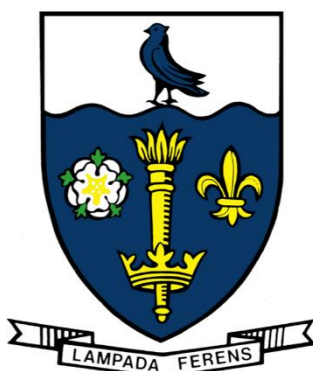


**THE UNIVERSITY OF HULL**



**Development of Radiolabeled Fatty Acid Derivatives for  
Imaging Cardiac Metabolism Using PET and SPECT**

being a Thesis submitted for the Degree of

Doctor of Philosophy

in the University of Hull

by

**Zainab Shakir Abdullah Al-Ali**

BSc (University of Basrah, Iraq, 1998)

MSc (University of Basrah, Iraq, 2001)

**April 2018**

## Abstract

Cardiac diseases are the leading cause of death worldwide. To address this problem, a better understanding of biochemical reasons underlying heart pathologies is needed. Fatty acid oxidation (FAO) plays a significant role in cardiac energy production and is therefore an important biomarker for heart disease. Positron emission tomography (PET) and single photon emission computed tomography (SPECT) are useful methods to quantify and qualify cardiac metabolic changes during either establishment of disease or therapeutic intervention. The extent of fatty acid oxidation can be visualised using radiolabeled thia-fatty acids. However, the uptake of these tracers as revealed by imaging also depends on their transport into cardiac cell mitochondria and general pharmacokinetics.

In this work, the synthesis of four types of 4-thia fatty acids, 4-thiacaprylic acid/caprylate derivatives (TCD1), 4-thiacapric acid/caprate derivatives (TCD2), 4-thiapalmitic acid/palmitate derivatives (TPD) and 4-thiaoleic acid/oleate derivatives (TOD) is described.

Fluorine-18 radiolabeling for the caprate, palmitate and oleate derivatives was optimised. The decay corrected radiochemical yields for the radiotracers, [ $^{18}\text{F}$ ]FTC2, [ $^{18}\text{F}$ ]FTP and [ $^{18}\text{F}$ ]FTO are  $16.15 \pm 2.60\%$ ,  $18 \pm 1.20\%$  and  $17.70 \pm 1.70\%$  respectively. [ $^{18}\text{F}$ ]FTP, [ $^{18}\text{F}$ ]FTO and [ $^{18}\text{F}$ ]FTC2 were found to be stable in serum after 3h at 37°C. PET imaging experiments in rats showed significant cardiac uptake for [ $^{18}\text{F}$ ]FTP and [ $^{18}\text{F}$ ]FTO but not for [ $^{18}\text{F}$ ]FTC2.

A thia-fatty acid delivery method to increase cardiac cell uptake was investigated, based on their coordination to mitochondria targeted transition metal complexes. The cross-bridged cyclam precursor compounds were produced in good yields and novel copper(II) cross-bridged cyclam complexes with a triphenylphosphonium moiety for mitochondria targeting were synthesised. Coordination of radiolabeled thiacapric acid to the complexes was attempted.

Novel  $^{99m}\text{Tc}$  radiolabeled long chain thia-fatty acids (palmitic and oleic acids) were investigated as potential new radiopharmaceuticals for use in fatty acid oxidation imaging, which would be metabolised by  $\beta$ -oxidation. The intermediate derivatives were synthesised in good yields and fully characterised to obtain the precursors for radiolabeling and to provide reference compounds.  $^{99m}\text{Tc}$  radiolabeled TACN –thia palmitic and thiaoleic acid were produced.

## Declaration of Authorship

I declare that the work presented in this thesis entitled **Development of Radiolabeled Fatty Acid Derivatives for Imaging Cardiac Metabolism Using PET and SPECT** was carried out in the School of Mathematics and Physical Sciences (Department of Chemistry) and School of Life Sciences (Positron Emission Tomography Research Centre) at The University of Hull by myself and under the supervision of Professor S. J. Archibald to fulfil the requirements of the University of Hull PhD degree in Chemistry (Biochemistry and medicinal inorganic chemistry). Except where indicated by references, this work is original and has not been submitted for any other degree.

**Zainab Shakir Abdullah Al-Ali (Reference Number: 201313469)**  
**University of Hull**

I confirm that the above information is correct.

**Professor S. J. Archibald**  
**Director of Positron Emission Tomography Research Centre**  
**University of Hull**  
**Cottingham Road**  
**Hull**  
**HU6 7RX**  
**UK**  
**Tel: 01482 465488**  
**FAX: 01482 466410**  
**Email: s.j.archibald@hull.ac.uk**

## Risk Assessment

All experiments were carried out in accordance with the University of Hull's Health and Safety guidelines. A full risk assessment was carried out for each new experiment, and all experiments were signed off by the supervisor (Prof. S. J. Archibald) and the departmental safety officer (Dr T. McCreedy or Dr G. Mackenzie) before any practical work started. Copies of each form were provided for reference to the departmental safety officer and supervisor. Radiochemistry experiments were assessed using the PET Research Facility Risk Assessment Form, signed by the undertaking student, supervisor (Prof. S. J. Archibald) and the radiation protection supervisor (Prof. S. J. Archibald/ Dr B. P. Burke/ Dr C. Cawthorne) before radiochemical experiments were carried out.

## Acknowledgements

I would like to express my sincere gratitude and thanks to my supervisor Prof. Steve Archibald, for his continuous guidance, constant support, encouragement and patience throughout my work. Without his valuable advice, it would be impossible to achieve my goals. I would like to thank Dr Chris Cawthorne for his contribution and carrying out all of the PET/CT imaging studies in this project.

I would like to thank Dr Juozas Domarkas and Dr Benjamin P. Burke. Juozas, for his help and advice throughout the project. Ben, I would like to thank for all of his ideas, which helped me to spot my mistakes more quickly and to become a more creative and independent researcher, and for the assistance that he gave me during the work in the laboratory. I would like address special thanks to the Archibald group members; Tahani, Rhiannon, Hayley, Boon-Uma, Fatmah, Ali, Bassim, Mustafa, Shubhanchi, Seraj, Fada, Farah, Alicja, Isaline, Dave and Beckie, who all made my PhD time easier. Special thanks to Goncalo dos santos Clemente for his help and support. I wish to thank Dr Anne Marie Seymour, Rob Atkinson, Faisal Nuhu and Shubhanchi Nigam for their assistance in the imaging studies. I would like to thank Carol Kennedy and Danny Mackenzie for performing the CHN analyses and Bob Knight for performing the ICP analyses. I also wish to thank Dr Kevin Welham for performing GC-MS and MS analyses.

My sincere thanks go to my family who were extremely supportive throughout this time; my great parents, my dear husband Mohanad for his incessant backing, tender care and support, my dear children (Mohammed, Hasan and Hashim), thank you very much for your patience with me throughout my PhD and my dear sisters and brothers. This work is dedicated to my husband and my children, they are always there for me, encouraging me to follow my instincts and supportive of any decisions I have made. I would not be where I am and who I am now, if not for them. I would like to thank the Iraqi Ministry of Higher Education and Scientific Research (MOHESR) for funding my scholarship. I give special acknowledgement goes for Iraqi Cultural Attaché and University of Basrah for their continued support.

## Abbreviations

[ <sup>123</sup> I]BMIPP	[ <sup>123</sup> I]-β-methyl- <i>p</i> -iodophenylpentadecanoic acid
[ <sup>123</sup> I]IPPA	15-( <i>p</i> -iodophenyl) pentadecanoic acid
[ <sup>18</sup> F]FDG	[ <sup>18</sup> F]-Fluorodeoxyglucose
[ <sup>18</sup> F]FHTA	[ <sup>18</sup> F]-Fluoro-6-thiaheptadecanoate
[ <sup>18</sup> F]FTC2	[ <sup>18</sup> F]-10-fluoro-4-thiacapric acid
[ <sup>18</sup> F]FTO	[ <sup>18</sup> F]-18-fluoro-4-thiaoleic acid
[ <sup>18</sup> F]FTP	[ <sup>18</sup> F]-16-fluoro-4-thiapalmitic acid
ACC	Acetyl CoA carboxylase
AMPK	AMP- activated protein kinase
ATP	Adenosine triphosphate
BFC	Bifunctional chelator
BM	Biomolecule
CAD	Coronary artery disease
CAT	Carnitine translocase
CoA	Coenzyme A
CPT	Carnitine palmitoyltransferase
CPT-I	Carnitine palmitoyltransferase I
CPT-II	Carnitine palmitoyltransferase II
CT	Computed tomography
DAST	Diethylaminosulfur trifluoride
DCM	Dichloromethane
DIPEA	Diisopropylethylamine
EC	Electron capture
EDTA	Ethylenediaminetetraacetic acid

ESI	Electrospray
FABP	Fatty acid binding protein
FACS	Fatty acyl CoA synthetase
FADH <sub>2</sub>	Flavin adenine dinucleotide
FAO	Fatty acid oxidation
FAT	Fatty acid transporters
FTO-CoA	Fatty acid oxidation CoA
FTP	Fluoro-4-thiapalmitate
GC-MS	Gas chromatography
HPLC	High-performance liquid chromatography
ICP	Inductively Coupled Plasma combine with mass spectrometry
IT	Isomeric transition
K <sub>222</sub>	Kryptofix
KCOs	Potassium channel openers
LAH	Lithium aluminum hydride
LDH	Lactate dehydrogenase
MBF	Myocardial blood flow
MCD	Malonyl CoA decarboxylase
MPC	Mitochondrial pyruvate carrier
MRI	Magnetic resonance imaging
MVo <sub>2</sub>	Myocardial oxygen consumption
NADH	Nicotinamide adenine dinucleotide
PALM	Palmitate
PALM-CoA	Palmitate Co A



PDH	Pyruvate dehydrogenase
PDK	Pyruvate dehydrogenase kinase
PDP	Pyruvate dehydrogenase phosphatase
PET	Positron emission tomography
PPTS	Pyridinium <i>p</i> -toluenesulfonate
QC	Quality control
QMA	Quaternary methyl ammonium
ROS	Reactive oxygen species
R <sub>t</sub>	Retention time
S <sub>N</sub> 2	Aliphatic nucleophilic substitution
S <sub>N</sub> Ar	Aromatic nucleophilic substitution
SPECT	Single-photon emission computed tomography
SUV	Standard uptake value
TBAF	Tetra- <i>n</i> -butylammonium fluoride
TBDMS	Dimethyl- <i>tert</i> -butylsilyl
TBDMSCl	Tetrabutyl-dimethylsilyl chloride
TCA	Tricarboxylic acid
TCD1	4-thiacaprylic acid/caprylate derivatives
TCD2	4-thiacapric acid/caprate derivatives
TEA	Triethylamine
TG	Triacylglycerol
THF	Tetrahydrofuran
THP	4-dihydro-2 <i>H</i> -pyran
TLC	Thin layer chromatography
TOD	4-thiaoleic acid/oleate derivatives

TPD	4-thiapalmitic acid /palmitate derivatives
TPP	Triphenylphosphonium
US	Ultrasound
VDAC	Voltage-dependent anion channel
$\beta^+$	Positron
$\gamma$	Gamma
$\Delta\Psi$	Mitochondrial membrane potential

# Table of Contents

Abstract.....	i
Declaration of Authorship.....	iii
Risk Assessment .....	iv
Acknowledgements.....	v
Abbreviations .....	vi
Table of Figures.....	xvi
Table of Schemes .....	xxi
Table of Tables .....	xxiv
Chapter One: Introduction.....	2
1.1 Cardiac disease .....	2
1.2 Cardiac disease and fatty acid metabolism.....	3
1.3 Myocardial metabolism in the healthy state .....	5
1.4 Myocardial metabolism in the pathologic state .....	8
1.5 What is difference between fatty acids and thia-fatty acids? .....	10
1.6 Medical imaging .....	12
1.6.1 Nuclear molecular imaging .....	13
1.6.2 What nuclear imaging techniques could bring to cardiology?.....	14
1.6.3 Single photon emission computed tomography (SPECT) imaging .....	15
1.6.3.1 Radiochemistry of technetium .....	17
1.6.3.2.3 SPECT tracers used to assess fatty acid metabolism.....	23
1.6.4 Positron emission tomography (PET) imaging.....	24
1.7 Proposed metabolism for thia-fatty acids in the cardiomyocytes.....	33
1.8 Summary.....	34
1.9 Research Aims .....	35

Chapter Two: Synthesis of thia-fatty acid derivatives .....	37
2.1 Aims and objectives .....	37
2.2 Previously reported synthetic methodologies to produce <sup>18</sup> F labeled fatty acid precursors.....	38
2.3 Synthesis of methyl 4-thiapalmitic acid/palmitate derivatives (TPD).....	43
2.3.1 Synthesis of 16-iodo or bromo-4-thiapalmitate ( <b>2</b> and <b>3</b> ).....	43
2.3.2 Synthesis of 16-fluoro-4-thiapalmitic acid (FTP) <b>6</b> .....	44
2.3.3 HPLC analysis of methyl 16-fluoro-4-thiapalmitate <b>5</b> and 16-fluoro-4-thiapalmitic acid (FTP) <b>6</b> .....	45
2.4 Novel synthetic routes for 4-thiacaprylic acid/caprylate derivatives (TCD1) ..	46
2.4.1 Synthesis of methyl 8-tosyl or bromo-4-thiacaprylate ( <b>13</b> and <b>18</b> ) .....	46
2.4.2 Synthesis of methyl 8-fluoro-4-thiacaprylic acid (FTC1) <b>21</b> .....	53
2.4.3 HPLC identification of 8-fluoro-4-thiacaprylic acid (FTC1) <b>21</b> .....	54
2.5 Synthesis of 4-thiacapric acid/ methyl-4-thiacaprate derivatives (TCD2) .....	55
2.5.1 Synthesis of methyl-10-iodo- or methyl-10-bromo-4-thiacaprate ( <b>22</b> and <b>23</b> ) .....	55
2.5.2 Synthesis of 10-fluoro-4-thiacapric acid (FTC2) <b>26</b> .....	56
2.5.3 HPLC identification of methyl-10-fluoro-4-thiacaprate <b>25</b> and 10-fluoro-4-thiacapric acid (FTC2) <b>26</b> .....	57
2.6 Novel synthesis of 4-thiaoleic acid/methyl-4-thiaoleate derivatives .....	58
2.6.1 Synthesis of methyl-18-tosyl-, methyl-18-bromo- or methyl-18-iodo-4-thiaoleate <b>32</b> , <b>33</b> and <b>34</b> .....	58
2.6.2 Synthesis of 18-fluoro-4-thiaoleic acid (FTO) <b>36</b> .....	61
2.6.3 HPLC identification of methyl 18-fluoro-4-thiaoleate <b>35</b> and 18-fluoro-4-thiaoleic acid (FTO) <b>36</b> .....	62
2.7 Conclusions.....	63

Chapter Three: Radiosynthesis and preclinical PET/CT imaging of <sup>18</sup> F-thia-fatty acids	66
3.1 Introduction	66
3.2 Aims and objectives	68
3.3 General radiolabeling method for fatty acid probe precursors	69
3.3.1 Radiosynthesis of [ <sup>18</sup> F]fluoro-4-thia-fatty acids ([ <sup>18</sup> F]FTC2, [ <sup>18</sup> F]FTP and [ <sup>18</sup> F]FTO)	71
3.3.2 Stability in Serum	73
3.4 [ <sup>18</sup> F]-16-fluoro-4-thiapalmitic acid ([ <sup>18</sup> F]FTP)	74
3.4.1 Radiosynthesis of [ <sup>18</sup> F]-16-fluoro-4-thiapalmitic acid ([ <sup>18</sup> F]FTP) [ <sup>18</sup> F]6	74
3.4.2 Preliminary preclinical evaluation of [ <sup>18</sup> F]16-fluoro-4-thiapalmitic acid ([ <sup>18</sup> F]FTP) [ <sup>18</sup> F]6	79
3.5 [ <sup>18</sup> F]10-fluoro-4-thiacapric acid ([ <sup>18</sup> F]FTC2) [ <sup>18</sup> F]26	81
3.5.1 Radiosynthesis of [ <sup>18</sup> F]-10-fluoro-4-thiacapric acid ([ <sup>18</sup> F]FTC2) [ <sup>18</sup> F]26	81
3.5.2 Preliminary preclinical imaging evaluation of [ <sup>18</sup> F]10-fluoro-4-thiacapric acid ([ <sup>18</sup> F]FTC2)/ [ <sup>18</sup> F]26	85
3.6 Synthesis and imaging of [ <sup>18</sup> F]18-fluoro-4-thiaoleic acid ([ <sup>18</sup> F]FTO) [ <sup>18</sup> F]36	86
3.6.1 Radiosynthesis of [ <sup>18</sup> F]-18-fluoro-4-thiaoleic acid ([ <sup>18</sup> F]FTO) [ <sup>18</sup> F]36	86
3.6.2 Preliminary preclinical PET/CT imaging evaluation of [ <sup>18</sup> F]-18-fluoro-4-thiaoleic acid ([ <sup>18</sup> F]FTO)/ [ <sup>18</sup> F]36	89
3.6.3 Evaluation of <i>in vivo</i> stability of [ <sup>18</sup> F]-18-fluoro-4-thiaoleic acid ([ <sup>18</sup> F]FTO)/[ <sup>18</sup> F]36	89
3.7 Cardiac uptake comparison between [ <sup>18</sup> F]FTP, [ <sup>18</sup> F]FTC2 and [ <sup>18</sup> F]FTO	90
3.8 Conclusion	91
Chapter Four: Fluorothiacapric acid complexes with copper(II) cross bridged cyclam derivatives	94
4.1 Introduction to azamacrocycles and mitochondrial targeting	94

4.1.1 Challenges with medium alkyl chain length thia-fatty acid probes .....	94
4.1.2 Macrocyclic chelators .....	94
4.1.3 Mitochondria structure and potential for targeting .....	95
4.2 Aims and objectives.....	99
4.3 Synthesis of cross-bridged cyclam chelators.....	101
4.4 Synthesis of the copper(II) cross-bridged cyclam complex with fluorothiaproic acid (non-targeted).....	104
4.5 Synthesis of the copper(II) cross-bridged cyclam complex with fluorothiaproic acid (mitochondria targeted).....	107
4.6 [ <sup>18</sup> F]-Fluorothiaproic acid complex with copper(II) cross-bridged cyclam (non-targeted).....	111
4.7 Conclusions.....	113
Chapter Five: Development of <sup>99m</sup> Tc labeled long alkyl chain thia-fatty acids .....	116
5.1 <sup>99m</sup> Tc labeled fatty acid imaging agents .....	116
5.2 Aims and objectives.....	119
5.3 Synthesis of <sup>99m</sup> Tc TACN-thiafatty acid radiolabeling precursors .....	120
5.4 Synthesis of rhenium(I) complexes with TACN-thiapalmitic acid/Re(CO) <sub>3</sub> <b>52</b> and TACN-thiaoleic acid/Re(CO) <sub>3</sub> <b>55</b> .....	124
5.5 <sup>99m</sup> Tc radiolabeling of TACN-thiapalmitic acid/ <sup>99m</sup> Tc(CO) <sub>3</sub> <b>52</b> .....	126
5.5.1 <sup>99m</sup> Tc(I) radiolabeling of thiafatty acid derivatives .....	127
5.5.4 Purification and isolation of the <sup>99m</sup> Tc(CO) <sub>3</sub> <b>52</b> .....	129
5.6 <sup>99m</sup> Tc radiolabeling of TACN-thiaoleic acid/ <sup>99m</sup> Tc(CO) <sub>3</sub> <b>55</b> .....	132
5.7 Conclusions.....	134
Chapter Six: Conclusions and Future work .....	136
6.1 Conclusions.....	136
6.1.1 Overview .....	136

6.1.2 Main achievements.....	136
6.2 Future work .....	144
6.2.1 Short term goals.....	144
6.2.2 Long-term goals.....	144
Chapter Seven: Experimental.....	147
7.1 Materials.....	147
7.2 General methodologies .....	147
7.3 Instrumentation.....	148
7.3.1 NMR spectroscopy.....	148
7.3.2 Mass spectrometry (MS) and gas chromatography mass spectrometry (GC-MS).....	148
7.3.3 CHN .....	148
7.3.3 ICP .....	149
7.3.4 Cyclotron.....	149
7.3.5 Hot cell .....	149
7.3.6 Elution for <sup>99</sup> Mo/ <sup>99m</sup> Tc generator .....	149
7.3.6 Radio-TLC scanner.....	149
7.3.7 High-Performance Liquid Chromatography HPLC and Radio- HPLC.....	150
7.3.8 PET/CT animal scanning.....	153
7.4 Experimental procedures .....	154
7.4.1 Synthesis of 4-thiapalmitic acid/palmitate derivatives (TPD) .....	154
7.4.2 Synthesis of 4-thiacaprylic acid/caprylate derivatives (TCD1) .....	160
7.4.2 Synthesis of 4-thiacapric acid/caprate derivatives.....	184
7.4.4 Synthesis of 4-thiaoleic acid/oleate derivatives (TOD) .....	190
7.4.5 Radio-fluorination of thia-fatty acid tracers.....	201
7.4.6 Stability in serum .....	206

7.4.7 Synthesis of copper-cross bridge cyclam complex which functionalise and not functionalise with a triphenylphosphonium .....	210
7.4.7.5 1-[4-Aminomethylbenzyl]-8-[methyl]-1,4,8,11-tetraazabicyclo [6.6.2]hexadecane ( <b>41</b> ) <sup>196, 199</sup> .....	214
7.4.7.9 (4-(Bromomethyl)benzyl)triphenylphosphonium bromide ( <b>43</b> ) <sup>205</sup> ...	219
7.4.7.10 (4-(((4-((11-methyl-1,4,8,11-tetraazabicyclo[6.6.2] hexadecane-4-yl)methyl)benzyl)amino)methyl)benzyl) triphenylphosphonium bromide ( <b>44</b> ).....	220
7.4.7.11 (4-(((4-((11-methyl-1,4,8,11-tetraazabicyclo[6.6.2] hexadecane-4-yl)methyl)benzyl)amino)methyl)benzyl) triphenylphosphonium bromide copper(II) chloride [Cu <b>44</b> Cl]Cl <sub>2</sub> .....	221
7.4.7.11 (4-(((4-((11-methyl-1,4,8,11-tetraazabicyclo[6.6.2] hexadecane-4-yl)methyl)benzyl)amino)methyl)benzyl) triphenylphosphonium bromide copper(II) perchlorate [Cu <b>44</b> (OH <sub>2</sub> )](ClO <sub>4</sub> ) <sub>2</sub> .....	222
7.4.7.12 (4-(((4-((11-methyl-1,4,8,11-tetraazabicyclo[6.6.2] hexadecane-4-yl)methyl)benzyl)amino)methyl)benzyl) triphenylphosphonium bromide copper(II) chloride and perchlorate [Cu <b>44</b> ( <b>26</b> )]X .....	223
7.4.7.8 Copper complexes of (4-(((4-((11-methyl-1,4,8,11-tetraazabicyclo[6.6.2] hexadecane-4-yl)methyl)benzyl)amino) methyl)benzyl) triphenylphosphonium bromide [ <sup>18</sup> F][Cu <b>40</b> ( <b>26</b> )] <sup>+</sup> .....	225
References.....	242



## Table of Figures

Figure 1: Non-invasive cardiac imaging techniques a. MRI, <sup>11</sup> b. SPECT, <sup>12</sup> c. CT, <sup>13</sup> d. PET <sup>14</sup> .....	3
Figure 2: The sources of energy for the heart .....	4
Figure 3: Myocardial metabolism under normal conditions .....	6
Figure 4: Schematic of $\beta$ -oxidation of fatty acids .....	7
Figure 5: Randle Cycle or the glucose/fatty acid cycle .....	8
Figure 6: Myocardial substrate metabolism in pathologic state (ischemic/reperfusion) .....	10
Figure 7: Schematic of metabolism of 4-thia fatty acid in mitochondria .....	11
Figure 8: Classification of medical imaging modalities <sup>40</sup> .....	13
Figure 9: Principles of single photon emission computed tomography (SPECT).....	15
Figure 10: A. <sup>99</sup> Mo/ <sup>99m</sup> Tc generator from Ultra-TechneKow™ DTE Generator. B. Illustration of the contents of <sup>99</sup> Mo/ <sup>99m</sup> Tc generator.....	18
Figure 11: Decay scheme of <sup>99</sup> Mo to <sup>99</sup> Ru.....	18
Figure 12: Radiolabeling of BMs containing endogenous sulfhydryl groups by the direct method .....	20
Figure 13: Schematic representation of the BFC approach .....	21
Figure 14: Chemical structures of [ <sup>123</sup> I] radiolabeled fatty acid analogues. ( <i>P</i> -IPPA) 15-( <i>p</i> -[ <sup>123</sup> I]-iodophenyl)pentadecanoic acid. ( <i>O</i> -IPPA) 15-( <i>O</i> -[ <sup>123</sup> I]-iodophenyl)pentadecanoic acid. (BMIPP) [ <sup>123</sup> I]- $\beta$ -methyl- <i>p</i> -iodophenylpentadecanoic acid.....	22
Figure 15: Chemical structure of <sup>99m</sup> Tc-sestamibi and <sup>99m</sup> Tc-tetrofosmin.....	23
Figure 16: Principle of positron emission tomography (PET) .....	24
Figure 17: Nucleophilic and electrophilic fluorination reactions.....	28
Figure 18: Cardiomyocyte substrate metabolism. [ <sup>18</sup> F]FHTA - [ <sup>18</sup> F]-18-fluoro-6-thiaheptadecanoic acid, [ <sup>18</sup> F]FTP - [ <sup>18</sup> F]-16-fluoro-4-thiapalmitic acid, [ <sup>18</sup> F]FTO - [ <sup>18</sup> F]-18-fluoro-4-thiaoleic acid, [ <sup>123</sup> I]BMIPP - beta-methyl- <i>p</i> -[ <sup>123</sup> I]-iodophenylpentadecanoic acid, [ <sup>18</sup> F]FDG - fluorodeoxyglucose .....	30
Figure 19: Proposed cardiomyocyte FTO metabolism.....	33
Figure 20: Chemical structures of target compounds .....	37

Figure 21: Chemical structure of thia-substituted fatty acids: [ <sup>18</sup> F]-14-fluoro-6-thiaoctadecanoic acid [ <sup>18</sup> F]14-FTHA; [ <sup>18</sup> F]-17-fluoro-6-thiaoctadecanoic acid [ <sup>18</sup> F]17-FTHA; [ <sup>18</sup> F]-16-fluoro-4-thiapalmitic acid [ <sup>18</sup> F]FTP; [ <sup>18</sup> F]-18-fluoro-4-thiaoleic acid [ <sup>18</sup> F]FTO; [ <sup>18</sup> F]-18-fluoro-4-thiastearic acid [ <sup>18</sup> F]FTS; [ <sup>18</sup> F]-18-fluoro-6-thiastearic acid [ <sup>18</sup> F]F-6-TS .....	38
Figure 22: Chemical structure for benzyl 14(R,S)-tosyloxy-6-thiaheptadecanoate <sup>113</sup> .....	39
Figure 23: HPLC traces of fluorinated ester intermediate 5 and 16-fluoro-4-thiapalmitic acid (FTP) 6 .....	45
Figure 24: HPLC traces of fluorinated ester intermediate 20 and 8-fluoro-4-thiacaprylic acid (FTC1) 21 .....	54
Figure 25: HPLC traces of fluorinated ester intermediate 25 and 10-fluoro-4-thiacapric acid (FTC2) 26.....	57
Figure 26: HPLC traces of fluorinated ester intermediate 33 and 18-fluoro-4-thiaoleic acid (FTO) 34 .....	62
Figure 27: Representation of cardiac uptake of [ <sup>18</sup> F]FTHA in patients <sup>31</sup> .....	66
Figure 28: Representative micro-PET images of thia-fatty acid tracers at 55–115 min <sup>4</sup> .....	67
Figure 29: Molecular structures of target compounds.....	68
Figure 30: <sup>18</sup> F-thia-fatty acid is administered to a rat to generate a PET/CT image of fatty acid metabolism .....	69
Figure 31: Schematic summary of the major steps in developing a routine preparation of a [ <sup>18</sup> F]thia-fatty acid tracers .....	70
Figure 32: Isolation of the [ <sup>18</sup> F]fluoride .....	71
Figure 33: Study of radiolabeling efficiency to form [ <sup>18</sup> F]5 at 75°C and 90°C, n=1 ...	75
Figure 34: Radio-TLC traces of [ <sup>18</sup> F]5 A: without using Silica Lite cartridge; B: with using Silica Lite cartridge.....	75
Figure 35: Radio-HPLC traces of [ <sup>18</sup> F]5 A: without cartridge purification; B: using Silica Lite cartridge .....	76
Figure 36: Radio-TLC trace of [ <sup>18</sup> F]6 with using Silica Lite cartridge, mobile phase pure acetonitrile.....	76

Figure 37: Radio-TLC trace of [ <sup>18</sup> F]6 with using Silica Lite cartridge, mobile phase DCM: MeOH (9: 1) .....	77
Figure 38: Radio-HPLC trace of [ <sup>18</sup> F]6 using a Silica Lite cartridge.....	77
Figure 39: Radio-HPLC trace of semi-preparative purification of [ <sup>18</sup> F]6.....	78
Figure 40: Radio-HPLC traces of [ <sup>18</sup> F]FTP-OH [ <sup>18</sup> F]6 eluted from Oasis C18 cartridge A: with ethanol; B: with diethyl ether.....	78
Figure 41: Radio-HPLC trace of [ <sup>18</sup> F]6 analysis of the final formulation .....	79
Figure 42: A. Sagittal PET-CT image of [ <sup>18</sup> F]FTP accumulation in nude mouse at different time points, B. [ <sup>18</sup> F]FTP liver and cardiac accumulation profile .....	80
Figure 43: A: Coronal maximum intensity projection images acquired 80-90 min post <i>iv</i> administration of [ <sup>18</sup> F]FTP. B: Time activity curves showing uptake of the tracer in indicated organs .....	81
Figure 44: Study of radiolabeling efficiency to form [ <sup>18</sup> F]25 at different time points, n= 1 .....	82
Figure 45: Radio-TLC trace of the radiolabeling reaction to form [ <sup>18</sup> F]25 .....	83
Figure 46: Radio-HPLC trace of [ <sup>18</sup> F]FTC2/ [ <sup>18</sup> F]26 .....	83
Figure 47: Radio-HPLC trace of semi-preparative HPLC purification of [ <sup>18</sup> F]26.....	84
Figure 48: Radio-HPLC of [ <sup>18</sup> F]FTC2/ [ <sup>18</sup> F]26 analysis of the final formulated radiotracer .....	84
Figure 49: A: Coronal maximum intensity projection images acquired 80-90 min post <i>iv</i> administration of [ <sup>18</sup> F]FTC2. B: Time activity curves showing uptake of the tracer in indicated organs.....	85
Figure 50: Radio-TLC of [ <sup>18</sup> F]35 from 18-tosyl, bromo or iodo-4-thiaoleate precursor 32, 33 and 34 (mobile phase DCM: MeOH 9:1).....	87
Figure 51: Radio-HPLC trace of [ <sup>18</sup> F]FTO/ [ <sup>18</sup> F]36 after hydrolysis.....	87
Figure 52: Radio-HPLC trace of semi-preparative purification of <sup>18</sup> F-FTO/ [ <sup>18</sup> F]36 ...	88
Figure 53: Radio-HPLC trace of <sup>18</sup> F-FTO/ [ <sup>18</sup> F]36 radiotracer in the final formulation .....	88
Figure 54: A: Coronal maximum intensity projection images acquired 80-90 min post <i>iv</i> administration of [ <sup>18</sup> F]FTO. B: Time activity curves showing uptake of the tracer in indicated organs.....	89

Figure 55: Comparison of HPLC trace of [ <sup>18</sup> F]FTO and urine fraction.....	90
Figure 56: Schematic representation of a mitochondrion and the mode of action of representative targeted compounds.....	97
Figure 57: Molecular design of mitochondrial targeting fatty acid metal complex ..	99
Figure 58: Molecular structures of the target compounds in this work.....	100
Figure 59: MS/MS of [Cu40(26)] <sup>+</sup> .....	106
Figure 60: HPLC trace of [Cu40(26)] <sup>+</sup> .....	106
Figure 61: HPLC trace for [Cu44(OH <sub>2</sub> )](ClO <sub>4</sub> ) <sub>3</sub> .....	109
Figure 62: HPLC trace of reaction to form [Cu44(26)]X .....	110
Figure 63: Radio-HPLC traces showing the results from four different attempts to synthesise [ <sup>18</sup> F][Cu40(26)] <sup>+</sup> under the same conditions (A, B, C and D). This shows the variability in the procedure. ....	112
Figure 64: Representative <sup>99m</sup> Tc-labeled fatty acids compounds that have been reported previously and showed high initial cardiac uptake .....	117
Figure 65: Molecular structure of the TACN chelator attached to thiapalmitic acid .....	118
Figure 66: Molecular structures of target compounds.....	119
Figure 67: HPLC traces of standard reference compounds Re(CO) <sub>3</sub> 52 and Re(CO) <sub>3</sub> 55 .....	125
Figure 68: HPLC traces of [ <sup>99m</sup> TcO <sub>4</sub> ] <sup>-</sup> and [ <sup>99m</sup> Tc(OH <sub>2</sub> ) <sub>3</sub> (CO) <sub>3</sub> ] <sup>+</sup> 56 .....	126
Figure 69: Radio-HPLC trace of <sup>99m</sup> Tc(CO) <sub>3</sub> 52 .....	128
Figure 70: The effect of varying the concentration of 52 on radiolabeling efficiency, n=1 .....	128
Figure 71: Radio-HPLC trace of semi-preparative separation of <sup>99m</sup> Tc(CO) <sub>3</sub> 52 .....	130
Figure 72: Radio-HPLC traces of <sup>99m</sup> Tc(CO) <sub>3</sub> 52; A: after C18 cartridge; B: after formulation .....	130
Figure 73: Radio-HPLC traces of <sup>99m</sup> Tc(CO) <sub>3</sub> 52 in serum over 3 hours (0, 1, 2 and 3 hours).....	131
Figure 74: Radio-HPLC trace of <sup>99m</sup> Tc(CO) <sub>3</sub> 52 in PBS after 3 hours.....	132
Figure 75: Radio-HPLC trace of <sup>99m</sup> Tc(CO) <sub>3</sub> 55 .....	133

Figure 76: Radio-HPLC trace $^{99m}\text{Tc}(\text{CO})_355$ after C18 cartridge purification and elution with different solvents.....	133
Figure 77: Proposed structure where a carbonyl (CO) group has been replaced by an ethanol moiety.....	134

## Table of Schemes

Scheme 1: Synthetic route to prepare [ <sup>18</sup> F]-17-fluoro-6-thiaoctadecanoic acid [ <sup>18</sup> F]17- FTHA precursor and standard reference <sup>115</sup> .....	39
Scheme 2: Synthetic routes to prepare [ <sup>18</sup> F]-16-fluoro-4-palmitic acid [ <sup>18</sup> F]FTP .....	40
Scheme 3: Synthetic routes to prepare [ <sup>18</sup> F]-16-fluoro-4-thiapalmitic acid [ <sup>18</sup> F]FTP “cold” reference standard <sup>115, 116</sup> .....	40
Scheme 4: Synthetic routes to prepare [ <sup>18</sup> F]-18-fluoro-4-thiaoleic acid [ <sup>18</sup> F]FTO precursor and “cold” reference standard <sup>117</sup> .....	41
Scheme 5: Synthetic routes to prepare of, [ <sup>18</sup> F]FTO, <sup>18</sup> F-clicked-FTO precursor and the cold standard, F-clicked-FTO <sup>118</sup> .....	41
Scheme 6: Schematic synthetic routes to prepare [ <sup>18</sup> F]-18-fluoro-4-thiastearic acid [ <sup>18</sup> F]FTS precursor and “cold” reference standard <sup>4</sup> .....	42
Scheme 7: Synthetic routes to prepare [ <sup>18</sup> F]-18-fluoro-6-thiastearic acid [ <sup>18</sup> F]F-6-TS precursor and “cold” reference standard <sup>4</sup> .....	42
Scheme 8: Synthesis of methyl 16-iodo or bromo-4-thiapalmitate 2, 3 respectively .....	44
Scheme 9: Synthesis of 16-fluoro-4-thiapalmitic acid (FTP) 6 .....	44
Scheme 10: Aliphatic nucleophilic substitution reaction (S <sub>N</sub> 2).....	46
Scheme 11: Synthesis of methyl 4-thiacaprylate derivatives in general .....	47
Scheme 12: Synthesis of methyl 4-thiacaprylate intermediate derivatives .....	48
Scheme 13: Attempting of synthesis methyl 8-tosyl-4-thiacaprylate 13, four methods: Method 1- DIPEA, DCM; Method 2- K <sub>2</sub> CO <sub>3</sub> , DCM; Method 3- Et <sub>3</sub> N, ACN; Method 4- pyridine, DCM .....	50
Scheme 14: Synthesis of methyl 8-alcohol-4-sulfinylcaprylate 15 .....	51
Scheme 15: Synthesis of methyl 8-tosyl-4-sulfinylcaprylate 17 .....	51
Scheme 16: Synthesis of methyl 8-tosyl-4-thiacaprylate 13.....	51
Scheme 17: Suggestion mechanism for compound 13.....	52
Scheme 18: Synthesis of methyl 8-bromo-4-thiacaprylate 18 .....	52
Scheme 19: Attempting of synthesis 8-fluoro-4-thiacaprylate 20.....	53
Scheme 20: Synthesis of 8-fluoro-4-thiacaprylic acid (FTC1) 21.....	54
Scheme 21: Synthesis of methyl 8-bromo or iodo-4-thiacaprylate 22, 23.....	55

Scheme 22: Synthesis of 10-fluoro-4-thiacapric acid (FTC2) 26 .....	56
Scheme 23: Synthesis of methyl 4-thiaoleate intermediate derivatives 27, 28 and 29 .....	59
Scheme 24: Synthesis of methyl-18-tosyl-, methyl-18-bromo- or methyl-18-iodo-4-thiaoleate 32, 33 and 34 .....	60
Scheme 25: Synthesis of 18-fluoro-4-thiaoleic acid (FTP) 36 .....	61
Scheme 26: Radiosynthesis of [ <sup>18</sup> F](10, 16 or 18)-fluoro-4-thia(capric, palmitic or oleic) acid ([ <sup>18</sup> F]FTC2, [ <sup>18</sup> F]FTP or [ <sup>18</sup> F]FTO) .....	72
Scheme 27: Radiosynthesis of [ <sup>18</sup> F]FTP/[ <sup>18</sup> F]6 from the iodo precursor (methyl 16-iodo-4-thiapalmitate 2).....	74
Scheme 28: Radiosynthesis of iodo precursor methyl 10-iodo-4-thiacaprate 23 .....	82
Scheme 29: Radiosynthesis of [ <sup>18</sup> F]36 from 18-tosyl, bromo or iodo-4-thiaoleate precursors (32, 33 and 34).....	86
Scheme 30: Synthetic route to produce the CB cyclam compounds.....	102
Scheme 31: Synthetic route to produce non-targeted copper(II) cross-bridged cyclam complexes [Cu40Cl]Cl and [Cu40(OH <sub>2</sub> )](ClO <sub>4</sub> ) <sub>2</sub> .....	104
Scheme 32: Synthetic route to form 10-fluorothiacapric acid with non-targeted copper(II) cross-bridged cyclam complexes [Cu40(26)] <sup>+</sup> .....	105
Scheme 33: Synthetic route to produce a triphenylphosphonium derivatised macrocyclic chelator 44 .....	108
Scheme 34: Synthetic route to produce mitochondria targeted copper(II) cross-bridged cyclam complexes.....	108
Scheme 35: Synthetic route to form 10-fluorothiacapric acid with the mitochondria targeted copper(II) cross-bridged cyclam complex, [Cu44(26)]X.....	109
Scheme 36: Synthetic route to form [ <sup>18</sup> F]10-thiacapric acid with non-targeted copper(II) cross-bridged cyclam complex [ <sup>18</sup> F][Cu40(26)] <sup>+</sup> .....	111
Scheme 37: Synthetic route to protect two of the amine nitrogens on TACN (47), to add cyano pendant arm (48) and to reduce the cyano group to an amino group (49).....	120
Scheme 38: Synthetic route to produce TACN-thiapalmitic acid 52 .....	122
Scheme 39: Synthetic route to produce TACN-thiaoleic acid 55.....	123

Scheme 40: Synthetic route to produce standard reference compounds $\text{Re}(\text{CO})_352$ and $\text{Re}(\text{CO})_355$ .....	125
Scheme 41: Synthesis of the organometallic precursor $[\text{}^{99\text{m}}\text{Tc}(\text{OH}_2)_3(\text{CO})_3]^+$ 56 .....	126
Scheme 42: Reaction pathway to $^{99\text{m}}\text{Tc}$ radiolabeling of novel precursor 52 .....	127
Scheme 43: Reaction pathway to $^{99\text{m}}\text{Tc}$ radiolabeling of novel precursor 55 .....	132
Scheme 44: Suggested synthetic route to produce gallium-68 radiolabeled thiapalmitic acid.....	145



## Table of Tables

Table 1: Common SPECT radioisotopes, decay characteristics and methods of production <sup>28, 51, 52</sup> .....	16
Table 2: Decay characteristics of common PET radionuclides <sup>10</sup> .....	25
Table 3: Molecular structures and yields for radiolabeling precursors .....	64
Table 4: Solvent/ pH used for <sup>99m</sup> Tc radiolabeling and yield obtained (90°C, 30 min, n=1) .....	127
Table 5: The effect of temperature on <sup>99m</sup> Tc radiolabeling yield of 52, n=1 .....	129
Table 6: The chemical structure for compounds synthesised and reported in Chapter Two .....	138
Table 7: Summary of radiosynthesis results for [ <sup>18</sup> F]FTP, [ <sup>18</sup> F]FTC2 and [ <sup>18</sup> F]FTO (Chapter Three).....	139
Table 8: Comparison study between radiolabeling of the 18-tosyl-, 18-iodo or 18-bromo-4-thiaoleate <b>32</b> , <b>33</b> and <b>34</b> precursors (Chapter Three).....	139
Table 9: The molecular structure for selected macrocyclic compounds synthesised (Chapter Four).....	141
Table 10: The molecular structures of key compounds produced for macrocycle attachment (Chapter Five).....	142
Table 11: The molecular structures for key rhenium and technetium compounds synthesised (Chapter Five).....	143
Table 12: HPLC gradient-method 1 .....	150
Table 13: HPLC gradient-method 2 .....	151
Table 14: HPLC gradient-method 3 .....	151
Table 15: HPLC gradient-method 4 .....	152
Table 16: HPLC gradient-method 5 .....	152
Table 17: HPLC gradient-method 6 .....	152
Table 18: Conditions, which use to synthesis compound [Cu40(26)] <sup>+</sup> .....	218
Table 19: Conditions, which use to synthesis compound [Cu44(26)]Cl <sub>2</sub> .....	224
Table 20: Conditions, which use to synthesis compound [Cu <b>44(26)</b> ](ClO <sub>4</sub> ) <sub>2</sub> .....	224
Table 21: Reaction conditions used in the synthesis of [ <sup>18</sup> F][Cu40(26)] <sup>+</sup> .....	227

# **Chapter One**

## **Introduction**

# Chapter One: Introduction

## 1.1 Cardiac disease

The heart works as a pump moving blood around the body. The circulating blood delivers oxygen and nutrients to the tissues and carries away generated carbon dioxide and other metabolic waste products. When the heart and peripheral veins or arteries are damaged, this system does not work properly, and it results in what is generally called “cardiac disease”. Since the last century, cardiac diseases have become a major public health problem and are, effectively, the greatest cause of mortality worldwide,<sup>1</sup> resulting in a challenge for modern clinical research.

The development of sensitive and preferably non-invasive methods for an early diagnosis of cardiac dysfunction is needed.<sup>2, 3</sup> Medical imaging is a generic name for a variety of such non-invasive diagnostic techniques. Non-invasive cardiac imaging (see Figure 1), refers to a combination of methods that can be used to obtain images relating to the structure and function of the heart.<sup>4</sup>

Cardiac imaging methods include echocardiography, magnetic resonance imaging (MRI), computed tomography (CT) and nuclear medicine techniques such as positron emission tomography (PET) and single-photon emission computed tomography (SPECT).<sup>5</sup> Echocardiography uses sound waves to provide an image of the heart in a similar way to ultrasound imaging.<sup>6</sup> Magnetic resonance imaging (MRI) uses contrast agents, which affect proton relaxation times in different environments. It is mainly used to examine perfusion of heart tissue but there are technical challenges related mainly to cardiac motion.<sup>7</sup> Computed tomography (CT) employs X-rays, which penetrate the body and are registered by a circular array of detectors. These data can be reconstructed into a 3D anatomical image of the heart.<sup>8</sup> Positron emission tomography (PET) and single-photon emission computed tomography (SPECT) offer the potential for focus on myocardial metabolism and require the use of radiopharmaceuticals. From the different techniques mentioned, only PET can reliably quantify the myocardial substrate metabolism.<sup>9, 10</sup> Thus, there is a clinical need for a further development of PET radiotracers capable of imaging heart

metabolism and answering important questions concerning the initial diagnosis or a follow-up/monitoring of effects of therapeutic intervention.

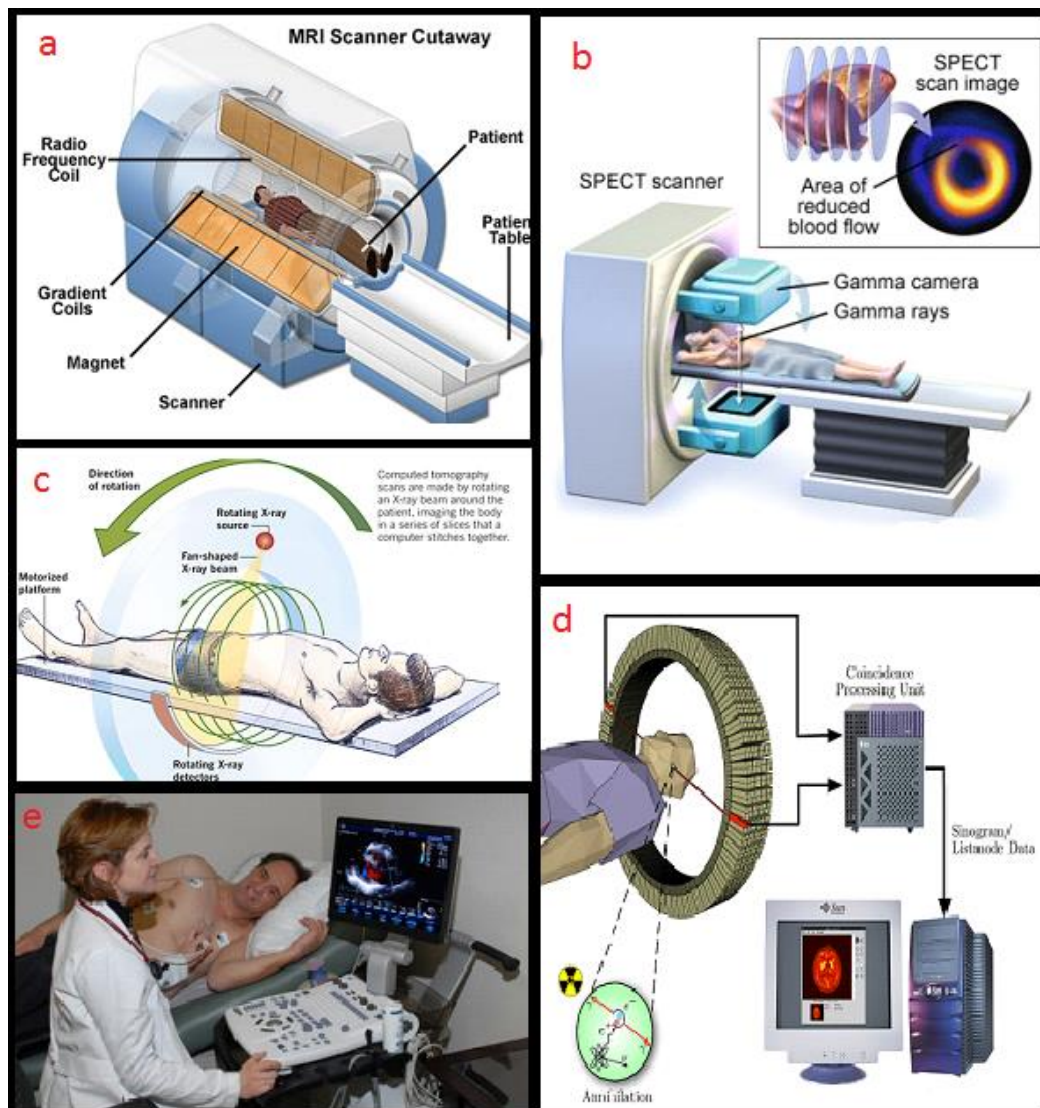


Figure 1: Non-invasive cardiac imaging techniques a. MRI,<sup>11</sup> b. SPECT,<sup>12</sup> c. CT,<sup>13</sup> d. PET<sup>14</sup> and e. Echocardiography<sup>15</sup>

## 1.2 Cardiac disease and fatty acid metabolism

To keep up the heart's rhythmic pumping activity, the cardiac muscle requires a lot of energy. Therefore, it uses large quantities of adenosine triphosphate (ATP) which is the ultimate energy source for contractile function. To assure a continuous supply of ATP, the heart can use different carbon substrates, such as glucose, lactate, fatty acids, ketone bodies (acetoacetate, beta-hydroxybutyrate and acetone) or even

amino acids (glutamate), as energy sources (see Figure 2). The main energy source in both healthy or dysfunctional heart is, however, fatty acid catabolism.<sup>16</sup>

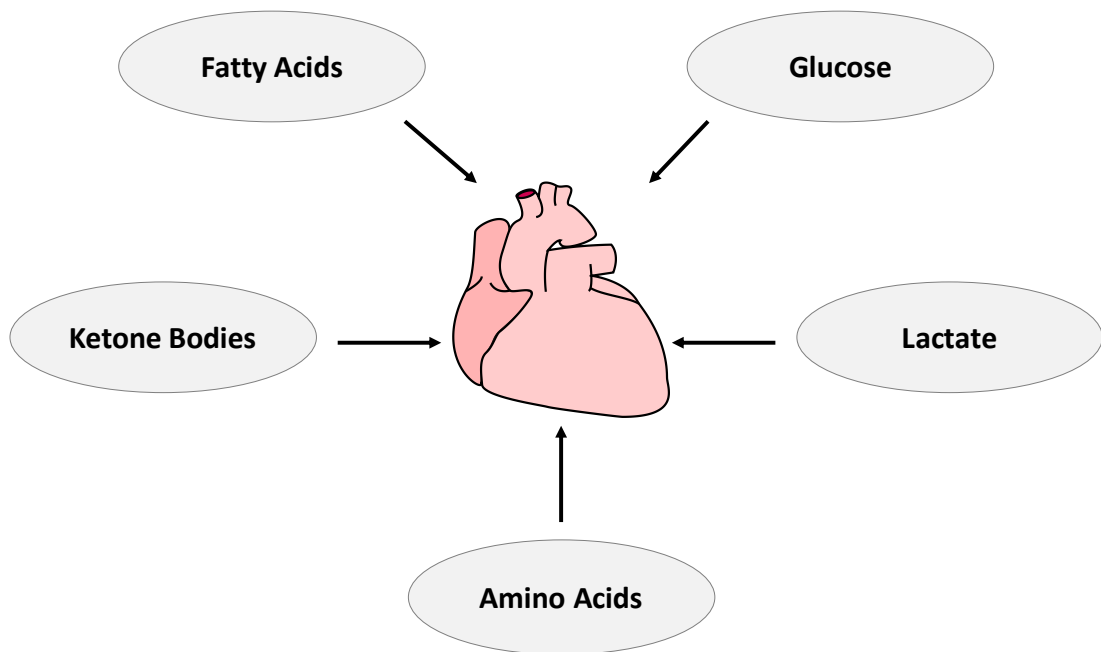


Figure 2: The sources of energy for the heart

The foetal heart, which functions in the environment with a low oxygen partial pressure, is driven by lactate and glucose catabolism.<sup>17</sup> After birth, there is a metabolic change towards mitochondrial fatty acid oxidation, which relies on a steady supply of both fatty acids and oxygen to the heart. Other variables, such as the presence of other energy sources such as glucose, proficiency in fatty acid uptake, esterification or mitochondrial transport, also play an important role in the exact composition of energy sources.<sup>16</sup> When there is an increase in blood glucose levels (non-fasting condition), the heart can be temporarily shifted back to “burning” glucose, lactate or ketone bodies (acetoacetate, beta-hydroxybutyrate and acetone). A similar shift may also occur in a disease state when oxygen supply is compromised, such as ischemia. Consequently, the myocardial substrate metabolism is an attractive target for diagnosis, because there is a strong relationship between changed myocardial metabolism and cardiac health.<sup>18</sup>

### 1.3 Myocardial metabolism in the healthy state

Knowledge of a healthy myocardial metabolism is critical in order to discern changes happening in the unhealthy heart (see Figure 3). Arterial blood contains various fatty acids. The most abundant (around 30%) is a palmitic acid, composed of saturated 16-carbon chain. All fatty acids including palmitic acid are too lipophilic to be soluble in blood and circulate either in free carboxylate form bound to albumin or as glycerol esters (triglycerides), carried by very-low-density lipoproteins or chylomicrons.

In the normal adult heart under fasting conditions, the glucose and insulin levels are low and fatty acid and catecholamine levels are high, resulting in an increased fatty acid uptake by myocardial cells. Palmitic acid enters the cell *via* a cell membrane-bound fatty acid transporter (FAT), composed of tissue-specific fatty acid transporter protein (CD36/FAT) and fatty acid binding protein (FABP). In the cytosol, free palmitate is conjugated with co-enzyme A (CoA) to form an activated PALM–CoA, which then can utilise the carnitine shuttle and be transported into the mitochondria (see Figure 3).

Carnitine palmitoyltransferase-I (CPT-I) exchanges CoA to carnitine and then the PALM-carnitine conjugate is transported into the mitochondrial matrix. Carnitine is released, while another carnitine palmitoyltransferase-II (CPT-II) exchanges it back to CoA. Activated PALM–CoA feeds directly into fatty acid oxidation process and released carnitine is transported back into cytosol allowing the shuttle process to continue (see Figure 3).<sup>8-11</sup>

When glucose and insulin levels increase after a meal, the myocardial glucose catabolism increases several fold while fatty acid catabolism is suppressed.<sup>16</sup> Briefly, glucose enters the cell by glucose transporters (GLUT1/4) (see Figure 3), is phosphorylated into glucose 6-phosphate and is then converted into a key intermediate pyruvate with a concurrent release of NADH. Pyruvate is then transported into the mitochondrial matrix and is converted into acetyl-CoA by pyruvate dehydrogenase (PDH). The acetyl CoA enters the TCA cycle, which releases NADH and FADH<sub>2</sub> and powers the ATP synthase, or is transformed by acetyl-CoA

carboxylase (ACC) into malonyl CoA which is a strong CPT-1 inhibitor, shutting down the carnitine shuttle and reducing fatty acid oxidation by compromising mitochondrial fatty acid supply.<sup>19-21</sup>

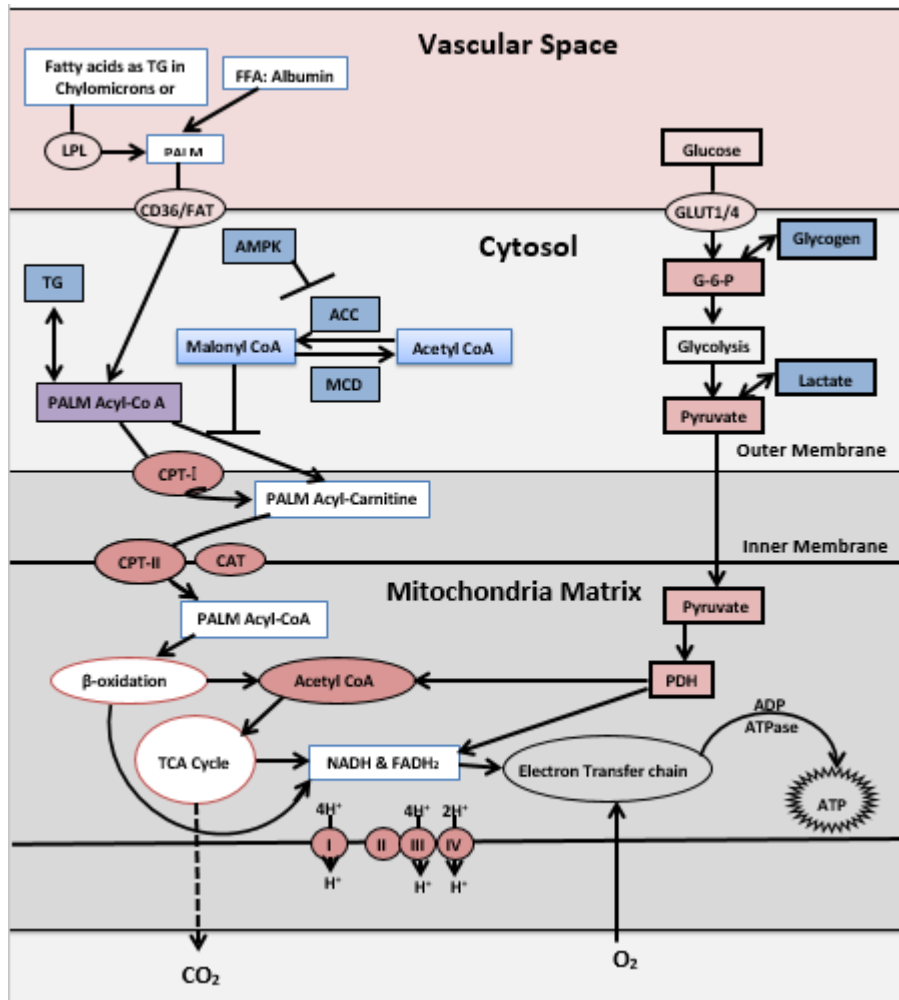


Figure 3: Myocardial metabolism under normal conditions

Each cycle of  $\beta$ -oxidation generates one acetyl-CoA molecule, which enters into the tricarboxylic acid (TCA) cycle (see Figure 4). In addition, one nicotinamide adenine dinucleotide (NADH) and one Flavin adenine dinucleotide ( $\text{FADH}_2$ ) molecules is also formed, which is required for ATP-synthase to generate the ATP.<sup>22</sup>

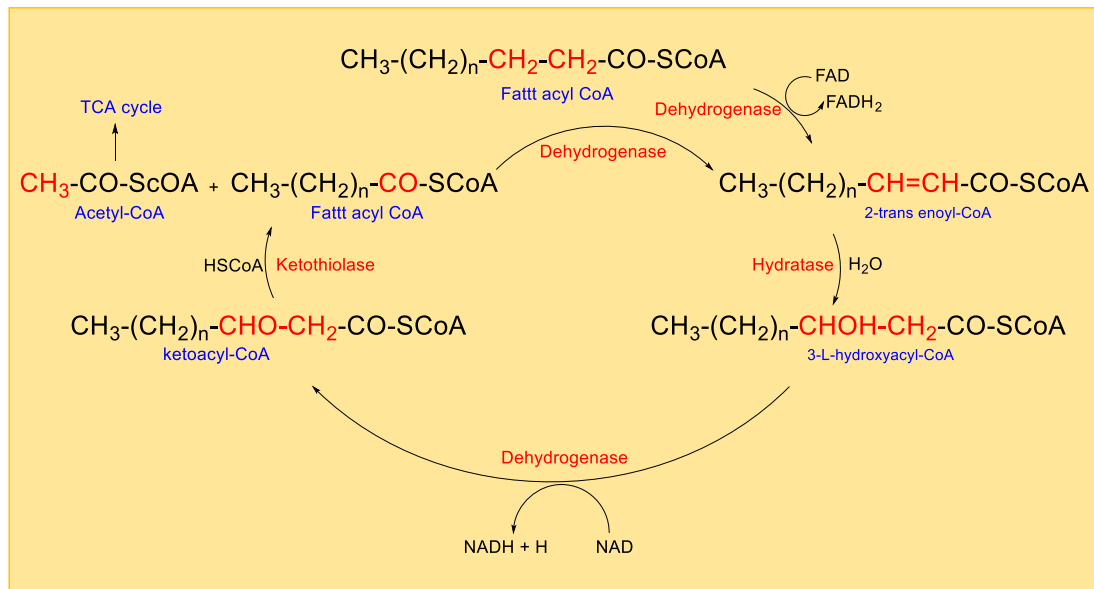


Figure 4: Schematic of  $\beta$ -oxidation of fatty acids

During intense exercise, when muscles function in the anaerobic regime, pyruvate formed from glycolysis is converted to lactate (non-oxidative glycolysis). Lactate is an important source of pyruvate and is used by cardiac muscle under hypoxic conditions.<sup>23</sup>

Glucose and fatty acid catabolism are connected in the Randle or glucose/fatty acid cycle.<sup>24</sup> Key glucose catabolism enzyme, PDH, is inhibited by  $\text{NADH}$  and acetyl-CoA, produced by fatty acid oxidation, and the key carnitine shuttle enzyme, CPT-1, is inhibited by glucose catabolism side product malonyl-CoA. (see Figure 5).<sup>19</sup>

The heart's ability to use different substrates for energy production under different conditions distinguishes it from other organs, such as the brain, which is powered almost exclusively by glucose catabolism. At the same time, it makes it vulnerable to issues caused by other tissues, *i.e.* skeletal muscles.<sup>25</sup>



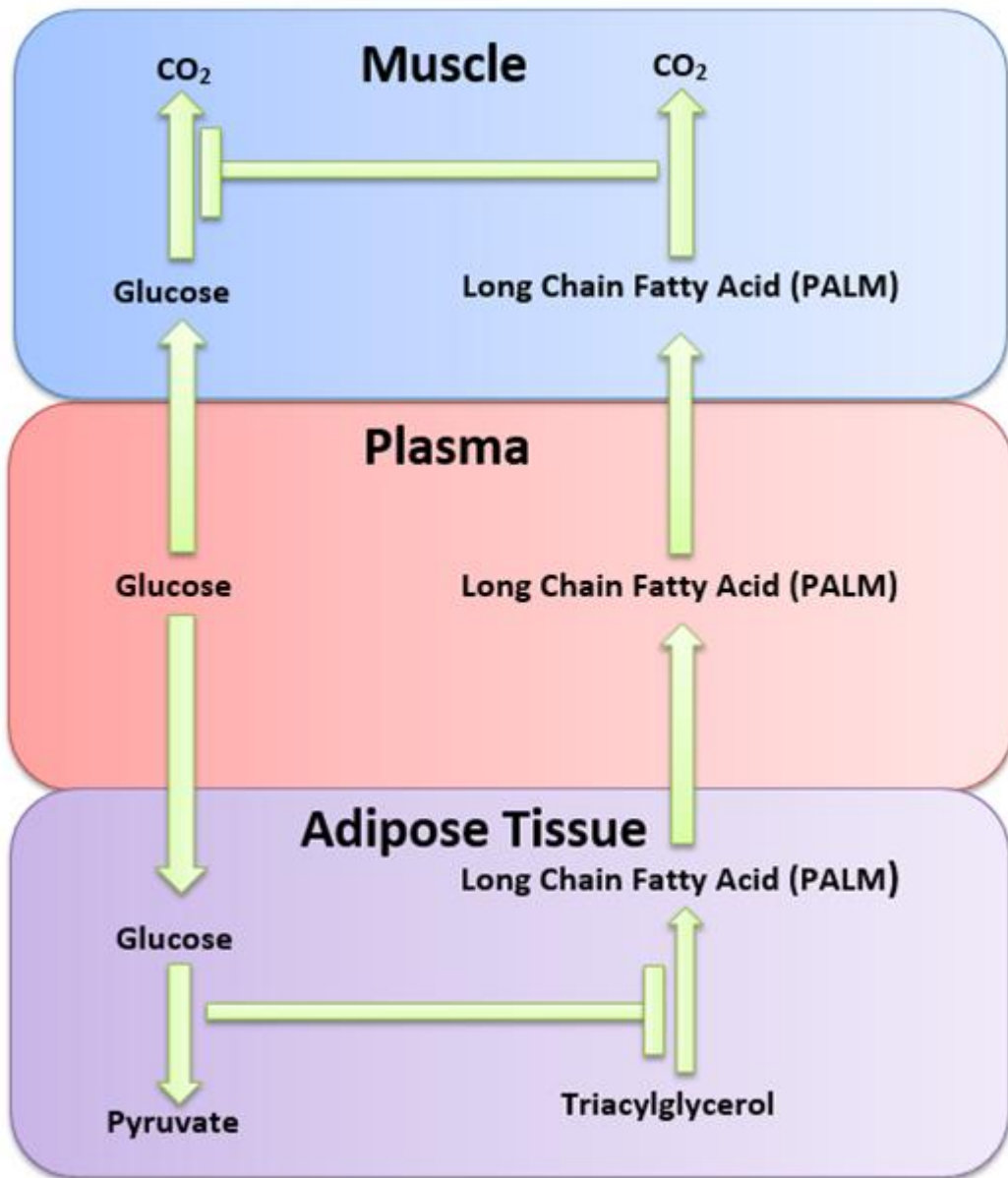


Figure 5: Randle Cycle or the glucose/fatty acid cycle

## 1.4 Myocardial metabolism in the pathologic state

In normal conditions, the process of fatty acid oxidation is the main source of energy for ATP synthesis. However, it consumes far more oxygen per mole of energy released than required by carbohydrate catabolism, thus, making it less economical regarding oxygen usage and inferior; under hypoxic conditions. This explains the shift towards carbohydrate catabolism observed in ischemic patients. There are many types of cardiac pathological states, *i.e.* ischemia, heart failure, diabetic cardiomyopathy, etc.<sup>19</sup> Changes in myocardial metabolism depends on the type of

disease; either fatty acid or glucose oxidation is increased. alteration in cardiac mitochondrial energy metabolism affects contractile function and cardiac efficiency.<sup>26</sup> However, the link between the metabolic state of the heart and different pathological states is not completely understood.

Under ischemic conditions, a decrease in oxygen supply to the heart causes an overall decrease of mitochondrial oxidative metabolism. This metabolic change resembles foetal cardiac metabolism, characterised by increased glycolysis and low mitochondrial oxidation. During a reperfusion of the heart after acute ischemic episode, the rate of fatty acid oxidation increases. This can be due either to higher levels of circulating fatty acids or to reduced efficiency of TCA cycle and increased malonyl-CoA levels.<sup>19</sup> As seen previously in the Randle cycle, a high rate of fatty acid oxidation dampens glucose catabolism by inhibiting the activity of pyruvate dehydrogenase (PDH). Reduced glucose catabolism may uncouple glycolysis from glucose oxidation in TCA cycle resulting in accumulation of lactate and acidification of cytosol, which compromises heart efficiency by diverting ATP reserves from contractile function to maintain ionic balance. Usually, excess protons from cytosol are removed by  $\text{Na}^+/\text{H}^+$  antiport pump, with the resulting increase in cytosolic  $\text{Na}^+$ , increasing  $\text{Ca}^{2+}$  flow into the cell *via* the  $\text{Ca}^{2+}/\text{Na}^+$  antiport.  $\text{Ca}^{2+}$  is an important cellular mediator, and its low cellular concentration is maintained by ATP powered transporter pushing  $\text{Ca}^{2+}$  out of the cell against the concentration gradient (see Figure 6).<sup>27</sup>

Consequently, even if increase in fatty acid oxidation after ischemia returns the heart to the natural metabolic state, if not properly managed, it might cause issues with longer-term cardiac health.<sup>28</sup>

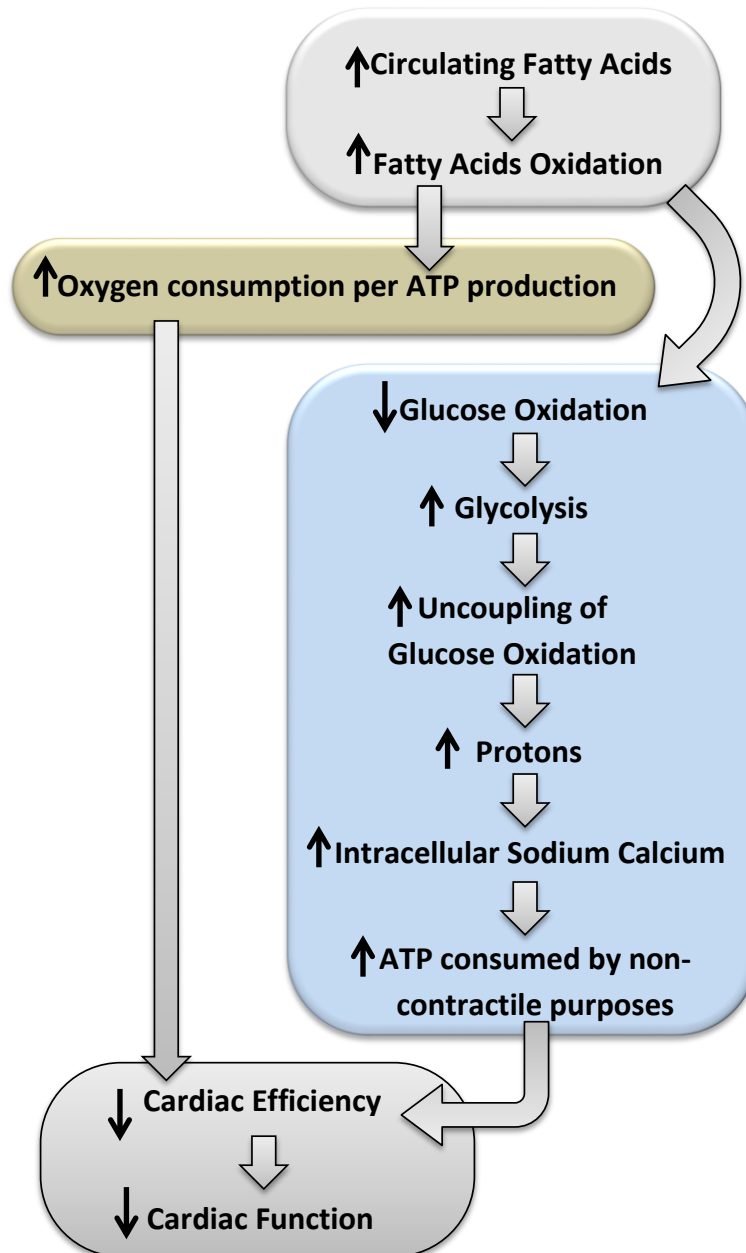


Figure 6: Myocardial substrate metabolism in pathologic state (ischemic/reperfusion)

### 1.5 What is difference between fatty acids and thia-fatty acids?

Fatty acid oxidation (FAO) plays a vital role for all living organisms. It is implicated in the production and storage of energy, integrated in the generation of all types of cell membranes and the regulation of cellular signalling pathways. Therefore, any disorder of FAO connected to various disease states such as cardiology,

endocrinology, neurology, and oncology.<sup>29</sup> The most problematic of these disorders is myocardial FAO.<sup>4</sup>

Recently, it has been found that fatty acid structural modification can be used to modulate crucial steps in fatty acid oxidation compared with the natural compound. This modification in fatty acid has a possibility to be useful both as a therapeutic and as diagnostic.<sup>30-32</sup>

Thia-fatty acids are fatty acids which are modified by insertion of a sulfur atom at specific positions in the carbon backbone, they have been found to potentially be of use as diagnostics in FAO. The chemical properties of thia-fatty acid are similar to a fatty acid, but, there are some important differences such as thia-fatty acid is more acidic and polar than identical fatty acid due to the increased electronegativity of the sulfur atom.<sup>33</sup> The metabolism of a thia-fatty acid is different from corresponding fatty acid, and this property can be exploited(see Figure 7).<sup>34</sup>

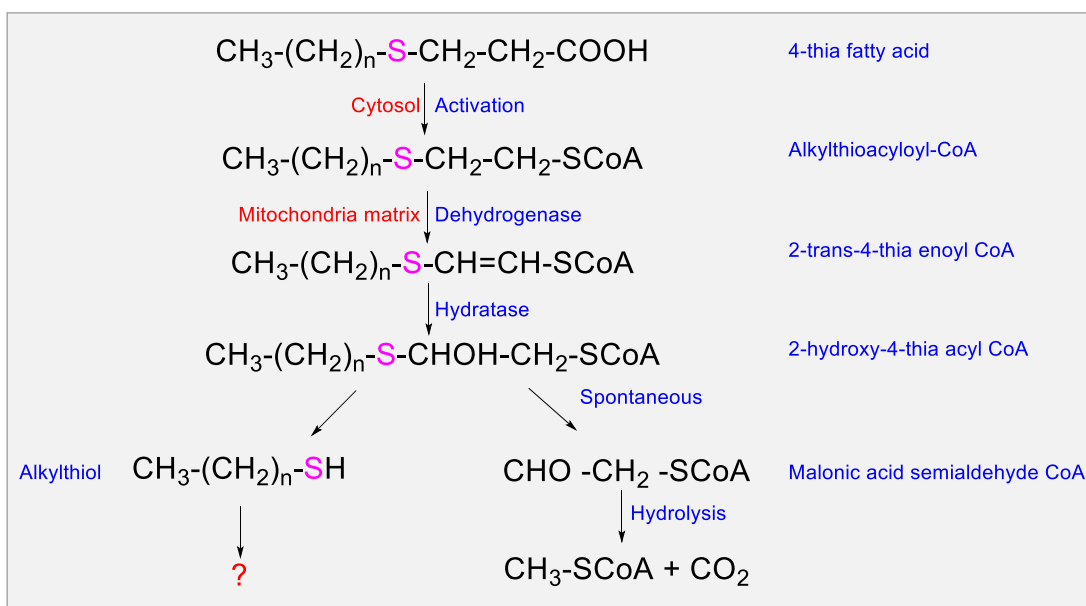


Figure 7: Schematic of metabolism of 4-thia fatty acid in mitochondria

The long chain 4-thia-fatty acid is activated in the cytosol in a similar mechanism the long-chain fatty acid, see Figure 3.<sup>34, 35</sup> After that, the majority of 4-thia-fatty acids are oxidised in  $\beta$ -oxidation in the mitochondria to alkylthioacyl-CoA ester which are poor substrates for mitochondrial hydratase.<sup>36</sup> They therefore accumulate and

slowly hydrolyse to 2-hydroxy-4-thiaacyl-CoA which transformed spontaneously to (1) alkylthiol, which has an unknown metabolic fate in the mitochondrial matrix,<sup>34, 37</sup> and (2) malonic acid semialdehyde- CoA ester, which is hydrolysed and metabolised to acyl-CoA and CO<sub>2</sub>.<sup>38</sup> 4-Thia fatty acid is of interest in the work reported here, due to its ability to become metabolically trapped in the mitochondria, which gives it suitable properties in radiotracer design for myocardial fatty acid oxidation.

## 1.6 Medical imaging

Molecular imaging is a type of medical imaging can be defined as the *in vivo* visualisation, characterisation and quantification of biological or biochemical pathways at the molecular level. The tools of molecular imaging allow imaging of complex physiological processes in health and disease states in living subjects without altering the system under investigation. In other words, molecular imaging allows visualisation of how the body is functioning and measurement of its chemical and biological processes.<sup>39, 40</sup>

Medical imaging modalities can be generally divided in two major categories: structural imaging and functional imaging. The structural and anatomical information of normal or pathological processes can be produced from imaging modalities, such as (CT), ultrasound (US) and (MRI). On the other hand, the functional imaging, which allows the visualisation and characterisation of biochemical pathways *in vivo*, requires imaging techniques such as PET, SPECT and optical imaging (OI) (e.g. bioluminescence and fluorescence) (see Figure 8).<sup>41</sup>

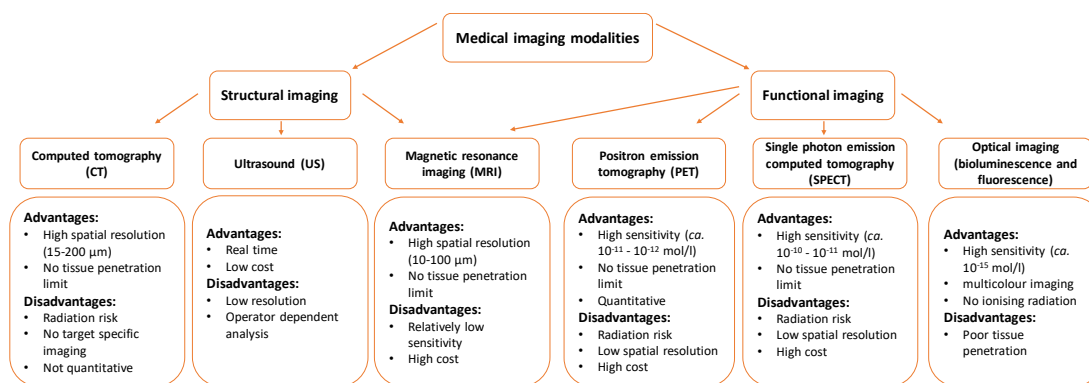


Figure 8: Classification of medical imaging modalities<sup>40</sup>

Each imaging modality has its own intrinsic advantages and disadvantages. Recently there has been a growing trend for the combinations of multiple imaging modalities; known as multimodality imaging. This allows the advantageous properties of multiple imaging techniques to be paired together affording more powerful diagnostics tools.<sup>42, 43</sup>

PET and SPECT are nuclear imaging techniques that are clinically used for diagnosis and developing therapeutic strategies in several diseases, such as cancer, cardiology and neurology fields.<sup>40</sup>

### 1.6.1 Nuclear molecular imaging

Nuclear imaging can be defined as a medical speciality that uses radiolabeled molecules (tracers) called radiopharmaceuticals that produce signals using radioactive decay for diagnosis and/or therapy of several diseases. Radiopharmaceuticals are compounds containing a radioisotope, which are used to either observe or change the biological system. When the compounds are used as imaging agents, they are used in tiny quantities and therefore have no pharmacological effects with the majority of radiopharmaceuticals administered *via* intravenous injection. A radiopharmaceutical can be a small organic molecule such as [<sup>18</sup>F]FDG, inorganic salts such as Na<sup>131</sup>I and Na<sup>18</sup>F, organometallic complexes such as <sup>99m</sup>Tc sestamibi, large molecules such as radiolabeled antibody fragments or an inhibitors of an enzyme.<sup>44-47</sup>

To serve as a radiolabel for diagnostic medicine, a radioisotope must meet certain conditions such as:

1. Commercial availability for use in a radiopharmacy (i.e. there is an established supply chain for production/delivery of the isotope or a generator to produce it)
2. Possess a physical half-life compatible with the synthesis and scanning requirements (this should be long enough to allow synthesis, purification and delivery of the tracer).
3. Emit radiation energetic enough to escape the body, but of low enough energy to be stopped by detectors.<sup>48</sup>

These conditions eliminate alpha and beta emitting radionuclides, thus, radioisotopes used in nuclear molecular imaging are either gamma ( $\gamma$ ) or positron ( $\beta^+$ ) emitters.

### 1.6.2 What nuclear imaging techniques could bring to cardiology?

A relationship between changes in myocardial metabolism and cardiac health has been shown, but there are still a lot of unanswered questions. For example, what are the key factors for myocardial substrate switch? Is the dominance of one metabolic pathway over another of predictive significance? Are the alterations in myocardial metabolism specific to different types of heart diseases? Therefore, new tools and strategies are needed for better understanding of cardiac pathologies.

PET and SPECT are the most notable techniques, which could be used to monitor metabolic changes in the cardiac disease *in vivo*. Radiotracers capable of revealing and quantifying metabolic switch would help to link different metabolic states to different heart diseases/states and, in this way, could contribute to the development of new and more scientific application of the available therapies.<sup>2,9</sup>

### 1.6.3 Single photon emission computed tomography (SPECT) imaging

A SPECT scan is a type of nuclear imaging technique, which depends on the radioactive decay of a radioisotope to form gamma rays (see Figure 9). These rays are emitted as single photons, which travels through tissues and can be detected on the position-sensitive detector of a gamma camera and an image of the localised radioactivity is produced. The position detection of the photons in SPECT does not carry enough information about its origin or the direction it was travelling, making the determination of a photon line of response impossible. To tackle this problem, a lead collimator between the source and the detector was added to determine the direction of the travelling photon.

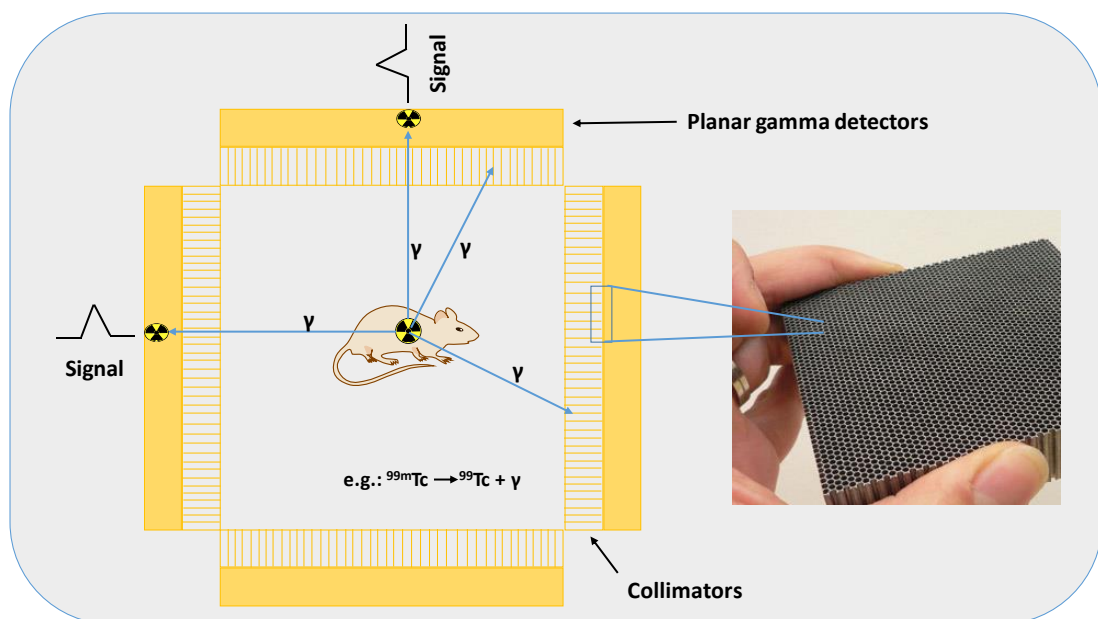


Figure 9: Principles of single photon emission computed tomography (SPECT)

The patient is surrounded by scintillation planar detectors with collimators which only allow detection of  $\gamma$ -rays falling normally onto the detectors blocks (see Figure 9). The collimator works as a filter rejecting most of the photons that are not travelling along the defined directions. In clinical systems, the collimator typically has parallel holes, producing no magnification; however, in pre-clinical systems the collimator has pinholes because of small animal imaging needs higher spatial



resolution. Spatial resolution can be increased by decreasing angle of collimation but sensitivity will be compromised by decreasing the angle. Thus, improving the design of the collimator leads to improvements in both sensitivity and resolution.<sup>49, 50</sup> The images obtained are usually two-dimensional cross-section slices of the image body, which later can be assembled into a three-dimensional image.<sup>51</sup>

SPECT scanners are widely found in hospitals around the world with a lot of the infrastructure already in place, making it cheaper to access than PET. However, limited spatial resolution does not always allow for accurate location of the abnormal tissue, to solve this problem SPECT is usually combined with CT to provide both structural and functional information.<sup>43</sup>

The majority of radioisotopes used in SPECT (<sup>123</sup>I, <sup>111</sup>In, <sup>67</sup>Ga and <sup>99m</sup>Tc) (see Table 1) decay by gamma emission *via* the electron capture mechanism (EC) or isomer transfer (IT). These nuclei contain too many protons but are unable to emit a positron and instead capture an electron and decompose by emitting a gamma ray.

Radionuclide	Half-life	Energy (keV)	Mode of decay	Method of production
<sup>99m</sup> Tc	6.02 h	149	IT	<sup>99</sup> Mo/ <sup>99m</sup> Tc generator
<sup>123</sup> I	13.22 h	159	EC	Cyclotron
<sup>111</sup> In	2.80 d	171, 245	EC	Cyclotron
<sup>67</sup> Ga	3.26 d	93, 185, 300, 394	EC	Cyclotron

Table 1: Common SPECT radioisotopes, decay characteristics and methods of production<sup>28, 51, 52</sup>

### 1.6.3.1 Radiochemistry of technetium

#### 1.6.3.1.1 Technetium

In 1869, technetium was predicted by Mendeleev and isolated, in 1937, by Segré and Perrier.<sup>53</sup> There are twenty-two isotopes of Tc and ten of them are man-made, elements  $^{88}\text{Tc}$  to  $^{113}\text{Tc}$  have been reported, and all of them are radioactive. The most common of these is technetium-99 which produced from the metastable state technetium-99m.<sup>53</sup>

Technetium-99m is the most isotope commonly used in diagnostic nuclear medicine. The main reasons for this are:<sup>54, 55</sup>

1. The half-life of 6.02 h is optimal for diagnosis because it is long enough to allow the radiopharmaceutical preparation, quality control, administration to the target (animal or patient), image acquisition and examine metabolic processes and is sufficiently short to induce low doses of radiation to the target.
2. The  $\gamma$  radiation emission (140 keV), is sufficiently low to prevent a high dose to the patient but sufficiently high to penetrate biological tissues and emerge from internal organs.
3. One of the greatest advantage of  $^{99\text{m}}\text{Tc}$  is availability from a cheap commercial source,  $^{99}\text{Mo}/^{99\text{m}}\text{Tc}$  generators (although there are ongoing concerns about the future supply chain of  $^{99}\text{Mo}$ )
4. The coordination chemistry of  $^{99\text{m}}\text{Tc}$  is varied. Thus, the synthesis of a wide variety of complexes with different physiochemical and biological properties is possible.

#### 1.6.3.1.2 Technetium-99m production and reduction

Sterile  $^{99\text{m}}\text{Tc}$  can produced in a closed system  $^{99}\text{Mo}/^{99\text{m}}\text{Tc}$  generator (e.g. Ultra-TechneKow™ DTE Generator, shown in Figure 10 which is prepared with fission-produced  $^{99}\text{Mo}$  adsorbed onto alumina column shielded by lead, tungsten, or depleted uranium. Sterile, non-pyrogenic isotonic solutions of sodium pertechnetate

( $\text{Na}^{99\text{m}}\text{TcO}_4$ ) in 0.9% sodium chloride (NaCl) solution can be obtained conveniently by periodic aseptic elution of the generator. These solutions should be clear, colourless, and free of visible foreign material.  $[\text{}^{99\text{m}}\text{TcO}_4]^-$  is a radiopharmaceutical in itself, and it may be used to radiolabel all other potential radiolabeling precursors *via* oxidation processes.<sup>45, 56</sup>

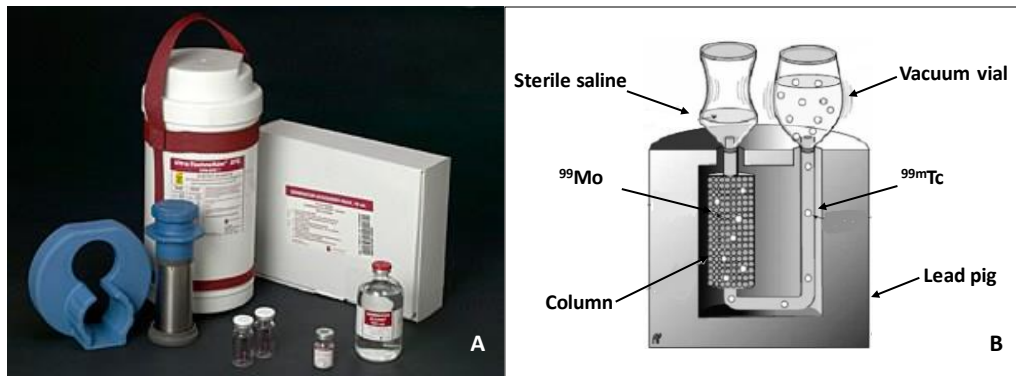


Figure 10: A.  $^{99}\text{Mo}/^{99\text{m}}\text{Tc}$  generator from Ultra-TechneKow™ DTE Generator. B. Illustration of the contents of  $^{99}\text{Mo}/^{99\text{m}}\text{Tc}$  generator

In  $^{99}\text{Mo}/^{99\text{m}}\text{Tc}$  generator  $^{99}\text{Mo}$  (half-life  $t_{1/2} = 66$  h) decays to  $^{99\text{m}}\text{Tc}$  by  $\beta^-$  decay (88.75%).  $^{99\text{m}}\text{Tc}$  is a nuclear isomer of  $^{99}\text{Tc}$  present in a metastable state, which decays to  $^{99}\text{Tc}$  by emitting a  $\gamma$  ray (11.25%) with an energy of 140 keV (see Figure 11). After that,  $^{99}\text{Tc}$  decays to  $^{99}\text{Ru}$  by  $\beta^-$  decay. The  $\gamma$  emission can be detected using a SPECT camera as discussed.<sup>53</sup>

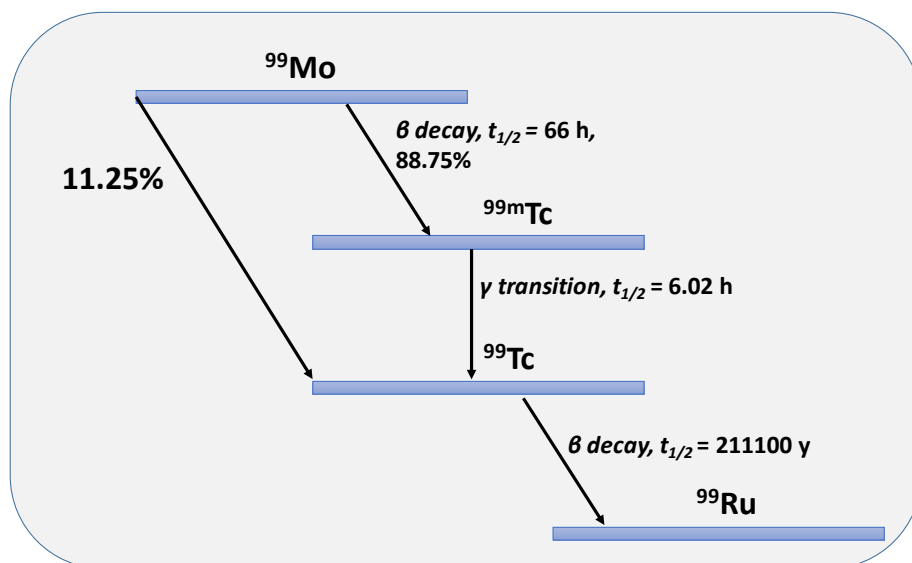


Figure 11: Decay scheme of  $^{99}\text{Mo}$  to  $^{99}\text{Ru}$

### 1.6.3.1.3 Coordination chemistry of technetium-99m

The design of  $^{99m}\text{Tc}$ -radiopharmaceuticals relies on the understanding of the coordination chemistry of  $^{99m}\text{Tc}$ . Many factors such as stable oxidation states and core structures are important in the design of effectively targeted  $^{99m}\text{Tc}$ -radiopharmaceuticals. Technetium has several different possible oxidation states (-I to +VII) and several coordination geometries that it can adopt. Therefore, the chemistry exhibited by technetium is diverse.

Technetium-99m was eluted from the generator as the  $[\text{}^{99m}\text{TcO}_4]^-$  anion in the highest oxidation state (VII). Although,  $^{99m}\text{Tc(VII)}$  is the most stable form in aqueous solution but does not bind directly to any ligand as it is an oxo-species. Thus,  $^{99m}\text{Tc(VII)}$  can be reduced to a lower oxidation state such as (V) or (I) in the presence of a suitable chelator to synthesise a  $^{99m}\text{Tc}$ -radiopharmaceutical.<sup>53</sup>

On reduction of  $^{99m}\text{Tc(VII)}$  in the presence of a suitable ligand, the  $[\text{}^{99m}\text{TcO}_4]^-$  does not always release all of the oxygen atoms, leading to complexes with different  $^{99m}\text{Tc}$  oxo species such as  $[\text{}^{99m}\text{TcO}]^{3+}$  or  $[\text{}^{99m}\text{TcO}_2]^+$ .<sup>55</sup> The  $[\text{}^{99m}\text{TcO}]^{3+}$  core has been extensively explored, and further advances are possible when other lower oxidation states are more comprehensively studied. One of the most promising and well developed organometallic cores for radiolabeling of biomolecules (BMs) for example, antibodies, peptides and fatty acids is the  $^{99m}\text{Tc(I)}$ - and  $\text{Re(I)}$ -tricarbonyl core  $[\text{M}(\text{H}_2\text{O})_3(\text{CO})_3]^+$  ( $\text{M} = ^{99m}\text{Tc}/^{188}\text{Re}$ ). The  $[\text{M}(\text{H}_2\text{O})_3(\text{CO})_3]^+$  core was reported for the first time by Alberto *et al.* as a useful precursor for the radiolabeling of BMs for diagnostic purposes.<sup>57</sup> The organometallic precursor  $[\text{}^{99m}\text{Tc}(\text{H}_2\text{O})_3(\text{CO})_3]^+$  was synthesised in one step by direct reduction of the  $[\text{}^{99m}\text{TcO}_4]^-$  from the oxidation state VII to I by using sodium boranocarbonate ( $\text{Na}_2[\text{H}_3\text{BCO}_2]$ ) as a reducing agent<sup>58</sup>, and has since been made commercially available in a lyophilised kit (IsoLink<sup>®</sup> kit, Mallinckrodt-Covidien, Petten, The Netherlands).<sup>53, 59</sup>

The organometallic core  $[\text{M}(\text{H}_2\text{O})_3(\text{CO})_3]^+$  ( $\text{M} = ^{99m}\text{Tc}/^{188}\text{Re}$ ) is stable, even at high temperature.<sup>60</sup> Complexes of  $[\text{M}(\text{H}_2\text{O})_3(\text{CO})_3]^+$  are kinetically inert due to the metal centre being in the low oxidation state and it forms  $d^6$  low-spin electron

configuration, octahedral complexes. The core  $[M(H_2O)_3(CO)_3]^+$  contains three tightly coordinated carbonyl ligands and three water molecules, which are very labile and can be readily replaced by mono-, bi- or tridentate chelators. Tridentate chelators can form  $^{99m}\text{Tc(I)}$ -tricarbonyl complexes to give high *in vivo* stability, which is essential for medical applications.<sup>52, 61</sup>

#### 1.6.3.1.4 Design of technetium-99m labeled biomolecules

There are two general classes of  $^{99m}\text{Tc}$  radiolabeling methods for the synthesis of labeled biomolecule targeted radiopharmaceuticals, the direct and indirect methods. The method selected depends on the biomolecules to be labeled.<sup>45, 52</sup> The direct radiolabeling method depends on the binding of  $^{99m}\text{Tc}$  to endogenous free sulfhydryl groups, generated by reduction of disulfide bonds in a protein or antibody to provide the binding sites (see Figure 12). It is only applicable if the molecule has disulfide bonds. The main advantage of this method is that it is easy to carry out, but the major disadvantage is that it requires a large amount of reducing agent; if too many disulfide bonds are reduced then the protein properties will be affected.<sup>62</sup>

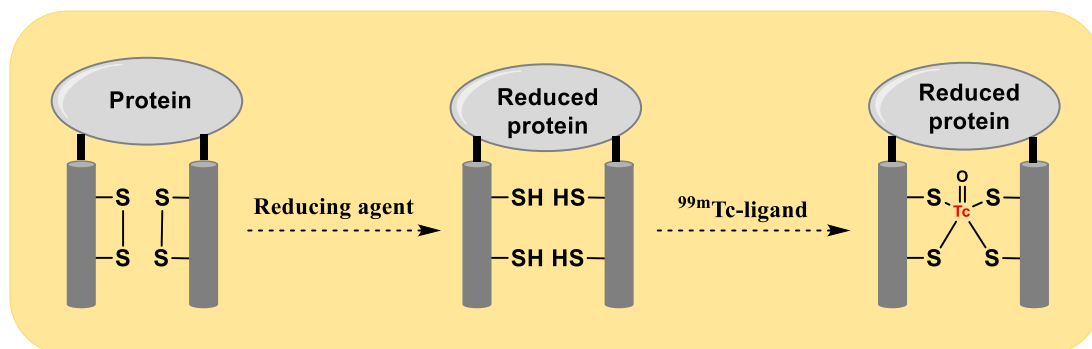


Figure 12: Radiolabeling of BMs containing endogenous sulfhydryl groups by the direct method

Indirect method radiolabeling methods are more generally applicable and are based on the incorporation of a bifunctional chelator (BFC). This method is the most popular strategy applied in the design of targeted radiopharmaceuticals, due to the higher probability of retaining the binding affinity of the biomolecule to its target with a careful selection of the BFC for radiolabeling. In addition, it can be applied to any biomolecule (antibody or a smaller molecule without sulfhydryl groups).<sup>53</sup>

A bifunctional chelator (BFC) consists three parts: a chelator framework, a linker and a functional group for the covalent attachment to the biomolecule.<sup>63</sup> There are a wide range of requirements for a BFC.<sup>44</sup> It should form a stable metal chelate complex with the required metal ion and it should coordinate to the radionuclide in a high yield with both high thermodynamic stability and kinetic inertness at neutral pH. These physicochemical properties are important because they reflect the rate of dissociation of metal ion from the BFC. Loss of the radiometal would cause undesirable side effects by accumulating in non-target organs increasing the background signal in the scans.<sup>63</sup> Selection of the correct BFC is dependent on the identity and oxidation state of a radioisotope and others specific factors, such as pH, temperature, reaction time, may be required for the radiolabeling reaction.<sup>64</sup>

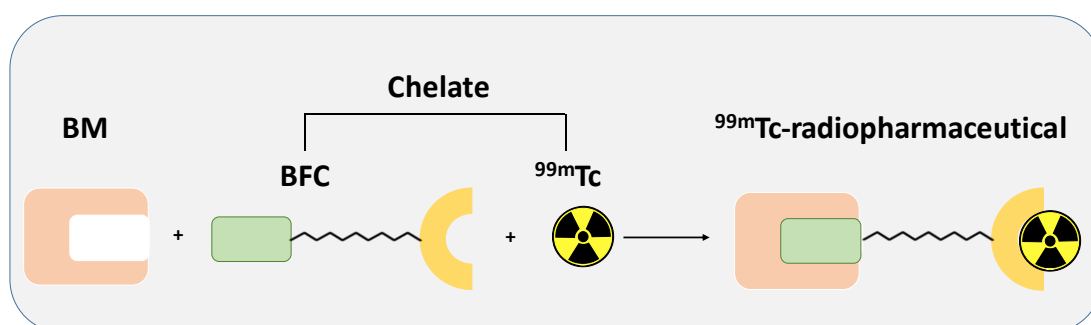


Figure 13: Schematic representation of the BFC approach

1,4,7-Triazacyclononane (TACN) and its derivatives are macrocycles with three nitrogen donor atoms which have applications as catalysts, bleaching agents, and chelators for medical imaging. Bifunctional chelators based on TACN meet many of the requirements with respect to chelation of <sup>99m</sup>Tc with high stability and fast chelation. TACN allows for facile modification to provide the functional group which is used to form covalent bond with the biomolecule (BM) *via* the linker.<sup>54</sup>

### 1.6.3.2 Single-photon emission computed tomography (SPECT) applied to cardiac metabolic imaging and blood flow

SPECT is used to provide an independent assessment of myocardial perfusion and viability either in resting state or after a dynamic exercise or pharmacologically induced stress. As SPECT radioisotopes are generally characterized by longer half-

lives (hrs-days) compared to PET radioisotopes, this technique is well suited for imaging during extended periods of time. However, because of the method of detection of single photons, sensitivity and resolution are not optimal.<sup>10, 65</sup> There are no specific SPECT radiotracers for measuring myocardial glucose metabolism. However, it can be examined using the PET radioisotope [<sup>18</sup>F]FDG.<sup>9</sup>

### 1.6.3.2.1 SPECT tracers for assessing myocardial fatty acid metabolism

The first SPECT tracer targeted to myocardial fatty acids metabolism was 15-(*p*-iodophenyl)pentadecanoic acid ([<sup>123</sup>I]IPPA) (see Figure 14). It worked because it was rapidly taken up in the myocardium and trapped there for a long time. However, it was not cleared fast enough to take advantage of the rapid uptake of [<sup>123</sup>I]IPPA. As a result, quantitative measurement of myocardial fatty acid metabolism was impossible, and the quality of the image was poor.<sup>66</sup> To counter pharmacokinetic problems, the branched chain analogue of [<sup>123</sup>I]IPPA, which did not suffer from extensive  $\beta$ -degradation, was developed. [<sup>123</sup>I]- $\beta$ -methyl-*p*-iodophenylpentadecanoic acid (<sup>123</sup>I-BMIPP) offered an increased cardiac retention leading to improved image quality. However, [<sup>123</sup>I]BMIPP did not find wide application in the clinic, because its uptake is subject to myocardial ischemia which reduces its uptake due to the metabolic switch from fatty acids to glucose.<sup>2, 66, 67</sup>

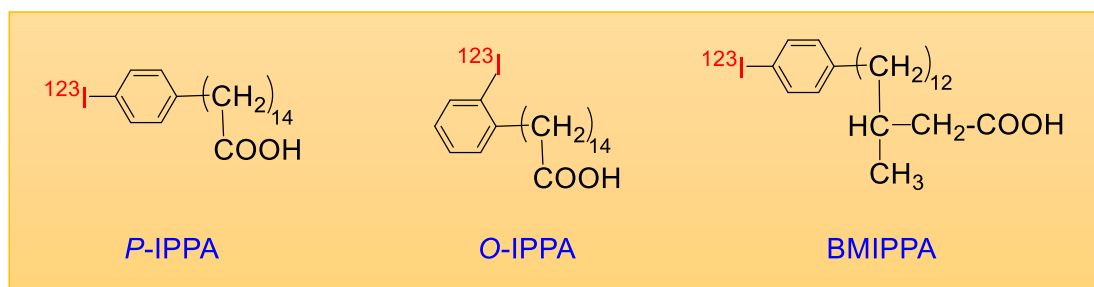


Figure 14: Chemical structures of [<sup>123</sup>I] radiolabeled fatty acid analogues. (*P*-IPPA) 15-(*p*-[<sup>123</sup>I]-iodophenyl)pentadecanoic acid. (*O*-IPPA) 15-(*o*-[<sup>123</sup>I]-iodophenyl)pentadecanoic acid. (BMIPP) [<sup>123</sup>I]- $\beta$ -methyl-*p*-iodophenylpentadecanoic acid

### 1.6.3.2.2 SPECT tracers used to measure blood flow

<sup>99m</sup>Tc-sestamibi and <sup>99m</sup>Tc-tetrofosmin were demonstrated as useful myocardial perfusion agents (see Figure 15) which are widely used. Generally, these tracers can

be classified as cationic tracers.<sup>54</sup> After intravenous administration, <sup>99m</sup>Tc-sestamibi shows cardiac uptake in proportion to regional mitochondrial membrane potentials in the heart muscle. Then, it clears rapidly from the blood with a fast initial/internal component with half-time of 4.3 min. <sup>99m</sup>Tc-tetrofosmin is rapidly taken up by myocardial tissue and reaches its maximum level in approximately 5 minutes.<sup>68</sup>

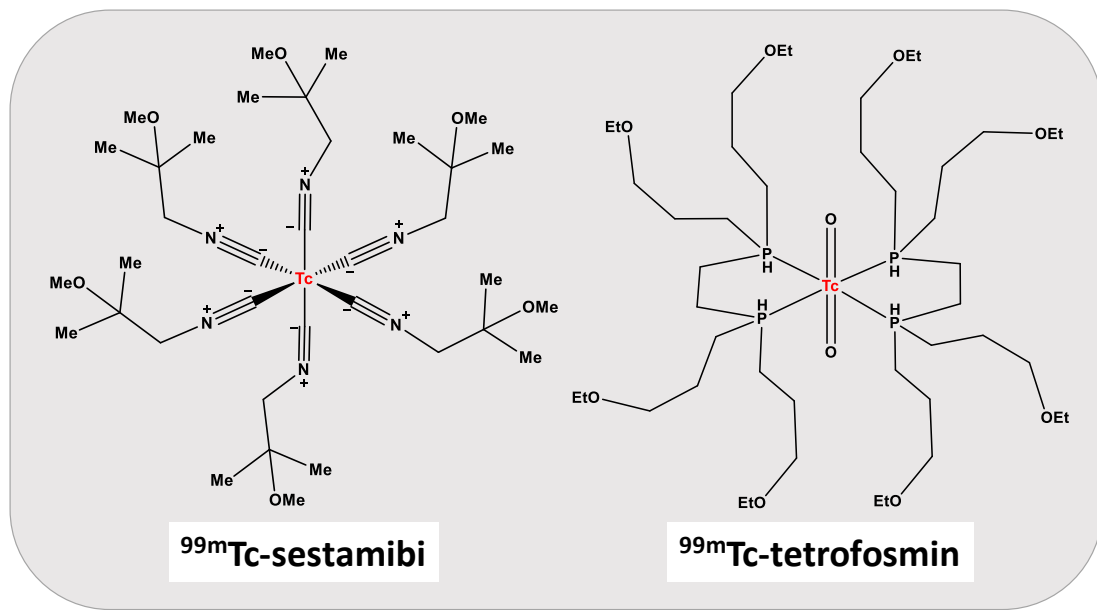


Figure 15: Chemical structure of <sup>99m</sup>Tc-sestamibi and <sup>99m</sup>Tc-tetrofosmin

### 1.6.3.2.3 SPECT tracers used to assess fatty acid metabolism

Techetium-99m labeled fatty acids have been designed and evaluated with different <sup>99m</sup>Tc cores such as *fac*-[<sup>99m</sup>Tc(CO)<sub>3</sub>(H<sub>2</sub>O)<sub>3</sub>]<sup>+</sup>, with *fac*-[<sup>99m</sup>Tc(O)MAMA] and *fac*-[<sup>99m</sup>Tc(N)(PNP)]<sup>2+</sup>. It has not yet been established whether these analogues are recognized and metabolized in the heart *via* beta-oxidation despite a number of *in vivo* studies. It was clearly shown that despite high initial accumulation in the heart, the radioactivity cleared rapidly and requires further optimisation for cardiac imaging.<sup>69-79</sup>



## 1.6.4 Positron emission tomography (PET) imaging

The radioisotopes used in PET decay by emitting a positron ( $\beta^+$ ). The emitted  $\beta^+$  travels a short distance (1-5 mm), gradually losing its kinetic energy until it slows down to the point where it annihilates with an electron. The mass of the positron and electron are converted into their energy equivalent ( $E = mc^2$ ) through the emission of two 511 keV gamma photons that are emitted in almost opposite directions. This energy is detected in coincidence by a gamma camera ring when they strike opposing detectors simultaneously (see Figure 16).<sup>80</sup>

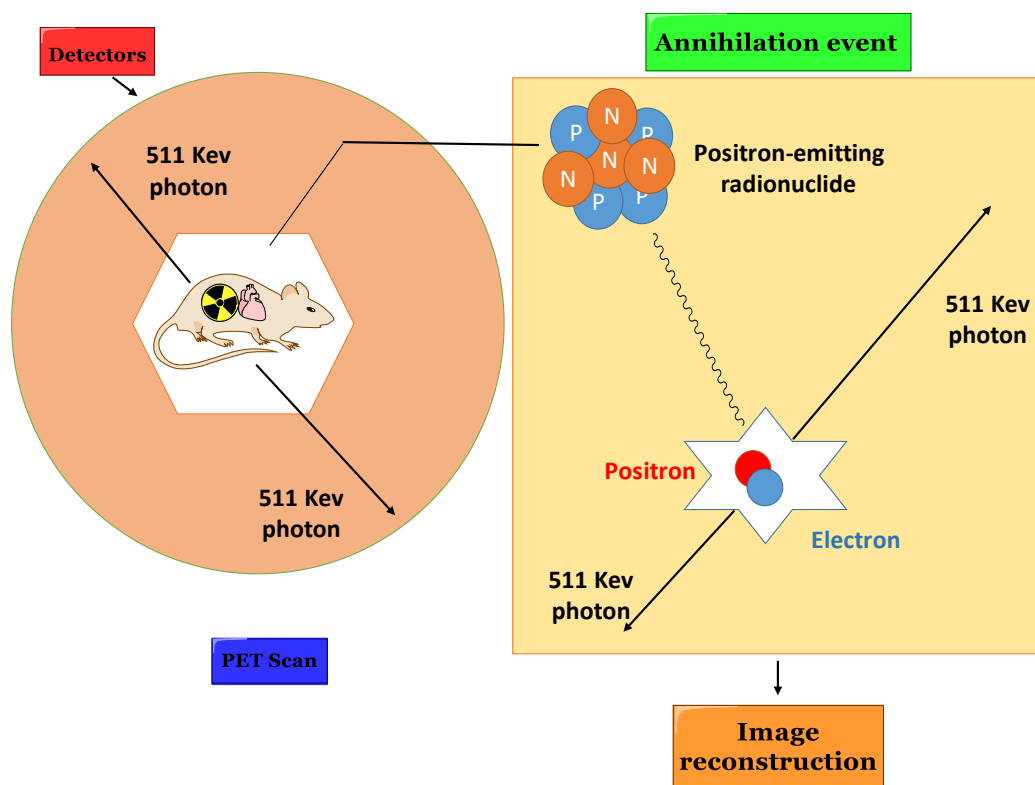


Figure 16: Principle of positron emission tomography (PET)

PET has several intrinsic advantages over SPECT: firstly, it offers greater sensitivity over single photon counting technique, which requires physical (lead or tungsten) collimation. Electronic collimation is applied in PET by dual photon coincidence counting. Secondly, positron emitting radioisotopes that can be exploited include oxygen-15, carbon-11, nitrogen-13 and fluorine-18 (see Table 2). All of these are organic radioisotopes and therefore biologically relevant. Labeled versions of

metabolic substrates can be synthesised, for example, [ $^{11}\text{C}$ ]glucose, [ $^{13}\text{N}$ ]NH<sub>3</sub>, [ $^{15}\text{O}$ ]H<sub>2</sub>O and [ $^{15}\text{O}$ ]CO<sub>2</sub> without any change in the biological properties of the radiolabeled molecule.<sup>81-83</sup>

Radionuclide	Half-life	Average $\beta^+$ Energy (keV)	Mode of decay	Method of production
$^{15}\text{O}$	2.03 min	1732	$\beta^+$	Cyclotron
$^{18}\text{F}$	109.8 min	633	$\beta^+$ EC	Cyclotron
$^{13}\text{N}$	9.97 min	1198	$\beta^+$	Cyclotron
$^{11}\text{C}$	20.4 min	960	$\beta^+$	Cyclotron
$^{68}\text{Ga}$	67.6 min	1899	$\beta^+$ EC	$^{68}\text{Ge}/^{68}\text{Ga}$ generator

Table 2: Decay characteristics of common PET radionuclides<sup>10</sup>

Thirdly, their short physical half-lives help to minimise radiation dose to the subject. However, some of these radionuclides have such short physical half-lives that it prevents their incorporation into more complex molecules and limits their usefulness in the clinic due to the required proximity to the production site (i.e cyclotron). In contrast, most of SPECT radioisotopes have half-lives of hours to days.<sup>81, 84</sup>

To acquire the scan, a radiotracer is injected into the subject (patient or animal). Dependent on the tracer's pharmacokinetic properties, it will be distributed between the different organs. If the target (a particular receptor, metabolic process or condition) is present, it accumulates in this particular area, with fast clearance in non-targeted organs desirable. At the appropriate time, the subject is placed inside the scanner and an image is acquired. An array of gamma detectors counts annihilation gamma rays and the image of the tracer's biological distribution is generated. PET is highly sensitive and quantitative but does not provide anatomical data, therefore it is often carried out in combination with an anatomical imaging technique such MRI or CT which are fused with the PET images.<sup>85, 86</sup>

## 1.6.4.1 Radiochemistry of fluorine-18

### 1.6.4.1.1 Fluorine-18

Fluorine is a unique element in chemical properties and also in the applications it has in the pharmaceutical and chemical industries. Carbon-fluorine bond strength (bond-dissociation energy up to 450 kJ/mol) is higher than other carbon-halogen bonds (240-330 kJ/mol) and carbon-hydrogen bonds (410 kJ/mol) and it has a very small steric size. A typical carbon-fluorine bond length (1.35 Å) is shorter than other carbon-halogen (1.77-2.14 Å) and longer than carbon-hydrogen (1.09 Å) bonds. Substitution of fluorine for hydrogen can produce significant and useful changes in physicochemical and biological properties of organic compounds, for drug molecules this can affect the pharmaceutical properties of these derivatives. Fluorine is modestly more lipophilic than a hydrogen atom and significantly more lipophilic than OH, CO, CN, or sulfoxide and sulfone substituents. These properties confer fluorine with considerable versatility such that it has been explored as a potential bioisostere of the hydrogen atom, carbonyl and sulfonyl functionalities, the carbinol moiety, and the nitrile, with effective functional mimicry very much dependent upon the biochemical context.<sup>87-90</sup>

Fluorine-18 has almost ideal radiochemical and biochemical properties. Its reasonably long physical half-life (109:8 min) permits transportation off-site, use in synthesis and allows acquisition of images over several hours. It is a pure positron emitter (97%) with a relatively low energy (maximum 0.63 MeV), resulting in a short linear range in tissue. This permits acquisition of images with a particularly high resolution. It is also readily available from two sources: nuclear reactor and particle accelerators (it is mainly produced in medical cyclotrons for clinical use).

### 1.6.4.1.2 Production of fluorine-18

Almost all fluorine-18 is currently produced in high specific activity using a cyclotron from enriched water [ $^{18}\text{O}$ ]H<sub>2</sub>O, ( $^{18}\text{O}(\text{p},\text{n})^{18}\text{F}$ ), as [ $^{18}\text{F}$ ]fluoride which can be used in a range of fluorination reactions.<sup>2, 54, 91-93</sup>

#### 1.6.4.1.3 Methods for fluorination

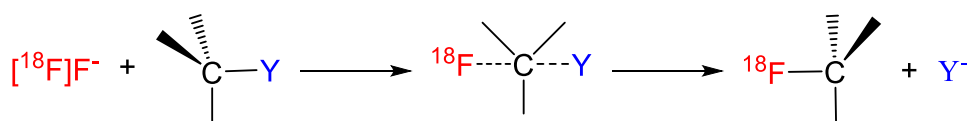
There are many chemical methods used to introduce the fluorine-18 isotope into target molecules. The main synthetic methods can be classified into two distinct areas: direct fluorination and indirect fluorination.

Direct fluorination, where the fluorine-18 isotope is introduced into target molecules in one-step directly. Indirect fluorination, which requires a multistep synthetic approach and the addition of fluorine-18 prosthetic groups. Prosthetic groups are small fluorine-18 labeled alkyl or aryl groups that also have a reactive functional group. They are designed to react with biological molecules which may be not stable enough for direct labelling with the fluorine-18 isotope.<sup>94</sup>

Direct fluorination can be subdivided into two main reaction types: nucleophilic substitution and electrophilic substitution. Nucleophilic substitution fluorine-18 labeling reactions are more routinely used than electrophilic substitution as they produce higher specific activity <sup>18</sup>F PET radiotracers (specific activity is defined as the amount of radioactivity per quantity of radiotracer (GBq/μmol)).

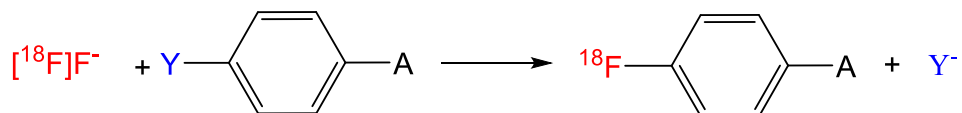
The fluoride ion [<sup>18</sup>F]F<sup>-</sup> from the target is trapped on an ion exchange column, then eluted from the column using base in water/acetonitrile solution. This purifies the radioisotope feedstock from contaminants and can allow recovery of the [<sup>18</sup>O]H<sub>2</sub>O if desired. Nucleophilic substitution reactions with fluoride can be subdivided into two general categories of chemical reaction: (1) Aliphatic nucleophilic substitution (S<sub>N</sub>2) and (2) Aromatic nucleophilic substitution (S<sub>N</sub>Ar) (see Figure 17). In S<sub>N</sub>2 reactions, the <sup>18</sup>F<sup>-</sup> attacks and binds to carbon atom of the precursor on the opposite side of the carbon to a leaving group, which is a weak base such as iodide, bromide and tosylate. In S<sub>N</sub>Ar reactions, the <sup>18</sup>F<sup>-</sup> is incorporated directly onto the aromatic ring of the molecule to be labeled with the leaving group such as iodide, nitrate and R<sub>3</sub>N, activated by the electron withdrawing groups in the *ortho* or *para* positions, such as CHO, CN, NO<sub>2</sub> or COOR.<sup>2</sup>

### Aliphatic Nucleophilic Substitution (S<sub>N</sub>2)



Y = Leaving group such as halide, tosylate, etc

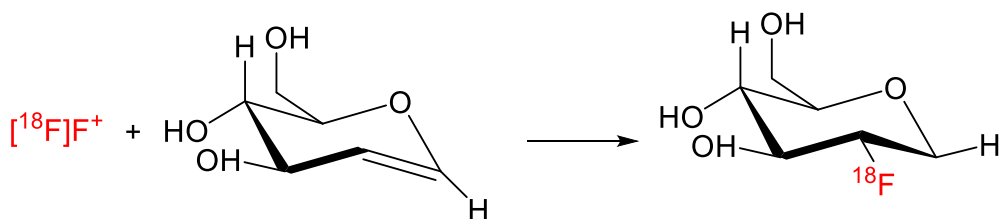
### Aromatic Nucleophilic Substitution (S<sub>N</sub>Ar)



Y = Leaving group such as halide, NO<sub>2</sub> or R<sub>3</sub>N

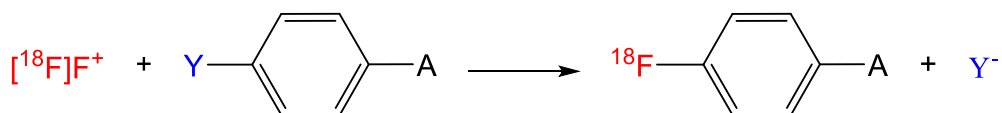
A = Electron withdrawing group such as CHO, COR, COOR, CN or NO<sub>2</sub>

### Aliphatic Electrophilic Fluorination



Aliphatic Electrophilic Fluorination using [<sup>18</sup>F]acetyl hypofluorite

### Aromatic Electrophilic Fluorination



Y = Leaving group such as H, SnR<sub>3</sub>, HgR or SiR<sub>3</sub>

A = Electron donating group such as OH, OCH<sub>3</sub>, NH<sub>2</sub>, CN or SR

Figure 17: Nucleophilic and electrophilic fluorination reactions

Electrophilic fluorine-18 labeling reactions have problems with specific activity as [<sup>18</sup>F]F<sub>2</sub> (or secondary compounds) are usually generated from <sup>18</sup>F with the addition of the stable fluorine-19 isotope. [<sup>18</sup>F]F<sub>2</sub> is highly reactive and so attempts have been made to decrease the reactivity of [<sup>18</sup>F]F<sub>2</sub> by conversion to a second reagent such as [<sup>18</sup>F]acetyl hypofluorite or xenon difluoride.<sup>10, 54, 95, 96</sup> Electrophilic reactions can be

subdivided into two general categories of chemical reaction (see Figure 17): (1) Aliphatic electrophilic fluorination and (2) Aromatic electrophilic fluorination. In an example of an aliphatic electrophilic fluorination reaction, the fluorine gas can be added to an alkene. This was the original method used to synthesise [ $^{18}\text{F}$ ]FDG. In aromatic electrophilic fluorination reaction [ $^{18}\text{F}$ ]F<sub>2</sub> or [ $^{18}\text{F}$ ]acetyl hypofluorite can be added to solutions of aromatic compounds resulting in addition/elimination reactions to produce [ $^{18}\text{F}$ ]aryl compounds.<sup>54</sup>

#### 1.6.4.2 Positron emission tomography (PET) applied to cardiac metabolic imaging

Cyclotron produced PET radioactive isotopes are short-lived (min-hrs), thus, this technique is well suited for a studying rapid biochemical processes (see Figure 18). High sensitivity and resolution, together with an accurate quantification, makes PET ideal for myocardial substrate metabolism (sugar or fatty acid) and storage (myocardial uptake) studies *in vivo*. With a suitable tracer, PET can be used to quantify the myocardial blood flow (MBF) and oxygen consumption, parameters that might be relevant and of interest in different clinical situations.<sup>97-99</sup> The downside of PET technology is the high cost of the infrastructure associated with radiotracer production, synthesis and validation, along with the dose of ionising radiation that is delivered to the patient during the scan.<sup>9</sup> However, the unique quality of the data that can be provided by PET scanning justifies this cost and risk in many cases.

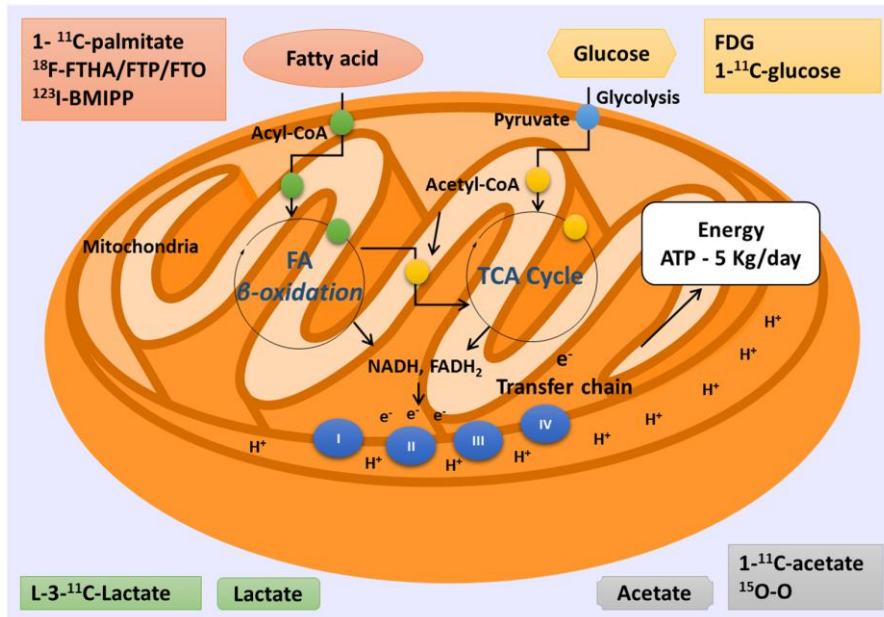


Figure 18: Cardiomyocyte substrate metabolism. [<sup>18</sup>F]FHTA - [<sup>18</sup>F]-18-fluoro-6-thiaheptadecanoic acid, [<sup>18</sup>F]FTP - [<sup>18</sup>F]-16-fluoro-4-thiapalmitic acid, [<sup>18</sup>F]FTO - [<sup>18</sup>F]-18-fluoro-4-thioleic acid, [<sup>123</sup>I]BMIPP - beta-methyl-*p*-[<sup>123</sup>I]-iodophenyl-pentadecanoic acid, [<sup>18</sup>F]FDG - fluorodeoxyglucose

### 1.6.4.3 PET tracers used to assess glucose metabolism

#### 1.6.4.3.1 [<sup>18</sup>F]-Fluorodeoxyglucose ([<sup>18</sup>F]FDG)

[<sup>18</sup>F]FDG is a fluorinated glucose analogue that can be used to quantify the myocardial glucose metabolism. Similar to glucose, it is up taken in cells *via* glucose transporters, but then gets trapped in the cytosol in [<sup>18</sup>F]-FDG-6-phosphate form. It is assumed that myocardial uptake of [<sup>18</sup>F]-FDG reflects the overall anaerobic and aerobic myocardial glycolytic flux. Due to [<sup>18</sup>F]-FDG-6-phosphate can no longer be transformed, [<sup>18</sup>F]FDG cannot be used to study further steps of glucose metabolism.<sup>100</sup>

#### 1.6.4.3.2 [<sup>11</sup>C]Glucose

Myocardial glucose metabolism can be quantified by [<sup>11</sup>C]glucose, which is identical to natural glucose with the 1-carbon atom replaced by the radioactive <sup>11</sup>C isotope. [<sup>11</sup>C]glucose has different applications to [<sup>18</sup>F]FDG, particularly in cardiac imaging, because it can be fully metabolised and provide information concerning its metabolic fate.<sup>23</sup> The main shortcomings of [<sup>11</sup>C]glucose are the short radiochemical half-life

(20 min) and complex synthesis, thus, both, radiolabel and tracer itself need to be produced in proximity to the patient.<sup>24</sup>

#### 1.6.4.3.3 [<sup>11</sup>C]Lactate

Lactate is one of the heart energy sources in particular during an intensity exercise. Herrero *et al.* developed a compartmental model for non-invasive measurements of myocardial lactate use and oxidation using [<sup>11</sup>C]-lactate, which suffers from similar problems as [<sup>11</sup>C]glucose.<sup>101</sup> The options for quantitative measurement of myocardial lactate metabolism are limited because of the lack of better radiotracers.<sup>9</sup>

#### 1.6.4.4 PET tracers used to measure blood flow

##### 1.6.4.4.1 [<sup>15</sup>O]Water

Myocardial perfusion images obtained with [<sup>15</sup>O]water are of high quality because it is metabolically inert and can diffuse across cell membranes resulting in an excellent first-pass extraction fraction. However, the short physical half-life of [<sup>15</sup>O]water (2 min) could demand multiple flow measurement at short intervals.<sup>102</sup>

##### 1.6.4.4.2 [<sup>13</sup>N]NH<sub>3</sub>

[<sup>13</sup>N]NH<sub>3</sub> is a more practical perfusion tracer.<sup>103, 104</sup> It has a longer physical half-life (9:8 min) compared to [<sup>15</sup>O]water, which leads to preferential distribution and prolonged retention in the myocardium and ultimately to better quality images. However, quantification using [<sup>13</sup>N]NH<sub>3</sub> is poor because its myocardial uptake depends not only on perfusion but also on integrity of cellular membranes, myocardial cells viability and metabolic conditions.<sup>105</sup>

##### 1.6.4.4.3 [<sup>82</sup>Rb]RbCl

The very short physical half-life of <sup>82</sup>Rb (76 s), together with acquisition times of 25-30 min, minimizes the patient's radiation exposure from cardiac imaging.<sup>106</sup> [<sup>82</sup>Rb]RbCl has the lowest myocardial extraction fraction when compared with other PET perfusion tracers. Moreover, it is extracted in a nonlinear fashion which, at higher flow, results in underestimation myocardial perfusion. Because of short



physical half-life and high activities injected, oversaturation might occur at the beginning of the acquisition.<sup>107</sup>

#### 1.6.4.5 PET tracers used to measure oxygen consumption

##### 1.6.4.5.1 [<sup>15</sup>O]Oxygen

[<sup>15</sup>O]oxygen has been used to estimate myocardial oxygen consumption (MVO<sub>2</sub>) based on the fact that oxygen is the final electron acceptor in all pathways of aerobic myocardial metabolism. In one PET scan, myocardial blood flow is measured, and the arterial oxygen content is assessed. Due to a very short radiochemical half-life (2 min), [<sup>15</sup>O]oxygen is suitable for studies requiring repetitive assessments, such as those assessing effects of acute pharmacological interventions. If measures of myocardial blood flow and blood volume are required, a second tracer usually is used adding complexity to data processing.<sup>27, 28</sup>

##### 1.6.4.5.2 [<sup>11</sup>C]Acetate

Acetic acid and acetate are direct substrates of tricarboxylic acid cycle there they are converted into acetyl-CoA. [<sup>11</sup>C]Acetate has been used to measure myocardial oxygen consumption. Obtained data was analysed using an exponential curve fitting or compartmental modelling. The exponential curve fitting method is easier to use and gives better results when cardiac output is low because the input function involves dispersion, whereas, compartmental modelling is more complex and requires correction of blood radioactivity for [<sup>11</sup>C]CO<sub>2</sub>.<sup>108</sup>

#### 1.6.4.6 PET tracers used to assess fatty acid metabolism

##### 1.6.4.6.1 [<sup>11</sup>C]Palmitate

Myocardial fatty acid metabolism could be measured using [<sup>11</sup>C]palmitate, which is identical to a natural fatty acid. As with its non-radiolabeled analogue, [<sup>11</sup>C]palmitate is transported into the mitochondria by the carnitine shuttle and is subject to β-oxidation. However, because the [<sup>11</sup>C] label is introduced at the C-1 position, it is lost after the first round of β-oxidation and is released, after passage through TCA cycle,

in [<sup>11</sup>C]CO<sub>2</sub> form. This short metabolic half-life explains the lack of specificity and poor image quality.<sup>4</sup>

#### 1.6.4.6.2 [<sup>18</sup>F]-Thia-fatty acids

Over the past three decades, development of tracers targeted to fatty acid metabolism moved away from using natural fatty acids as pharmacological moieties to sulfur atom containing thia-fatty acids. The introduction of the sulfur atom at 4<sup>th</sup> or 6<sup>th</sup> position blocks β-oxidation process, thus allowing the radiolabeled ω-terminus to remain trapped inside the cell. Multiple thia-fatty acids have been radiolabeled with fluorine-18.<sup>33, 109</sup>

### 1.7 Proposed metabolism for thia-fatty acids in the cardiomyocytes

Using FTO as an example, Pandey *et al.* proposed a mechanism for how long chain fatty acids are up taken and metabolically trapped in the myocardium (see Figure 19).<sup>110</sup>

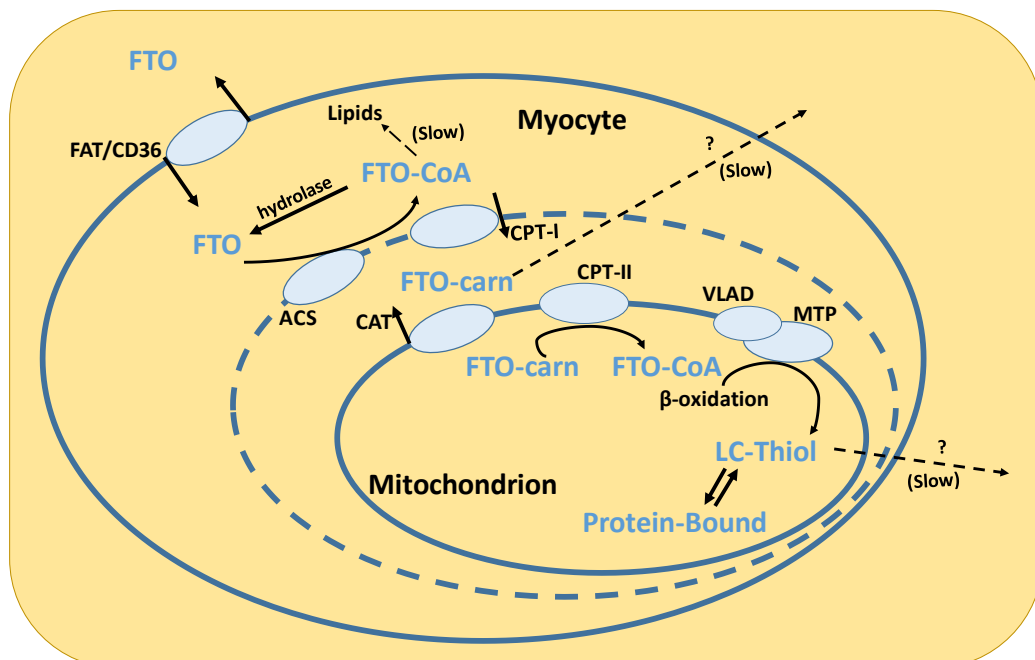


Figure 19: Proposed cardiomyocyte FTO metabolism

FTO enters into the cardiomyocyte *via* a fatty acid transporter (CD36 /FATP) (fatty acid trans- porter protein). In the cytosol, FTO is esterified to FTO-CoA by fatty acyl-CoA synthase. The CoA activating group is exchanged to carnitine by CPT-I and the acyl carnitine is then shuttled across the inner mitochondrial membrane where it gets converted back to FTO-CoA by CPT-II. In the mitochondrial matrix, FTO-CoA undergoes two rounds of  $\beta$ -oxidation forming the 3-hydroxy acyl-CoA moiety and a long-chain thiol, [ $^{18}\text{F}$ ]-14-fluoro-tetradecane-1-thiol, which then binds to various mitochondrial proteins. This theory is supported by the fact that, after administration to the rat, a predominant amount of radioactivity was retained in the mitochondrial fraction. Evidence of non-specific protein binding was presented by gel electrophoresis of heart extracts, which showed that the [ $^{18}\text{F}$ ] radioactivity was associated with a broad spectrum of molecular weights. Thus, the accumulation of protein-bound [ $^{18}\text{F}$ ] radioactivity in tissue is taken as a direct readout of the extent of fatty acid oxidation. Due to their high lipophilicity, thia-fatty acid tracers are cleared very slowly. Two likely mechanisms of clearance are the slow release of carnitine esters and  $\beta$ -oxidation metabolites.

## 1.8 Summary

Cardiac diseases are the leading cause of death worldwide, thus, an early detection and better understanding of different pathologies is needed. PET and SPECT are non-invasive medical imaging techniques capable of detecting metabolic changes during or preceding the establishment of a pathology. The rationale for developing fluorine-18 and technetium-99m radiolabeled thia-fatty acids as PET and SPECT probes of fatty acid oxidation for their potential used in cardiac imaging can be summarised as follows: 1. There is a strong clinical need to know the metabolic state of healthy and dysfunctional heart. 2. Fatty acids are the main source of energy in cardiac tissue. 3. Tissue trapping of thia-fatty acids is metabolism-dependent, which makes them ideal probes of natural fatty acid oxidation. 4. Knowledge of metabolic state could help to determine myocardial viability and provide information for better understanding and detection of ischemic heart disease and coronary artery disease (CAD).

## 1.9 Research Aims

The aims of this work are to synthesise and radiolabel in high radiochemical yields novel thia-fatty acids tracers for imaging cardiac metabolism to obtain new radiopharmaceuticals which might give more insight into cardiac metabolism.

To achieve these objectives, firstly, thia-fatty acids and their derivatives with various chain lengths including medium chain thia-fatty acids and long chain thia-fatty acids have been synthesised following novel and modified synthetic routes. Secondly, fluorine-18 radiolabeling of thia-fatty acid precursors have been developed and the cardiac uptake *in vivo* by PET in the different animal models have been investigated.

The third aim of this work is the development of a coordination chemistry delivery mechanism to  $^{18}\text{F}$ -thiacapric acid tracers for imaging cardiac metabolism by PET. To achieve this aim: an investigation of the coordination characteristics of thia-fatty acids with transition metal macrocyclic complexes known to coordinate carboxylates, using a fluorinated medium chain carboxylic acid as a model was attempted. Functionalisation of the macrocyclic transition metal complex with a triphenyl phosphinonium moiety was carried out in order to confer it mitochondrial targeting properties.

The fourth aim of the thesis is the development of novel  $^{99\text{m}}\text{Tc}$  labeled long chain thia-fatty acids (palmitic acid (C-16) and oleic acid (C-18)) for their potential use in cardiac metabolic imaging by SPECT. Synthesis and characterization of a BFC (TACN) chelating unit, which was conjugated to thia- palmitic and oleic acids, was carried out. In addition, synthesis and characterization of the analogous Re(I) complexes which are important for the characterisation of the  $^{99\text{m}}\text{Tc(I)}$  tracers was investigated.  $^{99\text{m}}\text{Tc}$  radiolabeling of both TACN-thiapalmitic acid and TACN-thiaoleic acid was attempted.

# **Chapter Two**

## **Synthesis of thia-fatty acid derivatives**

## Chapter Two: Synthesis of thia-fatty acid derivatives

### 2.1 Aims and objectives

Fatty acids that have alkyl chain lengths of sixteen carbons and longer, have to be transported inside the mitochondria *via* the carnitine shuttle. Shorter chain length fatty acids can access the site of metabolic degradation *via* passive diffusion.<sup>111, 112</sup> However, the utility of this or other alternative transport methods to the carnitine shuttle have not been investigated. Thus, synthesis of  $\omega$ -fluorinated medium chain eight and ten carbon chain length thia-fatty acids are proposed, in which cardiac uptake and retention could be compared with that of known fluorinated thiapalmitic acid (FTP, sixteen carbon chain) and an improved unsaturated fluorinated thia-oleic acid (FTO, eighteen carbon chain). To achieve this objective, the intermediate compounds, radiolabeling precursors and “cold” fluorine-19 containing reference compounds were investigated and synthetic results are reported in this chapter (see

Figure 20).

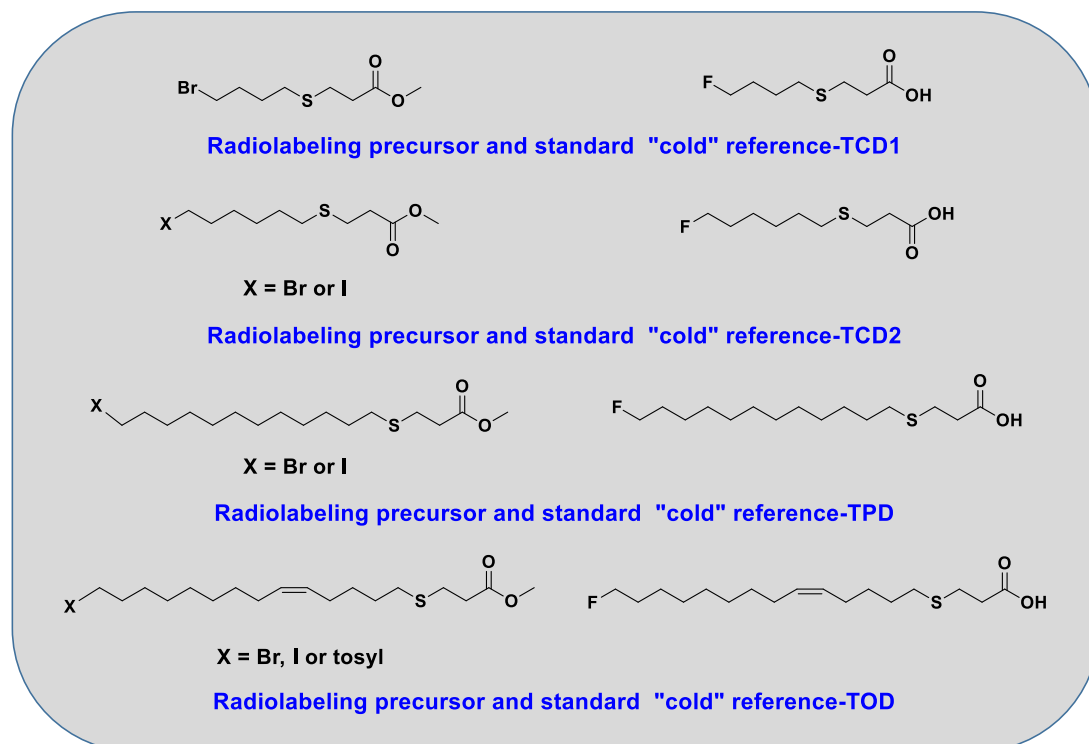


Figure 20: Chemical structures of target compounds

## 2.2 Previously reported synthetic methodologies to produce $^{18}\text{F}$ labeled fatty acid precursors

In the last 30 years, considerable attention has been paid to the development of fluorine-18 radiolabeled thia-substituted fatty acid analogues as metabolically trapped PET probes for myocardial fatty acid metabolism imaging. Metabolic trapping is the ideal method for imaging fatty acid metabolism i.e. that the fatty acid probe fluxes through at least the initial step(s) of  $\beta$ -oxidation then becomes metabolically trapped. The fatty acid probe should be specific to oxidation and should not undergo esterification as this will alter the accumulation pattern. To obtain high target cardiac uptake and retention, [ $^{18}\text{F}$ ]-labeled fatty acid tracers can contain heteroatoms (primarily sulfur) at the fourth or sixth position, which causes nearly exclusive fatty acid  $\beta$ -oxidation. Figure 21 shows the thia-fatty acid tracers that have been previously developed as PET probes for fatty acid oxidation.<sup>109</sup>

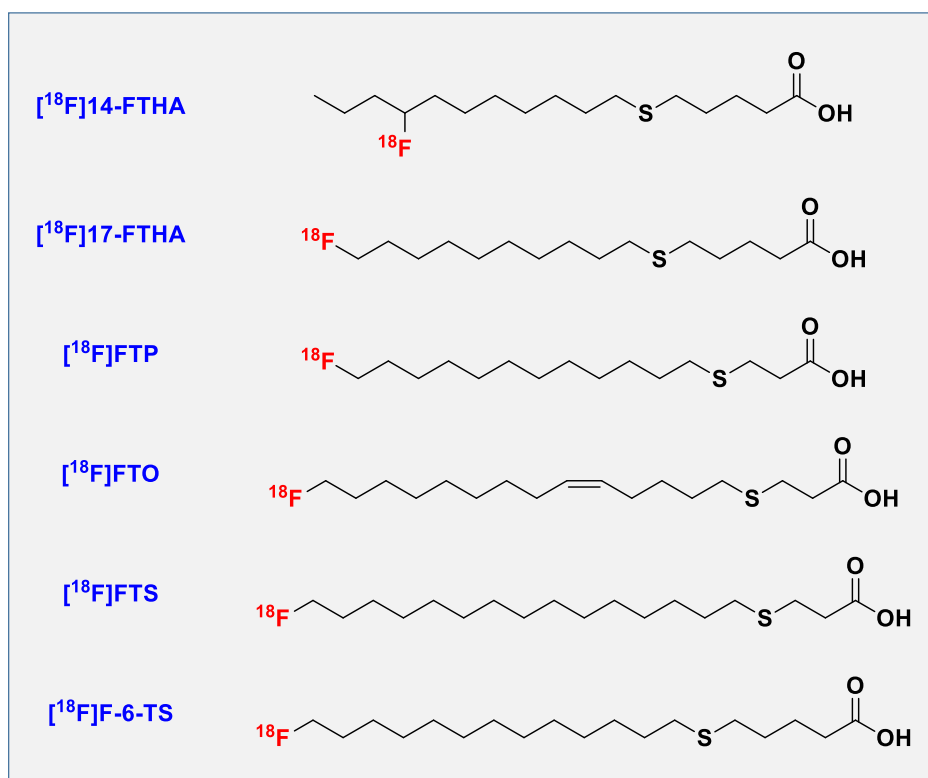


Figure 21: Chemical structure of thia-substituted fatty acids: [ $^{18}\text{F}$ ]-14-fluoro-6-thiaoctadecanoic acid [ $^{18}\text{F}$ ]14-FTHA; [ $^{18}\text{F}$ ]-17-fluoro-6-thiaoctadecanoic acid [ $^{18}\text{F}$ ]17-FTHA; [ $^{18}\text{F}$ ]-16-fluoro-4-thiapalmitic acid [ $^{18}\text{F}$ ]FTP; [ $^{18}\text{F}$ ]-18-fluoro-4-thiaoleic acid [ $^{18}\text{F}$ ]FTO; [ $^{18}\text{F}$ ]-18-fluoro-4-thiastearic acid [ $^{18}\text{F}$ ]FTS; [ $^{18}\text{F}$ ]-18-fluoro-6-thiastearic acid [ $^{18}\text{F}$ ]F-6-TS

Various synthetic routes have been developed previously to synthesise the precursors and “cold” reference standard compounds for these tracers. Some radiolabeling precursors are commercially available. Both the reference for [ $^{18}\text{F}$ ]-14-fluoro-6-thiaheptadecanoic acid ([ $^{18}\text{F}$ ]FTHA) and the radiolabeling precursor with a tosylate leaving group can be purchased (see Figure 22).<sup>113, 114</sup>

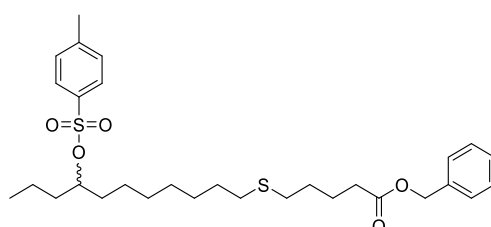
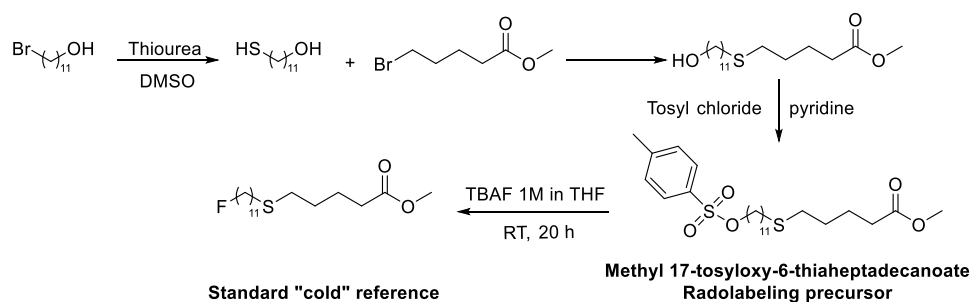


Figure 22: Chemical structure for benzyl 14(R,S)-tosyloxy-6-thiaheptadecanoate<sup>113</sup>

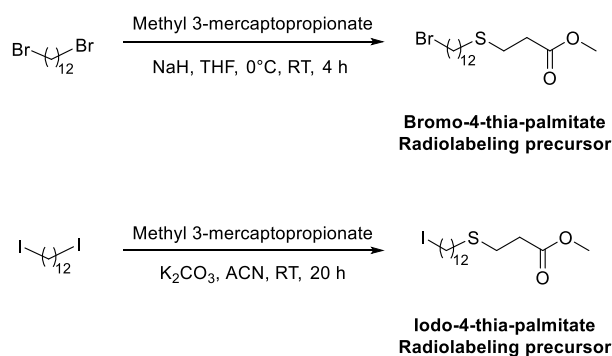
For the synthesis of [ $^{18}\text{F}$ ]-17-fluoro-6-thiaheptadecanoic acid ([ $^{18}\text{F}$ ]17-FTHA), 11-bromo-1-undecanol was converted to thiol 11-mercapto-undecanol by thiourea, then, methyl 5-bromopentanoate was added to insert the sulfur atom in position 6<sup>th</sup> in the carbon backbone and to extend the chain length. The resulting methyl 17-hydroxy-6-thiaheptadecanoate was tosylated to produce the target compound, methyl 17-tosyloxy-6-thiaheptadecanoate (see Scheme 1).<sup>115</sup>



Scheme 1: Synthetic route to prepare [ $^{18}\text{F}$ ]-17-fluoro-6-thiaheptadecanoic acid [ $^{18}\text{F}$ ]17-FTHA precursor and standard reference<sup>115</sup>

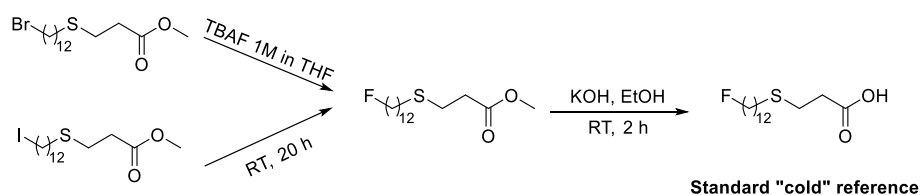
Belanger *et al.* and DeGrado *et al.* have reported two different synthetic routes to prepare [ $^{18}\text{F}$ ]FTP precursors<sup>115, 116</sup> (see Scheme 2). The alkylation method that Belanger *et al.* used depends on alkylation of bromo-4-thiapalmitate with 1,12-dibromododecane.<sup>116</sup> DeGrado *et al.* synthesised a similar compound using a diiodo derivative to give an iodide precursor for radiolabeling.<sup>115</sup>





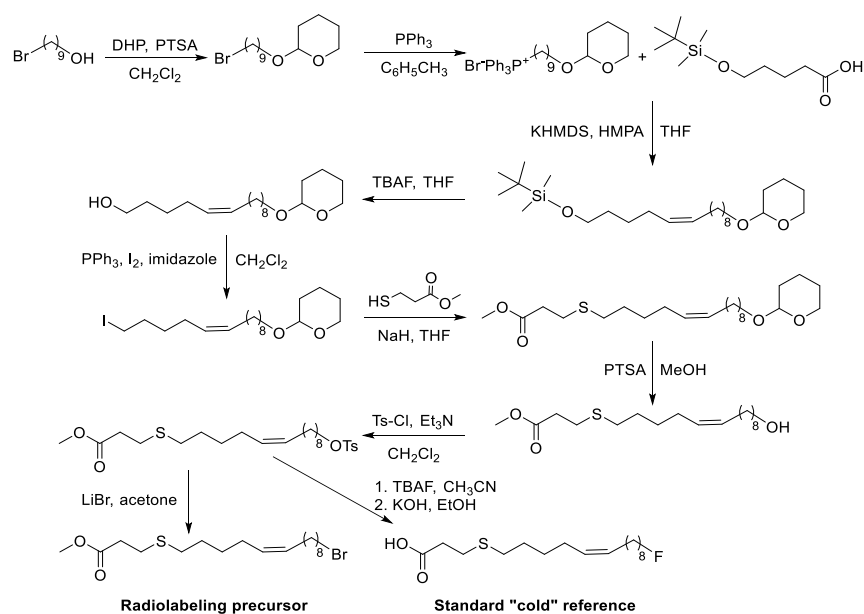
Scheme 2: Synthetic routes to prepare [ $^{18}\text{F}$ ]-16-fluoro-4-palmitic acid [ $^{18}\text{F}$ ]FTP precursors<sup>115, 116</sup>

Formation of non-radioactive fluorine-19 reference standards using the Belanger *et al.* and DeGrado *et al.* routes was performed by fluorination of the bromo and iodo terminating protected fatty acids with tetra-*n*-butylammonium fluoride (TBAF).<sup>115, 116</sup> The resulting fluoro-ester was hydrolysed with base (see Scheme 3).



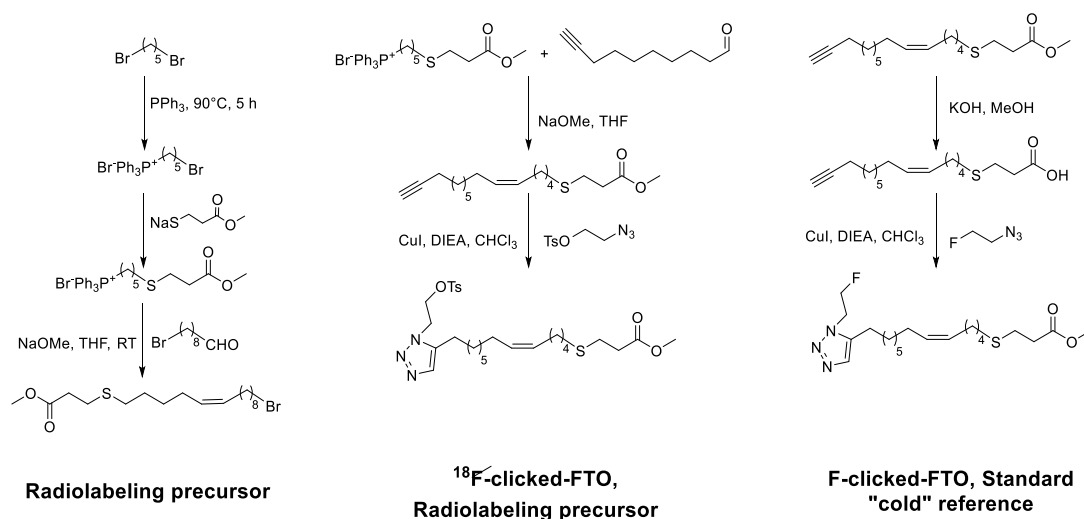
Scheme 3: Synthetic routes to prepare [ $^{18}\text{F}$ ]-16-fluoro-4-thiapalmitic acid [ $^{18}\text{F}$ ]FTP "cold" reference standard<sup>115, 116</sup>

There are two published methods for the synthesis of [ $^{18}\text{F}$ ]FTO precursors. In the first report, by DeGrado *et al.* the bromo precursor was prepared in nine steps. The non-radioactive reference compound 19-fluoro-4-thiaoleic acid (FTO) was produced by a nucleophilic substitution reaction between the precursor tetra-*n*-butylammonium fluoride (TBAF), and hydrolysed with base<sup>117</sup> (see Scheme 4).



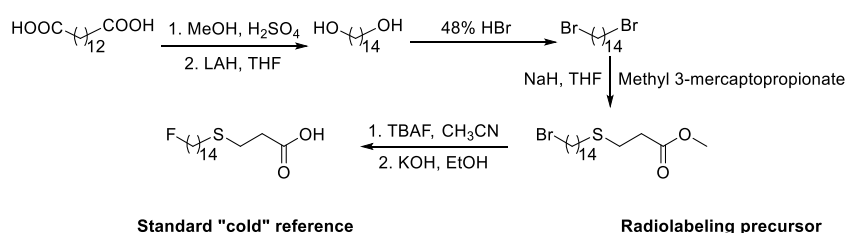
Scheme 4: Synthetic routes to prepare  $[^{18}\text{F}]$ -18-fluoro-4-thiaoleic acid  $[^{18}\text{F}]$ FTO precursor and "cold" reference standard<sup>117</sup>

In a report by Cai *et al.*, the radiolabeling precursor and non-radioactive reference compound were synthesised based on the corresponding clicked oleate analogue in five steps<sup>118</sup> (see Scheme 5). This research group also optimised the synthetic route to FTO to require only three steps from commercially available materials (see Scheme 5).



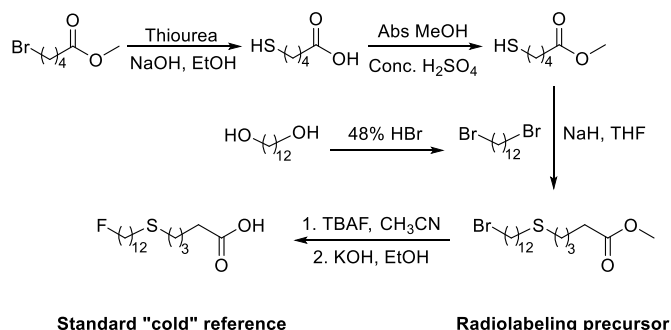
Scheme 5: Synthetic routes to prepare of,  $[^{18}\text{F}]$ FTO,  $^{18}\text{F}$ -clicked-FTO precursor and the cold standard, F-clicked-FTO<sup>118</sup>

The synthesis of [ $^{18}\text{F}$ ]-18-fluoro-4-thiastearic acid ([ $^{18}\text{F}$ ]FSTS) precursors has been reported.<sup>4</sup> 1,14-Tetradecadioic acid was converted to 1,14-tetradecane diol in two steps: esterification followed by reduction. The obtained diol was heated with HBr to yield 1,14-dibromotetradecane which on subsequent reaction with methyl 3-mercaptopropanoate in the presence of sodium hydride yielded bromostearate as precursor for radiofluorination. The bromostearate was treated with tetra-*n*-butylammonium fluoride (TBAF) followed by ester hydrolysis to obtain the non-radioactive reference standard (see Scheme 6).



Scheme 6: Schematic synthetic routes to prepare [ $^{18}\text{F}$ ]-18-fluoro-4-thiastearic acid [ $^{18}\text{F}$ ]FSTS precursor and "cold" reference standard<sup>4</sup>

To synthesise [ $^{18}\text{F}$ ]-18-fluoro-6-thiastearic acid ([ $^{18}\text{F}$ ]F-6-TS), the precursor has been prepared from methyl 5-bromopentanoate and thiourea followed by treatment and subsequent esterification with methanol. The product was treated with 1,12-dibromododecane in the presence of sodium hydride, forming the bromo stearate as the precursor for radiofluorination. To obtain the non-radioactive reference compound, the bromo stearate was treated with tetra-*n*-butylammonium fluoride (TBAF) followed by ester hydrolysis (see Scheme 7).



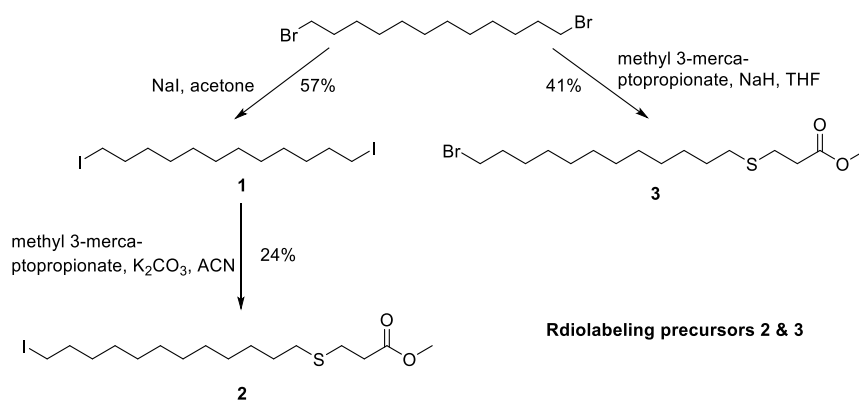
Scheme 7: Synthetic routes to prepare [ $^{18}\text{F}$ ]-18-fluoro-6-thiastearic acid [ $^{18}\text{F}$ ]F-6-TS precursor and "cold" reference standard<sup>4</sup>

## 2.3 Synthesis of methyl 4-thiapalmitic acid/palmitate derivatives (TPD)

Palmitate, a long chain fatty acid (sixteen carbon atoms), is one of the most prevalent in human blood. It is used to produce energy in the normoxic myocardium and it is rapidly metabolised by  $\beta$ -oxidation and easily passes through the mitochondrial membrane.<sup>112</sup> Thus, the 4-thiapalmitic acid tracer was developed for use as a metabolically trapped PET probe for myocardial fatty acid oxidation imaging.<sup>115</sup> However, the myocardial accumulation of [<sup>18</sup>F]-16-fluoro-4-thiapalmitic acid ([<sup>18</sup>F]FTP) is suboptimal in hypoxic tissues.<sup>115</sup> Overall, [<sup>18</sup>F]FTP is validated as a radiopharmaceutical for heart imaging and offers a well characterised control for radiolabeling and imaging experiments in this work.

### 2.3.1 Synthesis of 16-iodo or bromo-4-thiapalmitate (**2** and **3**)

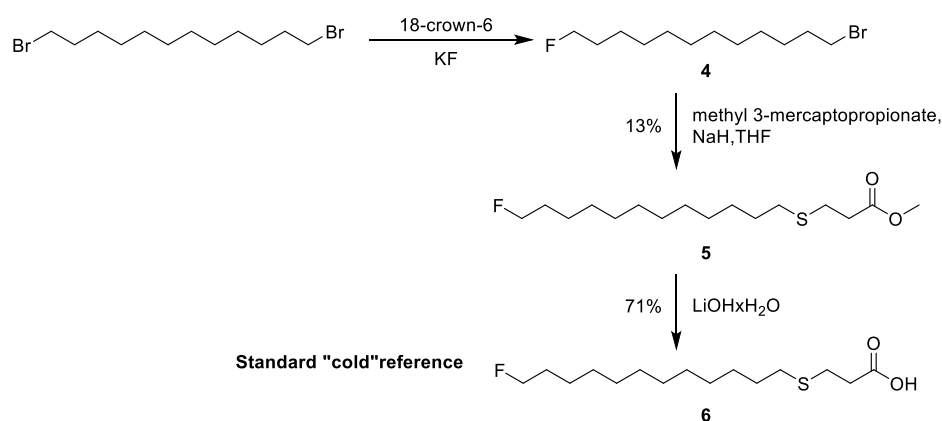
Two palmitate radiolabeling precursors, with iodo and bromo leaving groups, were synthesised. In order to facilitate a further nucleophilic attack by thiol of methyl 3-mercaptopropionate, commercially available 1,12-dibromododecane was iodinated with sodium iodide at refluxing in acetone to yield the diiodo product **1** in 57% yield (see Scheme 8). The approach was chosen based on the work by Sheibani and Wärnmark<sup>119</sup> who synthesised 1,12-diiodododecane in quantitative yield from 1,12-dibromododecane and methyl 3-mercaptopropionate following a modified procedure published by DeGrado *et al.*<sup>115</sup> and Pandey *et al.*<sup>4</sup> providing the expected iodinated thiapalmitate **2** in a 24% yield in an almost 1:1 mixture with the symmetric bis-substituted derivative. Although iodine is a better leaving group, bromide derivatives are also of interest. Therefore, bromate thiapalmitate **3** was prepared using sodium hydride activation<sup>4</sup> in a 41% yield (see Scheme 8).



Scheme 8: Synthesis of methyl 16-iodo or bromo-4-thiapalmitate **2**, **3** respectively

### 2.3.2 Synthesis of 16-fluoro-4-thiapalmitic acid (FTP) **6**

To obtain 16-fluoro-4-thiapalmitic acid (FTP) **6** as a standard for HPLC, fluorination of 1,12-dibromododecane was first carried out using KF/18-crown-6 complex in anhydrous acetonitrile (see Scheme 9). The fluorinated product **4** was reacted without isolation with methyl 3-mercaptopropionate using sodium hydride to form **5** in a yield of 13%.<sup>4</sup> 16-Fluoro-4-thiapalmitic acid **6** can then be formed *via* basic hydrolysis with LiOH in 60% ethanol/water solution in a 71% yield. The formation of compound **6** was observed in the <sup>1</sup>H NMR (disappearance of a singlet at  $\delta$  3.70 ppm, characteristic of methyl ester). As **6** was only required in small quantities for HPLC analysis, further optimisation to increase reaction yields was not attempted.



Scheme 9: Synthesis of 16-fluoro-4-thiapalmitic acid (FTP) **6**

### 2.3.3 HPLC analysis of methyl 16-fluoro-4-thiapalmitate **5** and 16-fluoro-4-thiapalmitic acid (FTP) **6**

Cold (non-radioactive) standard compounds are essential to allow method development *via* HPLC, allowing for radiotracer identification, reaction monitoring and purification.

In preparation for radiolabeling experiments, an HPLC method was developed and retention times for fluorinated ester intermediate **5** and 16-fluoro-4-thiapalmitic acid **6** were determined. The products eluted, respectively, at retention times ( $R_t$ ) of 14:20 min and 12:28 min (HPLC gradient-method 3, See Experimental, section 5.3.6.1) (see Figure 23).

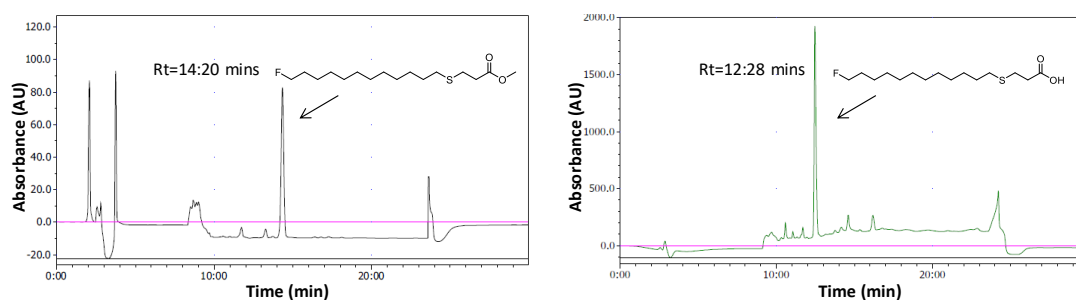


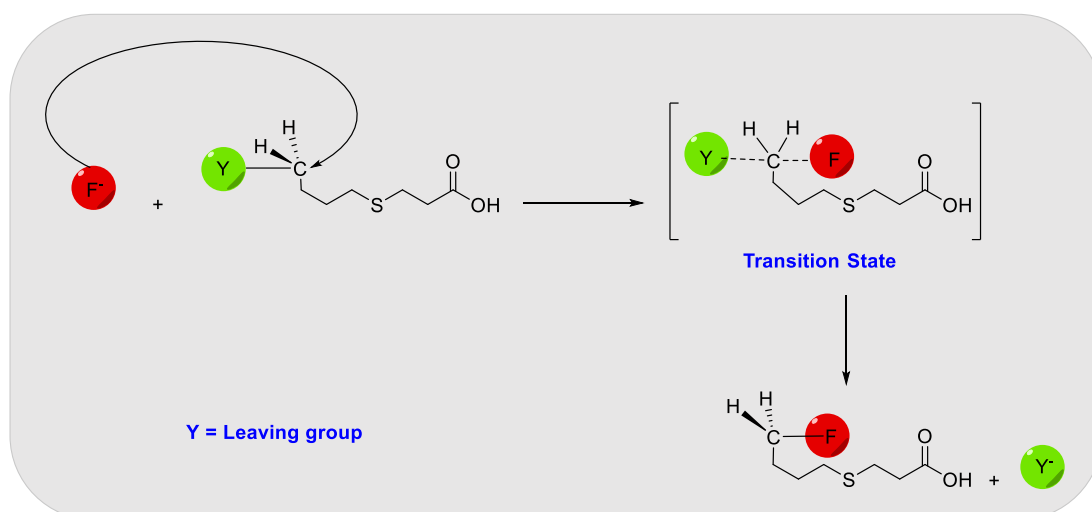
Figure 23: HPLC traces of fluorinated ester intermediate **5** and 16-fluoro-4-thiapalmitic acid (FTP) **6**

## 2.4 Novel synthetic routes for 4-thiacaprylic acid/caprylate derivatives (TCD1)

Medium chain thia-fatty acids may be interesting to compare with long chain thia-fatty acid tracers (C-16 to C-18) in regard to *in vivo* cardiac uptake. As noted in section 2.2, medium and short chain thia-fatty acid don't engage with the carnitine shuttle and appear to enter the mitochondria *via* a carnitine-independent process that is not yet fully characterised (likely to be passive diffusion).<sup>111, 112, 120</sup>

### 2.4.1 Synthesis of methyl 8-tosyl or bromo-4-thiacaprylate (**13** and **18**)

The most successful processes to synthesise high specific activity fluorine-18 radiotracers are based on aliphatic nucleophilic substitution reactions ( $S_N2$ ).<sup>2</sup> This reaction requires a good leaving group, such as halides (I, Br or Cl) or sulfonate (tosylate, nosylate, mesylate or triflate).<sup>121, 122</sup> In  $S_N2$  reactions, the fluoride ion  $F^-$  attacks and links to the primary carbon atom of the methyl 8-tosyl or bromo-4-thiacaprylate **13** and **18** respectively, on the opposite side to a leaving group, which is the weak base (see Scheme 10).

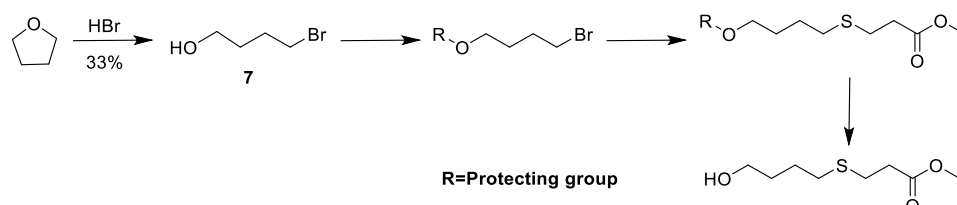


Scheme 10: Aliphatic nucleophilic substitution reaction ( $S_N2$ )

However, the main limitation of this method is the need to protect any potentially competing sites of nucleophilic attack in the molecule such as alcohol, acid or amine

groups.<sup>10</sup> As a result, additional synthesis and purification steps are required, increasing complexity and synthesis times.

The general synthesis of different thiacyprylate derivatives and protected intermediates to produce the radiolabeling precursors is shown in Scheme 11.



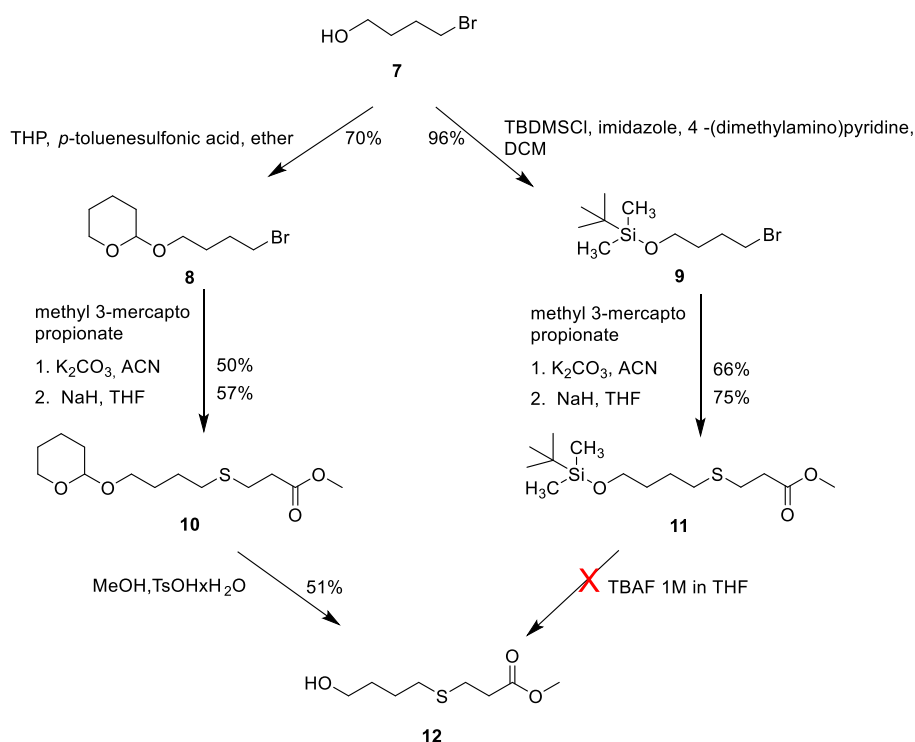
Scheme 11: Synthesis of methyl 4-thiacyprylate derivatives in general

4-Bromo-1-butanol **7** was prepared by acid hydrolysis of tetrahydrofuran by hydrobromic acid (HBr) following literature methods (see Scheme 11),<sup>123</sup> HBr is a strongly acidic reagent used for generating bromohydroxy compounds *via* ether cleavage.<sup>124</sup> **7** was prepared to react with methyl 3-mercaptopropionate. However, its hydroxyl group is a potential nucleophile and should be protected beforehand. Two protecting groups, tetrahydropyranyl (THP) and dimethyl-*tert*-butylsilyl (TBDMS) were explored.

The protecting group is introduced under mild acidic conditions and is stable to strongly basic reaction conditions, organometallics, hydrides, acylating reagents and alkylation reagents. One of the disadvantages of using THP protecting group is that it introduces an additional stereocentre that may lead to diastereomeric mixtures of the alcohol.<sup>125</sup> This was not a problem in our case due to the simplicity of the structure. The approach chosen in this work is based on the modified method by Grieco and Larsen (see Scheme 12).<sup>126</sup> The reaction was monitored by TLC until the starting material was consumed (24 h) rather than following the described reaction time (1 h). The formation of compound **8** was confirmed by the appearance of a characteristic triplet peak at  $\delta$  4.60 ppm corresponding to O-CH<sub>2</sub>-O proton. After flash chromatography purification, product **8** was isolated as a colourless oil in a 70% yield, lower than reported in literature (96%), although this was used without purification.<sup>126</sup>



An alternate protection strategy utilising dimethyl-*tert*-butylsilyl (TBDMS) group was also explored. Silyl protecting groups have the advantage of chemo-selective cleavage by fluoride ions which might be of interest if the protected compound contained other acid sensitive groups.<sup>125</sup> In this work, **9** was synthesised based on the method by Touh and Fallis.<sup>127</sup> TBDMS is introduced using tetrabutyldimetylsilyl chloride (TBDMSCl). Chloride is a poor leaving group and can be activated *in situ* by addition of imidazole. The group is introduced under mildly basic conditions. Acid-basic aqueous treatment gave the silyl ether **9** as a colourless oil in 96% yield, an improvement of the yield obtained in the literature (80%).<sup>127</sup> It was directly used in the next step without purification (see Scheme 12).



Scheme 12: Synthesis of methyl 4-thiacaprylate intermediate derivatives

To obtain novel thiaprylate derivatives, the THP protected compound **8** or TBDMS protected compound **9** is modified by insertion of a sulfur atom at specific positions in the chain backbone.<sup>33</sup> The thia fatty acids generally include a sulfur atom at the C-4 position, to facilitate metabolic trapping.<sup>2</sup> It is introduced by reacting a C<sub>n-4</sub> bromide derivative (in this case, protected bromobutanol) with methyl 3-mercaptopropionate. Two different procedures can be considered, heterogeneous

basic catalysis as described by Pandey *et al.*,<sup>4</sup> or activation of thiol by a strong base NaH as described by DeGrado *et al.*<sup>115</sup> (see Scheme 12). Both approaches were attempted and use an equimolar or slight excess of thiol to bromide derivative. However, the K<sub>2</sub>CO<sub>3</sub> method takes much longer (3 days) to achieve similar reaction yields as the NaH (50-60% vs. 57-75% respectively); hence, the NaH method is preferred. The formation of **10** and **11** was confirmed by the appearance of protons belonging to hydroxyl protective groups and a characteristic singlet at  $\delta$  3.70 ppm of methyl ester in <sup>1</sup>H NMR.

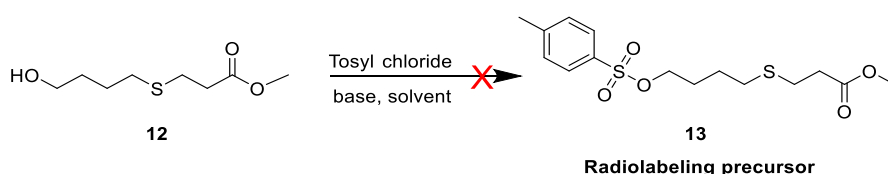
The THP protecting group was removed with an equimolar amount of *p*-toluenesulfonic acid, following literature methods.<sup>125</sup> The novel compound **12** was purified by flash chromatography and isolated as a colourless oil in 51% yield (see Scheme 12). The reaction can be followed by thin layer chromatography (TLC) or by <sup>1</sup>H NMR, monitoring the disappearance of characteristic O-CH-O proton at  $\delta$  4.60 ppm.

The TBDMS protecting group should be labile in the presence of fluoride ions. The de-protection of TBDMS is based on the work of Corey and Venkateswarlu.<sup>128</sup> However, the use of 2-3 fold excess of tetra-*n*-butyl ammonium fluoride in THF for 8 h at room temperature did not give the de-protected product (see Scheme 12). The mercapto group may compromise the stability of compound **11** or reactivity of fluoride, however, as the THP protecting strategy worked well, this has not been further investigated.

Tosylation of alcohols using *p*-toluenesulfonyl (tosyl) chloride is a typical transformation used to convert alcohols (a poor leaving group hydroxy) into tosyl (a good leaving group *p*-toluenesulfonyl or tosylate group) alkylating agents.<sup>129</sup> Many methods are available and were tested before identifying conditions suitable for the starting materials in this work.

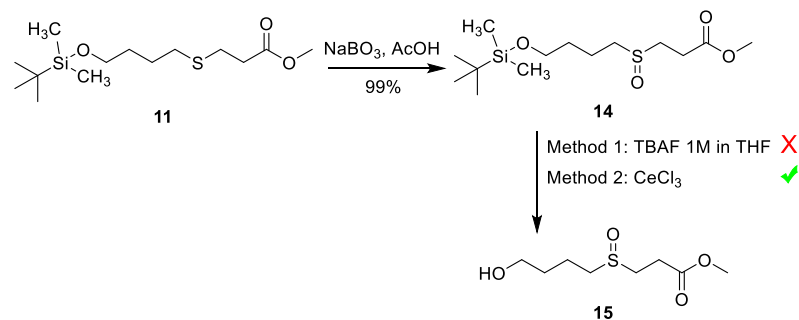
The general method for tosylation of an alcohol involves a tosyl chloride and a base, reacted in a polar solvent. To synthesise the previously unreported methyl 8-tosyl-4-

thiacaprylate **13**, three modified methods based on reports in the literature were attempted<sup>130, 131</sup> (Scheme 13). Using diisopropylethylamine (DIPEA) in dry dichloromethane (DCM) or K<sub>2</sub>CO<sub>3</sub> in dry DCM did not provide any tosylated product, as evidenced by the absence of aromatic protons in <sup>1</sup>H NMR of crude reactions. Attempts to activate the tosyl chloride into a pyridinium derivative using pyridine and 4-(dimethylamino)pyridine as a base in dry DCM using trimethylammonium derivative with triethylamine (TEA) as a base and trimethylamine hydrochloride as a catalyst were also not successful.



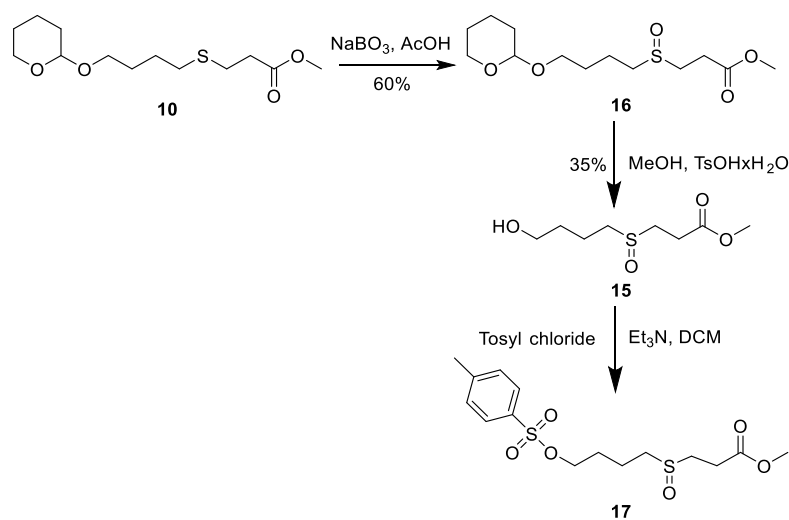
Scheme 13: Attempting of synthesis methyl 8-tosyl-4-thiacaprylate **13**, four methods: Method 1- DIPEA, DCM; Method 2- K<sub>2</sub>CO<sub>3</sub>, DCM; Method 3- Et<sub>3</sub>N, ACN; Method 4- pyridine, DCM

As these methods were proven to work with alcohols without sulfur atoms, protection of the mercapto derivatives was carried out by oxidation to a sulfinyl group using sodium perborate (NaBO<sub>3</sub>) in biphasic water/ethyl acetate solution acidified with a catalytic amount of glacial acetic acid, based on a method reported by Funakoshi *et al.*<sup>132</sup> Both TBDMS protected **11** and THP protected **10** (see Scheme 14) derivatives were prepared in 99% and 60% yield, respectively. Tetra-*n*-butylammonium fluoride de-protection of TBDMS to form **15** did not give the deprotected product compound **15**. Subsequently, a different method involving cerium(III) chloride (CeCl<sub>3</sub>) oxidation was used,<sup>84</sup> which gave a complex mixture in the <sup>1</sup>H NMR spectrum. TLC analysis of the reaction also indicated significant impurities which would require challenging purification. As the THP protection chemistry worked well, the TBDMS protection route was not investigated further (see Scheme 14).



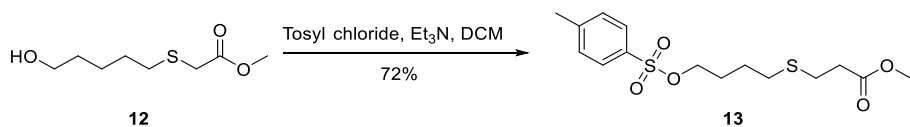
Scheme 14: Synthesis of methyl 8-alcohol-4-sulfinylcaprylate **15**

The THP derivative **10** was deprotected by stirring the protected sulfanyl-ester with an equimolar amount of *p*-toluenesulfonic acid in methanol to provide the sulfanyl alcohol **15** in a non-optimised yield of 35%. The sulfanyl alcohol **15** was tosylated using tosyl chloride, Me<sub>3</sub>N, HCl and Et<sub>3</sub>N to give **17** (see Scheme 15).<sup>130</sup> Multiple attempts at chromatographic purification failed because compound **17** hydrolysed to its precursor alcohol **15**.



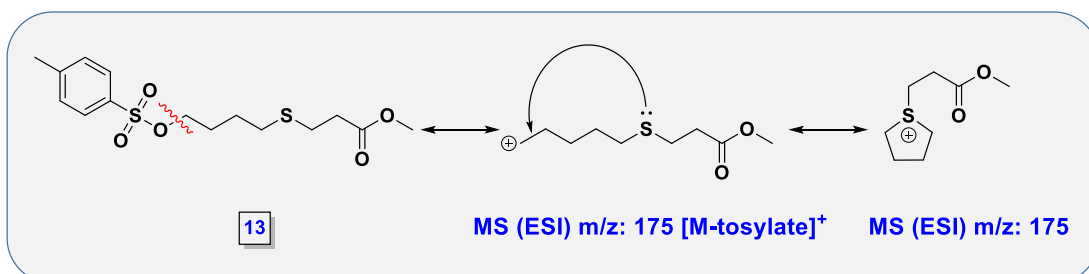
Scheme 15: Synthesis of methyl 8-tosyl-4-sulfinylcaprylate **17**

The tosylate derivative **13** was synthesised using a standard method, which was used to prepared tosylate derivative **17** (see Scheme 16).



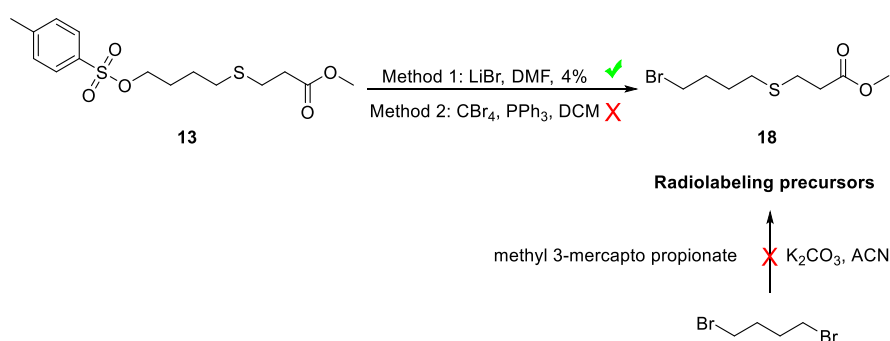
Scheme 16: Synthesis of methyl 8-tosyl-4-thaicaprylate **13**.

Problems were again encountered with the instability of this compound, which may be due to hydrolysis or potentially the cyclisation to form a sulfonium species, which was consistent with the fragment  $[M\text{-tosylate}]^+$  observed in the mass spectrum (see Scheme 17). This reactive species could subsequently be hydrolysed.



Scheme 17: Suggestion mechanism for compound **13**

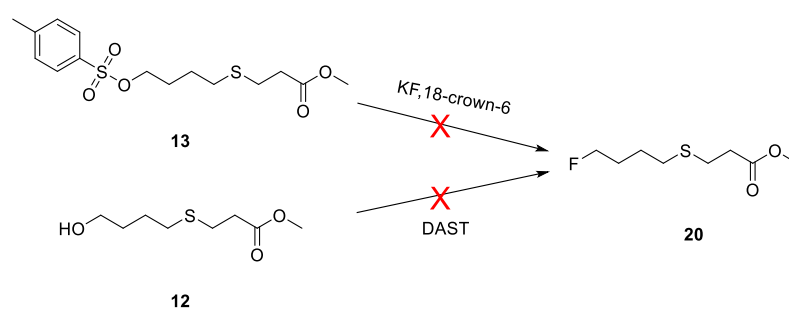
Bromide is also a good leaving group, thus could replace the tosyl group in an alternative radiolabeling precursor. The tosylate compound **13** was treated immediately after tosylation with lithium bromide in dimethylformamide (DMF) using a modified literature method (see Scheme 18).<sup>133</sup> After column chromatography purification, product **18** was isolated as a colourless oil in 4% yield, the low yield may be because of the instability of **13**. Other methods were attempted to prepare **18**, see Scheme 18, but the desired product was not isolated. Further optimisation is needed to increase the yield of the precursor but sufficient product has been isolated to proceed.



Scheme 18: Synthesis of methyl 8-bromo-4-thiacaprylate **18**

## 2.4.2 Synthesis of methyl 8-fluoro-4-thiacaprylate (FTC1) **21**

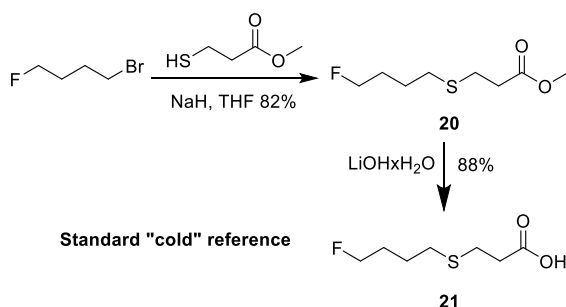
Synthesis of fluorine-19 containing 8-fluoro-4-thiacaprylate **20** was attempted by a nucleophilic substitution reaction between the radiolabeling precursor **18** and the fluoride ion carrier, followed by ester hydrolysis (see Scheme 19). Even though macroscale reaction conditions do not usually match radiolabeling conditions, the “cold” reaction might offer some insight. Two sources of fluoride, KF (activated with 18-crown-6) and tetra-*n*-butylammonium fluoride, were used. However, in both cases, complex mixtures of products were produced with the expected fluorinated derivative detected by mass spectrometry but not present in a recoverable quantity. Direct fluorination of alcohol **12** with diethylaminosulfur trifluoride (DAST), following literature methods,<sup>134</sup> was equally unsuccessful and was abandoned without further investigation.



Scheme 19: Attempting of synthesis 8-fluoro-4-thiacaprylate **20**

Therefore, the novel compound **20** was prepared by a different route to that used for the radiochemistry. Compound **20** was synthesised directly from commercially available 1-bromo-4-fluorobutane (see Scheme 20) and methyl 3-mercaptopropionate by using NaH as base, in an 82% yield. Its identity was confirmed by <sup>1</sup>H NMR (disappearance of  $\delta$  3.47 ppm triplet, characteristic of CH<sub>2</sub>-Br, and appearance of a singlet at  $\delta$  3.70 ppm, characteristic of methyl ester and a doublet of triplets at  $\delta$  4.46, characteristic of CH<sub>2</sub>-F). The novel reference “cold” standard 8-fluoro-4-thiacaprylic acid (FTC1) **21** was obtained from fluorinated ester precursor **20** by LiOH catalysed hydrolysis, carried out at room temperature in 60% ethanol/water solution in an 88% yield, following a modified literature method.<sup>135</sup> The identity was

confirmed by  $^1\text{H}$  NMR (disappearance of a singlet at  $\delta$  3.70 ppm, characteristic of methyl ester) and  $^{19}\text{F}$  NMR.



Scheme 20: Synthesis of 8-fluoro-4-thiacaprylic acid (FTC1) **21**

### 2.4.3 HPLC identification of 8-fluoro-4-thiacaprylic acid (FTC1) **21**

In preparation for radiolabeling experiments, an HPLC method was developed and retention times for fluorinated ester intermediate **20** and 8-fluoro-4-thiacaprylic acid (FTC1) (reference standard) **21** (see Figure 24), were determined. Products eluted, respectively, at a retention time ( $R_t$ ) 18:00 min and 15:22 min.

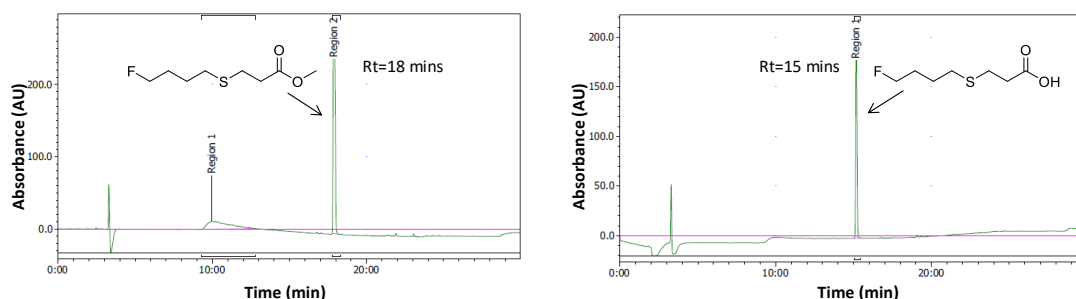


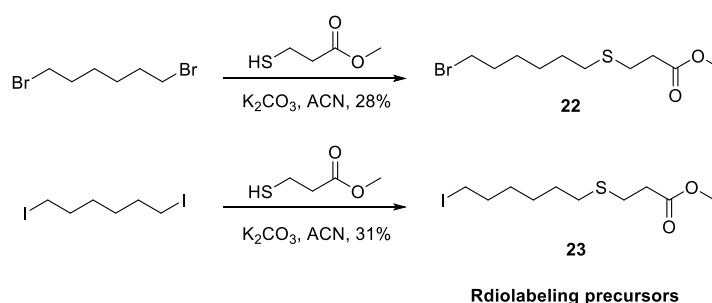
Figure 24: HPLC traces of fluorinated ester intermediate **20** and 8-fluoro-4-thiacaprylic acid (FTC1) **21**

## 2.5 Synthesis of 4-thiacapric acid/ methyl-4-thiacaprate derivatives (TCD2)

Capric acid, which has ten carbon atoms, is another medium chain thia-fatty acid, which was also investigated.

### 2.5.1 Synthesis of methyl-10-iodo- or methyl-10-bromo-4-thiacaprate (**22** and **23**)

Similar to the previously described work, to obtain [ $^{18}\text{F}$ ]-10-fluoro-4-thiacapric acid, a precursor which has a good leaving group should be synthesised. Bromo and iodo precursors, **22** and **23** respectively, were synthesised (see Scheme 21) by reaction of methyl 3-mercaptopropionate with 1,6-dibromo or iodo-hexane in acetonitrile in the presence of  $\text{K}_2\text{CO}_3$ . The synthesis of **22** is a modified version of a procedure reported by DeGrado *et al.*<sup>115, 136</sup> The number of molar equivalents used by DeGrado (1:1, methyl 3-mercaptopropionate: 1,6-dibromohexane) only gave symmetric bis-substituted product when followed. To tackle this problem, multiple experiments were attempted, to give optimised conditions (0.5:1, methyl 3-mercaptopropionate: 1,6-dibromohexane with the reaction time is increased to 3 days) **22** was purified by column chromatography and isolated as a colourless oil in 28% yield (lower than reported by DeGrado, 35%). The formation of compound **22** was characterised by the presence of two triplet peaks in the  $^1\text{H}$  NMR spectrum, one at  $\delta$  3.40 ppm for two protons ( $\text{CH}_2\text{-Br}$ ) and another at  $\delta$  2.73 ppm for two protons ( $\text{CH}_2\text{-S}$ ).



Scheme 21: Synthesis of methyl 8-bromo or iodo-4-thiacaprate **22**, **23**

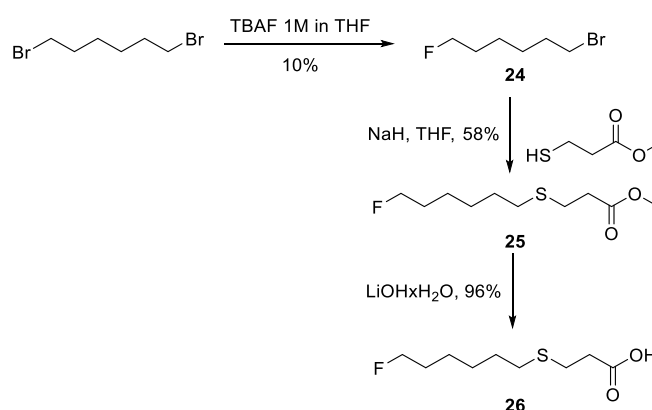
The novel methyl 10-iodo-4-thiacaprate **23** was synthesised by applying the same conditions used to prepare the bromo precursor **22** and was prepared in 31% yield.



The structure of compound **23** was confirmed by the appearance of two characteristic triplets peaks one at  $\delta$  3.19 ppm for two protons ( $\text{CH}_2\text{-I}$ ) and another at  $\delta$  2.78 ppm for two protons ( $\text{CH}_2\text{-S}$ ) in the  $^1\text{H}$  NMR spectrum.

### 2.5.2 Synthesis of 10-fluoro-4-thiacapric acid (FTC2) **26**

To synthesise **26** (see Scheme 22), 1,6-dibromohexane was first fluorinated by the addition of TBAF at room temperature for 72 h. The resulting fluoro-bromo crude compound **24** was purified by distillation and isolated as a colourless oil in 10% yield. The low yield in this reaction is not a major issue as the starting material is commercially available and inexpensive (see Scheme 29). 1-Bromo-6-fluorohexane **24** was subsequently alkylated by the addition of methyl-3-mercaptopropionate to form **25** in a 58% yield. The identity has been confirmed by  $^{19}\text{F}$  NMR and  $^1\text{H}$  NMR with the disappearance of  $\delta$  3.40 ppm triplet, characteristic of  $\text{CH}_2\text{-Br}$ , and appearance of a singlet at  $\delta$  3.70 ppm, characteristic of methyl ester and a doublet of triplets at  $\delta$  4.53, characteristic of  $\text{CH}_2\text{-F}$ . The novel reference “cold” standard 8-fluoro-4-thiacaprylic acid (FTC2) **26** was obtained from fluorinated ester precursor **25** by LiOH catalysed hydrolysis, carried out at room temperature in 60% ethanol/water solution in an 96% yield, following a modified literature method.<sup>135</sup> The identity was confirmed by  $^1\text{H}$  NMR (disappearance of a singlet at  $\delta$  3.70 ppm, characteristic of methyl ester) and  $^{19}\text{F}$  NMR.



Scheme 22: Synthesis of 10-fluoro-4-thiacapric acid (FTC2) **26**

### 2.5.3 HPLC identification of methyl-10-fluoro-4-thiacaprate **25** and 10-fluoro-4-thiacapric acid (FTC2) **26**

A HPLC method was developed for the fluorinated ester **25** and 10-fluoro-4-thiacapric acid (FTC2) **26** (see Figure 25). The products eluted, respectively, with retention times of ( $R_t$ ) 19:08 min and 14:14 min.

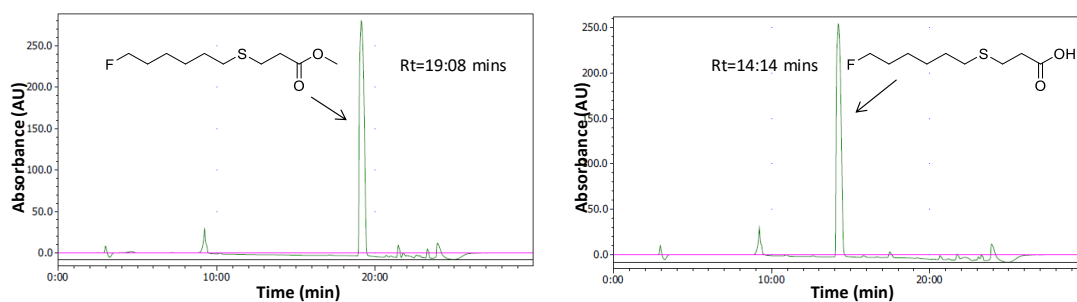


Figure 25: HPLC traces of fluorinated ester intermediate **25** and 10-fluoro-4-thiacapric acid (FTC2) **26**

## 2.6 Novel synthesis of 4-thiaoleic acid/methyl-4-thiaoleate derivatives

Oleate is a long chain fatty acid (18 carbon atoms), longer than palmitate by two carbon atoms and contains a double bond. As with palmitate, it has ideal properties for development as radiopharmaceutical agent<sup>117</sup> because of the chain length and degree of unsaturation.<sup>4</sup> Therefore, [<sup>18</sup>F]-18-fluoro-4-thiaoleic acid ([<sup>18</sup>F]FTO) is a potential optimised metabolically trapped fatty acid oxidation tracer. It has shown increased higher myocardial accumulate and excellent myocardial imaging compared to [<sup>18</sup>F]-16-fluoro-4-thiapalmitic acid ([<sup>18</sup>F]FTP)<sup>117</sup>.

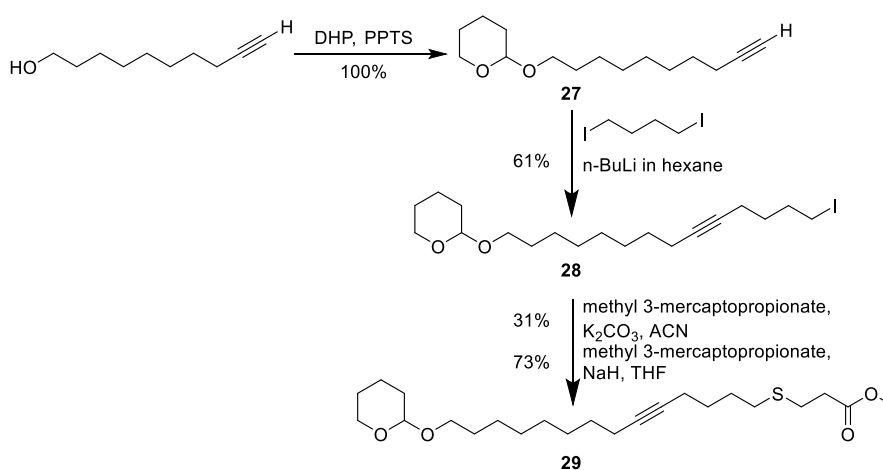
As mentioned before in section 2.1,<sup>117, 118</sup> two different synthetic route have previously been used to synthesise [<sup>18</sup>F]-4-thiaoleic acid radiolabeling precursors (bromo and tosyl). In this work, new synthetic routes were investigated to reduce the number of synthetic steps. Also, three different precursors (tosylate, iodo and bromide) were prepared to compare the precursor yield, number of synthetic steps and radiolabeling yield. The reference compound 18-fluoro-4-thiaoleic acid (FTO), was also synthesised.

### 2.6.1 Synthesis of methyl-18-tosyl-, methyl-18-bromo- or methyl-18-iodo-4-thiaoleate **32**, **33** and **34**

Tetrahydropyranyl (THP) was added to a solution of acetylenic alcohol and pyridinium *p*-toluenesulfonate (PPTS). PPTS is used as a weakly acidic catalyst in such reaction when a substrate is unstable to stronger acid catalysts. Protected dec-9-yn-1-ol **27** was produced as a colourless oil in 100% yield, consistent with that achieved by Goerger & Hudson<sup>137</sup> (see Scheme 23). The <sup>1</sup>H NMR spectrum showed the appearance of a characteristic triplet at  $\delta$  4.57 ppm corresponding to O-CH-O proton.

To extend the fatty acid chain, a novel synthetic route was developed, inspired by analogous functional group chemistry.<sup>138</sup> The acetylenic hydrogen atom can be easily removed by strong bases, such as *n*-BuLi, to give the acetylide anion. The protected dec-9-yn-1-ol **27** was deprotonated by addition of *n*-BuLi and then alkylated with

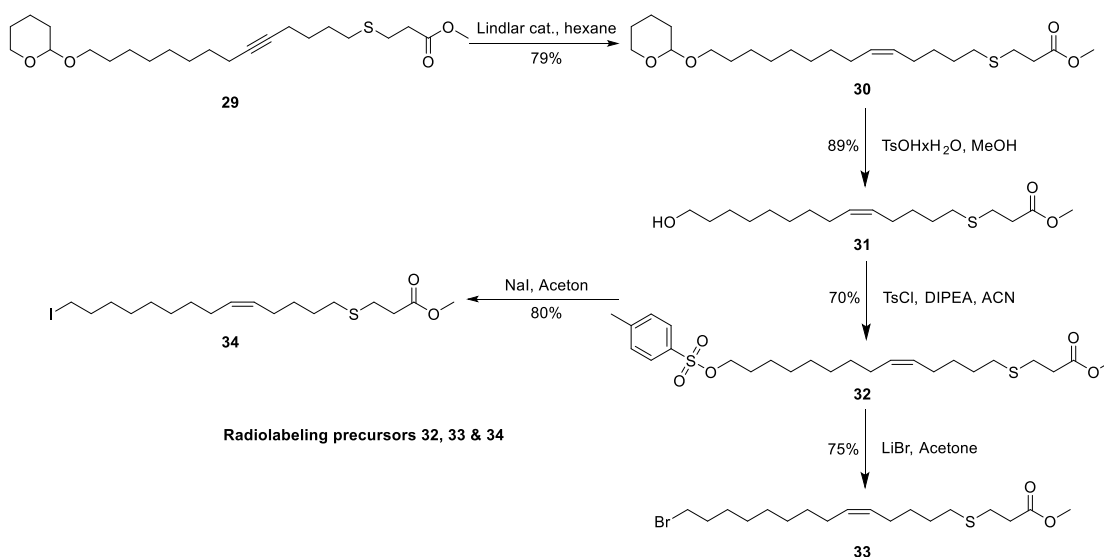
diiodobutane at room temperature overnight. After column chromatography purification the novel protected alkyne iodide **28** was isolated as a colourless oil in 61% yield (see Scheme 23). The  $^1\text{H}$  NMR showed disappearance of the triplet at  $\delta$  1.93 ppm characteristic of terminal alkyne and the appearance of a peak at  $\delta$  2.21-2.13 ppm for four protons  $\text{H}_2\text{C}\equiv\text{CH}_2$ .



Scheme 23: Synthesis of methyl 4-thiaoleate intermediate derivatives **27**, **28** and **29**

To synthesise novel methyl-4-thiaoleate derivatives (see Scheme 23), the compound **28** must be modified by insertion of a sulfur atom at position four in the alkyl chain. An alkylation reaction of **28** with methyl-3-mercaptopropionate gave the protected long chain 4-thiaoleate **29** in a 31% yield. Modification of the procedure to use sodium hydride increased the yield to 73%. The  $^1\text{H}$  NMR spectrum showed disappearance of a triplet at  $\delta$  3.21 ppm, characteristic of  $\text{CH}_2\text{-I}$ , and appearance of a singlet at  $\delta$  3.71 ppm, characteristic of the methyl ester.

Hydrogenation of alkyne **29** was performed using the Lindlar catalyst (5% Pd/ $\text{CaCO}_3$ ) to give the cis alkene **30** (see Scheme 24).<sup>139</sup> The addition of quinoline to the reaction mixture is necessary to prevent alkane formation. After column chromatography purification, the novel compound **30** was isolated as a colourless oil in 79% yield. The formation of **30** was characterised by the presence of a multiplet peak in the  $^1\text{H}$  NMR spectrum at  $\delta$  5.29 ppm for the two alkene protons ( $\text{HC}=\text{CH}$ ).



Scheme 24: Synthesis of methyl-18-tosyl-, methyl-18-bromo- or methyl-18-iodo-4-thiaoleate **32**, **33** and **34**

The THP protecting group was removed using *p*-toluenesulfonic acid.<sup>125</sup> The compound **31** (see Scheme 24) was purified by flash chromatography and isolated as a colourless oil in 89% yield. The reaction can be followed by TLC or by <sup>1</sup>H NMR (monitoring the disappearance of characteristic O-CH-O proton at  $\delta$  4.57 ppm) (see Scheme 24).

Tosylation of methyl-18-hydroxy-4-thiaoleate **31** was carried out and, after column chromatography purification, **32** was isolated as a colourless oil in 70% yield. The <sup>1</sup>H NMR spectrum showed the appearance of two characteristic multiplet peaks (one at  $\delta$  7.82 ppm for two protons (Ar-H) and another at  $\delta$  7.34 ppm for two protons (Ar-H)). The tosylate compound **32** was used to form the bromo and iodo derivatives (see Scheme 24).

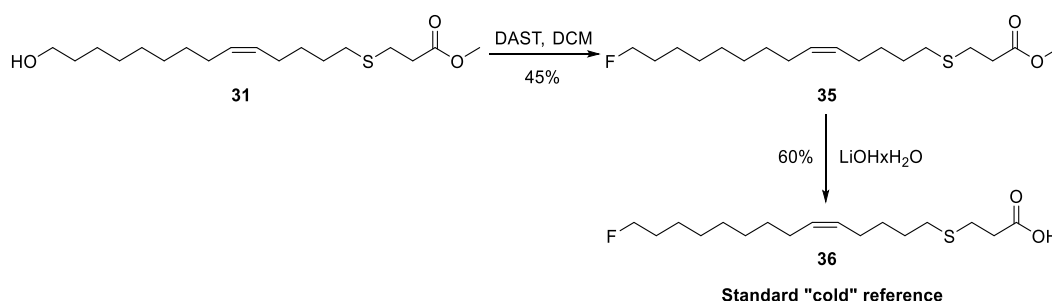
The bromo precursor **33** was synthesised by reacting methyl-18-tosyl-4-thiaoleate with LiBr, the crude product was purified by column chromatography, and **33** was isolated as a colourless oil in 75% yield (see Scheme 24). The product has been synthesised previously using a different synthetic route.<sup>117</sup> The formation of **33** was characterised by the presence of a triplet peak in the <sup>1</sup>H NMR spectrum at  $\delta$  3.42 ppm (CH<sub>2</sub>-Br).

Synthesis of a novel methyl-18-iodo-4-thiaoleate (**34**) was achieved by adding of NaI to the methyl-18-tosyl-4-thiaoleate.<sup>115</sup> After column chromatography purification, **34** was isolated as a colourless oil in 80% yield (see Scheme 24).

## 2.6.2 Synthesis of 18-fluoro-4-thiaoleic acid (FTO) **36**

The synthesis of the HPLC reference for radiochemistry, was carried out using a nucleophilic substitution reaction. The methyl-18-hydroxy-4-thiaoleate **31** was fluorinated directly by adding of diethylaminosulfur trifluoride (DAST). The fluorinated compound **35** was purified by column chromatography and isolated as a colourless oil in 45% yield (see Scheme 25). The formation of the product was confirmed by <sup>1</sup>H NMR with the appearance of a doublet of triplets at  $\delta$  4.43 ppm (CH<sub>2</sub>-F).

18-Fluoro-4-thiaoleate was hydrolysed with LiOH to give **36** in 60% yield, as shown in the <sup>1</sup>H NMR with the disappearance of the singlet at  $\delta$  3.70 ppm, characteristic of the methyl ester.



Scheme 25: Synthesis of 18-fluoro-4-thiaoleic acid (FTP) **36**

### 2.6.3 HPLC identification of methyl 18-fluoro-4-thiaoleate **35** and 18-fluoro-4-thiaoleic acid (FTO) **36**

HPLC conditions for the reference compounds **35** and **36** were developed (see Figure 26). Products eluted, respectively, with a retention time ( $R_t$ ) 22:28 min and 18:45 min.

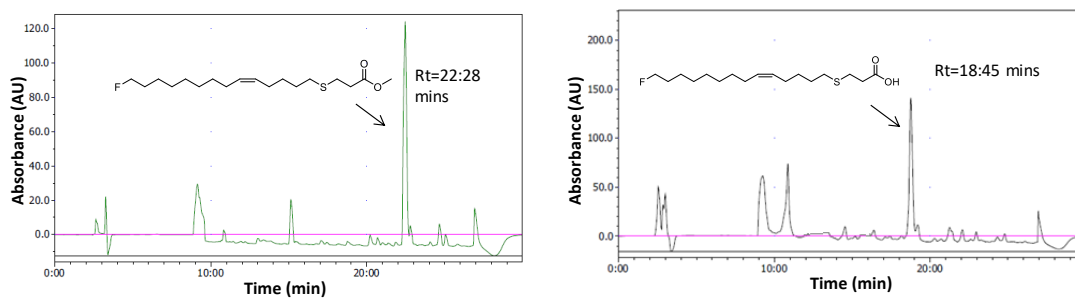


Figure 26: HPLC traces of fluorinated ester intermediate **33** and 18-fluoro-4-thiaoleic acid (FTO) **34**

## 2.7 Conclusions

This chapter details the synthesis of radiolabeling precursors and fluorinated reference compounds for two types of thia-fatty acids; medium chain thia-fatty acids (thiacaprylic acid FTC1, 8 carbon atoms and thiacapric acid FTC2, 10 carbon atoms) and long-chain thia-fatty acids (thiapalmitic acid FTP, 16 carbon atoms and thiaoleic acid FTO, 18 carbon atoms).

Novel synthetic strategies were investigated and protocols were optimised in order to improve yields or to facilitate purification. Novel radiolabeling precursor **18** and “cold” reference standard **21** for 4-thiacaprylic acid (FTC1) were prepared. New synthesis routes to produce radiolabeling precursors (tosyl **32**, bromo **33** and iodo **34**) and “cold” reference standard **36** for thiaoleic acid (FTO) were developed. Thiapalmitic acid (FTP) and thiacapric acid (FTC2) were produced together with iodo and bromo methyl ester precursors (**2**, **3** and **22**, **23**) respectively. “Cold” reference standards have also been successfully synthesised using modifications of the published methods (see Table 3). Tetrahydropyranyl (THP) and dimethyl-*tert*-butylsilyl (TBDMS) groups were investigated as protecting groups for the terminal alcohol group with THP preferred. Two alkylation protocols were explored to access to 4-thia-fatty acid derivatives.

HPLC methods were developed and retention times determined for the fluorinated ester intermediate and “cold” reference standard for all of the synthesised thia-fatty acid compounds.



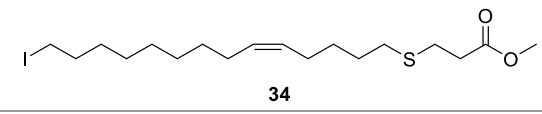
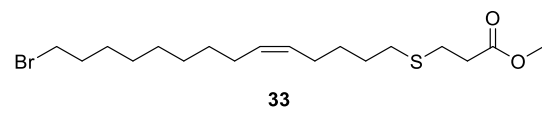
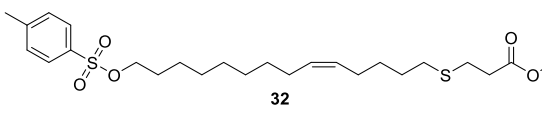
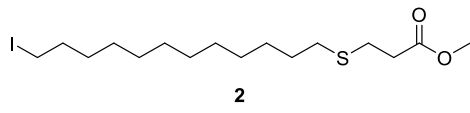
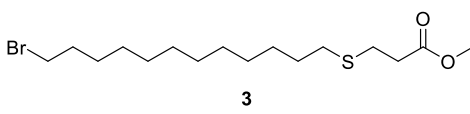
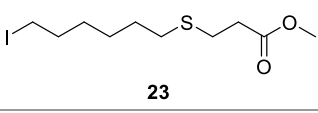
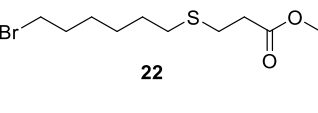
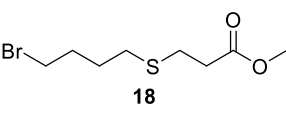
Tracers	Radiolabeling precursors	Synthetic steps No.	Overall yield %	Ref.
$[^{18}\text{F}]\text{FTO}$	 34	Six steps	18%	Novel compound
	 33	Six steps	16%	Novel synthetic route to known compound
	 32	Five steps	22%	Novel synthetic route to known compound
$[^{18}\text{F}]\text{FTP}$	 2	Two steps	14%	Standard synthetic route to known compound <sup>115</sup>
	 3	One step	41%	Standard synthetic route to known compound <sup>4</sup>
$[^{18}\text{F}]\text{FTC2}$	 23	One step	31%	Novel compound
	 22	One step	28%	Novel synthetic route to known compound <sup>136</sup>
$[^{18}\text{F}]\text{FTC1}$	 18	Six steps	0.19%	Novel compound

Table 3: Molecular structures and yields for radiolabeling precursors

# **Chapter Three**

## **Radiosynthesis and preclinical PET/CT imaging of $^{18}\text{F}$ -thia-fatty acids**

## Chapter Three: Radiosynthesis and preclinical PET/CT imaging of $^{18}\text{F}$ -thia-fatty acids

### 3.1 Introduction

The first thia-fatty acid tracer developed was [ $^{18}\text{F}$ ]-14-fluoro-6-thiaheptadecanoic acid [ $^{18}\text{F}$ ]FTHA, a 17 carbon fatty acid analogue. DeGrado *et al.*<sup>140</sup> showed accumulation of [ $^{18}\text{F}$ ]FTHA in the mouse heart, where it is metabolised to a protein-bound species which is a metabolic by-product from  $\beta$ -oxidation. [ $^{18}\text{F}$ ]FTHA was then approved for clinical use and has been applied in various studies to assess the long chain fatty acid  $\beta$ -oxidation rate. One such clinical study, showed an increase in uptake of [ $^{18}\text{F}$ ]FTHA in patients with heart failure (see Figure 27).<sup>31</sup>

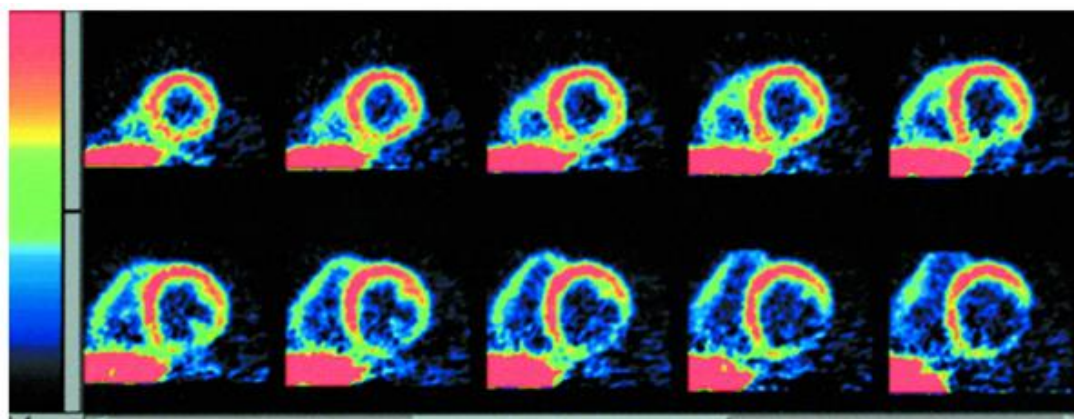


Figure 27: Representation of cardiac uptake of [ $^{18}\text{F}$ ]FTHA in patients<sup>31</sup>

However, [ $^{18}\text{F}$ ]FTHA uptake and metabolic trapping are not hypoxia-sensitive which disagrees with the expectation that a lower level of oxygen should result in reduced  $\beta$ -oxidation.<sup>141</sup> This may be due to the myocardial retention of the radiotracer resulting in accumulation despite a reduction of  $\beta$ -oxidation.<sup>115, 141</sup> Analysis has shown that the metabolites of [ $^{18}\text{F}$ ]FTHA predominantly accumulated in liver and skeletal muscle tissues in lipid pools which limits its application as a general mitochondrial fatty acid oxidation probe.<sup>4</sup>

This has led to the development of new thia-fatty acid analogue compounds. The second radiotracer developed was [ $^{18}\text{F}$ ]-16-fluoro-4-thiapalmitic acid ([ $^{18}\text{F}$ ]FTP). [ $^{18}\text{F}$ ]FTP has increased specificity for myocardial fatty acid oxidation, correlating with

fatty acid oxidation rates of natural fatty acids in the hypoxic state.<sup>142</sup> Unfortunately, it showed poor myocardial retention as “trapped metabolite” in rat myocardium over a 2 h period. Also, the uptake of [<sup>18</sup>F]FTP was not sensitive to carnitine palmitoyltransferase I (CPT-I) inhibition as would be expected (see Figure 28).<sup>115, 142</sup>

As a result, [<sup>18</sup>F]-18-fluoro-4-thiaoleic acid ([<sup>18</sup>F]FTO) was developed. [<sup>18</sup>F]FTO showed increased cardiac uptake and myocardial retention in rat myocardium (see Figure 28), and the myocardial uptake of [<sup>18</sup>F]FTO was decreased on treatment with a CPT-I inhibitor, showing excellent sensitivity to alterations in myocardial fatty acid oxidation.<sup>115, 117</sup> Pandey *et al.*<sup>4</sup> believed that increase the cardiac uptake and retention in myocardium is due to the presence of a double bond and the longer chain length. In the other words, the alterations in structure for [<sup>18</sup>F]FTO are responsible for its favourable cardiac uptake properties.

As the structure of the thia-fatty acid analogue is of key importance, properties may be further optimised by further structural modifications of the thia-fatty acids.<sup>4</sup> [<sup>18</sup>F]-18-fluoro-4-thiastearic acid ([<sup>18</sup>F]FTS) and [<sup>18</sup>F]-18-fluoro-6-thiastearic acid ([<sup>18</sup>F]F-6-TS) were synthesised and examined in comparison with [<sup>18</sup>F]FTP and [<sup>18</sup>F]FTO. The results showed that the chain length has an effect on cardiac uptake ([<sup>18</sup>F]FTP vs. [<sup>18</sup>F]FTS), as does the sulfur atom position ([<sup>18</sup>F]F-6-TS vs. [<sup>18</sup>F]FTS), and the presence of a double bond ([<sup>18</sup>F]FTO vs. [<sup>18</sup>F]F-6-TS) (see Figure 28).<sup>4</sup>

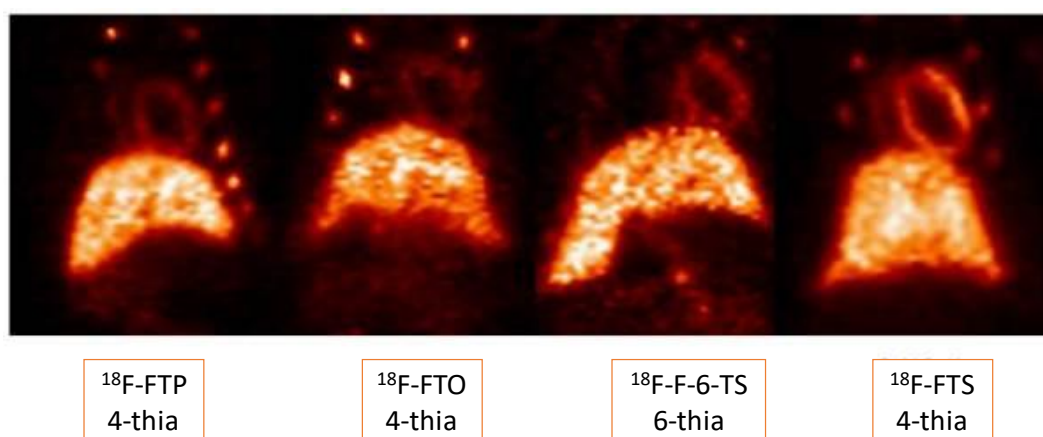


**Figure 28: Representative micro-PET images of thia-fatty acid tracers at 55–115 min<sup>4</sup>**

## 3.2 Aims and objectives

The main aim of the research reported in this chapter is the radio-fluorination of precursors synthesised in chapter two to produce 10- $^{18}\text{F}$ -fluoro-4-thiacapric acid ( $^{18}\text{F}$ FTC2),  $^{18}\text{F}$ -16-fluoro-4-thiapalmitic acid ( $^{18}\text{F}$ FTP) and  $^{18}\text{F}$ -18-fluoro-4-thiaoleic acid ( $^{18}\text{F}$ FTO) (see Figure 29). The stability of these radiotracers was tested in serum and uptake/retention in the myocardium investigated *in vivo* using PET/CT in rat or mouse models to provide a basis for rational design of PET imaging probes for FAO.

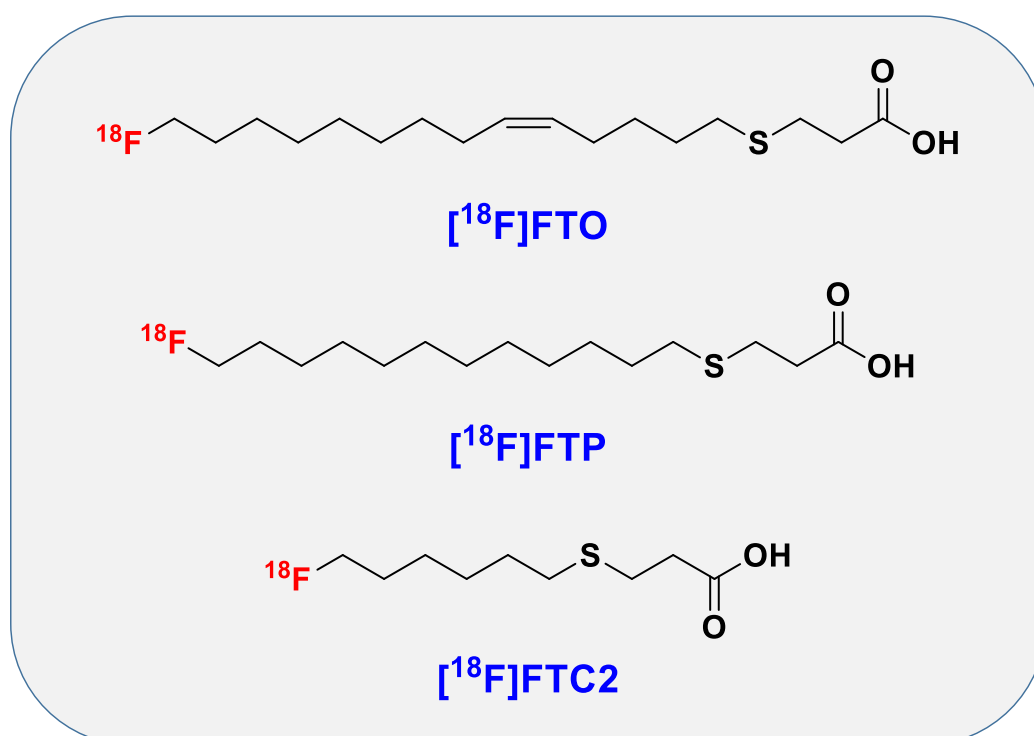


Figure 29: Molecular structures of target compounds

### 3.3 General radiolabeling method for fatty acid probe precursors

Fluorine-18 is by far the most frequently utilised PET-isotope in nuclear medicine. Fluorine-18 nucleophilic substitution reactions with [<sup>18</sup>F]fluoride are routinely used to produce the commonly used <sup>18</sup>F PET radiotracers.<sup>80</sup> A preclinical PET/CT study requires labeling of biological active compounds such as fatty acid or glucose with a positron imaging radionuclide such as fluorine-18 (see Figure 30).

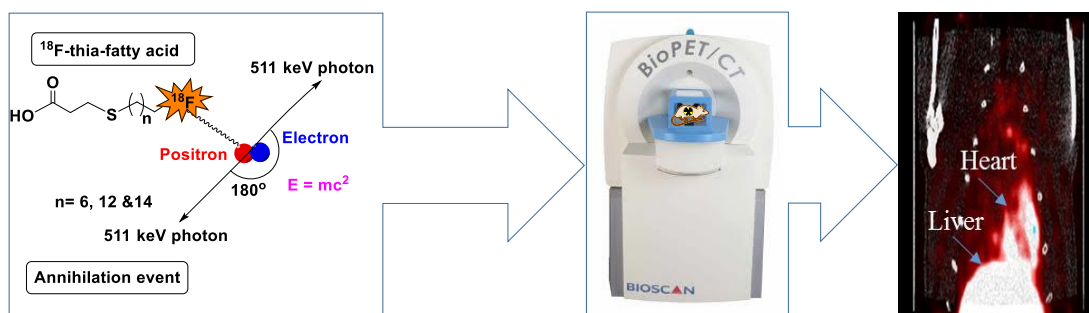


Figure 30: <sup>18</sup>F-thia-fatty acid is administered to a rat to generate a PET/CT image of fatty acid metabolism

Figure 31 shows the steps in the preparation of a radiotracer that need to be carried out (and tested in advance) with focus on production methods for a thia-fatty acid tracer. Radiotracers are typically administered intravenously for *in vivo* studies and so the radiotracer should not only be radiochemically pure but also sterile and free from pyrogens.<sup>143, 144</sup>

The development of a rapid and efficient radiosynthesis is often highly dependent on the availability of suitably radiolabeling precursor (in this case a thia-fatty acid precursor compound) and suitable HPLC conditions from “cold” reference standard compounds.

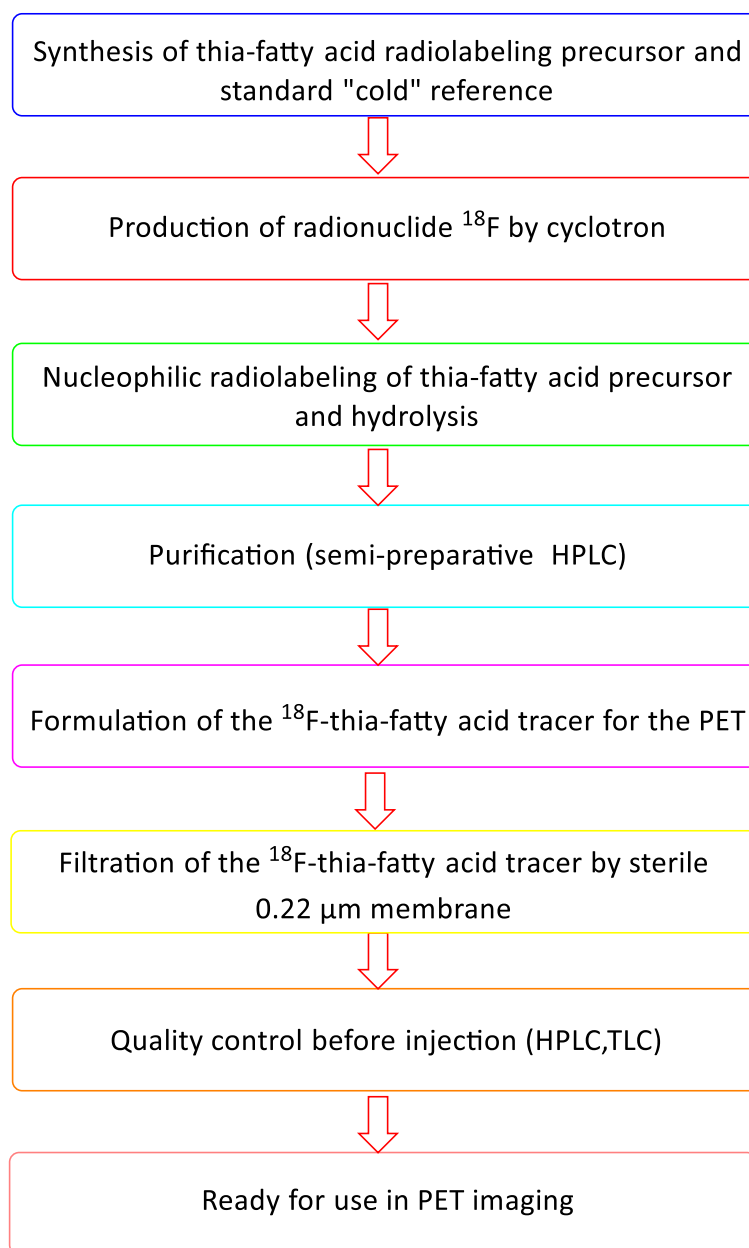


Figure 31: Schematic summary of the major steps in developing a routine preparation of a [<sup>18</sup>F]thia-fatty acid tracers

Production of [<sup>18</sup>F] fluoride in a cyclotron *via* a reaction  $^{18}\text{O}(p,n)^{18}\text{F}$  nuclear reactions is the first step in the use of fluorine-18 and an acceptable amount of radioactivity must be allocated (0.7-2.2 GBq is appropriate) for these reactions.<sup>145</sup> Syntheses of [<sup>18</sup>F]thia-fatty acid tracers typically involve two purification steps to separate the desired labeled product from radiochemical impurities. Firstly, semi-preparative high-performance liquid chromatography (HPLC), and, secondly, solid-phase extraction (SPE) methods. The SPE cartridges are made of materials such as octadecyl

bonded silica gel (C-18) or ion exchange resins, and are used for purification and formulation of the final product.<sup>146</sup> It is vital to carry out radiochemical quality control (QC) of the radiotracers before administration. QC is typically performed out using chromatographic techniques that have high sensitivity and chemical resolution, such as radio-HPLC or radio-TLC.

### 3.3.1 Radiosynthesis of [<sup>18</sup>F]fluoro-4-thia-fatty acids ([<sup>18</sup>F]FTC2, [<sup>18</sup>F]FTP and [<sup>18</sup>F]FTO)

The radiosynthetic procedures to produce [<sup>18</sup>F]16-fluoro-4-thiapalmitic acid ([<sup>18</sup>F]FTP), [<sup>18</sup>F]10-fluoro-4-thiacapric acid ([<sup>18</sup>F]FTC2) and [<sup>18</sup>F]18-fluoro-4-thioleic acid ([<sup>18</sup>F]FTO) were developed by modifying procedures from the work of DeGrado *et al.*<sup>117</sup> and Li and Conti.<sup>10</sup> First of all, to avoid contamination of the reaction and to remove the bulk [<sup>18</sup>O]H<sub>2</sub>O, the [<sup>18</sup>F]fluoride must be isolated. It is strongly solvated in water due to strong hydrogen bonding and, therefore, is inactive as a nucleophile.<sup>147, 148</sup> Thus, [<sup>18</sup>F]fluoride was trapped on a pre-activated weak anion exchange cartridge (QMA Light) by addition of the aqueous solution containing the radioisotope, the cartridge was then air-dried and the [<sup>18</sup>F]fluoride eluted with a solution of K<sub>2</sub>CO<sub>3</sub> in acetonitrile/ aqueous solution (see Figure 32).

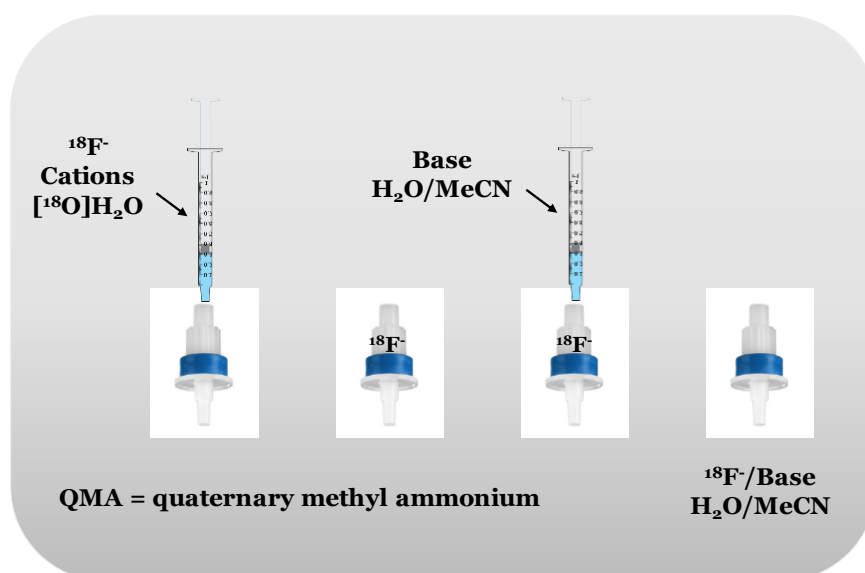
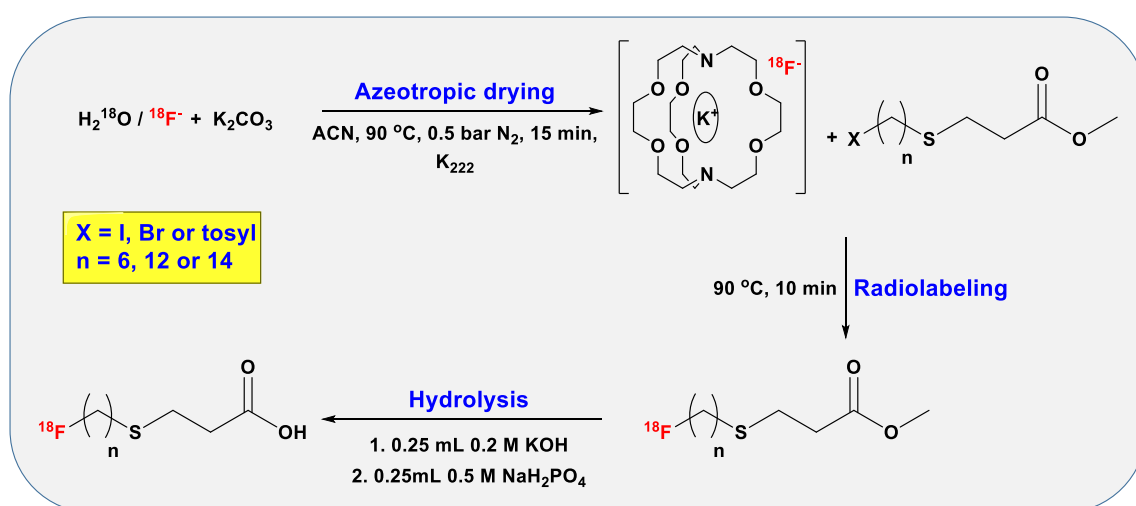


Figure 32: Isolation of the [<sup>18</sup>F]fluoride



The  $[^{18}\text{F}]$ fluoride ion forms a strong interaction with the positively charged ion ( $\text{K}^+$ ), hence it is important to weaken this interaction (and improve the reactivity of the fluoride) by coordination of the metal ion by the cryptand Kryptofix ( $\text{K}_{222}$ ) (see Scheme 26).<sup>2</sup>  $\text{K}_{222}$  (one eq. to  $\text{K}^+$ ) was added, dissolved in acetonitrile, to the  $[^{18}\text{F}]$ fluoride/ potassium carbonate solution and the mixture was dried with heating under a stream of argon. To ensure removal of water acetonitrile was added and the azeotropic drying procedure was repeated twice (overall this takes 15-20 min). The three thia-fatty acid compounds,  $[^{18}\text{F}]$ FTP,  $[^{18}\text{F}]$ FTC2 and  $[^{18}\text{F}]$ FTO, can be prepared in two steps from their respective precursors. In the first step, the leaving group on the precursor is replaced by  $[^{18}\text{F}]$ fluoride and, in the second step, ester is hydrolysed to give the carboxylic acid. The iodo, bromo or tosyl precursors were dissolved in anhydrous acetonitrile and added to the dried  $[^{18}\text{F}]\text{KF}/\text{K}_{222}$  complex and the reaction mixture was heated in a closed vial at  $90^\circ\text{C}$  for 10 min. The fluorination reactions were analysed by radio-TLC and analytical HPLC to monitor reaction progress. Then, the reaction vial was cooled down to room temperature, and 0.2 M KOH was added to hydrolyse the ester, and the reaction mixture was heated at  $90^\circ\text{C}$  for 5 min. The reaction was quenched by addition of 0.5 M  $\text{NaH}_2\text{PO}_4$  and the crude mixture was purified by semi-preparative HPLC using a gradient elution (see Scheme 26).



Scheme 26: Radiosynthesis of  $[^{18}\text{F}]$ (10, 16 or 18)-fluoro-4-thia(capric, palmitic or oleic) acid ( $[^{18}\text{F}]$ FTC2,  $[^{18}\text{F}]$ FTP or  $[^{18}\text{F}]$ FTO)

The fluorinated ester and acid compounds are lipophilic and do not move on a C18 stationary phase until the eluent has 70-80% acetonitrile content. High water content (80-90%) is used at the start of the HPLC run to elute any unreacted fluoride, followed by an increase in acetonitrile percentage to subsequently elute the thia-fatty acid derivatives. The same gradient was used for both, analytical and semi-preparative HPLC. The radiotracer is eluted in a large volume of a solvent containing acetonitrile which is not biocompatible. Thus, for *in vivo* administration, the [<sup>18</sup>F]thia-fatty acid containing fraction was trapped on a solid phase extraction cartridge and the acetonitrile was replaced by ethanol (or another biocompatible solvent). To achieve this, the radiotracer containing fraction was with water and loaded on the C18 cartridge. Then, the cartridge was washed with water and dried with compressed air prior to elution of the product. The solution containing the radiolabeled product was evaporated under a stream of argon at RT and it was then re-suspended in a 3% albumin solution in isotonic saline and filtered through a syringe filter into an Eppendorf tube for administration. For quality control, 10 µL of the formulated tracer was mixed with 0.5 mL of acetonitrile (to precipitate the albumin), centrifuged and the supernatant analysed by radio-HPLC.

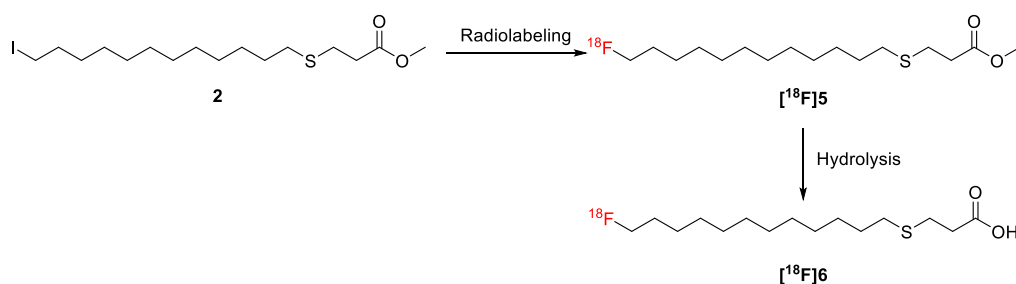
### 3.3.2 Stability in Serum

High radiotracer stability to defluorination is crucial for a compound to be useful as an imaging agent. The stability of radiotracer in serum can give an indication of the properties *in vivo*. If released, [<sup>18</sup>F]fluoride is taken up by bone due to the high affinity for hydroxyapatite in bone. The stability of [<sup>18</sup>F]thia-fatty acid in human serum was determined *in vitro*, the approach chosen in this work is based on modification of the method reported by Al Jammaz *et al.*<sup>149</sup> The [<sup>18</sup>F]thia-fatty acid was incubated with human serum at 37°C for up to 3 hours with analysis by radio-HPLC at a number of time points.

### 3.4 [<sup>18</sup>F]-16-fluoro-4-thiapalmitic acid ([<sup>18</sup>F]FTP)

#### 3.4.1 Radiosynthesis of [<sup>18</sup>F]-16-fluoro-4-thiapalmitic acid ([<sup>18</sup>F]FTP) [<sup>18</sup>F]6

As [<sup>18</sup>F]-16-fluoro-4-thiapalmitic acid ([<sup>18</sup>F]FTP) has been previously reported,<sup>115</sup> it was selected as the first molecule to radiolabel. The iodo precursor 16-iodo-4-thiapalmitate **2** was radiolabeled ([<sup>18</sup>F]**5**) and hydrolysed to produce [<sup>18</sup>F]**6** in a 120 min total synthesis time (see Scheme 27).



Scheme 27: Radiosynthesis of [<sup>18</sup>F]FTP/[<sup>18</sup>F]**6** from the iodo precursor (methyl 16-iodo-4-thiapalmitate **2**)

Radiolabeling efficiency was studied at 75°C and 90°C, assessing fluorine-18 and [<sup>18</sup>F]**5** ratios at different time points by radio-TLC. At 75°C, the yield of [<sup>18</sup>F]**5** steadily increases from 6% (5 min) to 19% (30 min). At 90°C, the yield of [<sup>18</sup>F]-FTP-OMe [<sup>18</sup>F]**5** is steady at around 60% for the first few measurements and then declines to 37% at 30 min time point, indicating thermal decomposition of the fluorinated ester (see Figure 33). Based on these findings, the radiolabeling reaction was carried at 90°C for 10 min. Apart from temperature and reaction time, the amount of activity used also influences the fluorine-18 incorporation efficacy. The amount of activity used in this work varied from 678 MBq to 1180 MBq, to give fluorine-18 incorporation of 63±8%.

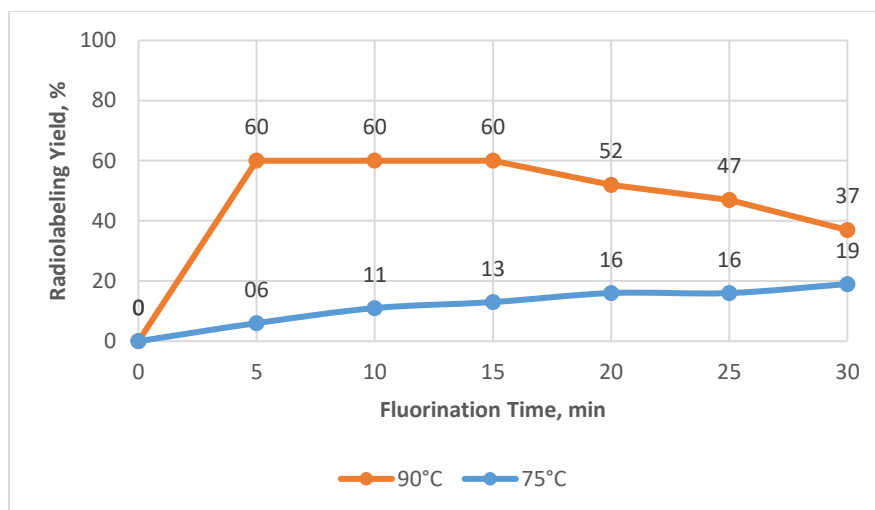


Figure 33: Study of radiolabeling efficiency to form  $[^{18}\text{F}]\mathbf{5}$  at 75°C and 90°C, n=1

Studies on the hydrolysis step have been carried out by sampling reaction mixture every minute for the first 5 min and then every 3 min until 15 min by quenching the aliquots with  $\text{NaH}_2\text{PO}_4$  buffer solution. However, the results from the TLC and HPLC analyses were not consistent. Moreover, the quenching was not efficient and hydrolysis continued even after the addition of the buffer (data not shown). Therefore, the hydrolysis step was run at 90°C for 5 min, ensuring complete hydrolysis without noticeable degradation. Before proceeding to the hydrolysis step, removal of unreacted  $[^{18}\text{F}]$ fluoride was carried out by passing the reaction mixture through a Silica Lite cartridge. Figure 34 and Figure 35 are present distribution of radioactive products as revealed by radio-TLC and radio-HPLC, respectively. Figure 34 shows that the unreacted fluorine-18 was decreased from 40% to 18.9% according to radio-TLC

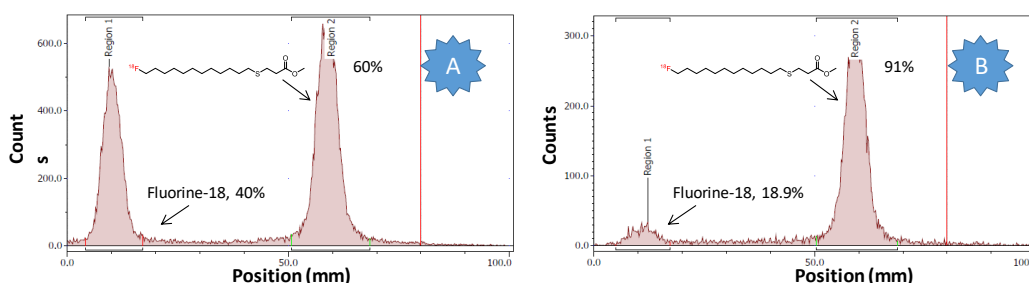


Figure 34: Radio-TLC traces of  $[^{18}\text{F}]\mathbf{5}$  A: without using Silica Lite cartridge; B: with using Silica Lite cartridge

However, Figure 35 shows that the unreacted fluorine-18 was decreased from 40% to 9% according to radio-HPLC. Also, radio-HPLC suggests that some hydrolysis takes place during fluorination step, with a peak for  $[^{18}\text{F}]\mathbf{6}$  at 12:57 min. Therefore, the overall yield may be reduced by using silica cartridge purification, as it could remove some of the deprotected acid as well as the unreacted  $[^{18}\text{F}]\text{fluoride}$ .

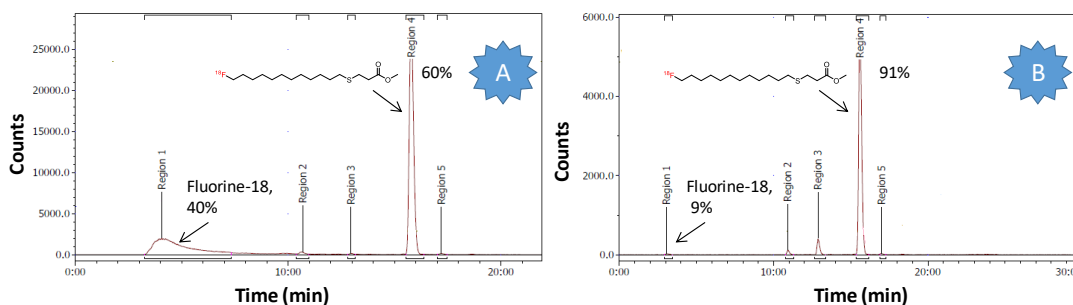


Figure 35: Radio-HPLC traces of  $[^{18}\text{F}]\mathbf{5}$  A: without cartridge purification; B: using Silica Lite cartridge

It was found that radio-TLC analysis with acetonitrile as eluent is less accurate than radio-HPLC for reaction monitoring after hydrolysis step (if unreacted  $[^{18}\text{F}]\text{fluoride}$  had not been removed beforehand) because it is not capable of separating free fluoride from fluorinated acid or some by-products of fluorination (see Figure 36).

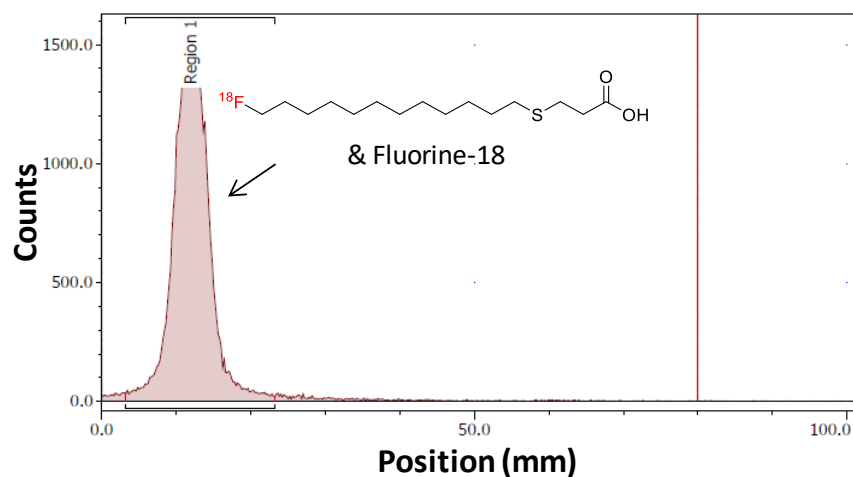


Figure 36: Radio-TLC trace of  $[^{18}\text{F}]\mathbf{6}$  with using Silica Lite cartridge, mobile phase pure acetonitrile

Other mobile phases were tested to find conditions (DCM: MeOH (9: 1)) that separated [ $^{18}\text{F}$ ]**6** from unreacted [ $^{18}\text{F}$ ]fluoride (see Figure 37).

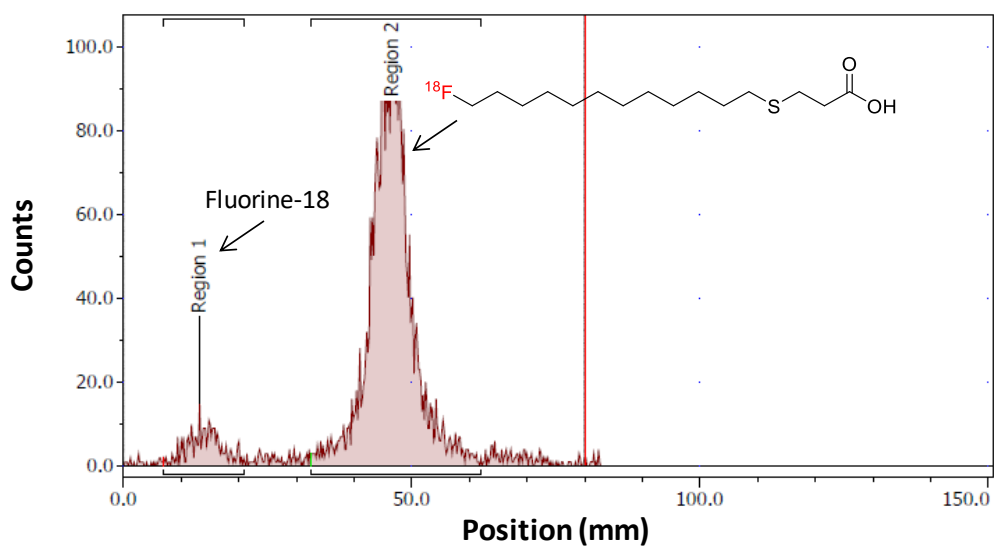


Figure 37: Radio-TLC trace of [ $^{18}\text{F}$ ]**6** with using Silica Lite cartridge, mobile phase DCM: MeOH (9: 1)

Radio-TLC is useful as it can be carried out more rapidly than radio-HPLC. The radio-HPLC chromatogram after hydrolysis (see Figure 38) shows a change in retention time to 12:57 min and the disappearance of the peak for [ $^{18}\text{F}$ ]**5**, indicating that the hydrolysis step is complete.

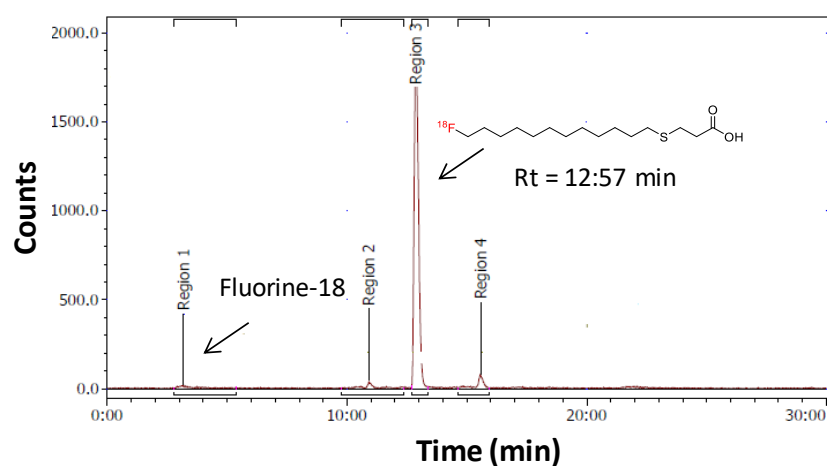


Figure 38: Radio-HPLC trace of [ $^{18}\text{F}$ ]**6** using a Silica Lite cartridge

Radiolabeled [ $^{18}\text{F}$ ]fluorothiopalmitic acid crude was purified by semi-preparative HPLC (see Figure 39) with [ $^{18}\text{F}$ ]**6** eluting from 10:50 to 12:22 min. All fractions were collected and the activity contained in each fraction measured.

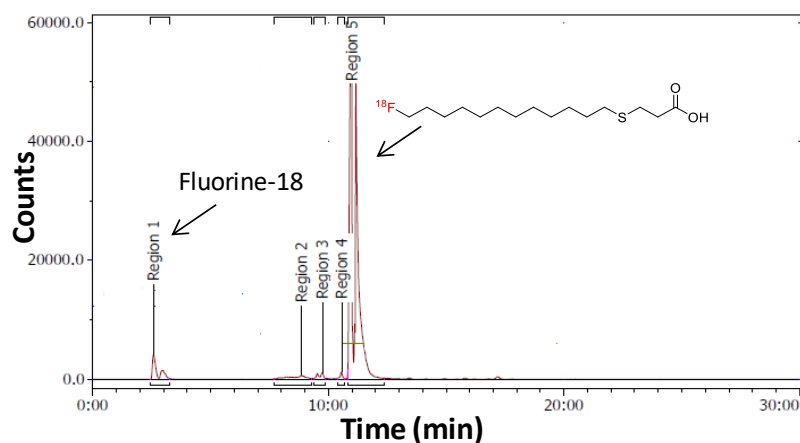


Figure 39: Radio-HPLC trace of semi-preparative purification of [ $^{18}\text{F}$ ]**6**

[ $^{18}\text{F}$ ]FTP is eluted in a large volume of a solvent containing acetonitrile, which is not biocompatible. Thus, for *in vivo* administration, [ $^{18}\text{F}$ ]FTP containing fraction was prepared as discussed in section 3.3.1, using an Oasis C18 cartridge without a noticeable loss of activity (< 3%). The literature report on this compound<sup>117</sup> describes a formulation containing ethanol and bovine serum albumin (BSA). However, using ethanol with [ $^{18}\text{F}$ ]FTP was shown to result in ester formation (see Figure 40). To avoid this and to speed up the evaporation of the collected fraction, ethanol was replaced by diethyl ether which showed a similar elution efficiency (71%, 2 mL). After efficient evaporation of the ether solution, [ $^{18}\text{F}$ ]FTP was prepared into an injectable formulation with 3% BSA in isotonic saline. This reduced reformulation time from 20 min down to 5 min.

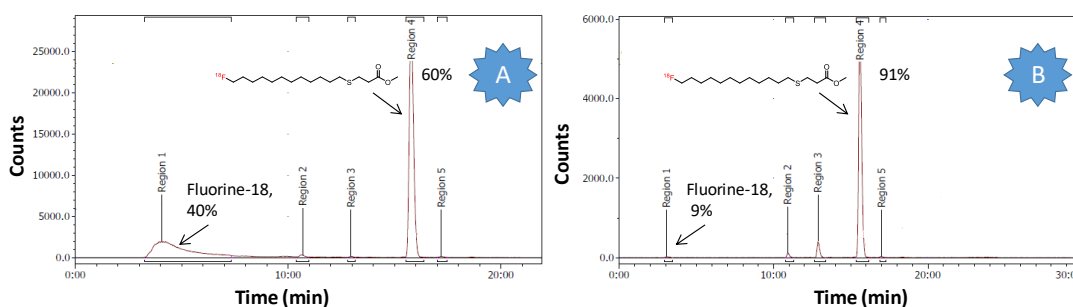


Figure 40: Radio-HPLC traces of [ $^{18}\text{F}$ ]FTP-OH [ $^{18}\text{F}$ ]**6** eluted from Oasis C18 cartridge A: with ethanol; B: with diethyl ether

[ $^{18}\text{F}$ ]FTP (50-100 MBq/500  $\mu\text{L}$  in the formulated solution) has been prepared in a sufficiently high activity for *in vivo* administration with an overall decay corrected

yield of  $18 \pm 1.2$  %. HPLC analysis of the final formulation showed radiochemical purity  $> 95\%$  (see Figure 41).

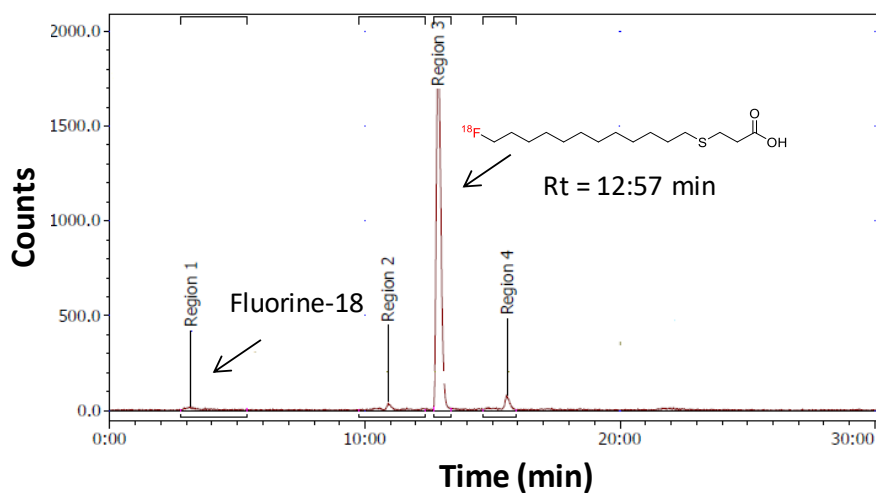


Figure 41: Radio-HPLC trace of  $[^{18}\text{F}]\mathbf{6}$  analysis of the final formulation

The degradation of the  $[^{18}\text{F}]16$ -fluoro-4-thiapalmitic acid ( $[^{18}\text{F}]\text{FTP}$ ) was investigated in human serum *in vitro* by HPLC analysis showing that it was stable ( $> 95\%$ ) during incubation at  $37^\circ\text{C}$  at up to 3 hours.

### 3.4.2 Preliminary preclinical evaluation of $[^{18}\text{F}]16$ -fluoro-4-thiapalmitic acid ( $[^{18}\text{F}]\text{FTP}$ ) $[^{18}\text{F}]\mathbf{6}$

All PET /CT imaging studies were carried out under the project licence of Dr Anne Marie Seymour and supervised by Dr Chris Cawthorne. The imaging studies and data processing were carried out by Rob Atkinson, Faisal Nuhu and Shubhanchi Nigam. PET/CT imaging of  $[^{18}\text{F}]\text{FTP}$   $[^{18}\text{F}]\mathbf{6}$  was carried out in nude mice ( $n = 2$ ).  $[^{18}\text{F}]\text{FTP}$  (5.61 MBq) was injected into the tail vein and data were acquired for 90 minutes in the preclinical scanner. Following reconstruction, the region of interest (ROI) analysis of the heart was performed. Interestingly, no significant cardiac uptake or accumulation of  $[^{18}\text{F}]\text{FTP}$  was observed. The main organs of uptake were liver, kidney, brown fat and, in the later time points, paraspinal muscle (see Figure 42).



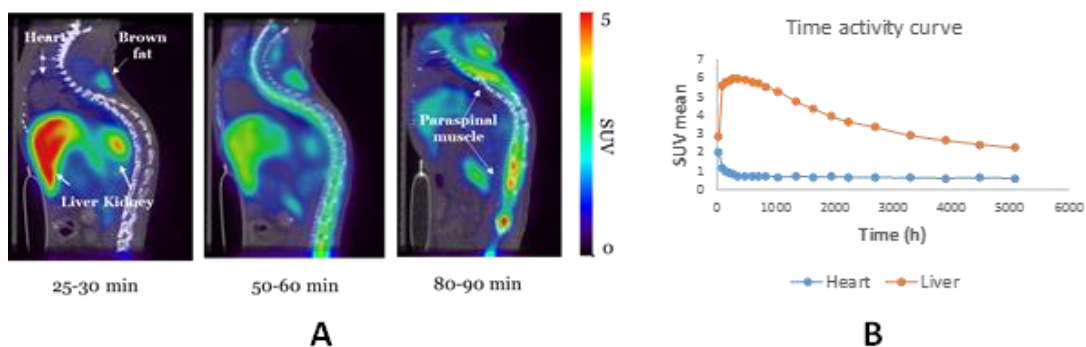


Figure 42: A. Sagittal PET-CT image of  $[^{18}\text{F}]$ FTP accumulation in nude mouse at different time points, B.  $[^{18}\text{F}]$ FTP liver and cardiac accumulation profile

Previous reports in the literature<sup>4, 110, 117, 142, 150</sup> which study the cardiac uptake of  $[^{18}\text{F}]$ FTP,  $[^{18}\text{F}]$ FTO,  $[^{18}\text{F}]$ FTS and  $[^{18}\text{F}]$ F-6-TS *in vivo* by PET used rats as the animal model. Cai *et al.*<sup>118</sup> used mice to study the cardiac uptake of  $[^{18}\text{F}]$ FTO, which showed sufficient uptake for visualisation of the myocardium in mice, although the preliminary metabolism data suggests that only a fraction of the uptake was due to fatty acid  $\beta$ -oxidation. The cardiac uptake for  $[^{18}\text{F}]$ FTHA was also studied in mice and humans, The results indicate metabolic trapping of  $[^{18}\text{F}]$ FTHA in myocardium subsequent to its entry into the mitochondria.<sup>31, 140</sup>

Cicone *et al.*<sup>151</sup> confirmed that key differences could be observed between different rodent animal models. Rats are more commonly used than mice for cardiac imaging. Mice have small heart dimensions and the heart rate is fast, this is challenging to image and also the energy demand will be increased.

Based on the low cardiac uptake observed in this work in mouse models, other animal models were utilised to study the accumulation of tracer as PET probes of fatty acid oxidation (FAO). Cardiac uptake for  $[^{18}\text{F}]$ FTP was determined *in vivo* in a male Sprague–Dawley rat (n=3). Rats was anaesthetized with isoflurane and  $[^{18}\text{F}]$ FTP (12.29 MBq) was injected into the tail vein and data were acquired for 90 minutes in the PET/CT scanner. Following data acquisition, and reconstruction, the region of interests (ROI) were analysed for the heart. Figure 43 shows an image of the cardiac uptake of the tracer (or  $[^{18}\text{F}]$ metabolite) after intravenous administration of  $[^{18}\text{F}]$ FTP

at 80-90 minutes after injection. The highest uptake was seen in liver, followed by the heart (see Figure 43).

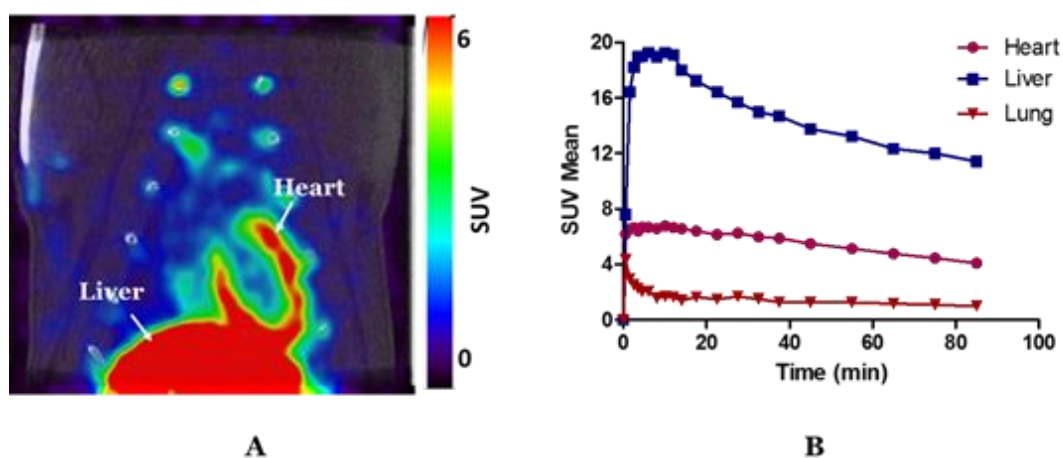


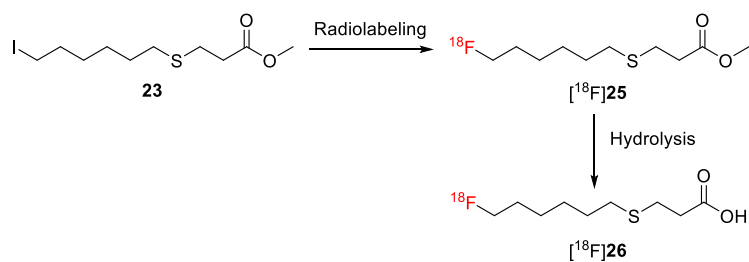
Figure 43: A: Coronal maximum intensity projection images acquired 80-90 min post iv administration of  $[^{18}\text{F}]\text{FTP}$ . B: Time activity curves showing uptake of the tracer in indicated organs

The dynamic quantification of  $[^{18}\text{F}]\text{FTP}$  uptake in the heart (see Figure 43) was analysed (left side of the heart). The mean standard uptake value (SUV Mean) at 10 min was compared with previously published work by Degrado *et al.*<sup>117</sup> and showed consistency. In both rat imaging studies, the long chain tracer  $[^{18}\text{F}]\text{FTP}$  shows significant cardiac uptake.

### 3.5 $[^{18}\text{F}]\text{10-fluoro-4-thiacapric acid } ([^{18}\text{F}]\text{FTC2}) [^{18}\text{F}]\mathbf{26}$

#### 3.5.1 Radiosynthesis of $[^{18}\text{F}]\text{-10-fluoro-4-thiacapric acid } ([^{18}\text{F}]\text{FTC2}) [^{18}\text{F}]\mathbf{26}$

Once a potential radiolabeling precursor and a suitable labeling method have been developed, radiosynthesis procedures can be evaluated for the synthesis of  $[^{18}\text{F}]\text{FTC2}$  following the same method as discussed for  $[^{18}\text{F}]\mathbf{6}$ . The precursor methyl 10-iodo-4-thiacaprate **23** was radiolabeled ( $[^{18}\text{F}]\mathbf{25}$ ) and hydrolysed to produce  $[^{18}\text{F}]\mathbf{26}$  (Scheme 28).



Scheme 28: Radiosynthesis of iodo precursor methyl 10-iodo-4-thiacaprate **23**

Radiolabeling efficiency at 90°C was studied in a test reaction by radio-TLC at different time points up to 40 min (see Figure 44). At 10 min, production of  $[^{18}\text{F}]25$  reaches 47%, and then starts to decline indicating thermal decomposition of the fluorinated ester as was observed for  $[^{18}\text{F}]6$ . Therefore, 10 min is an ideal time for the radiolabeling reaction.

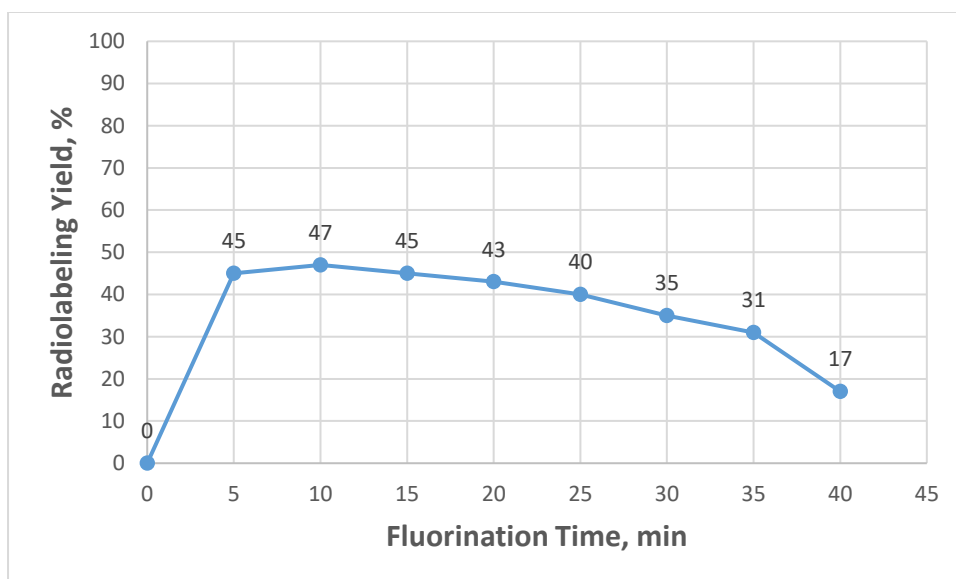


Figure 44: Study of radiolabeling efficiency to form  $[^{18}\text{F}]25$  at different time points,  $n = 1$

Radiolabeling of the iodo precursor **23** proceeded efficiently on a larger scale, with  $47 \pm 4\%$  (fluoride incorporation yield analysed by radio-TLC, see Figure 45).

Hydrolysis of the  $[^{18}\text{F}]$ -10-4-thiacaprate ester,  $[^{18}\text{F}]25$  was achieved in a quantitative yield by the addition of KOH and heating (see Figure 45).

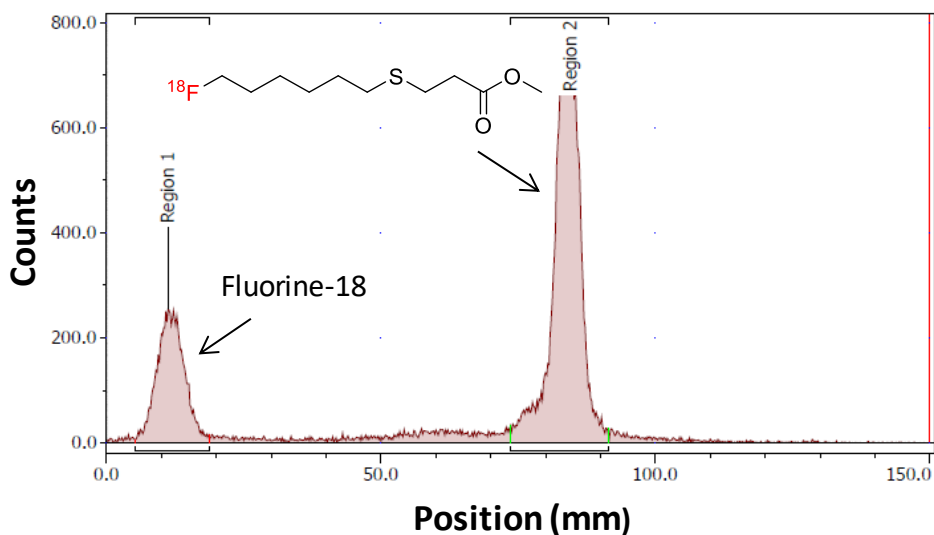


Figure 45: Radio-TLC trace of the radiolabeling reaction to form  $[^{18}\text{F}]\mathbf{25}$

$[^{18}\text{F}]\mathbf{25}$  was hydrolysed to produce  $[^{18}\text{F}]\text{FTC2}/[^{18}\text{F}]\mathbf{26}$ , (see Figure 47) which was then purified by using semi-preparative HPLC. The chromatogram shows elution of unreacted  $[^{18}\text{F}]\text{fluoride}$  with the solvent front and then  $[^{18}\text{F}]\mathbf{26}$  eluting from 13:27 to 14:59 min followed by some unidentified radiolabeled compounds. All fractions were collected and the activity measured for each fraction (see Figure 47)

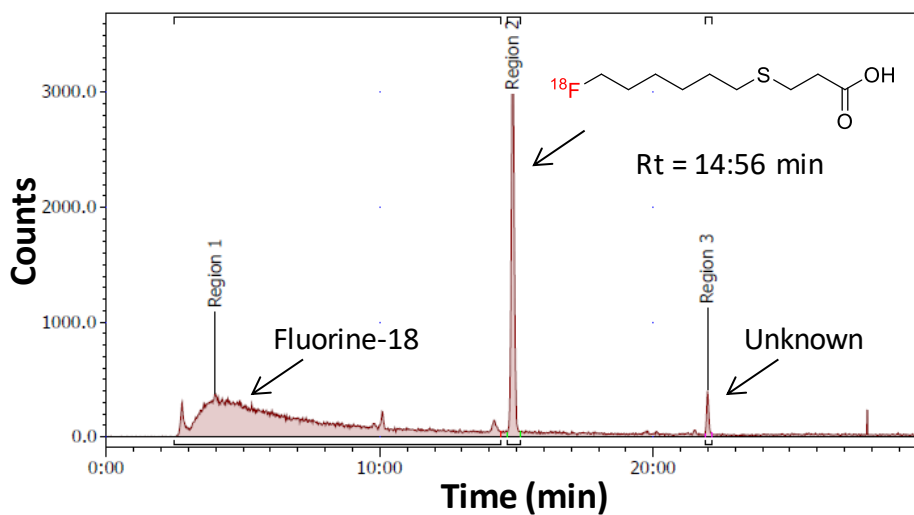


Figure 46: Radio-HPLC trace of  $[^{18}\text{F}]\text{FTC2}/[^{18}\text{F}]\mathbf{26}$

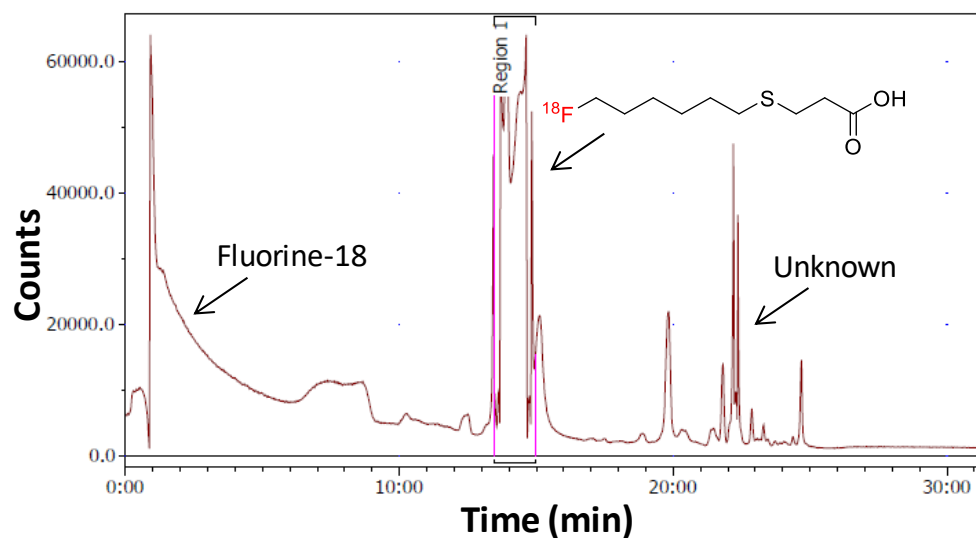


Figure 47: Radio-HPLC trace of semi-preparative HPLC purification of  $[^{18}\text{F}]\mathbf{26}$

Preparation of  $[^{18}\text{F}]\text{FTC2}$  (50-100 MBq) produces enough activity for *in vivo* administration in an overall decay corrected yield  $16.15 \pm 2.6\%$ . HPLC analysis of the final formulated radiotracer showed radiochemical purity  $>98\%$  (see Figure 48).

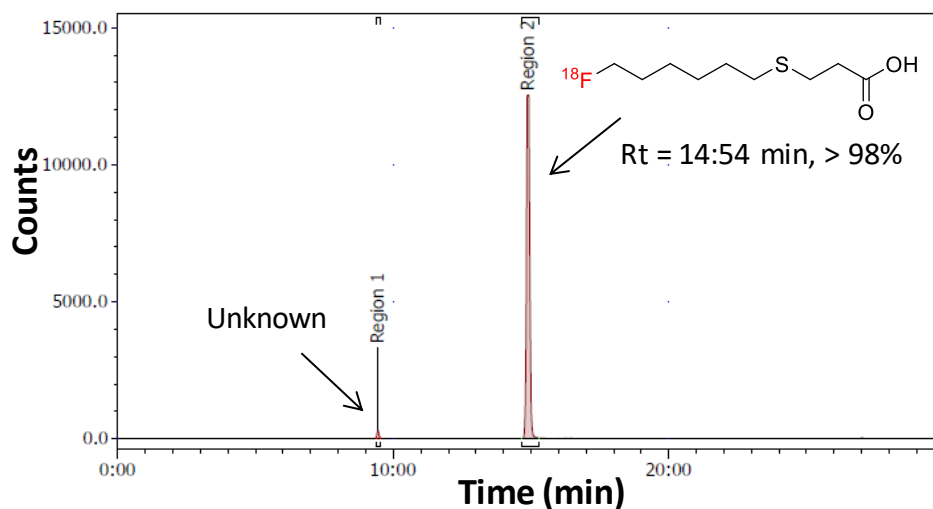


Figure 48: Radio-HPLC of  $[^{18}\text{F}]\text{FTC2}/ [^{18}\text{F}]\mathbf{26}$  analysis of the final formulated radiotracer

The stability of  $[^{18}\text{F}]\text{10-fluoro-4-thiacapric acid}$  ( $[^{18}\text{F}]\text{FTC2}$ ) in human serum was studied by radio-HPLC analysis to show no degradation ( $> 98\%$ ) during incubation at  $37^\circ\text{C}$  at timepoints up to 3 hours.

### 3.5.2 Preliminary preclinical imaging evaluation of [<sup>18</sup>F]10-fluoro-4-thiacapric acid ([<sup>18</sup>F]FTC2)/ [<sup>18</sup>F]26

PET scanning of the novel medium alkyl chain length tracer [<sup>18</sup>F]FTC2/ [<sup>18</sup>F]26 was carried out *in vivo* in male Sprague–Dawley rats (n=3) anaesthetised with isoflurane. [<sup>18</sup>F]-FTC2 (12.01 MBq) was injected into the tail vein and data were acquired for 90 minutes using the preclinical PET/CT scanner. After reconstruction, the image was produced, Figure 49, that shows the cardiac uptake of fluorine-18 radioactivity after intravenous administration of [<sup>18</sup>F]FTC2 at 80-90 minutes after injection and ROI analysis of the heart could be performed at different time points.

[<sup>18</sup>F]FTC2/[<sup>18</sup>F]26 did not show significant cardiac uptake and the highest uptake was seen in liver. The dynamic quantification of [<sup>18</sup>F]FTC2 uptake in the heart (see Figure 49) was compared with an area of the liver by the mean standard uptake value (SUV Mean) at 3 minute intervals (for the early timepoints). These results indicated that the medium alkyl chain tracer [<sup>18</sup>F]FTC2 does not utilise the carnitine shuttle to enter the mitochondria (only passive diffusion) as discussed in section 2.4.<sup>111, 112, 120</sup>

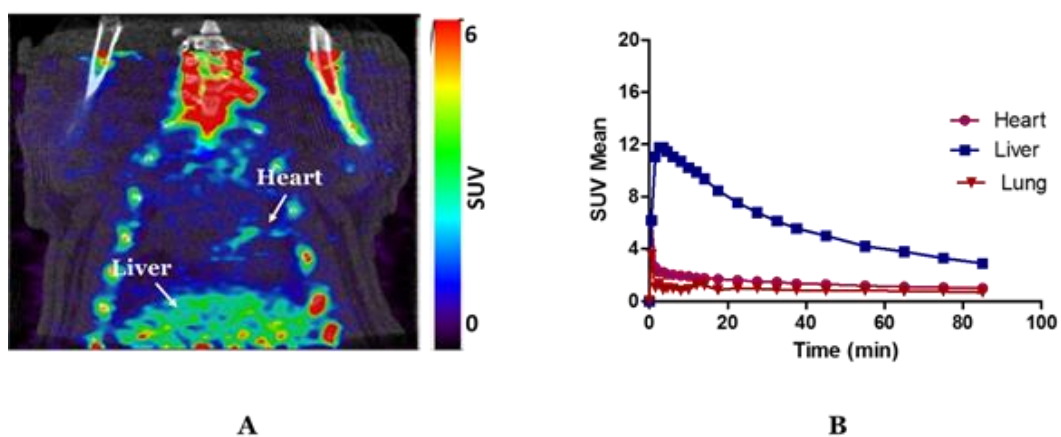
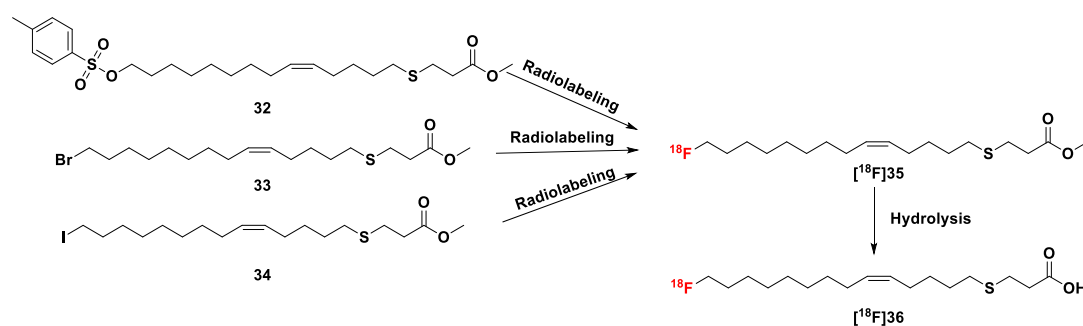


Figure 49: A: Coronal maximum intensity projection images acquired 80-90 min post *iv* administration of [<sup>18</sup>F]FTC2. B: Time activity curves showing uptake of the tracer in indicated organs

### 3.6 Synthesis and imaging of [<sup>18</sup>F]18-fluoro-4-thiaoleic acid ([<sup>18</sup>F]FTO) [<sup>18</sup>F]**36**

#### 3.6.1 Radiosynthesis of [<sup>18</sup>F]-18-fluoro-4-thiaoleic acid ([<sup>18</sup>F]FTO) [<sup>18</sup>F]**36**

Three radiolabeling precursors, methyl 18-tosyl-4-thiaoleate **32**, methyl 18-bromo-4-thiaoleate **33** and methyl 18-iodo-4-thiaoleate **34** had been synthesized and were used to provide a comparison for the radiolabeling yields with [<sup>18</sup>F]fluoride (see Scheme 29).



Scheme 29: Radiosynthesis of [<sup>18</sup>F]**36** from 18-tosyl, bromo or iodo-4-thiaoleate precursors (**32**, **33** and **34**)

Theoretically, iodo group is the best leaving group, followed by bromo then tosyl ( $I > Br > OTs$ ), however this does not account for competing reactions. The experimental results show that, as expected, the tosyl precursor **32** is not reactive enough to give high fluoride radiolabeling yields ( $50 \pm 5\%$  ( $n=4$ )). However, the iodo precursor **34** gave a similar  $50 \pm 2\%$  yield and the HPLC trace shown in Figure 50 shows that other products are formed. The bromo precursor **33** shows the best radiolabeling yield of  $72 \pm 1\%$  (see Figure 50). Hence the bromo precursor was selected for the radiolabeling reactions to produce radiotracer for *in vivo* imaging.

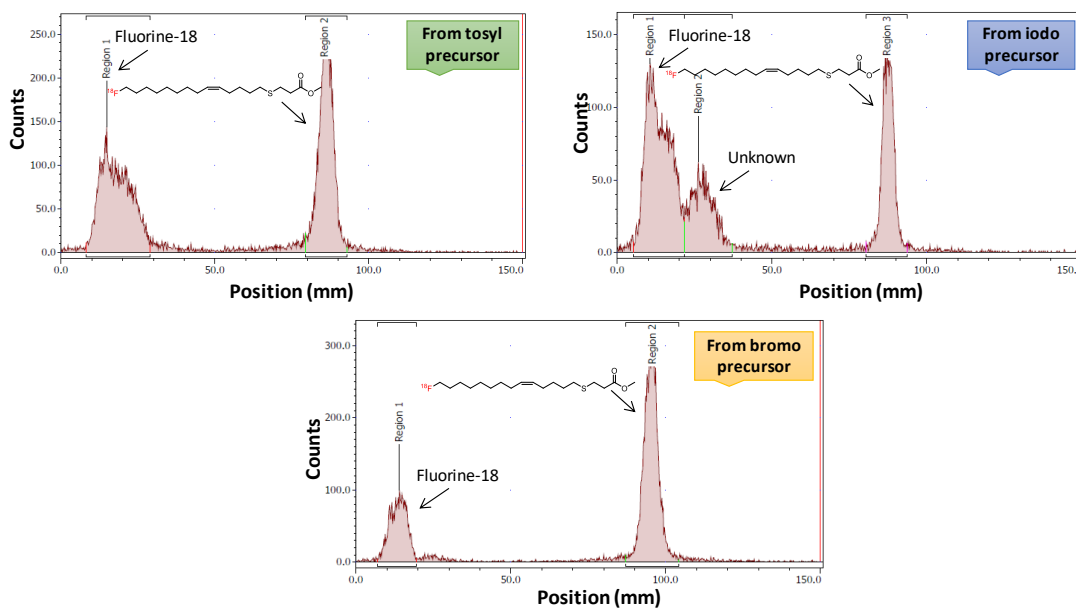


Figure 50: Radio-TLC of  $[^{18}\text{F}]\mathbf{35}$  from 18-tosyl, bromo or iodo-4-thiaoleate precursor  $\mathbf{32}$ ,  $\mathbf{33}$  and  $\mathbf{34}$  (mobile phase DCM: MeOH 9:1)

$[^{18}\text{F}]\mathbf{35}$  was hydrolysed quantitatively by the same method used for  $[^{18}\text{F}]\mathbf{5}$  and  $[^{18}\text{F}]\mathbf{25}$  with the addition of KOH (see Figure 51).

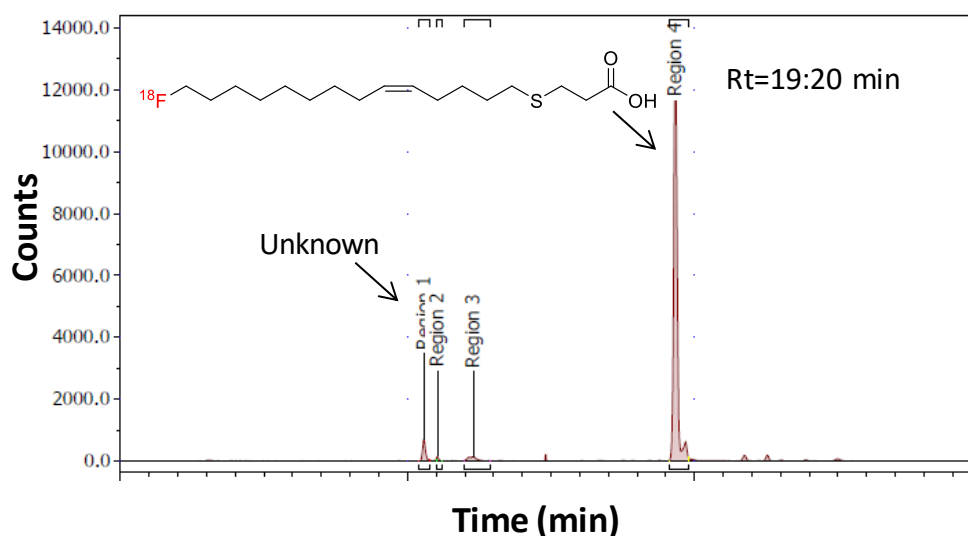


Figure 51: Radio-HPLC trace of  $[^{18}\text{F}]\text{FTO}/[^{18}\text{F}]\mathbf{36}$  after hydrolysis

After hydrolysis, purification of the crude  $[^{18}\text{F}]\text{FTO}/[^{18}\text{F}]\mathbf{36}$  was carried out *via* semi-preparative HPLC. The chromatogram shows some unidentified radiolabeled products eluting at less than 15 min and  $[^{18}\text{F}]\text{FTO}/[^{18}\text{F}]\mathbf{36}$  eluting from 17:14 to 18:24 min. All fractions were collected and the amount of radioactivity measured for each (see Figure 52).



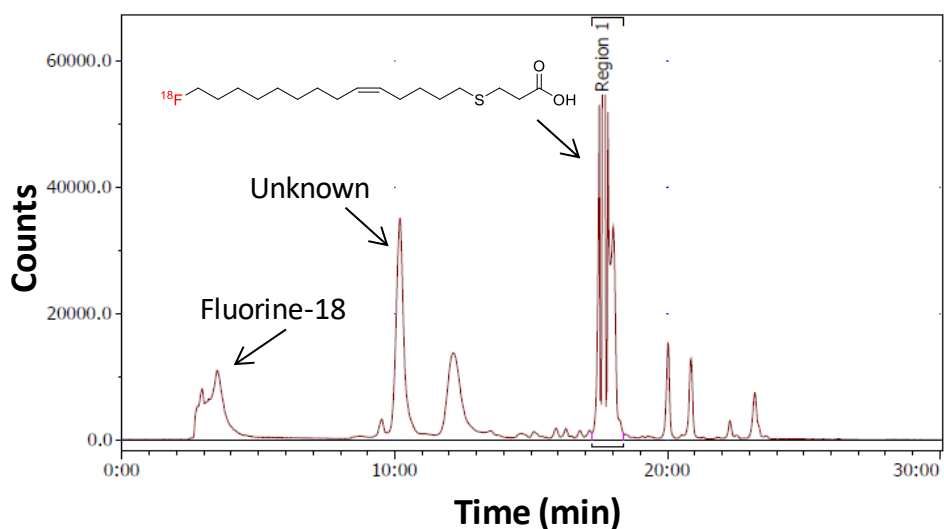


Figure 52: Radio-HPLC trace of semi-preparative purification of  $^{18}\text{F}$ -FTO/  $[^{18}\text{F}]\mathbf{36}$

$[^{18}\text{F}]\text{FTO}/[^{18}\text{F}]\mathbf{36}$  (50-75 MBq) was prepared in a sufficient amount for *in vivo* imaging experiments and formulated as described previously. The radiochemical yield (decay corrected) was  $17.75 \pm 1.70$  %. HPLC analysis of the final formulated radiotracer showed radiochemical purity >96% (see Figure 53).

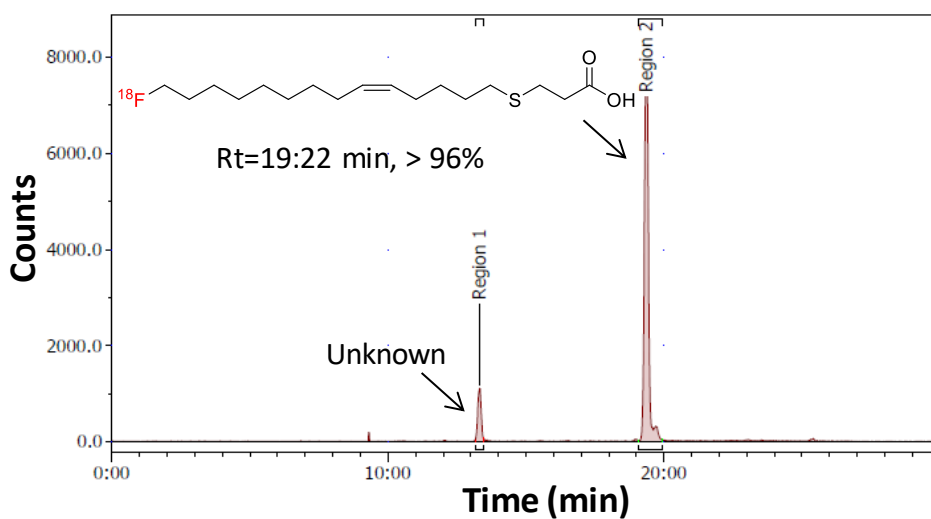


Figure 53: Radio-HPLC trace of  $^{18}\text{F}$ -FTO/  $[^{18}\text{F}]\mathbf{36}$  radiotracer in the final formulation

As with the previous tracers, the serum stability of  $[^{18}\text{F}]\text{FTO}/[^{18}\text{F}]\mathbf{36}$  was determined in human serum *in vitro*. HPLC analysis revealed that the  $[^{18}\text{F}]\text{FTO}$  was sufficiently stable (> 90%) during incubation at  $37^\circ\text{C}$  up to 3 hours.

### 3.6.2 Preliminary preclinical PET/CT imaging evaluation of [<sup>18</sup>F]-18-fluoro-4-thiaoleic acid ([<sup>18</sup>F]FTO)/ [<sup>18</sup>F]36

PET/CT scanning of long alkyl chain tracer [<sup>18</sup>F]FTO/ [<sup>18</sup>F]36 was carried out in male Sprague–Dawley rats (n=3). As previously described, the rats were anaesthetized with isoflurane and [<sup>18</sup>F]FTO (12.01 MBq) was injected into the tail vein and data were acquired in for 90 minutes in the preclinical PET/CT scanner. Following reconstruction, an image showing the cardiac uptake of the tracer (or metabolite) of [<sup>18</sup>F]FTO at 80-90 minutes after intravenous administration was produced, see Figure 54. This shows significant cardiac uptake with the highest uptake was seen in liver. The dynamic quantification of [<sup>18</sup>F]FTO uptake in the heart was again carried out by mean standard uptake value (SUV Mean) at initial 3 min intervals (see Figure 54). Previous reports on this radiotracer also show significant cardiac uptake.<sup>117</sup>

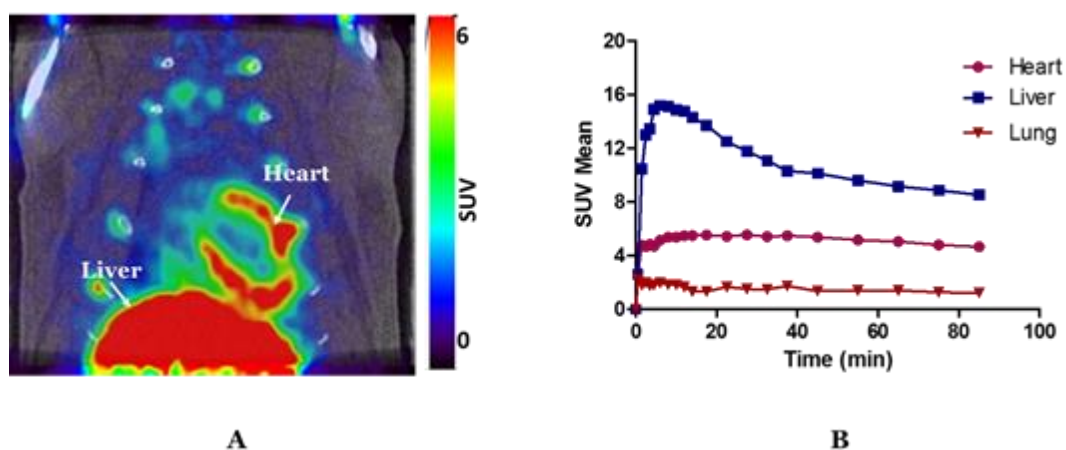


Figure 54: A: Coronal maximum intensity projection images acquired 80-90 min post *iv* administration of [<sup>18</sup>F]FTO. B: Time activity curves showing uptake of the tracer in indicated organs

### 3.6.3 Evaluation of *in vivo* stability of [<sup>18</sup>F]-18-fluoro-4-thiaoleic acid ([<sup>18</sup>F]FTO)/[<sup>18</sup>F]36

To evaluate the *in vivo* stability of the fatty acid analogues to fatty acid oxidation FAO, [<sup>18</sup>F]FTO was analysed in the isolated urine and blood from a male Sprague–Dawley rat (n=1) sampled two hours after administration of the tracer. This was analysed by mixing the biological fluid (urine or blood) with five equivalents by volume of ice cold

MeOH, followed by vortex and centrifugation. The supernatant was then analysed by radio-HPLC.

The results show that no tracer was present in the blood, although this may be due to the extraction procedure for [ $^{18}\text{F}$ ]FTO from blood if it has remained protein bound. However, the urine fraction shows two different peaks with retention times of 1:0 and 4:32 min while the [ $^{18}\text{F}$ ]FTO reference appears at 5:21 min with this gradient method (see Figure 55). The results indicated that the [ $^{18}\text{F}$ ]FTO was metabolised and some of the metabolites were detected in the urine.

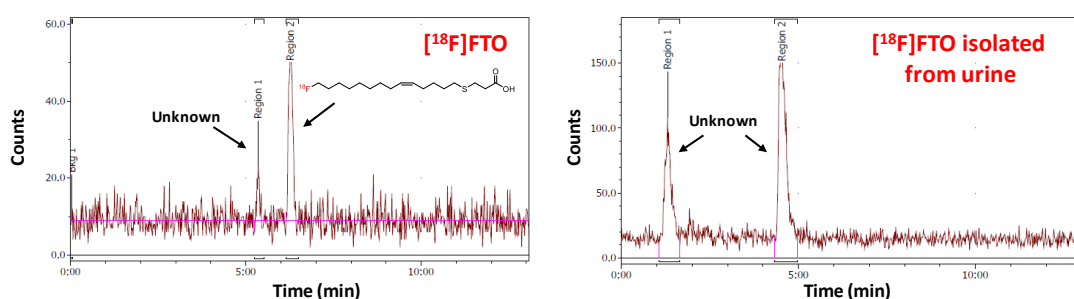


Figure 55: Comparison of HPLC trace of [ $^{18}\text{F}$ ]FTO and urine fraction

### 3.7 Cardiac uptake comparison between [ $^{18}\text{F}$ ]FTP, [ $^{18}\text{F}$ ]FTC2 and [ $^{18}\text{F}$ ]FTO

In this study, a preliminary evaluation of the PET imaging properties of [ $^{18}\text{F}$ ]FTP, [ $^{18}\text{F}$ ]FTC2 and [ $^{18}\text{F}$ ]FTO in rats as probes for myocardial fatty acid oxidation (FAO) showed that the cardiac uptake of [ $^{18}\text{F}$ ]FTP is greater than [ $^{18}\text{F}$ ]FTO. According to a study reported in the literature<sup>117</sup>, greater uptake was observed for [ $^{18}\text{F}$ ]FTO than [ $^{18}\text{F}$ ]FTP. This was thought to be due to the presence of monounsaturated linker along with improved retention in the myocardium that can be attributed to the longer chain length.<sup>4, 117</sup>

The variability in the observed results between this work and that of Degrado *et al.*<sup>115</sup> work may be linked with the animal models used or some other aspect of the imaging experiment. Palmitic acid is the most abundant fatty acid in arterial blood, comprising 25% to 30% of plasma fatty acids and the high levels of this compound may influence the uptake mechanism.<sup>152-156</sup>

The results of the preliminary evaluation of the novel tracer [ $^{18}\text{F}$ ]FTC2 in rats appeared as expected with no significant cardiac uptake. This is likely due, as mentioned before in this chapter (section 3.3.2) and chapter two (section 4.2) to the fact that medium-chain fatty acids carnitine-shuttle independent.<sup>112, 120</sup>

### 3.8 Conclusion

In this chapter, several long alkyl chain, thia-fatty acid analogues were radiolabeled and preliminary evaluation of the imaging properties carried out in rats as PET probes for myocardial fatty acid oxidation (FAO). All of the radiotracers in the current study were radiolabeled with  $^{18}\text{F}$  at the terminal ( $\omega$ ) position, a site known to undergo metabolic defluorination in liver.

Radiosynthesis of several long thia-fatty acids; [ $^{18}\text{F}$ ]16-fluoro-4-thiapalmitic acid ([ $^{18}\text{F}$ ]FTP) / [ $^{18}\text{F}$ ]6, a novel [ $^{18}\text{F}$ ]10-fluoro-4-thiacapric acid ([ $^{18}\text{F}$ ]FTC2)/ [ $^{18}\text{F}$ ]26 and [ $^{18}\text{F}$ ]-18-fluoro-4-thiaoleic acid ([ $^{18}\text{F}$ ]FTO)/ [ $^{18}\text{F}$ ]36 were achieved in good yields. The decay corrected yields for these tracers are  $18.0 \pm 1.2\%$ ,  $16.15 \pm 2.6\%$  and  $17.7 \pm 1.7\%$ , respectively.

Radiolabeling of these tracers was carried out from different precursors. [ $^{18}\text{F}$ ]FTP/ [ $^{18}\text{F}$ ]6 and a [ $^{18}\text{F}$ ]FTC2/ [ $^{18}\text{F}$ ]26 were produced from bromo and iodo precursors. However, [ $^{18}\text{F}$ ]FTO/[ $^{18}\text{F}$ ]36 was produced from all of the bromo, iodo and tosyl precursors. This showed that the highest and most consistent yields could be achieved with the bromo precursor. [ $^{18}\text{F}$ ]FTP/ [ $^{18}\text{F}$ ]6, [ $^{18}\text{F}$ ]FTC2/ [ $^{18}\text{F}$ ]26 and [ $^{18}\text{F}$ ]FTO/ [ $^{18}\text{F}$ ]36 were shown stable in serum for the timescale of the PET scan.

Significant cardiac uptake was shown for [ $^{18}\text{F}$ ]FTP and [ $^{18}\text{F}$ ]FTO in this work, with [ $^{18}\text{F}$ ]FTP > [ $^{18}\text{F}$ ]FTO (although some variability was observed). However, Pandey *et al.* have previously reported that the greater uptake was observed for [ $^{18}\text{F}$ ]FTO over [ $^{18}\text{F}$ ]FTP. This may be due to variability in the parameters of the imaging experiments. A novel tracer, [ $^{18}\text{F}$ ]FTC2 shows no significant cardiac uptake, as was expected.

The type of animal model plays an important role in testing of the tracer *in vivo*. Imaging experiments in nude mice rather than rats with [<sup>18</sup>F]FTP showed no significant cardiac uptake or accumulation of tracer. Therefore, the cardiac uptake of all of the tracers was studied in rat models.

These results confirm that cardiac retention of thia-fatty acids is likely to reflect the extent of fatty acid metabolism. Long alkyl chain thia-fatty acids, [<sup>18</sup>F]FTP [<sup>18</sup>F]**6** and [<sup>18</sup>F]FTO [<sup>18</sup>F]**36** are actively taken up by myocytes, but show poor blood solubility and fast liver-based elimination due to their high lipophilicity. There is no active transport of medium length alkyl chain thia-fatty acids which may result in more favourable pharmacokinetics/ clearance as their lipophilicity is lower than the long alkyl chain thia-fatty acids. This may be important if delivery mechanisms can be developed to accumulate medium chain length fatty acid tracers in cardiac tissues.

## **Chapter Four**

# **Fluorothiacapric acid complexes with copper(II) cross bridged cyclam derivatives**

## Chapter Four: Fluorothiacapric acid complexes with copper(II) cross bridged cyclam derivatives

### 4.1 Introduction to azamacrocycles and mitochondrial targeting

#### 4.1.1 Challenges with medium alkyl chain length thia-fatty acid probes

As discussed in the introduction, section 1.3, long-chain fatty acid metabolism is a major pathway of energy production in the normal perfused myocardium with uptake *via* the carnitine shuttle. Under hypoxic conditions, production of the messenger-RNA encoding muscle carnitine palmitoyltransferase I (the key enzyme in the carnitine shuttle) may be blocked.<sup>157</sup> Fatty acids can still access the site of metabolic change *via* passive diffusion.<sup>112, 120</sup> Therefore, cardiac retention of long chain thia-fatty acids is expected to reflect the extent of fatty acid metabolism under conditions where active uptake by the heart occurs. Mechanisms to accumulate radiolabeled fatty acid derivatives of short, medium and long alkyl chain lengths are of interest. One potential area to exploit is the coordination interaction with a metal centre to influence the biodistribution. Building on previous work in the Archibald group macrocyclic metal complexes that are known to have high affinity for carboxylate ligands can be combined with mitochondrial targeting groups in an attempt to deliver the fatty acid payload to the cardiac (or tumour) tissue.

#### 4.1.2 Macrocyclic chelators

Chelating ligands, such as macrocycles, are generally utilised to form thermodynamically and kinetically stable metal ion complexes. They can also be used to modify the physical and chemical properties of the metal ion(s), such as reactivity, lipophilicity, stabilisation of specific oxidation states and inertness to donor atom/ligand substitution. The chelate effect exploits the entropic energy gain to give enhanced thermodynamic stability for metal complexes with polydentate/chelating ligands compared with monodentate ligands.<sup>158, 159</sup> Polydentate chelators can be divided into macrocyclic chelators (such as cyclam and DOTA) and acyclic chelators

(such as ethylenediaminetetraacetic acid, EDTA). Macrocyclic chelators can benefit from additional thermodynamic stability due to the macrocyclic effect (an extension of the chelate effect) and often form more kinetically inert complexes than acyclic chelators. However, complex formation can require longer reaction times and increased temperatures.<sup>159</sup>

Macrocyclic chelators can be defined as having a ring structure with at least nine atoms including at least three donor atoms oriented to bind to a central metal ion.<sup>160</sup> The ring size of macrocyclic chelators and the type of donor atoms play a significant role in the chelator properties.<sup>161, 162</sup> If appropriately designed, macrocycles can also be good hosts for anions, neutral molecules and organic cation guests. Macrocycles with nitrogen donors, such as TACN, cyclam and cyclen, have been used in many different applications including catalysis, medical imaging and functional materials.<sup>163</sup> In some cases, these macrocycles contain rings that have a large enough central cavity for first row transition metal ions to fit into the plane of the macrocycle. Azamacrocycles, such as cyclam and cyclen, form stable complexes with transition metals such as zinc(II) and copper(II).<sup>164</sup> These tetraazamacrocycles can be arranged in different conformations to encapsulate the metal ion, and can be functionalised with additional donor atoms with pendant arms on the ring nitrogens.<sup>165, 166</sup> In some cases, additional ligands are also bound to complete the coordination sphere (e.g. solvent or coordinating anions).

### 4.1.3 Mitochondria structure and potential for targeting

Mitochondria structure can be divided into four main parts: the outer membrane, the inner membrane, the intermembrane space and the mitochondrial matrix. The main mitochondrial functions are as follows: (1) to produce energy in the form of adenosine triphosphate (ATP) by oxidation of fatty acids and carbohydrates; (2)  $\text{Ca}^{2+}$  homeostasis, which acts as a metabolic regulator; (3) the regulation of heme metabolism, cell cycle regulation, redox homeostasis, thermogenesis and to regulate the levels of reactive oxygen species (ROS). These functions are interconnected through the bioenergetics of the proton electrochemical gradient across the inner



membrane.<sup>167-169</sup> Mitochondria play a multifunctional role in cell survival and death processes and a key parameter is the mitochondrial membrane potential ( $\Delta\Psi$ ). It provides an indicator of cellular viability by reporting on the capacity of the electron transport chain to pump protons across the inner membrane for fatty acid oxidation and ATP generation.<sup>71</sup> Thus,  $\Delta\Psi$  is an important characteristic of both tumours and in cardiac diseases as an indicator of mitochondrial dysfunction.<sup>170-173</sup>

A survey of the literature shows that many agents have been investigated to deliver a drug or biochemically active compound into the mitochondria, as it represents an attractive target for disease diagnosis or treatment. The administered compound can be taken up into the mitochondria through various pathways. While the outer mitochondrial membrane is relatively permeable due to the abundance of the voltage-dependent anion channel (VDAC) protein, the inner mitochondrial membrane is highly impermeable and acts as a rigid barrier to the passive diffusion of many molecules. It is also rich in the unusual phospholipid CL and maintains a strong negative internal potential.<sup>169</sup> Murphy and Smith<sup>174</sup> reviewed this topic and showed that exploitation of this biophysical property has been a widely used strategy for targeting mitochondria. Cationic molecules are attracted to and accumulate preferentially within the negatively charged mitochondrial matrix if they have appropriate lipophilicity properties. Hoye *et al.*<sup>175</sup> based an alternate targeting strategy on the affinity of an agent to mitochondrial membrane components, such as the phospholipid CL, which is only found in the inner mitochondrial membrane. As mentioned, appropriate lipophilicity is also required to achieve significant accumulation in the mitochondria.

Many approaches have been used for selective delivery of bioactive cargo molecule into mitochondria (see Figure 56)<sup>176</sup> including:

(1) Specific peptide sequences with appropriate physicochemical properties can be used.<sup>177</sup> Peptides can infiltrate the mitochondria of mammalian cells and trigger apoptosis. Thus, they are attractive as targeted anticancer agents because they can be conjugated to tissue- or tumour-specific peptides or antibodies.<sup>178</sup> Recently, the

mitochondrial localisation and membrane-disrupting activity of the widely used cationic and amphipathic  $\alpha$ -helical peptide d-(KLAKLAK)<sub>2</sub> has been investigated.<sup>179</sup>

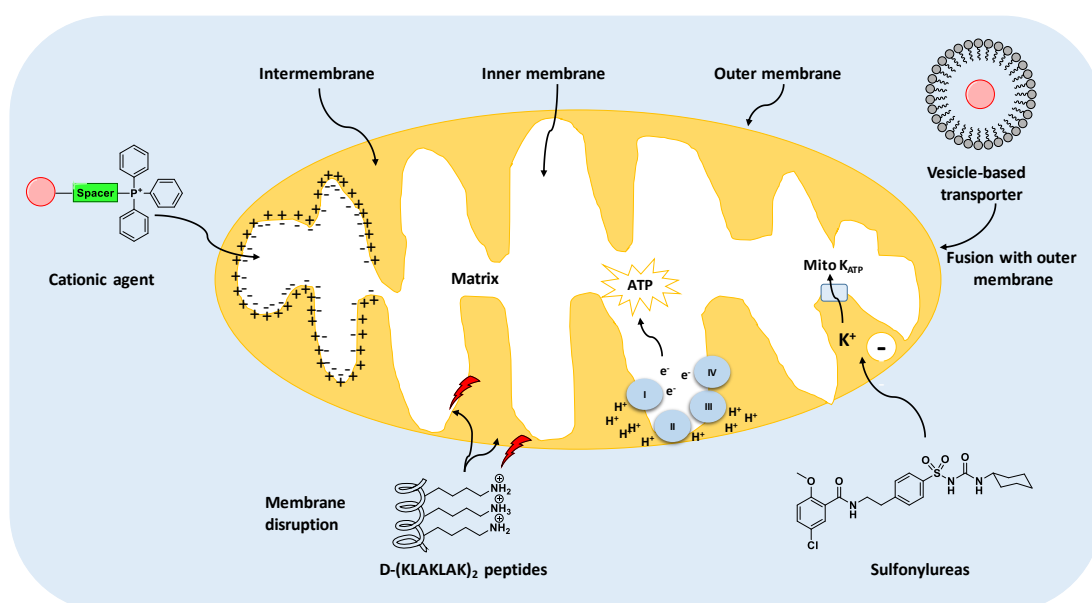


Figure 56: Schematic representation of a mitochondrion and the mode of action of representative targeted compounds

(2) Non-peptide mitochondria-targeted agents are also well characterised. Triphenylphosphonium (TPP) compounds can be used to exploit the substantial negative electrochemical potential maintained across the inner mitochondrial membrane. This class of delocalized lipophilic cations is particularly effective at crossing the hydrophobic membranes and, hence, preferentially accumulate within the mitochondrial matrix by passive diffusion.<sup>174, 180, 181</sup> TPP derivatives have been developed for molecular imaging. Over the past 20-30 years, many research groups have investigated fluorine-18 radiolabeled TPP cations as PET radiotracers for both tumour and cardiac imaging.<sup>182-190</sup> Therefore, TPP functionalised metal complexes which accumulate in mitochondria could be used to deliver medium alkyl chain length fatty acids across the mitochondria membranes.

(3) An alternative to targeted agents, it is possible to encapsulate compounds or tracers in a cationic liposome transporter system which undergoes cellular internalisation and subsequent fusion with the outer mitochondrial membrane.<sup>191</sup>

This approach is suitable for the uptake of large molecules that would normally not permeate the mitochondria.<sup>176</sup>

(4) Sulfonylureas and related compounds bind to high affinity sulfonylurea receptors (SURs) in the plasma membrane of various cell including cardiac cells. Also, these compounds were observed to both activate and inhibit mitochondrial potassium ATP-regulated ion channels (mitoK<sub>ATP</sub>). The mitoK<sub>ATP</sub> channel that is linked to the SURs was detected in the inner membrane of mitochondria and identified as the target of sulfonylurea compounds, although the exact mechanism of action and specificity have not been determined.<sup>175</sup>

## 4.2 Aims and objectives

The aim of this work is the development of a thiocaproic acid delivery vehicle, which is retained in cardiac cells. The molecular design is based on the coordination interaction with a transition metal complex functionalised with TPP to target the mitochondria. [ $^{18}\text{F}$ ]Fluorothiocaproic acid (precursors synthesised and radiolabeling discussed in Chapters 2 and 3) can coordinate with transition metals. Ethylene cross-bridged macrocyclic complexes (copper(II) and zinc(II)) were selected as they have a free coordination site and a particularly high affinity for carboxylates.<sup>192</sup> [ $^{18}\text{F}$ ]Fluorothiocaproic acid and the non-radioactive fluorine-19 derivatives were reacted with the metal macrocycle complex that has been functionalised with TPP to guide fatty acid tracer to the mitochondria (see Figure 57).

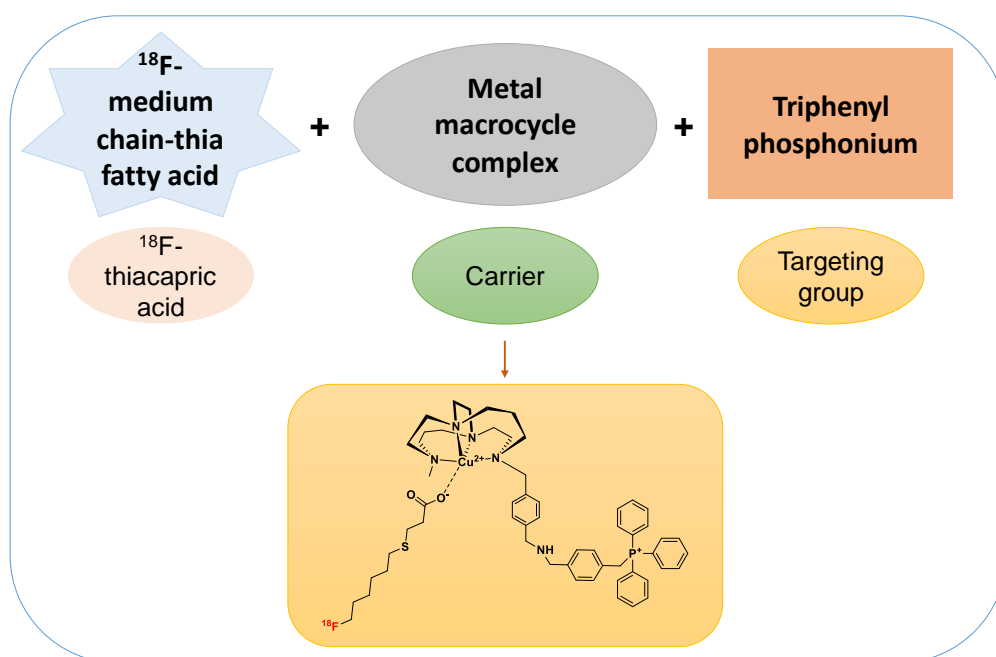


Figure 57: Molecular design of mitochondrial targeting fatty acid metal complex

To confirm whether the behaviour of the compounds is due to the TPP group, a control compound is needed, and this could be produced by using one of the macrocycle precursors to form the complex with the fluorothiocaproic acid with no TPP present. This compound, which requires fewer steps to produce, could also be useful in the development of the protocols for complex formation with the radiolabeled fatty acid and HPLC separation. Non-radioactive “cold” reference standards are also

needed for both the non-targeted and mitochondria targeted compounds to develop the HPLC methods to follow the radiosynthesis and to purify the final product (see Figure 58).

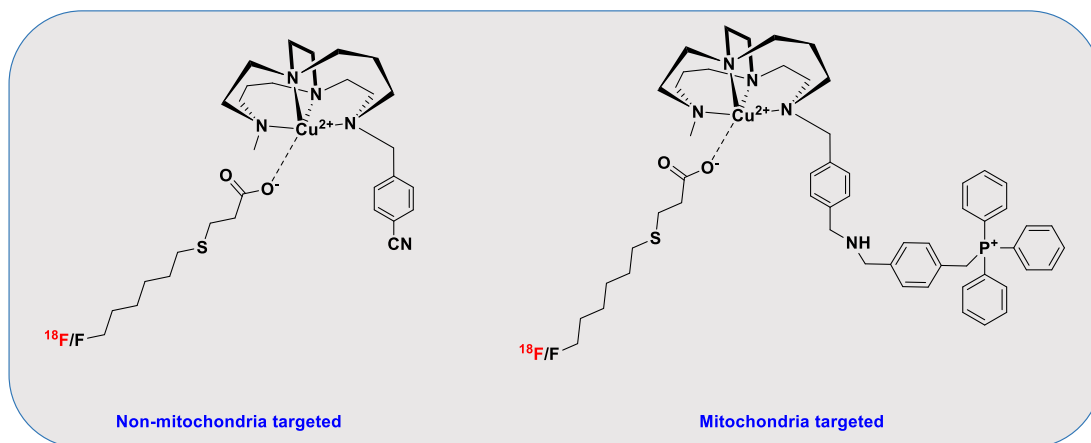


Figure 58: Molecular structures of the target compounds in this work

### 4.3 Synthesis of cross-bridged cyclam chelators

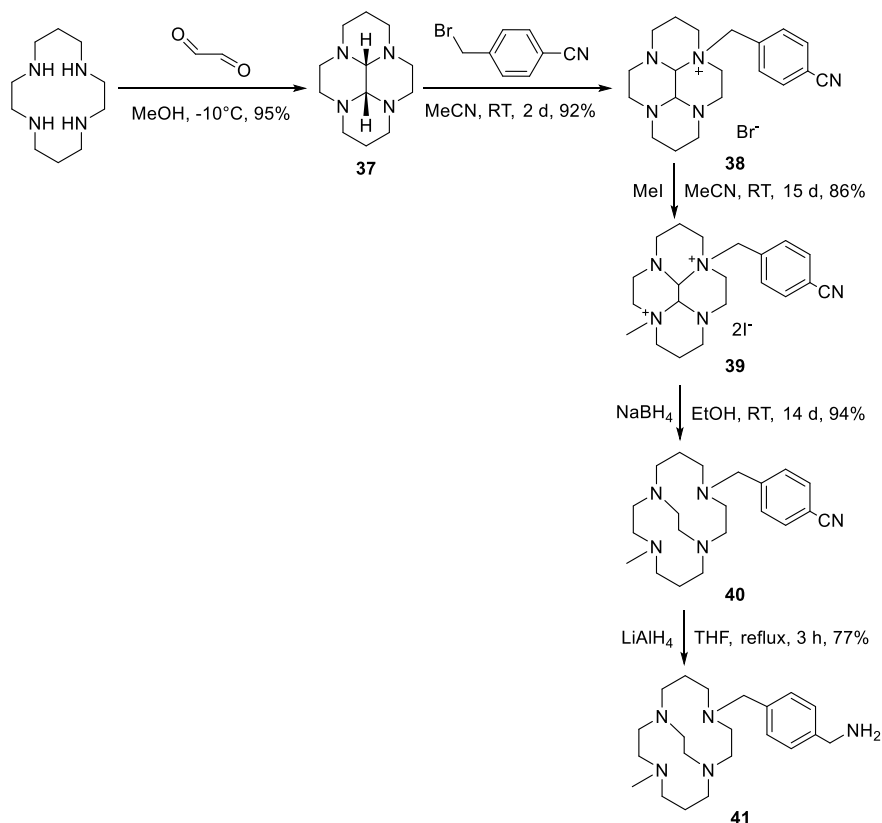
The carnitine shuttle independent targeting approach based on the coordination of the fatty acid (e.g. [<sup>18</sup>F]fluorothiicapric acid) with a mitochondria targeted metal complex requires the design of a suitable chelator to form the metal complex component. To fully understand any biological results, a non-targeted metal complex equivalent should also be synthesised.

Cyclam was selected as the macrocycle component, and has the following properties:<sup>193</sup>

1. Cyclam is a fourteen-membered, N<sub>4</sub>-donor macrocyclic ring, which can be functionalised through carbon or nitrogen atoms. A wide variety of available pendant arms can be used to produce a range of related but structurally different macrocyclic ligands.
2. The carbon skeleton is rigid enough to provide strong metal binding sites and orient functional groups stereoselectively. However, they are flexible enough to provide the structural changes needed to interact with biological targets.
3. The addition of pendant arm(s) can increase the number of donor atoms for coordination to a metal centre or can be used to provide additional functionality to the compound/ conjugate to other molecules.
4. The conformation or configuration can be restricted by linking the ring nitrogens with two or three carbon linkers, which can increase the compound stability and optimise the available coordination site for selective binding (e.g. to carboxylates).

Ethylene cross-bridged (CB) cyclam derivatives have been used in the development of radiopharmaceuticals as copper radioisotope chelators for tumour targeting applications. The increased kinetic stability of such complexes due to the configurational restriction is a key feature.<sup>194</sup> However, there are issues with the cross-bridged as harsh conditions are required to form the complex with the metal ion in the macrocycle cavity.<sup>195, 196</sup> Many research groups<sup>197-200</sup> have worked on a variety of synthetic routes to produce a wide range of cross bridge cyclam chelators

and protein binding compounds based on this component. Cyclam is the precursor used to synthesis the functionalised CB cyclam compounds in this work (see Scheme 30). The addition of a pendant arm, methylation and reduction of the macrocyclic ligand is performed by following previously reported procedures.



Scheme 30: Synthetic route to produce the CB cyclam compounds

Glyoxal is used to bridge the cyclam and form the bisaminal **37** in a 95% yield.<sup>201</sup> During the addition of the glyoxal the temperature of the reaction mixture must be kept below  $-10^{\circ}\text{C}$  to prevent polymerisation and then **37** is extracted into diethyl ether to separate it from any polymeric material formed. The identity of **37** was confirmed by the  $^1\text{H}$  NMR spectrum with the presence of a singlet at 3.07 ppm assigned to the aminal CH protons. A pendant arm is required to provide the site for functionalisation with TPP. Costamagna *et al.*<sup>202</sup> have shown the use of pendant arms on macrocycles to provides functional groups for conjugation to other molecules, such as fluorescent dyes or radiolabeled groups. The rigid *cis* arrangement of the bisaminal means that only two of the nitrogen lone pairs are correctly oriented to be

reactive. Also, to control the reactivity to a single substitution product, an appropriate solvent can be selected to precipitate the mono-quaternised product. Although in this case the reaction to form **38** proceeded in acetonitrile with a good yield and pure product (see Scheme 30).<sup>196, 199</sup> 4-(Bromomethyl)benzotrile was used as a pendant arm (with a cyano group in the *para*-position) to give **38** in 92%. The <sup>1</sup>H NMR spectrum contains two aromatic proton signals at 7.96 and 7.70 ppm respectively and the <sup>13</sup>C NMR has a peak for Ar-CH<sub>2</sub> at 61.54 ppm. The alkylation step was followed by methylation with methyl iodide to give **39** in 86% yield. Subsequent reduction of **39** with excess sodium borohydride (37 molar equiv.) in ethanol to cleave the quaternary nitrogen to carbon bonds afforded the cross-bridged product **40** in 86% yield, with the disappearance of the aminal proton signals in the <sup>1</sup>H NMR spectrum.

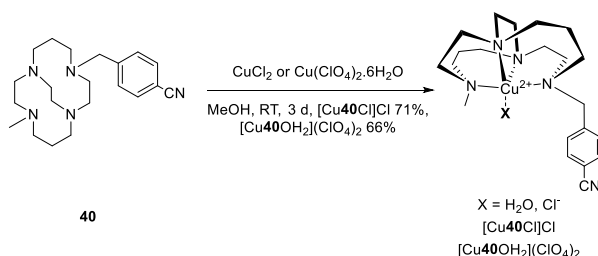
The cyanobenzyl group was reduced with LiAlH<sub>4</sub> to give the (amino)xylyl group on **41** in 77% yield, following previously reported protocols literature.<sup>203</sup> Analysis showed the appearance of a peak assigned to the CH<sub>2</sub>NH<sub>2</sub> protons in the <sup>1</sup>H NMR spectrum and the disappearance of the cyano peak in the <sup>13</sup>C NMR spectrum.



## 4.4 Synthesis of the copper(II) cross-bridged cyclam complex with fluorothiacapric acid (non-targeted)

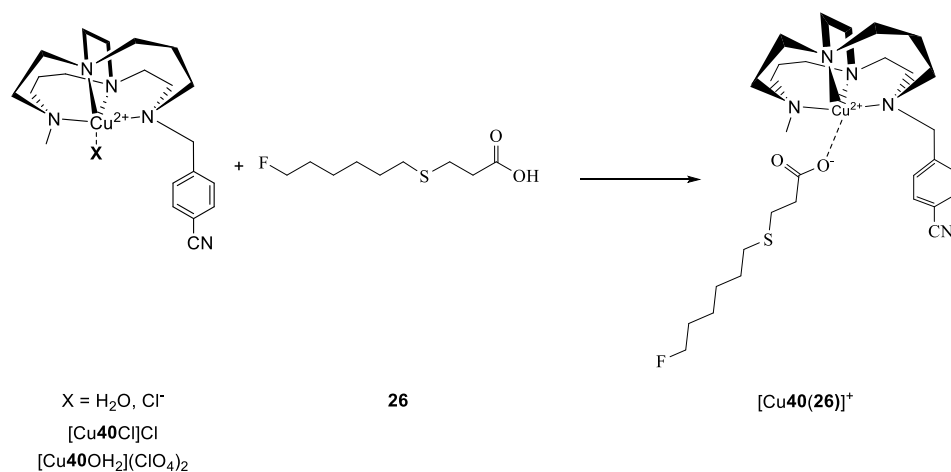
The cross-bridged cyclam chelators **40** and **41** can be used to form complexes with transition metal ions such as copper(II), nickel(II) and zinc(II). Previous work has shown high stability for copper(II) complexes that are stable to reduction and re-oxidation, hence remain intact in biological systems.<sup>192, 204</sup> The cross-bridged cyclam with cyano group **40** was selected for formation of the control complex with copper(II). This complex can be characterised and utilised to develop the HPLC method that is needed to follow the radiosynthesis reaction and to purify the product.

**40** was reacted with either anhydrous copper(II) chloride or copper(II) perchlorate hexahydrate (see Scheme 31). The chloride and perchlorate anions were selected as it is known for these compounds that facile replacement with a carboxylate anion is possible especially for the non-coordinating perchlorate anion. This should allow for subsequent to coordinate the thia fatty acid to the metal ion without affecting the coordination to the macrocycle. Other anions, such as acetate may compete more effectively for this coordination site at the metal centre.  $\text{Cu40Cl}_2$  was purified *via* size exclusion chromatography (Sephadex LH20) and  $\text{Cu40}(\text{ClO}_4)_2$  was isolated by filtration as the compound precipitated with sufficient purity, the yields of complexes were 71% and 66% respectively. The presence of solvent (MeOH) was observed in both the CHN and ICP analyses.



Scheme 31: Synthetic route to produce non-targeted copper(II) cross-bridged cyclam complexes  $[\text{Cu40Cl}]\text{Cl}$  and  $[\text{Cu40}(\text{OH}_2)](\text{ClO}_4)_2$

These complexes can now be used to coordinate with 10-fluoro-4-thiacapric acid **26** by exchange of the water molecule or anion bound to the metal centre to give.  $[\text{Cu40(26)}]^+$  (see Scheme 32).



Scheme 32: Synthetic route to form 10-fluorothiacaipric acid with non-targeted copper(II) cross-bridged cyclam complexes  $[\text{Cu40(26)}]^+$

For the fatty acid coordination reaction, a range of procedures was attempted with changes to the solvent and/or the reaction temperature. All attempts made showed formation of the desired compound  $[\text{Cu40(26)}]^+$  after 5 min reaction time with analysis by mass spectrometry, however peaks were also observed for the copper complex of **40** and 10-fluoro-4-thiacapric acid **26**. In order to further characterise the formed compound, HRMS was carried out to confirm the identity of the complex and MS/MS (see Figure 59) showed that the peaks for the copper(II) complex of **40** and **26** appeared as fragments of the desired product  $[\text{Cu40(26)}]^{2+}$ .

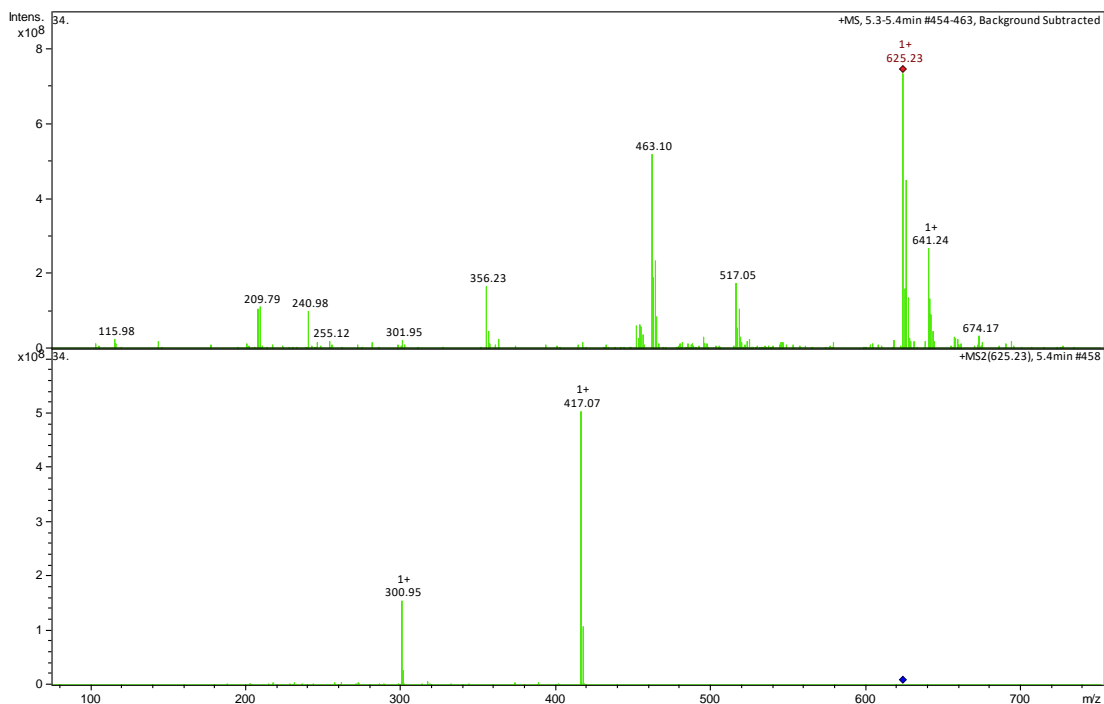


Figure 59: MS/MS of  $[\text{Cu}40(26)]^+$

The HPLC analysis of  $[\text{Cu}40(26)]^+$  used the same method which was applied to the purification of 10-fluoro-4-thiacapric acid **26** with the product eluted at a retention time ( $R_t$ ) 09.66 min (see Figure 60).

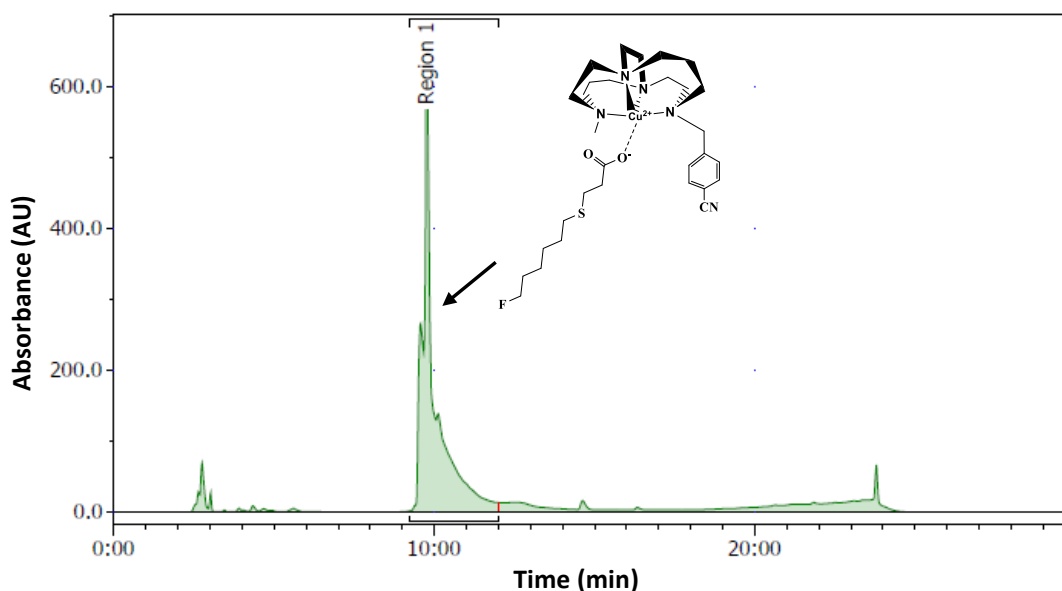


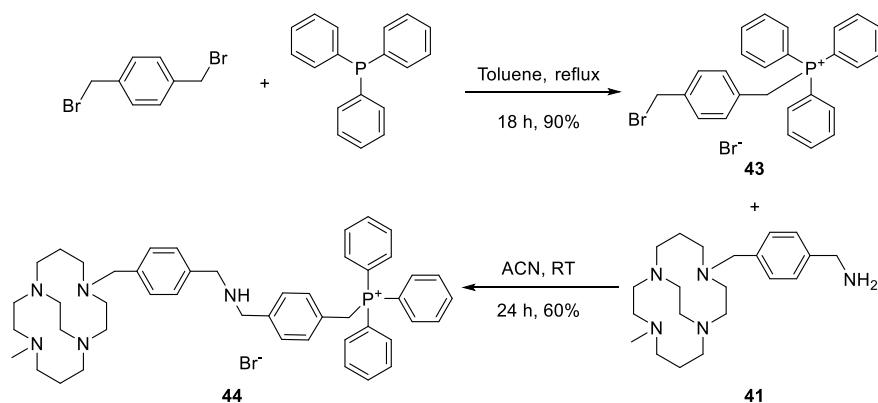
Figure 60: HPLC trace of  $[\text{Cu}40(26)]^+$

## 4.5 Synthesis of the copper(II) cross-bridged cyclam complex with fluorothiacypric acid (mitochondria targeted)

[<sup>18</sup>F]Fluoride radiolabeling of thiacypric acid precursors is high yielding but does not give a tracer that is preferentially taken up into the myocardium. In order to increase the utility of this radiolabeled molecule in PET imaging, a mechanism for delivery to cardiac tissue is required. The aim of this part of the research is to develop a triphenylphosphonium functionalised macrocycle that forms a stable complex with copper(II) and has an available high affinity site for additional binding of a carboxylate such as fluorothiacyprylate. This compound could ultimately be tested for specific mitochondrial uptake *in vitro* and potentially investigated for *in vivo* biodistribution and cardiac uptake.

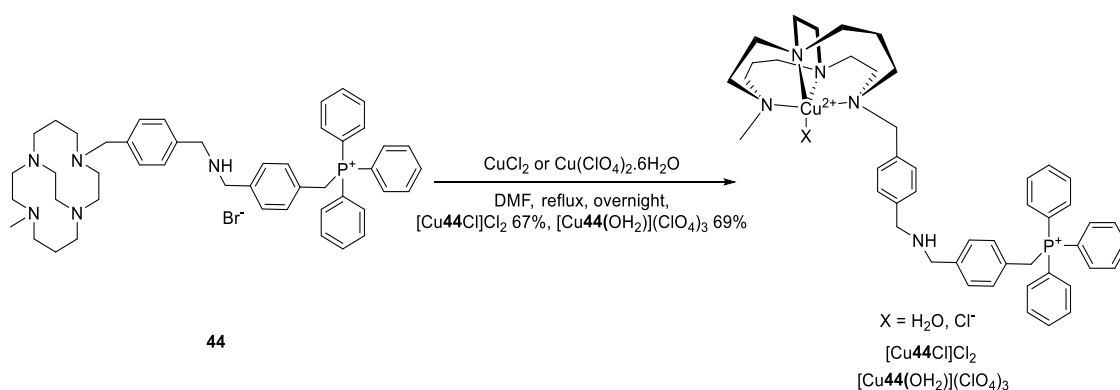
(4-(Bromomethyl)benzyl)triphenylphosphonium bromide **43** (see Scheme 33) was synthesized,<sup>205</sup> by reacting triphenylphosphine with  $\alpha,\alpha'$ -dibromomethyl-*p*-xylene. This compound can be used to generate a triphenylphosphonium pendant arm on the azamacrocycle. **43** was purified by silica gel column chromatography and isolated as a white powder in 90% yield, matching the yield reported in the literature by Wang *et al.*<sup>205</sup> The formation of compound **43** was characterized by the presence of a singlet peak in the <sup>1</sup>H NMR spectrum at  $\delta$  1.68 ppm for two protons (CH<sub>2</sub>-P). The product formation and purity was further confirmed by <sup>31</sup>P NMR ( $\delta$  24.08 ppm).

The bromine in **49** is a good leaving group, thus it was expected to react effectively with **41** (see Scheme 33) to produce **44**. 0.6 equivalents of **43** were used in the preparation of compound **44** to avoid quaternisation products and the reaction was followed by mass spectrometry showing formation of the **44** by detection of the molecular ion. The identity of the product was confirmed by the presence of two singlet peaks in the <sup>1</sup>H NMR spectrum at  $\delta$  3.40 and 3.49 ppm for the two CH<sub>2</sub>-NH groups. Compound **44** was further characterised by <sup>31</sup>P NMR showing a single peak ( $\delta$  23.71 ppm).



Scheme 33: Synthetic route to produce a triphenylphosphonium derivatised macrocyclic chelator **44**

However, it was also clear from the analysis that the 0.4 equivalents of the aminobenzyl cross-bridged cyclam starting material were still present in the isolated compound. No satisfactory purification method was found and so an attempt was made to form the metal complex with a view to purification at this stage. The metal complexes were formed with **44** using anhydrous copper(II) chloride and copper(II) perchlorate hexahydrate as previously utilized for the formation of complexes with **40** (see Scheme 34).



Scheme 34: Synthetic route to produce mitochondria targeted copper(II) cross-bridged cyclam complexes

$[\text{Cu44Cl}]\text{Cl}_2$  and  $[\text{Cu44(OH}_2\text{)](ClO}_4\text{)}_3$  were both purified *via* size exclusion chromatography (Sephadex LH20) to remove metal salts and give the products in 67% and 69% yield respectively. Complexes were characterised by MS, ICP and CHN analysis with some impurities still present. Inductively coupled plasma (ICP) analysis also suggested that there might be impurities present in both complexes. The HPLC

analysis of  $[\text{Cu44}(\text{OH}_2)](\text{ClO}_4)_3$  was carried out and did show some peaks for other minor by-products. The main product peak, which was confirmed to be the desired product by MS, was eluted with a retention time ( $R_t$ ) of 13:78 min (see Figure 61).

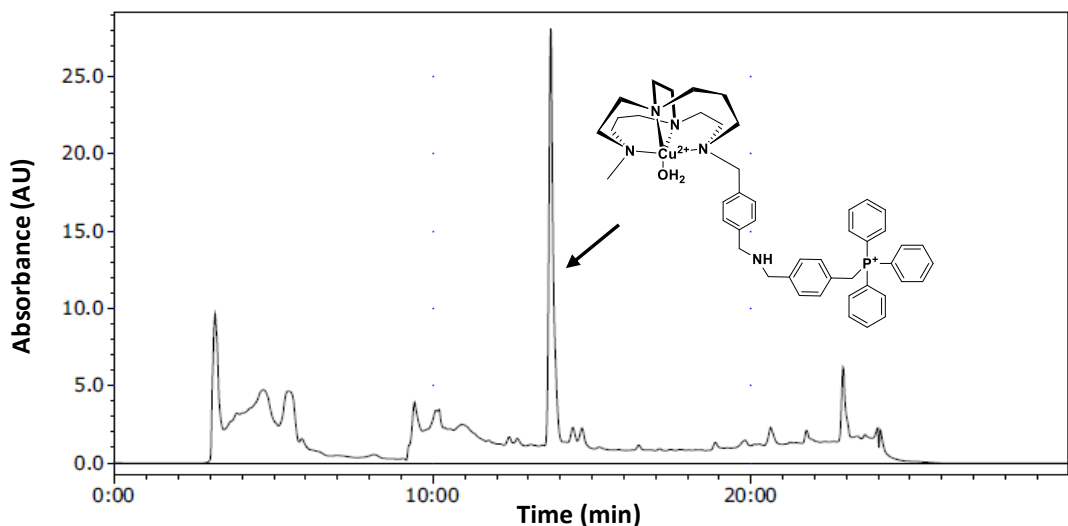
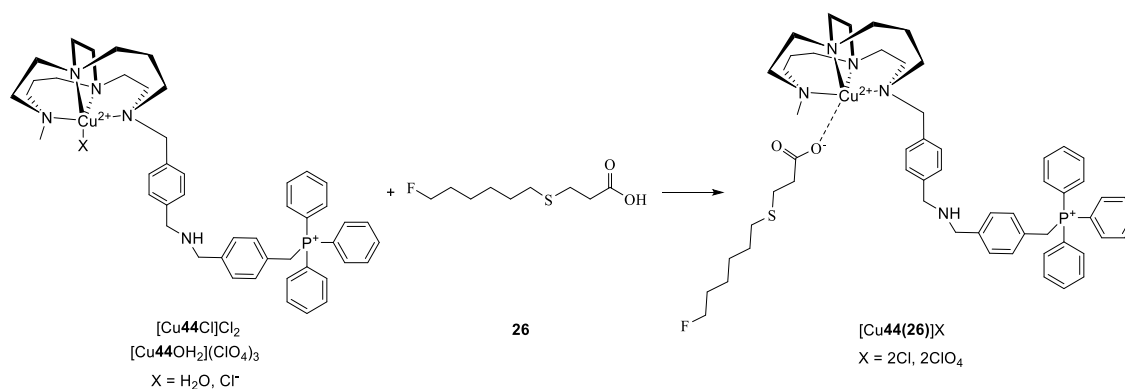


Figure 61: HPLC trace for  $[\text{Cu44}(\text{OH}_2)](\text{ClO}_4)_3$

The next step was to test whether these complexes react with 10-fluorothiaproic acid **26** to produce compound  $[\text{Cu44}(\mathbf{26})]^+$ . This cation should be able to pass across the mitochondrial membranes due to the mitochondrial transmembrane potential,  $\Delta\Psi$ , which acts to concentrate lipophilic cations inside the mitochondria.



Scheme 35: Synthetic route to form 10-fluorothiaproic acid with the mitochondria targeted copper(II) cross-bridged cyclam complex,  $[\text{Cu44}(\mathbf{26})]\text{X}$

Different solvent mixtures were used to form the 10-fluorothiaproate complex with the TPP derivative based on the previous work carried out with the cyano complex. Solvent systems used included a mixture of acetonitrile and water, or PBS and water.

Some of challenges are associated with this reaction are with the solubilities of the two compounds. The identity of  $[\text{Cu44(26)}]\text{X}$  was confirmed by mass spectrometry (including HRMS) and HPLC analysis. The product eluted with a retention time ( $R_t$ ) of 11:20 min and, as expected some starting material was observed at 13:78 min. The retention times suggest that the fluorocapric acid copper(II) complex is more lipophilic than the starting copper(II) compound, as would be expected (see Figure 62).

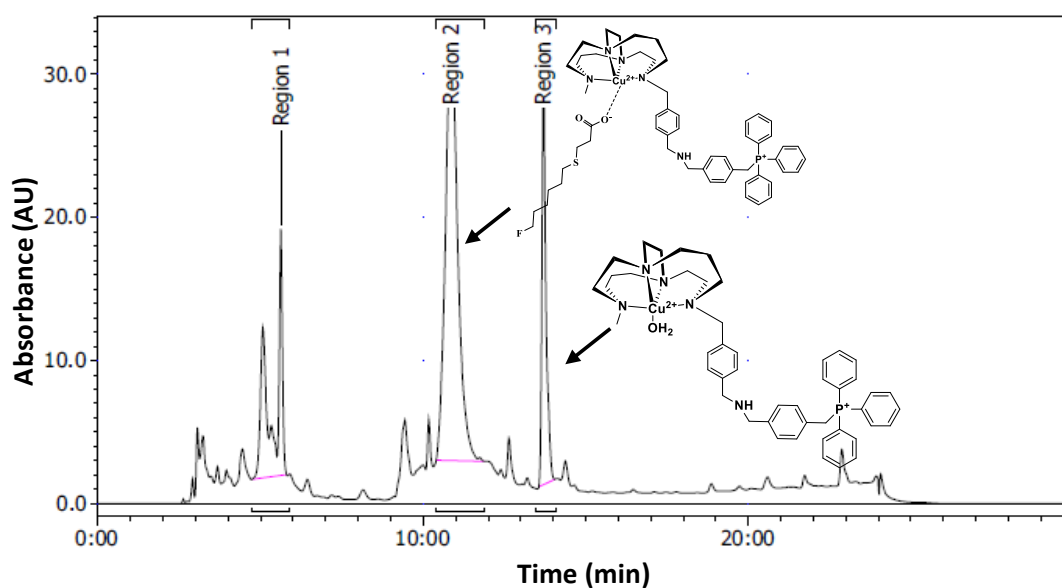
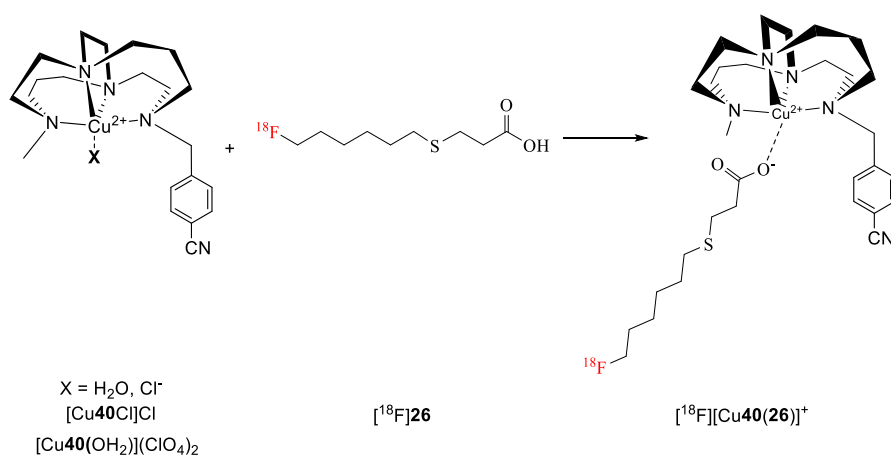


Figure 62: HPLC trace of reaction to form  $[\text{Cu44(26)}]\text{X}$

## 4.6 [ $^{18}\text{F}$ ]-Fluorothiacticapric acid complex with copper(II) cross-bridged cyclam (non- targeted)

The reaction with the radiolabeled 10-fluoro-4-thiacticapric acid [ $^{18}\text{F}$ ]**26** was first developed with the non-targeted metal complexes, [ $\text{Cu40Cl}$ ] $\text{Cl}$  and [ $\text{Cu40}(\text{OH}_2)$ ]( $\text{ClO}_4$ ) $_2$ . [ $^{18}\text{F}$ ]**26** was synthesised following the procedure reported in chapter three, which includes [ $^{18}\text{F}$ ]fluoride radiolabeling of precursor **22**, hydrolysis, purification (semi-prep HPLC), solid phase extraction drying and analysis. The aim was then to form [ $^{18}\text{F}$ ][ $\text{Cu40}(\mathbf{26})$ ] $^+$  (Scheme 36) by using the same protocols developed to synthesise [ $\text{Cu40}(\mathbf{26})$ ] $^+$ . The key difference is the concentration of the radiolabeled thiacticapric acid precursor which is much lower than the “cold” equivalent.



Scheme 36: Synthetic route to form [ $^{18}\text{F}$ ]10-thiacticapric acid with non-targeted copper(II) cross-bridged cyclam complex [ $^{18}\text{F}$ ][ $\text{Cu40}(\mathbf{26})$ ] $^+$

The reaction to produce [ $^{18}\text{F}$ ][ $\text{Cu40}(\mathbf{26})$ ] $^+$  was monitored by HPLC and radio-TLC and was attempted under many different conditions to optimise yields (see table 18 in section 7.4.7.8). Different mixture solvent mixtures, temperatures and reaction times were investigated (e.g. temperature varied from RT to 50°C). Base was added in some reactions ( $\text{Cs}_2\text{CO}_3$ , one equiv. to the complex) and the “cold” compound 10-fluorothiacticapric acid was added to increase the effective concentration of the fatty acid under “carrier-added” conditions.



The results appeared to show that the reaction was successful with PBS/ water as the solvent mixture (see table 18 in experimental section; reaction 16, 62% yield and reaction 17, 93% yield). However, on repeating the reaction under the same or similar conditions the results were variable (for example, see table 18; reaction 18, 7% yield and reaction 19, 42% yield) (see Figure 63 for HPLC traces).

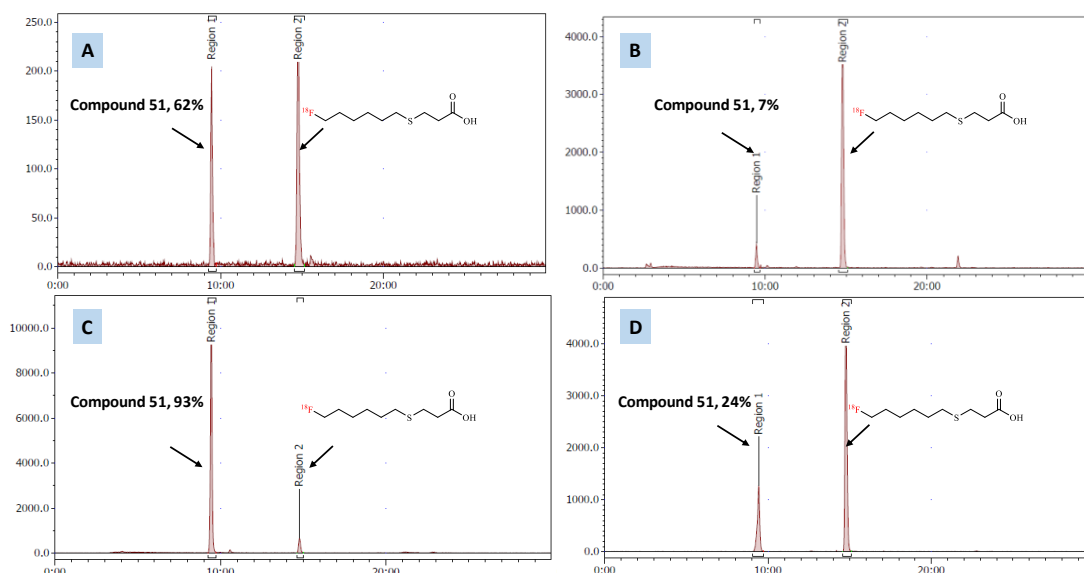


Figure 63: Radio-HPLC traces showing the results from four different attempts to synthesise  $^{18}\text{F}$ [Cu40(26)]<sup>+</sup> under the same conditions (A, B, C and D). This shows the variability in the procedure.

The peak in the HPLC trace at 9:26 min was assigned as the desired product in comparison to the cold standard (retention time 9:66 min). Then different distance to the detectors from the sampling module gives variation in retention time between UV and radiation detectors and so the difference was not thought to be significant. The HPLC mobile phase was changed to replace TFA by perchloric acid to prevent the possibility of the fluorothiaccaprate being displaced by trifluoroacetate. The peak at 9:26 min was separated by semi-prep HPLC and then reinjected into the analytical HPLC; the chromatogram shows the same peak, indicating that the compound is pure. To provide further evidence that the peak at 9:26 min is related to the complex, reagents and albumin were mixed in the absence of the complex and analysed by HPLC (i.e. solvent with  $^{18}\text{F}$ 10-fluoro-4-thiacapric acid/ $^{18}\text{F}$ 26 or solvent with  $^{18}\text{F}$ fluoride) with only the peaks for the starting materials observed. This indicates

that the peak at 9:26 min is not due to the interaction of the radiolabeled component with the albumin in the reaction mixture. The variability and inconsistency of this reaction is problematic and its origins were not identified in the course of these experiments. Further optimisation of this synthesis is required before it can be progressed to the TPP derivative. The reaction may be highly sensitive to the order and timing of reagent addition, maintaining solubility of all of the components is highly important and could be further investigated.

## 4.7 Conclusions

This research resulted in the synthesis of a series of novel compounds. A triphenylphosphonium derivatised macrocyclic chelator **44** was produced and the copper(II) complex formed. The triphenylphosphonium group was added to give the potential for mitochondrial targeting, although this was not validated in the current work it is an established approach. However, based on previous work to design systemically administered mitochondrial targeting agents, optimisation of the properties such as lipophilicity may be required to influence the biodistribution.

The chelators were synthesised using previously characterised precursors and for the TPP derivative, quaternisation of the amino nitrogen was avoided by reducing the molar ratio of the triphenylphosphonium precursor. Copper(II) complexes were synthesised from chloride and perchlorate salts as these anions were to either be non-coordinating (perchlorate) or to exchange with carboxylates (chloride).

Both a cyano derivatised and the TPP derivatised copper(II) cross bridged cyclam complex were reacted with 10-fluoro-4-thiacapric acid to form complexes where the anion or solvent molecule interacting with the metal centre was displaced to give the 10-fluoro-4-thiacaprate complexes  $[\text{Cu}\mathbf{40}(\mathbf{26})]^+$  and  $[\text{Cu}\mathbf{44}(\mathbf{26})]^+$ . The complexes were analysed by mass spectrometry and HPLC and showed formation of the desired compounds, however some impurities that were present in **44** were carried through to the copper(II) complex and the final compound

The formation of the [<sup>18</sup>F]10-fluoro-4-thiacapric acid was investigated for the copper(II) complex of **40** to give [<sup>18</sup>F][Cu**40(26)**]<sup>+</sup>. This compound seemed to be formed successfully despite the significant reduction in the concentration of the fatty acid precursor when moving to the radiolabeled compounds (due to the radioactive nature of the compound). However, the reaction was not reproducible and the problematic factors were not identified. Further study is required before the TPP complex can also be investigated.

## **Chapter Five**

# **Development of $^{99m}\text{Tc}$ labeled long alkyl chain thia-fatty acids**

## Chapter Five: Development of $^{99m}\text{Tc}$ labeled long alkyl chain thia-fatty acids

### 5.1 $^{99m}\text{Tc}$ labeled fatty acid imaging agents

A SPECT radiotracer for cardiac imaging requires sufficient cardiac uptake with rapid background clearance. This has been a key issues in the development of SPECT based fatty acid radiotracers for cardiac imaging, as the radiotracer is cleared *via* the liver which can be problematic for cardiac images, as the clearance rates correlate directly with  $\beta$ -oxidation.<sup>9</sup>

As discussed previously, long alkyl chain fatty acids (C-13 to C-21) have been identified as the most important source of energy in cardiac cells.<sup>153, 206, 207</sup> Single photon gamma emitting isotopes, such as  $^{99m}\text{Tc}$  and  $^{123}\text{I}$ , have been used to radiolabel long alkyl chain fatty acids to give radiopharmaceuticals for the assessment of myocardial fatty acid metabolism and diagnoses of cardiac disease.<sup>72, 73, 75, 208, 209</sup> As mentioned in introduction,  $^{123}\text{I}$ -IPPA (15-(*p*-[ $^{123}\text{I}$ ]iodophenyl)pentadecanoic acid) and  $^{123}\text{I}$ -BMIPP (15-(*p*-[ $^{123}\text{I}$ ]iodophenyl)-3-(*R,S*)-methylpentadecanoic acid) were widely used SPECT radiotracers which demonstrated rapid accumulation in the cardiac tissue and were clinically successful in detecting heart disease.<sup>67</sup> However, facile loss of the radioiodine *in vivo* is a key problem in application of these tracers. In addition,  $^{123}\text{I}$  is high cost with limited availability. Hence, technetium-99m is attractive for radiolabeling fatty acids, due to its well-developed of coordination chemistry, widespread availability from a cost effective source ( $^{99}\text{Mo}/^{99m}\text{Tc}$  generator) and suitable decay characteristics with a 6.02 hours half-life.<sup>210, 211</sup>

A number of technetium-99m labeled long alkyl chain fatty acids have been investigated for their potential use in metabolic cardiac imaging.<sup>69, 75, 212, 213</sup> Some of these radiotracers showed relatively poor extraction and/or rapid washout from the heart in rat models. Some radiotracers showed higher initial cardiac uptake (see Figure 64):  $^{99m}\text{Tc}$ -MAMA-HDA<sup>75</sup> was a key advance as it was shown that the fatty acid was metabolised to  $^{99m}\text{Tc}$ -MAMA-butyric acid *via*  $\beta$ -oxidation.  $^{99m}\text{Tc}(\text{CO})_3$ -15-[*N*-(acetyloxy)-2-picolylamino]pentadecanoic acid<sup>214</sup>,  $^{99m}\text{Tc}$ -CpTT-16-PA<sup>73</sup> and  $^{99m}\text{Tc}$ -

CpTT-16-oxo-HDA<sup>215</sup> were initially metabolised to  $^{99m}\text{Tc}(\text{CO})_3\text{-[N-acetyloxy-2-picolylamino]pentanoic acid}$ ,  $^{99m}\text{Tc-CpTT-propionic acid}$  and  $^{99m}\text{Tc-CpTT-4-butyric acid}$ , respectively, *via*  $\beta$ -oxidation in myocardium. Based on these prior investigations, technetium-99 fatty acid tracers for cardiac imaging need to be modified to increase their retention time of in the heart. Also, the  $^{99m}\text{Tc}$  core must maintain a relatively small molecular size and high stability.<sup>213</sup>

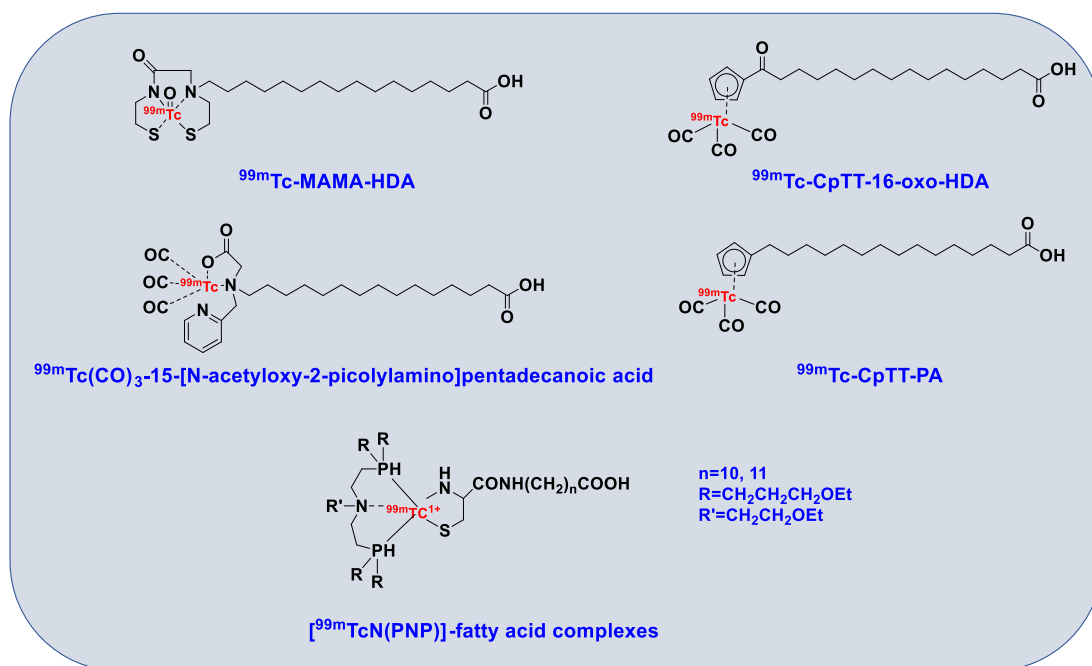


Figure 64: Representative  $^{99m}\text{Tc}$ -labeled fatty acids compounds that have been reported previously and showed high initial cardiac uptake

*In vivo* biodistribution of the  $^{99m}\text{TcN(PNP)}$ -fatty acid complexes<sup>216</sup> showed rapid clearance from the myocardium up to 10 min post-injection followed by retention in the myocardium up to 30 min but the amount of activity retained in the myocardium was low. Thus, the development of  $^{99m}\text{Tc}$ -labeled fatty acid tracers metabolised by  $\beta$ -oxidation in the myocardium with suitable uptake and retention is an unsolved challenge.

The design of a BFC for radiolabeling of the fatty acid should allow it to be easily linked and it should not unduly influence the biochemical properties of the fatty acid. Thus, development of a synthetic pathway for appropriate structural modification is a key step. A balance between taking part in the fatty acid metabolism and

accumulating in the tissues is required. Ideally the  $^{99\text{m}}\text{Tc}$  complex used in the radiolabeling should not be bioactive i.e. interact with proteins or be involved in metabolic pathways.<sup>217-219</sup> A bifunctional chelator (BFC) that strongly coordinates the metal ion ( $^{99\text{m}}\text{Tc}$ ), through appropriate donor atoms, and can easily be covalently attached to the biomolecule (a thia-fatty acid in the case of this work) without disrupting the biological properties, is required.

The type of BFC selected depends on the identity of the metal ion and its oxidation state. A spacer/linker between the metal and the biomolecule may be included, to modulate either the pharmacokinetics of the compound and/or its biological activity.<sup>220</sup> In this case, the amine nitrogen donor chelator 1,4,7-triazacyclononane (TACN) was selected. It forms a highly stable coordination complex with the  $[\text{M}(\text{CO})_3]^+$  core ( $\text{M} = ^{99\text{m}}\text{Tc}$  and  $\text{Re}$ ) where the N-M-N bond angles are close to  $90^\circ$ . The chelator binds as a facial tridentate ligand to complete the octahedral geometry around the technetium(I) metal ion.<sup>221</sup> It has been shown that this complex is stable for up to 6 hours when incubated in saline at room temperature and in mouse serum at  $37^\circ\text{C}$ .<sup>222</sup> These characteristics make TACN attractive candidate to coordinate strongly with technetium(I) to develop a novel  $^{99\text{m}}\text{Tc}$  radiolabeled long alkyl chain thia-fatty acid as a novel tracer to potentially increase initial cardiac uptake and extend the retention time in the heart (see Figure 65).

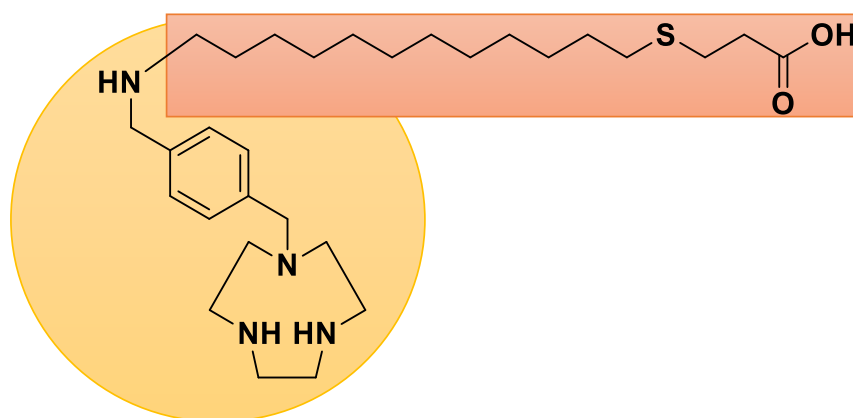


Figure 65: Molecular structure of the TACN chelator attached to thiapalmitic acid

## 5.2 Aims and objectives

The aims of the work reported in this chapter were to synthesise precursors and radiolabel long alkyl chain thia-fatty acids (C-16 palmitic acid and C-18 oleic acid) with  $^{99m}\text{Tc}$  to form tracers (see Figure 66) for use in cardiac imaging that are metabolised by  $\beta$ -oxidation but retained in the tissues. The initial steps in this process are the synthesis of a precursor for radiolabeling, with the chelator component and to synthesise a “cold” reference standard. TACN was selected as the chelator for  $^{99m}\text{Tc}$  radiolabeling. This required functionalisation of a bis-BOC protected TACN with a cyanobenzyl arm followed by reduction to give a primary amine group that is suitable for reaction with bromo- or iodo-thiapalmitate ester (or thiaoleate ester derivatives). Deprotection steps to remove both the BOC and the ester groups could then be carried out.

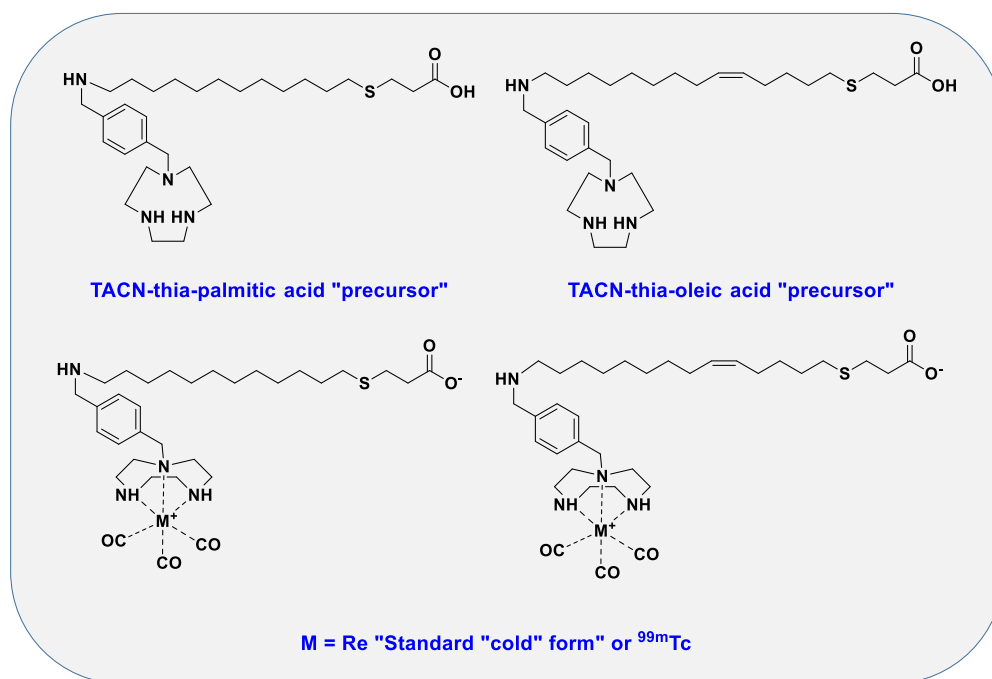


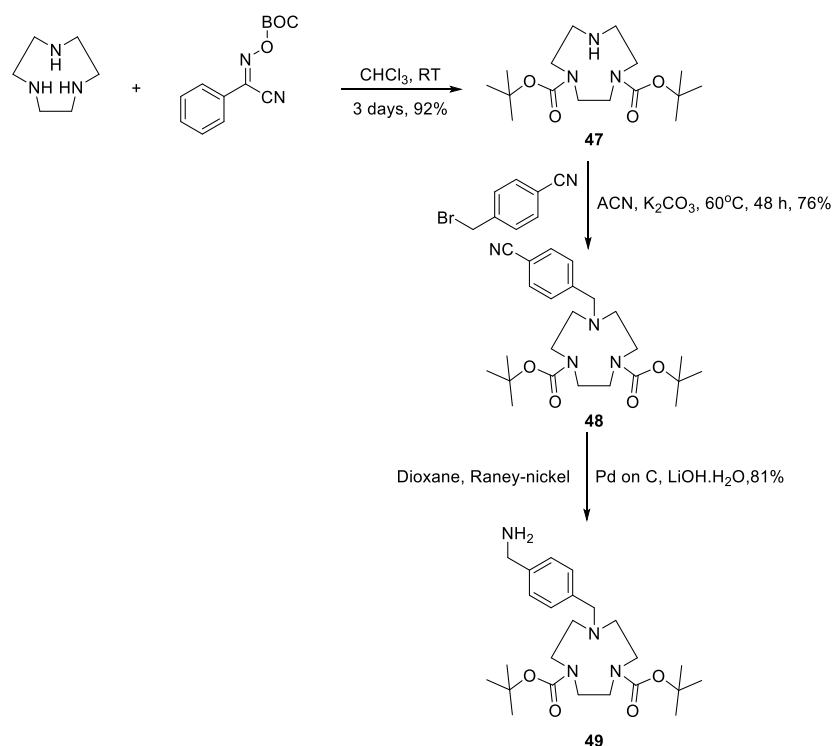
Figure 66: Molecular structures of target compounds

“Cold” standard reference compounds cannot be synthesized with technetium as there are no stable isotopes. The most closely related element is the third row congener of technetium, rhenium. Hence the rhenium(I) complex can be synthesised and used to develop HPLC analysis and separation methods (see Figure 66).



### 5.3 Synthesis of $^{99m}\text{Tc}$ TACN-thiafatty acid radiolabeling precursors

The  $^{99m}\text{Tc}$  radiolabeling precursor was synthesised from TACN which was initially functionalised on one of the ring nitrogens with a cyanobenzyl arm. TACN has three secondary amine groups, therefore, to achieve selective reaction, protection of two of the amine groups is required. The BOC-ON group ((2-(*t*-butoxycarbonyloxyimino)-2-phenylacetonitrile)) was used to add BOC protecting groups to the secondary amines.<sup>223, 224</sup> Di-*tert*-butyl 1,4,7-triazanonane-1,4-dicarboxylate **47** was prepared by protecting the TACN with BOC-ON following previously reported protocols (see Scheme 37).<sup>225</sup> The ratio of TACN to BOC-ON used was 1: 2 to ensure that only two of the three secondary amine nitrogens were protected.



Scheme 37: Synthetic route to protect two of the amine nitrogens on TACN (**47**), to add cyano pendant arm (**48**) and to reduce the cyano group to an amino group (**49**).

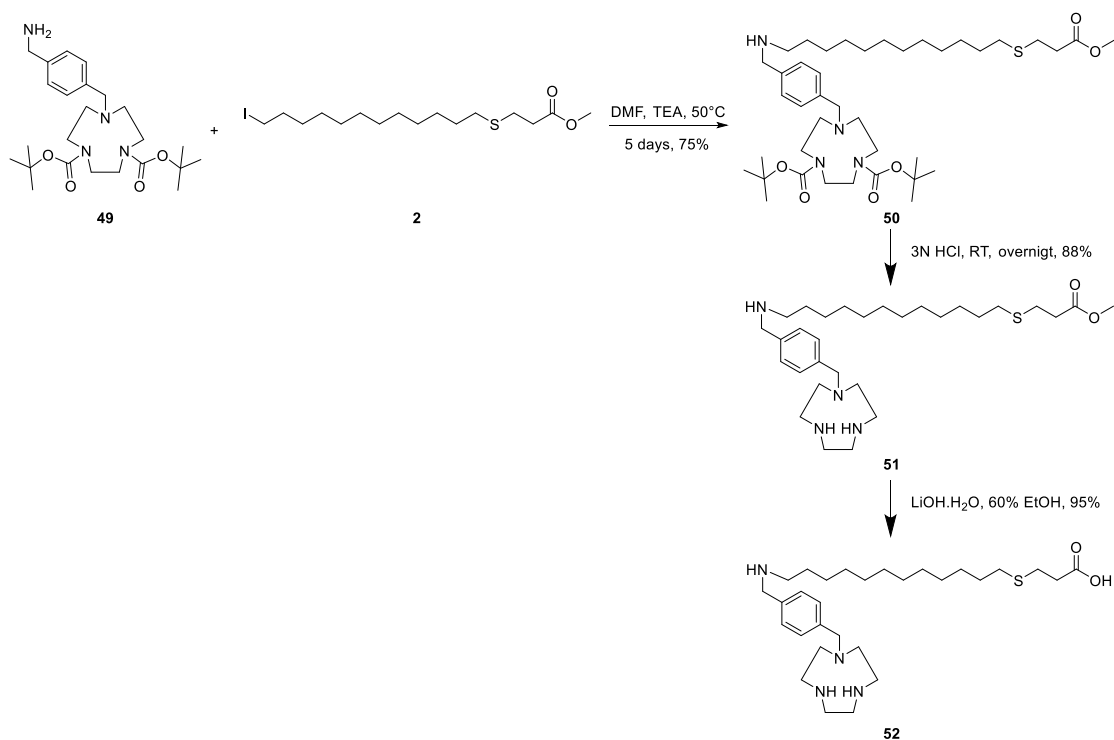
**47** was obtained in a 92% yield as a colourless oil, in line with the literature reports.<sup>225</sup> Di-*tert*-butyl 7-(4-(cyanomethyl)benzyl)-1,4,7-triazanonane-1,4-dicarboxylate **48** was synthesised *via* modification of the method reported by Ortiz *et al.*<sup>226</sup> which was used to

synthesise a related compound (4,4',4''-((1,4,7-triazonane-1,4,7-triyl)tris(methylene))-tribenzonitrile). The conditions were modified to increase the reaction time to 48 h and decrease the temperature to 60°C. **48** was then purified by silica gel column chromatography and isolated as white crystalline solid in a 76% yield.

Nitriles are a versatile synthon for amines and can be prepared by a variety of methods.<sup>227</sup> To conjugate the thia-fatty acid ester with the bis-protected TACN the nitrile group needs to be converted to the amino group (see Scheme 37). Reduction of nitriled in the presence of Boc-protected amino groups was carried out using Raney-nickel following a literature procedure used to prepare the related compound *N*<sup>1</sup>,*N*<sup>9</sup>-di(*tert*-butyloxycarbonyl)-*N*<sup>1</sup>,*N*<sup>9</sup>-di(3-aminopropyl)-1,9-nonanediamine.<sup>227</sup>

The primary amine product **49** was formed within 24 h at 50°C by using Raney nickel and 10% palladium on carbon as catalysts in 1,4-dioxane/water (4: 1) with LiOH as base under an H<sub>2</sub> atmosphere. 1,4-Dioxane was chosen as an inert solvent to repress the formation of N-alkylated by-products. The presence of water was required for the reaction to proceed. Neither Raney-nickel nor palladium on carbon alone affected any reaction under a range of conditions. After column chromatography purification, **49** was isolated as a white crystalline compound in 81% yield.

To produce a novel radiolabeling precursor **52**, three further steps were required. Firstly, reaction of methyl 16-iodo-4-thiapalmitate **2** with the bis-protected TACN benzyl amine **49** to produce compound **50**. Secondly, to remove the BOC-groups to give **51** and finally, to hydrolyse the ester group to give **52** (see Scheme 38).

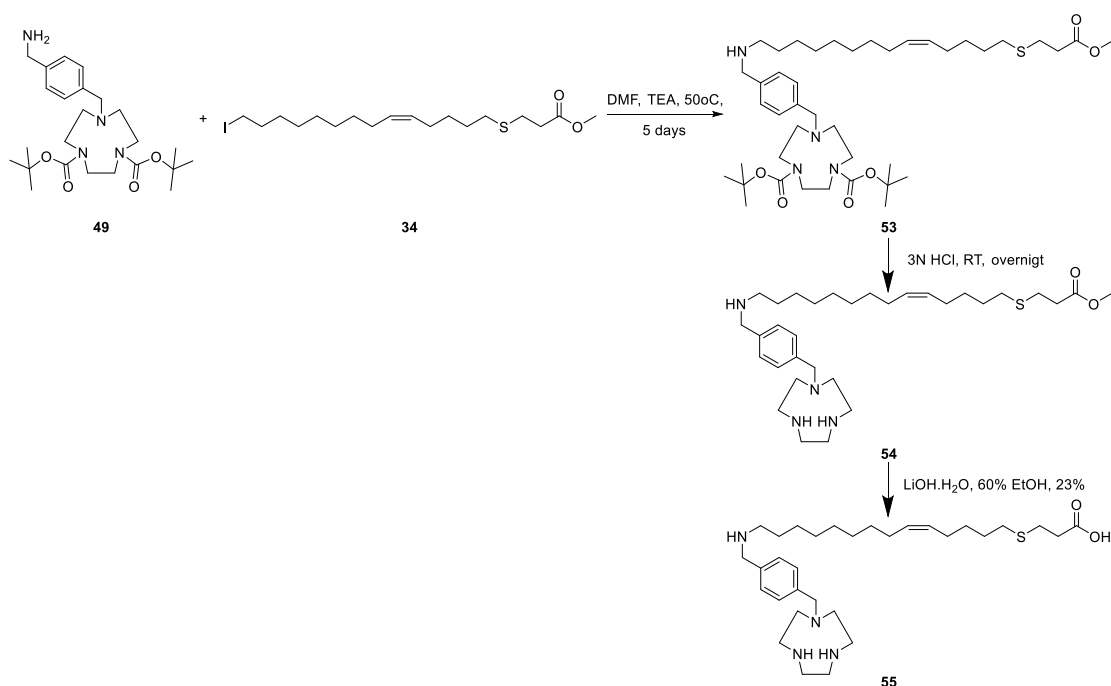


Scheme 38: Synthetic route to produce TACN-thiapalmitic acid **52**

The alkylation reaction was carried out under basic conditions using triethylamine (TEA) as base with dimethylformamide (DMF) as solvent at 50°C for five days to give **50** as a yellow oil in a 75% yield (see Scheme 38). The BOC deprotection was carried out by stirring in a solution of 3 N hydrochloric acid (HCl)/MeOH at room temperature for 24 hours to give the product as a yellow solid in an 88% yield. The hydrolysis of the ester group was carried out using lithium hydroxide monohydrate (LiOH.H<sub>2</sub>O) in 60% EtOH at room temperature for 5 hours. This reaction proceeds *via* a nucleophilic acyl substitution mechanism whereby the hydroxide ion from lithium hydroxide attacks the carbonyl carbon to form a four coordinate, tetrahedral intermediate. This intermediate then collapses to reform the C=O in an acyl-oxygen cleavage resulting in the loss of an alkoxide to form the carboxylic acid. The base, in this case lithium hydroxide, then deprotonates the carboxylic acid group to form a lithiated salt. This salt is converted back into this carboxylic acid during the work up. After 5 hours, HCl (0.1 N) was added dropwise until the pH of the solution reached around 7. The ethanol was removed *in vacuo*, to leave an aqueous fraction which was extracted with DCM. Upon extraction, it was evident that the product had been retained in the

aqueous phase as it had been protonated by the addition of the acid. The aqueous phase also contained lithium chloride and so further separation was required. A solid phase extraction was used with a reverse phase Waters C18 Sep-pak cartridge. After the salts had been washed through, the C18 column was washed with ethanol to elute the product **52**, which was isolated as a brown solid in 35% yield.

The thiaoleic acid derivative **55** was synthesised following the same procedure used to produce **52** (see Scheme 39). The intermediate compounds were isolated with



Scheme 39: Synthetic route to produce TACN-thiaoleic acid **55**

lower purity. The radiolabeling precursor, which was obtained in a 23% yield as a viscous oil, was shown to be of lower purity by elemental analysis (outside the required 0.4% limits) which is likely due to the challenges of analysing an oil as well as potential salt impurities.

## 5.4 Synthesis of rhenium(I) complexes with TACN-thiapalmitic acid/Re(CO)<sub>3</sub>**52** and TACN-thiaoleic acid/Re(CO)<sub>3</sub>**55**

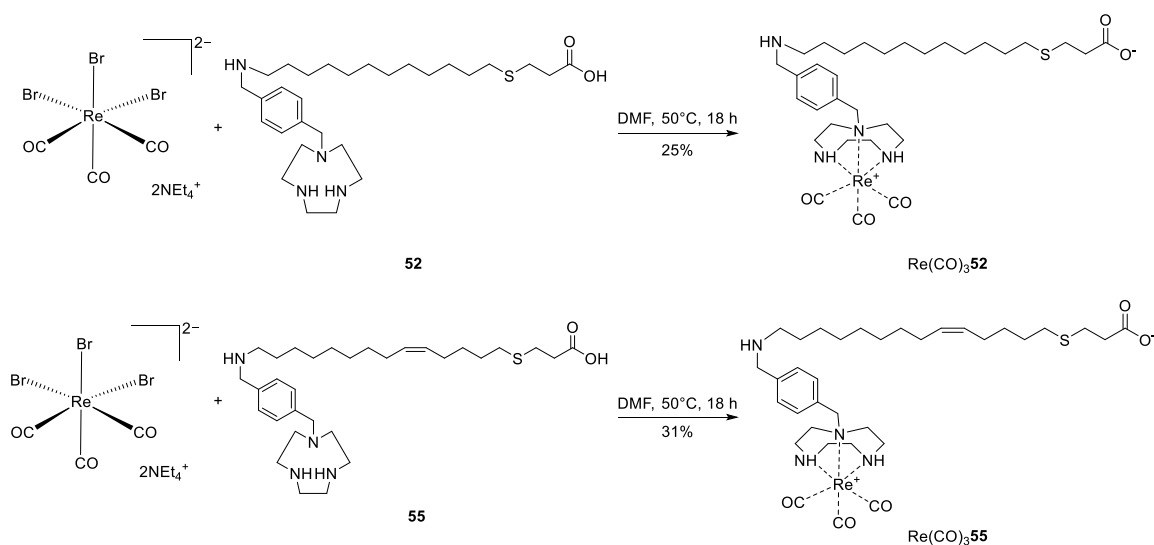
Radiochemistry experiments are challenging to implement without having the HPLC conditions for a non-radioactive “cold” reference compound or standard. In general, radiochemistry is carried out with a very low amount/ concentration of the radioactive isotope. All technetium isotopes are radioactive, thus, the best alternative is to form the reference compound using a metal ion with similar properties to use in the investigation of complex formation reactions and HPLC analysis method development.

Rhenium is the third row congener to technetium in group seven of the transition series. The ionic radii of rhenium is very similar to technetium due to the lanthanide contraction (Tc 1.36 Å; Re 1.37 Å) and so it forms structurally analogous complexes. Technetium and rhenium complexes can have the metal in oxidation states up to +VII (d<sup>0</sup>). Rhenium has been used previously as a non-radioactive replacement ion in order to characterise <sup>99m</sup>Tc radiopharmaceuticals. In spite of the similarities, there are some variations that should be taken into consideration in the preparation of Tc and Re complexes, the most relevant being the easier oxidation of rhenium complexes and their higher kinetic inertness.<sup>56, 221, 228-230</sup>

The rhenium(I) tricarbonyl complex was formed by addition of TACN-thiapalmitic acid **52** or TACN-thiaoleic acid **55** in DMF to a stirred solution of [Et<sub>4</sub>N]<sub>2</sub>[Re(CO)<sub>3</sub>(Br)<sub>3</sub>]<sup>2+</sup> and then, heating to 50°C for 18 hours (see Scheme 40). [Et<sub>4</sub>N]<sub>2</sub>[Re(CO)<sub>3</sub>(Br)<sub>3</sub>]<sup>2+</sup> was prepared by a member of the Archibald group and supplied for us in this project (Mrs. Rebecca Hargreaves).

The rhenium(I) tricarbonyl unit coordinates with the TACN moiety which acts as a tridentate face-capping ligand, with the three nitrogens acting as donor atoms, to give an octahedral geometry. Therefore, this complex is positively charged and the carboxylic acid can be deprotonated to balance the charge. [Re(CO)<sub>3</sub>]<sup>+</sup> complexes are

low spin  $d^6$  configuration, with no unpaired electrons, rendering the rhenium(I) metal inert to ligand substitution and consequently increasing its stability *in vivo*.<sup>221</sup>



Scheme 40: Synthetic route to produce standard reference compounds  $\text{Re}(\text{CO})_3\mathbf{52}$  and  $\text{Re}(\text{CO})_3\mathbf{55}$

The rhenium(I) TACN-thiaoleic acid complex  $\text{Re}(\text{CO})_3\mathbf{55}$  and TACN-thia palmitic acid complex  $\text{Re}(\text{CO})_3\mathbf{52}$  were isolated as yellow/brown oils in yields of 31% and 25% respectively. The low yields may be due to the small scale and washing step required to remove salts formed in the reaction. The formation of the desired products was confirmed by mass spectrometry. HPLC method development for  $\text{Re}(\text{CO})_3\mathbf{52}$  and  $\text{Re}(\text{CO})_3\mathbf{55}$  gave retention times (see Figure 67), respectively, at 17:17 min and 19:27 min.

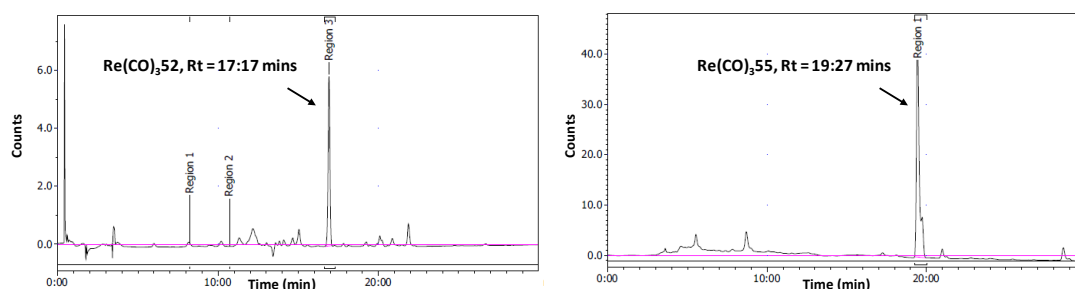
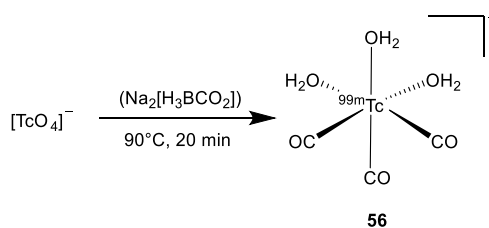


Figure 67: HPLC traces of standard reference compounds  $\text{Re}(\text{CO})_3\mathbf{52}$  and  $\text{Re}(\text{CO})_3\mathbf{55}$

## 5.5 $^{99m}\text{Tc}$ radiolabeling of TACN-thiapalmitic acid/ $^{99m}\text{Tc}(\text{CO})_3\mathbf{56}$

As mentioned in the introduction, the favourable properties of the isotope including the half-life, gamma emission energy, generator production and flexible coordination chemistry/ oxidation states make it a good choice for SPECT imaging applications.  $[\text{}^{99m}\text{TcO}_4]^-$ , which is eluted from the generator is as anion with technetium in the highest oxidation state (+VII) and is used as the precursor in the synthesis of all  $^{99m}\text{Tc}$ -based complexes for imaging applications. However, in order to form complexes with chelating ligands,  $[\text{}^{99m}\text{TcO}_4]^-$  must be reduced from Tc(VII) to a lower oxidation state, then the  $^{99m}\text{Tc}$ -radiopharmaceutical can be synthesised.<sup>57, 231, 232</sup> In this work,  $^{99m}\text{Tc}$  was eluted from the  $^{99}\text{Mo}/^{99m}\text{Tc}$  generator as  $[\text{}^{99m}\text{TcO}_4]^-$  and reduced to give **56**  $[\text{}^{99m}\text{Tc}(\text{OH}_2)_3(\text{CO})_3]^+$  (see Scheme 41).<sup>58</sup> Sodium boranocarbonate ( $\text{Na}_2[\text{H}_3\text{BCO}_2]$ ) is as a reducing agent and is also an *in situ* source of carbon monoxide (CO).



Scheme 41: Synthesis of the organometallic precursor  $[\text{}^{99m}\text{Tc}(\text{OH}_2)_3(\text{CO})_3]^+$  **56**

**56** was analysed by HPLC and the retention times of  $^{99m}\text{TcO}_4^-$  and  $[\text{}^{99m}\text{Tc}(\text{OH}_2)_3(\text{CO})_3]^+$  were found to be 5:50 min and 13:35 min respectively (see Figure 68).

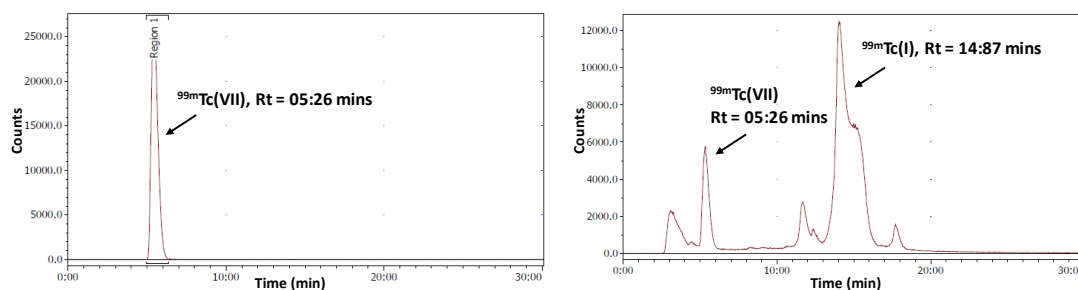


Figure 68: HPLC traces of  $[\text{}^{99m}\text{TcO}_4]^-$  and  $[\text{}^{99m}\text{Tc}(\text{OH}_2)_3(\text{CO})_3]^+$  **56**





= 17:17 min. All conditions tested showed high radiolabeling yields with sodium acetate at pH 11 selected for the subsequent studies.

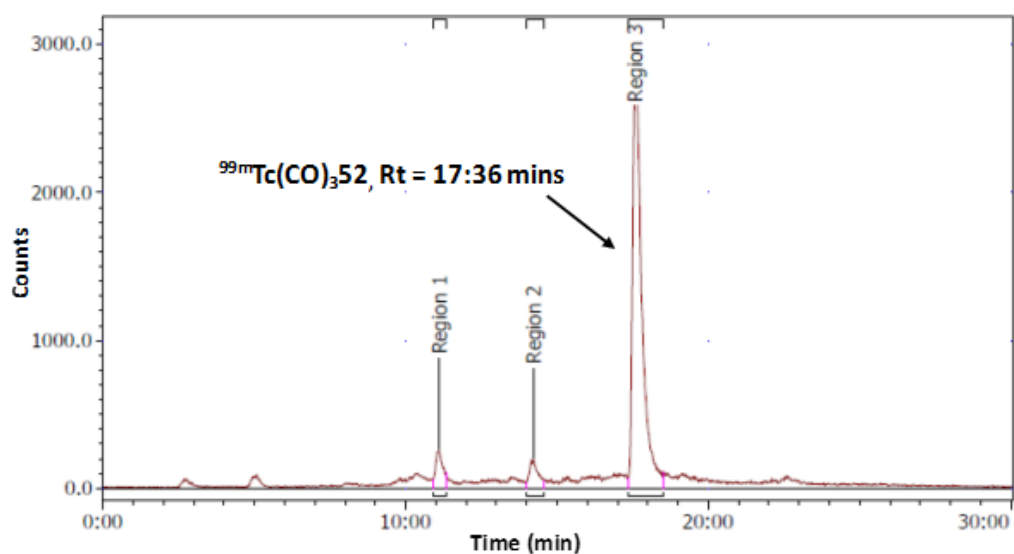


Figure 69: Radio-HPLC trace of  $^{99m}\text{Tc}(\text{CO})_3\mathbf{52}$

### 5.5.2 Radiolabeling of the precursor **52** at a range of concentrations

A solution of  $[\text{}^{99m}\text{Tc}(\text{OH}_2)_3(\text{CO})_3]^+$  **56** was added to different concentrations of **52** in sodium acetate buffer at pH 11. The total volume of reaction mixture used was 200  $\mu\text{L}$  with the reaction mixture shaken at  $90^\circ\text{C}$  for 30 min and the analysed by HPLC. Figure 70 shows the yields over the concentration range, indicating that 3.22 mmol is the lowest concentration to give a reasonable radiolabeling yield.

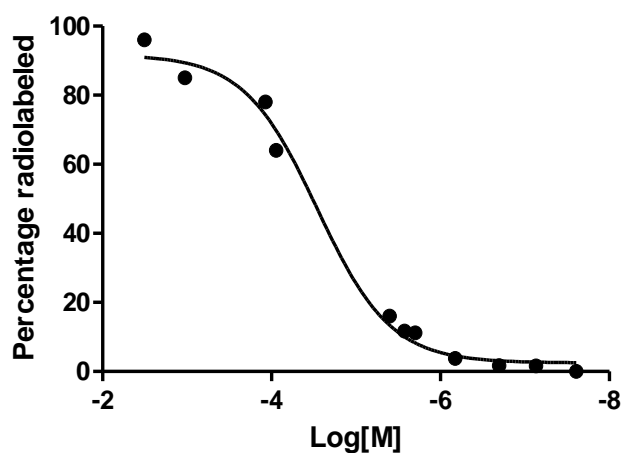


Figure 70: The effect of varying the concentration of **52** on radiolabeling efficiency,  $n=1$

### 5.5.3 Radiolabeling of the precursor **52** at various temperatures

A solution of [ $^{99m}\text{Tc}(\text{OH}_2)_3(\text{CO})_3$ ] $^+$  **56** was added to precursor **52** (3.22 mmol) in sodium acetate at pH 11. The total volume of the reaction mixture was 200  $\mu\text{L}$  and it was shaken at different temperatures (RT, 50°C and 90°C) for 30 min (see Table 5), and analysed by HPLC. Carrying out the reaction at 90°C gives the highest yield but reasonable yields are also achieved at 50°C and RT. Based on this work the  $^{99m}\text{Tc}$  radiolabeling reaction of **52** was carried out at 90°C for 30 min in sodium acetate at pH 11 using 3.22 mmol of the precursor.

Temperature °C	Radiolabeling yield %
90	96
50	88
RT	80

Table 5: The effect of temperature on  $^{99m}\text{Tc}$  radiolabeling yield of **52**, n=1

### 5.5.4 Purification and isolation of the $^{99m}\text{Tc}(\text{CO})_3$ **52**

The crude radiolabeled compound,  $^{99m}\text{Tc}(\text{CO})_3$ **52**, was synthesised on a larger scale and was purified using semi-preparative HPLC. The results are slightly different to those observed by analytical HPLC with the lower amounts of activity. Figure 71 shows a typical chromatogram with unreacted  $^{99m}\text{Tc}(\text{I})$  tricarbonyl compound,  $^{99m}\text{Tc}(\text{VII})$  and some unidentified radiolabeled products eluted prior to the  $^{99m}\text{Tc}(\text{CO})_3$ **52** at 17:40 to 17:88 min. All fractions were collected and activity in each was measured. 73 MBq of the radioactive crude compound was injected and the amounts of the identified fractions collected were:  $^{99m}\text{Tc}(\text{VII})$  0.13 MBq,  $^{99m}\text{Tc}(\text{I})$  1.4 MBq and  $^{99m}\text{Tc}$ -TACN-thiapalmitic acid 30 MBq.

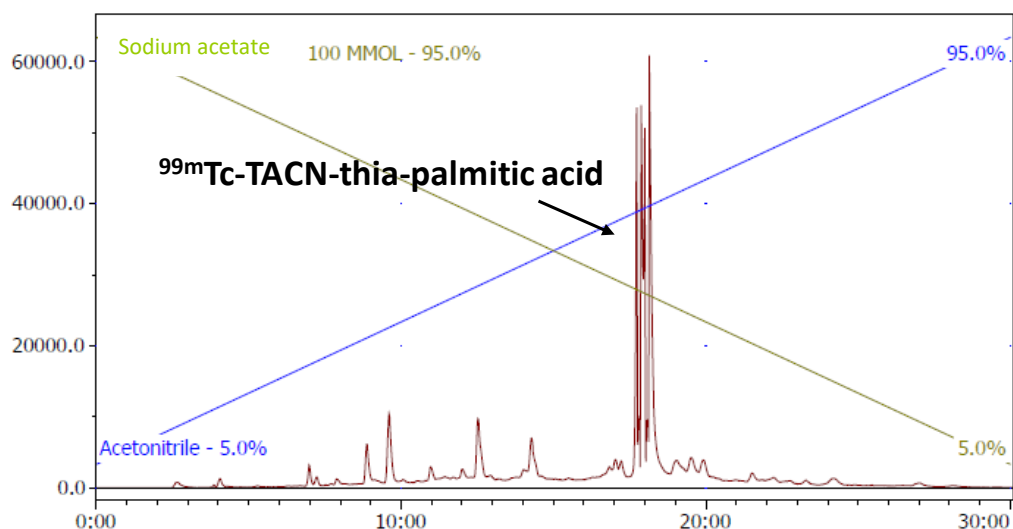


Figure 71: Radio-HPLC trace of semi-preparative separation of  $^{99m}\text{Tc}(\text{CO})_3\mathbf{52}$

$^{99m}\text{Tc}(\text{CO})_3\mathbf{52}$  is eluted in acetonitrile/ sodium acetate buffer which is not biocompatible. Thus, for *in vivo* administration of the  $^{99m}\text{Tc}(\text{CO})_3\mathbf{52}$ , the acetonitrile needs to be replaced by ethanol or another suitable solvent to ensure biocompatibility. A solid phase extraction is preferred to evaporation and this was carried out using an Oasis C18 cartridge.

The  $^{99m}\text{Tc}(\text{CO})_3\mathbf{52}$  containing fraction was diluted three-fold with water and loaded onto the C18 cartridge. The retention varied from 85% to almost quantitative. Then, the cartridge was washed with water without a noticeable loss of activity (< 3%) and dried by passing argon through it. 29 MBq of  $^{99m}\text{Tc}(\text{CO})_3\mathbf{52}$  was trapped on the cartridge which could be eluted using EtOH to release 17 MBq (leaving 12 MBq stuck in the cartridge). Analysis of this fraction by HPLC showed that another peak was present ( $R_t = 15:34$  min) as well as the peak for the desired product (see Figure 72).

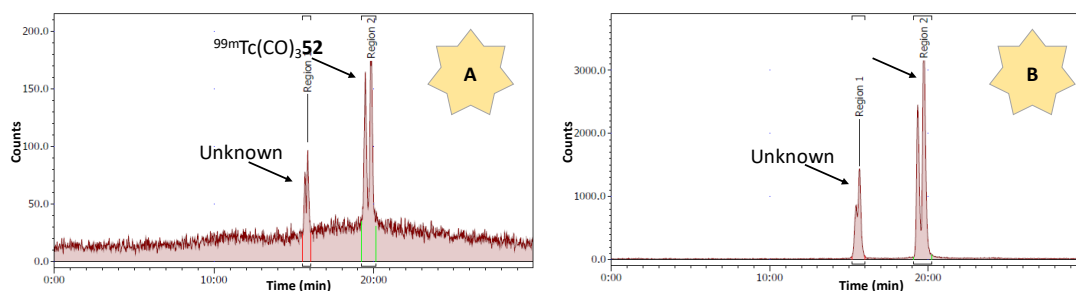


Figure 72: Radio-HPLC traces of  $^{99m}\text{Tc}(\text{CO})_3\mathbf{52}$ ; A: after C18 cartridge; B: after formulation

The ethanol fraction was dried and dissolved in 3% bovine serum albumin (BSA) in isotonic saline. It was then analysed again with HPLC (after precipitation of the BSA by addition of acetonitrile and centrifugation) by sampling the supernatant solution. This gave the same HPLC chromatogram observed before formulation (see Figure 72). The identity of the new peak is unknown but, as it appears on the addition of ethanol, potentially a solvent molecule could be replacing one of the carbonyl (CO) groups. Further investigation is required. In an attempt to clarify what had occurred, alternative solvents to ethanol (acetonitrile, ether and THF) were investigated for elution of the  $^{99m}\text{Tc}(\text{CO})_3\mathbf{52}$  from the C18 cartridge. All of these solvents failed to elute the activity. In a further experiment, the crude  $^{99m}\text{Tc}(\text{CO})_3\mathbf{52}$  (prior to semi-preparative HPLC purification) was diluted three times with water and loaded on the C18 cartridge, following the same process including the ethanol elution as with the purified compound. HPLC analysis showed that the same unidentified peak was present in the chromatogram. This indicates that it is the ethanol that is reacting or causing reaction of  $^{99m}\text{Tc}$ - $^{99m}\text{Tc}(\text{CO})_3\mathbf{52}$ , and that this is occurring in the solid phase extraction step not on the semi-prep HPLC. Stability of the crude  $^{99m}\text{Tc}(\text{CO})_3\mathbf{52}$  was investigated in serum. HPLC analysis revealed that the  $^{99m}\text{Tc}(\text{CO})_3\mathbf{52}$  was sufficiently stable during incubation at 37°C up to 3 hours in serum (see Figure 73).

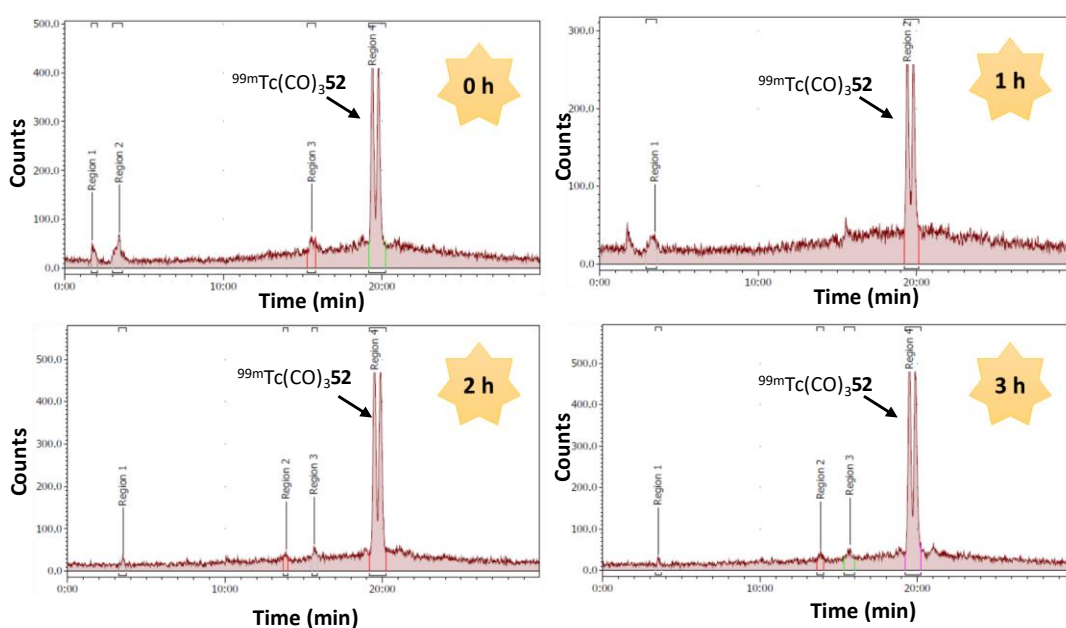


Figure 73: Radio-HPLC traces of  $^{99m}\text{Tc}(\text{CO})_3\mathbf{52}$  in serum over 3 hours (0, 1, 2 and 3 hours)

The stability of  $^{99m}\text{Tc}(\text{CO})_3\mathbf{52}$  in phosphate buffer solution (PBS) was also studied, again showing that the compound was stable according to HPLC analysis (see Figure 74).

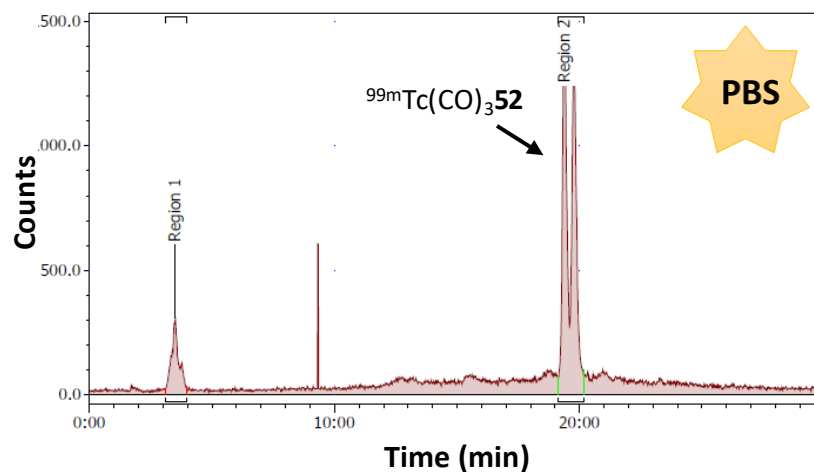
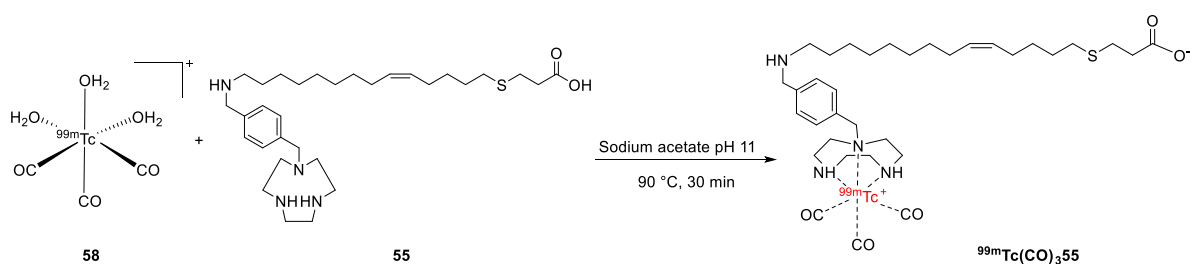


Figure 74: Radio-HPLC trace of  $^{99m}\text{Tc}(\text{CO})_3\mathbf{52}$  in PBS after 3 hours

## 5.6 $^{99m}\text{Tc}$ radiolabeling of TACN-thiaoleic acid/ $^{99m}\text{Tc}(\text{CO})_3\mathbf{55}$

$^{99m}\text{Tc}(\text{CO})_3\mathbf{55}$  was studied using similar conditions to those used for  $^{99m}\text{Tc}$  radiolabeling of  $^{99m}\text{Tc}(\text{CO})_3\mathbf{52}$  (sodium acetate buffer at pH 11, heated at 90°C for 30 min). One variation in the conditions was a slightly higher amount of the precursor at 4.58 mmol (see Scheme 43).



Scheme 43: Reaction pathway to  $^{99m}\text{Tc}$  radiolabeling of novel precursor  $\mathbf{55}$

One main radioactive peak was observed in the radio-HPLC trace, eluting at 19:55 min (see Figure 75). This was identified as  $^{99m}\text{Tc}(\text{CO})_3\mathbf{55}$  by comparison with the UV detector HPLC trace of the  $\text{Re}(\text{CO})_3\mathbf{55}$ , which eluted at 19:27 min.

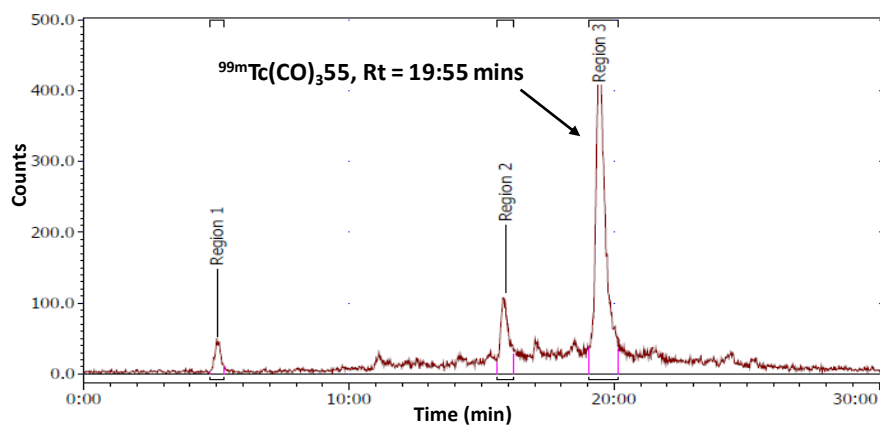


Figure 75: Radio-HPLC trace of  $^{99m}\text{Tc}(\text{CO})_3\mathbf{55}$

$^{99m}\text{Tc}(\text{CO})_3\mathbf{55}$  was purified by semi-preparative HPLC. Then, the same procedure was followed to isolate the potential radiotracer into a more appropriate solvent system (the collected fraction was diluted 3 fold with water and loaded on the C18 cartridge). The cartridge was washed and dried as previously and the trapped activity was eluted using ethanol. On analysis of the purified compound by HPLC, again an unidentified peak had appeared ( $R_t = 17:40$  min).

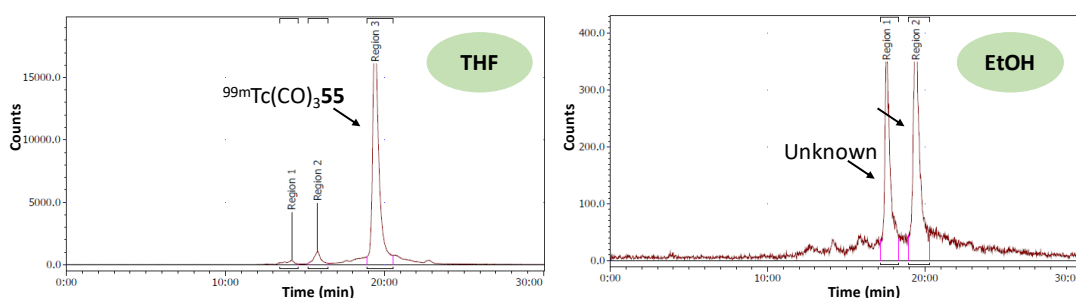


Figure 76: Radio-HPLC trace  $^{99m}\text{Tc}(\text{CO})_3\mathbf{55}$  after C18 cartridge purification and elution with different solvents

In this case it was possible to use different solvents to elute the product from the C18 cartridge with THF effective in releasing the product (see Figure 76). When THF was used as the elution solvent the unidentified peak was no longer present. This supports the idea that one of the carbonyl (CO) groups was replaced by a coordinating ethanol moiety (see Figure 77).

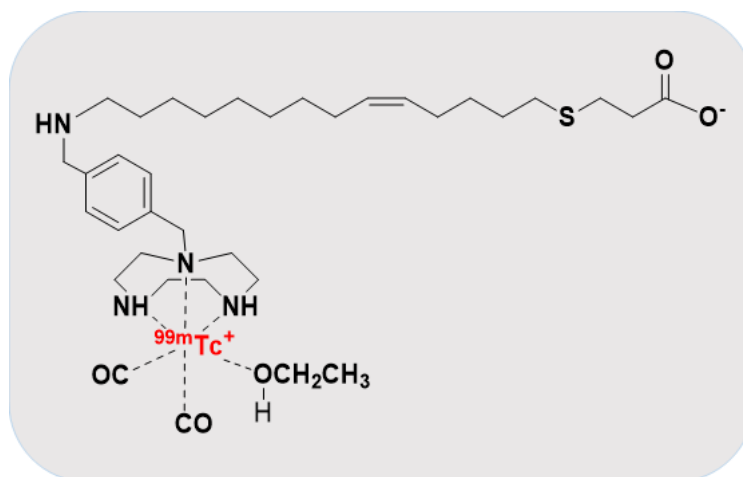


Figure 77: Proposed structure where a carbonyl (CO) group has been replaced by an ethanol moiety

## 5.7 Conclusions

The synthesis of novel TACN-thiapalmitic and TACN-thiaoleic acid compounds has been achieved to give compounds suitable for radiolabeling with a  $^{99m}\text{Tc}(\text{CO})_3^+$  unit. The protected macrocycle **47** was synthesised and functionalised with a cyano-benzyl arm to give **48** followed by reduction of the cyano group to a primary amine (**49**). Following purification by silica gel column chromatography, this compound was reacted with bromothiopalmitate or iodothiaoleate followed by deprotection of the BOC groups and hydrolysis of the ester to give TACN-thiapalmitic acid **52** and TACN-thiaoleic acid **55**. The “cold” reference standard compounds with rhenium(I) tricarbonyl were successfully synthesized ( $\text{Re}(\text{CO})_3$ **52** and  $\text{Re}(\text{CO})_3$ **55**) and an HPLC separation method was developed. The conditions for  $^{99m}\text{Tc}$  radiolabeling of TACN-thiapalmitic acid and TACN-thiaoleic acid were investigated (with optimal conditions from those tested; sodium acetate buffer at pH 11, heated to 90°C for 30 min to label 3.22-4.58 mmol of the precursor). Issues were encountered on formulation following purification by semi-preparative HPLC with an impurity appearing when the solid phase extraction cartridge was eluted with ethanol. Where it was possible to elute with an alternative solvent (THF), this could be avoided.

# **Chapter Six**

## **Conclusions and Future work**



## Chapter Six: Conclusions and Future work

### 6.1 Conclusions

#### 6.1.1 Overview

The importance of cardiac imaging agents as drug development and clinical research tools drives the development of tracers capable of quantifying the extent of cardiac fatty acid metabolism. Existing thia-fatty acid tracers present suboptimal myocardial retention and suffer from nonspecific uptake and slow elimination.

New, more specific cardiac PET tracers with improved pharmacokinetic profiles, would be a useful tool for finding better diagnostic and therapeutic strategies in the battle against the cardiac disease.

#### 6.1.2 Main achievements

The synthesis of a four different chain length (8 atoms (caprylic), 10 atoms (capric), 16 atoms (palmitic) and 18 atoms (oleic)) thiafatty acid derivatives is described in this work. Three of the  $^{18}\text{F}$  target compounds have been synthesised previously. Novel synthetic strategies to give target compounds were developed and protocols optimized in order to improve yields or to facilitate purification (see Table 6).

A novel radiolabeling precursor **18** and “cold” reference standard **21** for thiacaprylic acid (FTC1) were prepared. A modified synthetic route was used to prepare known thiapalmitic acid radiolabeling precursors (iodo derivative **2** and bromo derivative **3**) and the “cold” reference standard **6**. The radiolabeling precursors (bromo **22** and iodo **23** (novel)) and “cold” reference standard **26** for thiacapric acid (FTC2) were prepared by a modified synthetic route.

The completion of a novel multi-step synthetic route (six steps) to obtain the labeling precursors **32**, **33** and **34** and “cold” reference standard **36** for thia-oleic acid have been outlined. In particular, tetrahydropyranyl (THP) and dimethyl-*tert*-butylsilyl (TBDMS) groups were investigated for temporary protection of terminal alcohol group, with selection of the former.

Two alkylation methods giving access to 4-thia fatty acid derivatives were explored. Early problems with tosylation of sulfur containing derivatives were solved, and the synthesis of tosylated-thiafatty acid was optimised. The fluorination reaction was successful and the HPLC methods for analysis of the “cold” reference standards were developed.

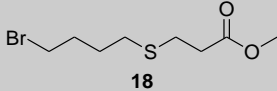
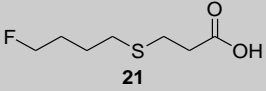
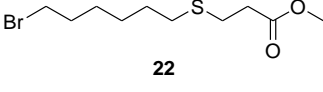
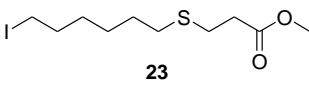
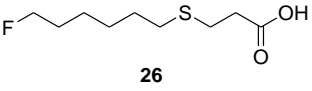
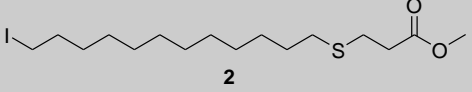
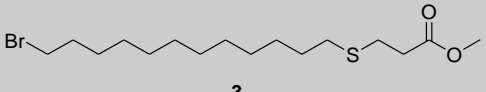
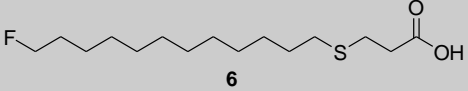
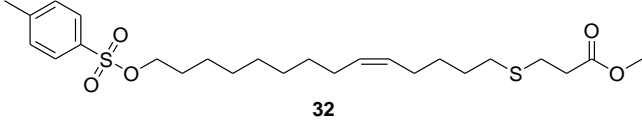
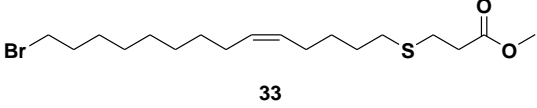
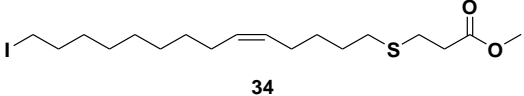
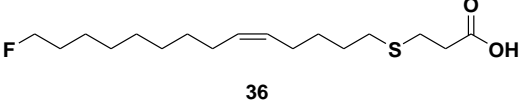
Thia fatty acid	Radiolabeling precursors	Ref.	"cold" reference standards	Ref.	Novelty
TCD1	 18	This work	 21	This work	Novel compounds
TCD2	 22  23	130  This work	 26	130	<b>16</b> and <b>17</b> modified synthesis from literature and <b>14</b> novel precursor
TPD	 2  3	109  4	 6	4, 109	<b>22</b> and <b>23</b> modified synthetic from literature and <b>26</b> new synthetic routes
TOD	 32  33  34	111  111  This work	 36	111	<b>32</b> and <b>33</b> modified synthetic from literature and <b>36</b> new synthetic routes

Table 6: The chemical structure for compounds synthesised and reported in Chapter Two

Radiolabeling methods for preparation of  $\omega$ -fluorinated thia-fatty acids, [ $^{18}\text{F}$ ]FTP, [ $^{18}\text{F}$ ]FTC2 and [ $^{18}\text{F}$ ]FTO were developed to give the target compounds in good yields (see Table 7).

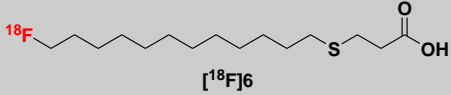
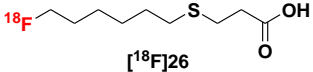
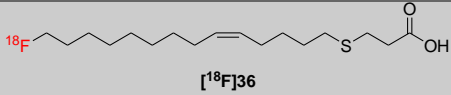
Precursors	Radiotracers	Fluorine incorporation yield	Decay corrected yield	Activity for <i>in vivo</i> administration
Iodo precursor <b>2</b>	 [ $^{18}\text{F}$ ]6	63 $\pm$ 8 %	18.00 $\pm$ 1.2 %	50-100 MBq/ 500 $\mu\text{L}$
Iodo precursor <b>22</b>	 [ $^{18}\text{F}$ ]26	47 $\pm$ 4 %	16.15 $\pm$ 2.6%	50-100 MBq/ 500 $\mu\text{L}$
Bromo precursor <b>33</b>	 [ $^{18}\text{F}$ ]36	72 $\pm$ 1 %	17.75 $\pm$ 1.7%	50-75 MBq/ 500 $\mu\text{L}$

Table 7: Summary of radiosynthesis results for [ $^{18}\text{F}$ ]FTP, [ $^{18}\text{F}$ ]FTC2 and [ $^{18}\text{F}$ ]FTO (Chapter Three)

The comparison study between radiolabeling of the 18-tosyl-, 18-iodo- or 18-bromo-4-thiaoleate **32**, **33** and **34** precursors show that radiolabeling of the bromo precursor provides the highest fluorine incorporation yield (see Table 8).

Precursors	Fluorine incorporation yield
Tosyl precursor <b>32</b>	50 $\pm$ 5 %
Bromo precursor <b>33</b>	50 $\pm$ 2 %
Iodo precursor <b>34</b>	72 $\pm$ 1 %

Table 8: Comparison study between radiolabeling of the 18-tosyl-, 18-iodo or 18-bromo-4-thiaoleate **32**, **33** and **34** precursors (Chapter Three)

Cardiac uptake of [ $^{18}\text{F}$ ]FTP and [ $^{18}\text{F}$ ]FTO *in vivo* using a rat model was confirmed by PET/CT imaging. In the same model, [ $^{18}\text{F}$ ]FTC2 did not show significant cardiac accumulation. These results confirmed that cardiac retention of thia-fatty acids is expected to reflect the extent of fatty acid metabolism. Long alkyl chain thia-fatty

acids are actively taken up by myocytes, but show poor blood solubility and fast liver-based elimination due to their high lipophilicity. There is no active transport of medium fatty acids, which may result in more favourable pharmacokinetics. [<sup>18</sup>F]FTP, [<sup>18</sup>F]FTC2 and [<sup>18</sup>F]FTO are all stable in serum. PET imaging studies did not reveal any significant cardiac uptake or accumulation of [<sup>18</sup>F]FTP in nude mice. Thus, the animal model selected plays an important role in the *in vivo* imaging study.

The successful synthesis of novel copper(II) cross-bridged cyclam complexes functionalised with a triphenylphosphonium group to target the mitochondria was carried out. A multi-step synthetic route to obtain the cross-bridged cyclam ligands was designed and completed. All relevant compounds (**37**, **38**, **39**, **40** and **41**) were produced in good yields and fully characterised.

A cross-bridged cyclam chelator bearing a benzylcyano pendant arm was synthesised, along with the copper(II) complexes with different anion (chloride and perchlorate). The exchange of bound solvent or anion for 10-fluoro-4-thiacapric acid to form a complex with the bound fatty acid [Cu**40(26)**]<sup>+</sup> and also the fluorine-18 labelled equivalent [<sup>18</sup>F][Cu**40(26)**]<sup>+</sup> was investigated and HPLC analysis conditions developed (see Table 9). The formation of the [<sup>18</sup>F]10-fluoro-4-thiacaprate complex with copper(II) cross-bridged cyclam compound requires further optimisation before the process can be applied to the phosphonium derivative.

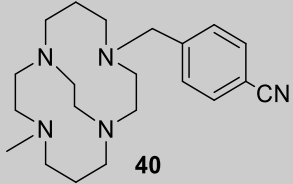
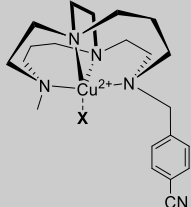
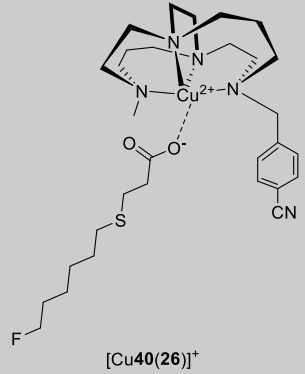
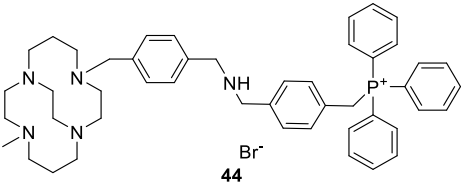
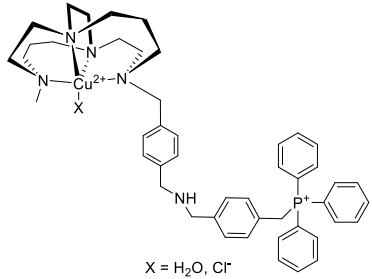
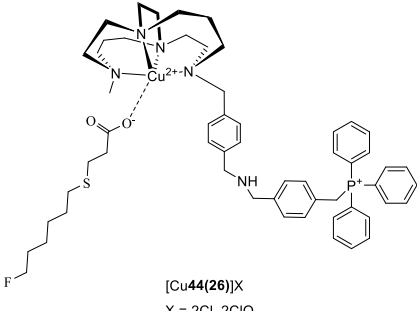
Ligands	Ref.	Complexes	Ref.	Non-targeted and targeted mitochondria	Ref.	Novelty
 <p><b>40</b></p>	190, 193	 <p>X = H<sub>2</sub>O, Cl<sup>-</sup> [Cu<b>40</b>Cl]Cl [Cu<b>40</b>H<sub>2</sub>](ClO<sub>4</sub>)<sub>2</sub></p>	This work	 <p>[Cu<b>40</b>(<b>26</b>)]<sup>+</sup></p>	This work	The ligand <b>40</b> was synthesised following literature, novel compounds are complexes and non-targeted mitochondria
 <p><b>44</b> Br<sup>-</sup></p>	This work	 <p>X = H<sub>2</sub>O, Cl<sup>-</sup> [Cu<b>44</b>Cl]Cl<sub>2</sub> [Cu<b>44</b>H<sub>2</sub>](ClO<sub>4</sub>)<sub>3</sub></p>	This work	 <p>[Cu<b>44</b>(<b>26</b>)]X X = 2Cl, 2ClO<sub>4</sub></p>	This work	Novel compounds

Table 9: The molecular structure for selected macrocyclic compounds synthesised (Chapter Four)

The synthesis of novel intermediates and  $^{99m}\text{Tc}$  radiolabeled TACN-thiapalmitic and thiaoleic acid was carried out (see Table 10).

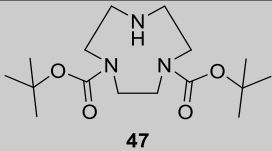
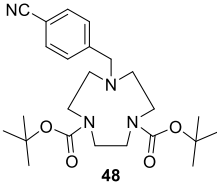
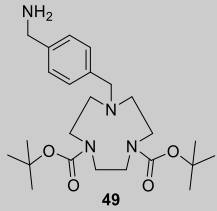
Intermediate derivatives	Yield%	Ref.	Novelty
 <p style="text-align: center;">47</p>	92%	219	Known compound
 <p style="text-align: center;">48</p>	76%	This work	Novel compound
 <p style="text-align: center;">49</p>	81%	This work	Novel compound

Table 10: The molecular structures of key compounds produced for macrocycle attachment (Chapter Five)

The synthesis of novel TACN-thiapalmitic and thiaoleic acid compounds that incorporate a macrocyclic chelator suitable for radiolabeling with a  $^{99m}\text{Tc}(\text{CO})_3^+$  core was achieved. The precursor compounds **52** and **55** were radiolabelled. The “cold” reference standards, containing rhenium were synthesized for both precursors,  $\text{Re}(\text{CO})_3\mathbf{52}$  and  $\text{Re}(\text{CO})_3\mathbf{55}$ , and the HPLC analysis method was developed. The conditions for  $^{99m}\text{Tc}$  radiolabeling of TACN-thiapalmitic acid and TACN-thiaoleic acid were developed to give  $^{99m}\text{Tc}(\text{CO})_3\mathbf{52}$   $^{99m}\text{Tc}(\text{CO})_3\mathbf{55}$  respectively (see Table 11).

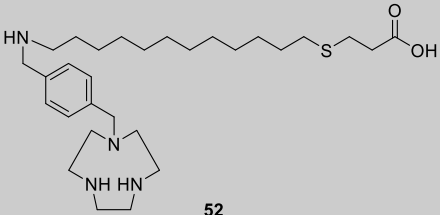
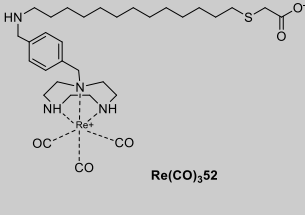
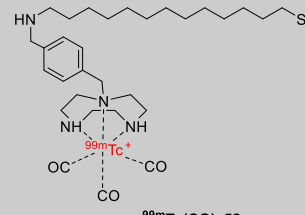
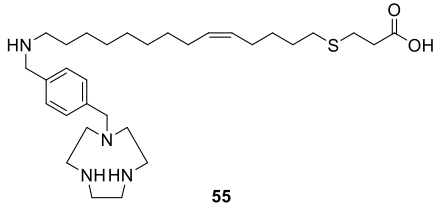
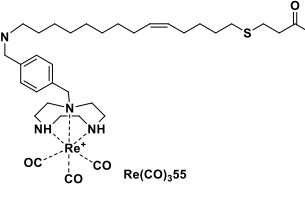
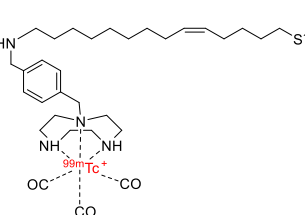
Radiolabeling precursor	Ref.	"cold" reference standard	Ref.	<sup>99m</sup> Tc-tracers	Ref.	Novelty
 <p>52</p>	This work	 <p>Re(CO)<sub>3</sub>52</p>	This work	 <p><sup>99m</sup>Tc(CO)<sub>3</sub>52</p>	This work	Novel compounds
 <p>55</p>	This work	 <p>Re(CO)<sub>3</sub>55</p>	This work	 <p><sup>99m</sup>Tc(CO)<sub>3</sub>55</p>	This work	Novel compounds

Table 11: The molecular structures for key rhenium and technetium compounds synthesised (Chapter Five)



## 6.2 Future work

This section describes future work, including potential short term and long term goals to extend the scope of this study.

### 6.2.1 Short term goals

- To optimise the synthesis of radiolabeling precursor **12** to improve the low overall yield.
- To compare *in vivo* blocking of cardiac uptake of [<sup>18</sup>F]FTP, [<sup>18</sup>F]FTO and [<sup>18</sup>F]FTC2. This could be achieved by treating the rat to be imaged with mitochondrial enzyme CPT-I inhibitor “Etomoxir”.
- To optimise the formation of the [<sup>18</sup>F]10-fluoro-thiacapric acid complex with copper(II) cross-bridged cyclam compound [Cu**40**(OH<sub>2</sub>)]X<sub>2</sub>
- To optimise the <sup>99m</sup>Tc radiolabeling and purification of TACN-thiapalmitic acid **52** and TACN-thiaoleic acid **55** derivatives.

### 6.2.2 Long-term goals

A key aim would be to extend the formation of the [<sup>18</sup>F]10-fluoro-4-thiacapric acid to potentially mitochondria targeted copper cross-bridged cyclam complexes and to validate their targeting properties. Key aspects include:

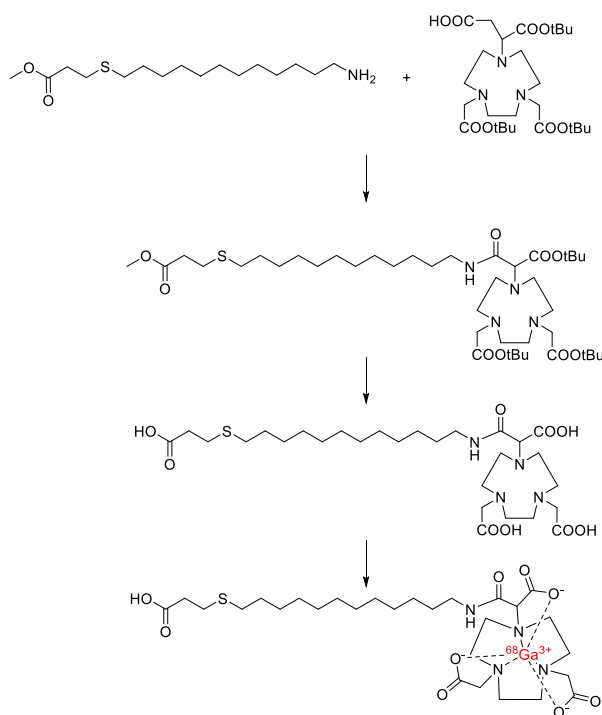
- Investigating cellular uptake and *in vivo* pharmacokinetic properties of the copper(II) macrocycle-thiacaprylic acid complexes.
- Comparison of cardiac uptake of mitochondria-targeted radiolabelled thiacaprylic acid complexes with cardiac uptake of the free medium chain acid tracer and free long-chain/ oleic fatty acid tracers (which would show active uptake *via* the carnitine shuttle).

It would be of high interest to study radiotracer <sup>99m</sup>Tc(CO)<sub>3</sub>**52** and <sup>99m</sup>Tc(CO)<sub>3</sub>**52** *in vivo*.

- An initial study of *in vivo* cardiac uptake in a healthy rat (control)

- Followed by a study with *in vivo* blocking of cardiac uptake (where the rat is treated with mitochondrial enzyme CPT-I inhibitor “Etomoxir”).

It would be interesting to radiolabel the long and medium chain thiafatty acids with another radionuclide such as  $^{68}\text{Ga}$ , for which a similar strategy as that used for technetium-99m labelling could be adopted utilising a different chelator (see Scheme 44).



Scheme 44: Suggested synthetic route to produce gallium-68 radiolabeled thiapalmitic acid

# **Chapter Seven**

## **Experimental**

## Chapter Seven: Experimental

### 7.1 Materials

All chemicals and solvents were purchased from Sigma-Aldrich (Dorset, UK) and Alfa Aesar (Heysham, Lancashire, UK), Fisher Scientific Ltd (Loughborough, UK), VWR International S.A.S (EC) or Fisher Scientific Ltd (Loughborough, UK) and were either laboratory or analytical grade. Deuterated solvents were purchased from Cambridge Isotopes Laboratories Ltd (London, UK) or Goss Chemicals (Crewe, Cheshire, UK). Anion exchange cartridge QMA, Oasis C18 Plus and Silica Lite are all manufactured by Waters (Milford, MA). Filter (Millex-GS, Millipore, Bedford, MA, U.S.). “Cold” reference standard compounds and radiolabeling precursors were synthesized as described below.

### 7.2 General methodologies

All reactions were performed at room temperature and under an inert (argon/nitrogen) atmosphere unless otherwise stated. Solvents were used as received or, if necessary, dried over 3 Å molecular sieves (dried at 200°C, 14 h) following a literature method<sup>233</sup> and handled under an inert (argon/nitrogen) atmosphere.

Solvents were removed under reduced pressure using a rotary evaporation on a Buchi RE 111 evaporator equipped with a diaphragm vacuum pump. Further drying before analysis was carried out using a Schlenk line and vacuum pump.

TLC analyses were performed on silica gel 60 f254 plates (Merck, New Jersey, USA). When UV active chromophore was present in the analysed structure/mixtures, they were developed under UV light ( $\lambda = 254$  nm); otherwise, they were stained with iodine or basic potassium permanganate solution, prepared by the reported method.<sup>234</sup> Synthetic intermediates and final products were purified by flash chromatography on silica gel (60 Å (35–75  $\mu$ m), Fluorochem, Hadfield, Derbyshire, UK) using an appropriate mixture of solvents as eluent. Cartridge pre-activated: QMA

by flushing with 5 mL of NaHCO<sub>3</sub> (8.4%), air, 10 mL of water, and air, Silica Lite cartridge by flushing 5 mL of ACN, followed by air, Oasis C18 Plus cartridge by flushing with 10 mL Ethanol, 20 mL of water, and dried with air.

## 7.3 Instrumentation

### 7.3.1 NMR spectroscopy

<sup>1</sup>H, <sup>13</sup>C, <sup>19</sup>F and <sup>31</sup>P NMR results were recorded on a JEOL JNM-LA400 spectrometer at 400 MHz, 100 MHz, 376 MHz and 162 MHz, respectively. All NMR spectra were referenced to a deuterated solvents, namely, <sup>1</sup>H NMR (CDCl<sub>3</sub>) δ 7.26 ppm; <sup>13</sup>C NMR (CDCl<sub>3</sub>) δ 77.0 ppm, <sup>1</sup>H NMR (D<sub>2</sub>O) δ 4.79 ppm and <sup>1</sup>H NMR (CD<sub>3</sub>OD) δ 3.31 ppm; <sup>13</sup>C NMR (CD<sub>3</sub>OD) δ 49.00 ppm. Spectra were processed using MestReNova software (Mestrelab Research, version 6.0.2-5475). Chemical shifts (δ) were recorded in parts per million (ppm). for <sup>1</sup>H NMR and <sup>13</sup>C NMR spectra and coupling constants, (*J*), reported in Hertz, Hz. Splitting patterns were denoted by s (singlet), d (doublet), t (triplet), m (multiplet), q (quartet), quin (quintet), td (triple doublet) and br (broad signal).

### 7.3.2 Mass spectrometry (MS) and gas chromatography mass spectrometry (GC-MS)

Low-resolution MS data were recorded using a Varian 500 ion trap a Finnegan MAT 900 XLT mass spectrometer and Advion, expression Compact Mass Spectrometer. GC-MS spectral data were obtained from the Agilent 5973 GC-MS system.

### 7.3.3 CHN

CHN analysis (Elemental analysis) was performed using a CHN analyser EA1108 (Carlo Erba). Most compounds were within the limit of 0.4% of the expected ratios (exceptions are [Cu<sup>44</sup>Cl]Cl, [Cu<sup>44</sup>(OH<sub>2</sub>)]ClO<sub>4</sub> and **55**). Issues may be due to products being viscous oils which make elemental analysis challenging, higher solvent retention or impurities causing the larger deviation from the predicted values.

### 7.3.3 ICP

ICP analysis (Inductively Coupled Plasma combine with mass spectrometry) was performed using by using ICP-OES Perkin Elmer (Optima 5300 DV).

### 7.3.4 Cyclotron

No-carrier-added fluorine-18 was produced from  $^{18}\text{O}$ -enriched water by a table top cyclotron BG75 (ABT Molecular Imaging Ltd) located in the PET Research Centre, University of Hull. After 1-2 h of bombardment, 0.7-2.2 GBq of fluorine-18 contained in 0.2-0.3 mL of target  $[^{18}\text{O}]\text{H}_2\text{O}$  was delivered and used in the next step. (Produced by David P Roberts, technician).

### 7.3.5 Hot cell

All radiochemical work was carried out in a lead shielded hot cell equipped with compressed gases (air, nitrogen, helium and argon), a camera and a Capintec CRC-55tPET dose calibrator (Capintec, New Jersey, USA). The dose calibrator is indispensable for measuring amounts of radioactivity present in a given volume of radioactive materials.

### 7.3.6 Elution for $^{99}\text{Mo}/^{99\text{m}}\text{Tc}$ generator

Technetium-99m was produced from an UltraTechnekow FM generator (Mallinckrodt Medical Cat. No. DRN 4329). The generator contains the parent isotope molybdenum-99 absorbed to an aluminium oxide column. Instructions proved by the manufacturer were followed with sterile saline used to elute sodium pertechnetate ( $\text{Na}[^{99\text{m}}\text{TcO}_4]$ ).

### 7.3.6 Radio-TLC scanner

Radiochemical reactions were monitored by thin layer radio chromatography. Samples were eluted on silica gel 60 F254 chromatographic plates (Merck, USA) and read by LabLogic Scan-Ram scanner running LabLogic Laura (version 4.1.7.70) software.

### 7.3.7 High-Performance Liquid Chromatography HPLC and Radio- HPLC

HPLC chromatograms for cold chemistry were recorded on Agilent Technologies 1200 series HPLC. Analytical analyses were performed on an ACE5 C18 4.6×250 mm 5 Å column using detection at 220 nm.

Radiochemical reactions were monitored, and final products were purified by HPLC (Agilent Technologies 1200 series) equipped with UV and gamma radiation detector (Bioscan) running LabLogic Laura (version 4.1.7.70) software. The analysis was done on ACE5 C18 4.6×250 mm 5 Å column, and final products were purified on ACE5 C18 10×250 mm 5 Å semi-preparative column, purchased from Hichrom Limited.

#### 7.3.7.1 Standard HPLC methods

These methods were used to identify the “cold” reference standard and hot chemistry for radiolabeling precursors.

Method 1: HPLC gradient for 4-thiacaprylic acid/caprylate derivatives (TCD1) and [<sup>18</sup>F]-8-fluoro-4-thiacaprylic acid ([<sup>18</sup>F]FTC1) (see Table 12).

<b>Time (mm:ss)</b>	<b>Acetonitrile + 0.1% TFA (%)</b>	<b>Water + 0.1% TFA (%)</b>
0	10.00	90.00
5	10.00	90.00
20	95.00	05.00
25	95.00	05.00
30	10.00	90.00

Table 12: HPLC gradient-method 1

Method 2: HPLC gradient for 4-thiacapric acid/caprato derivatives (TCD2) and [<sup>18</sup>F]-10-fluoro-4-thiacapric acid ([<sup>18</sup>F]FTC2) (see Table 13).

<b>Time (mm:ss)</b>	<b>Acetonitrile + 0.1% TFA (%)</b>	<b>Water + 0.1% TFA (%)</b>
0	20.00	80.00
5	20.00	80.00
5.1	40.00	60.00
15	60.00	40.00
20	95.00	05.00
21	20.00	80.00
30	20.00	80.00

Table 13: HPLC gradient-method 2

Method 3: HPLC gradient for 4-thiapalmitic acid/palmitate derivatives (TPD) and [<sup>18</sup>F]-16-fluoro-4-thiapalmitic acid ([<sup>18</sup>F]FTP) (see Table 14).

<b>Time (mm:ss)</b>	<b>Acetonitrile + 0.1% TFA (%)</b>	<b>Water + 0.1% TFA (%)</b>
0	20.00	80.00
5	20.00	80.00
5.1	90.00	10.00
20	90.00	10.00
20.1	20.00	80.00
30	20.00	80.00

Table 14: HPLC gradient-method 3



Method 4: HPLC gradient for 4-thiaoleic acid/oleate derivatives (TOD) and [<sup>18</sup>F]-8-fluoro-4-thiaoleic acid ([<sup>18</sup>F]FTO) (see Table 15).

Time (mm:ss)	Acetonitrile + 0.1% TFA (%)	Water + 0.1% TFA (%)
0	10.00	90.00
5	10.00	90.00
5.1	60.00	40.00
20	95.00	05.00
20.1	95.00	05.00
23	95.00	05.00
24	10.00	90.00
30	10.00	90.00

Table 15: HPLC gradient-method 4

Method 5: HPLC gradient for evaluation of *in vivo* stability of [<sup>18</sup>F]-18-fluoro-4-thiaoleic acid ([<sup>18</sup>F]FTO) (see Table 16)

Time (mm:ss)	Acetonitrile + 0.1% TFA (%)	Water + 0.1% TFA (%)
0	10.00	90.00
3	10.00	90.00
3	95.00	05.00
9	95.00	05.00
10	10.00	90.00
13	10.00	90.00

Table 16: HPLC gradient-method 5

Method 6: HPLC gradient for <sup>99m</sup>Tc radiolabeling of (TACN-thiapalmitic acid) <sup>99m</sup>Tc(CO)<sub>3</sub>**52** and (TACN-thiaoleic acid) <sup>99m</sup>Tc(CO)<sub>3</sub>**55** and their standard “cold” form rhenium complexes Re(CO)<sub>3</sub>**52** and Re(CO)<sub>3</sub>**55** (see Table 17).

Time (mm:ss)	Acetonitrile	Sodium acetate pH 5, 100 mmol
0	05.00	95.00
30	95.00	05.00

Table 17: HPLC gradient-method 6

### 7.3.8 PET/CT animal scanning

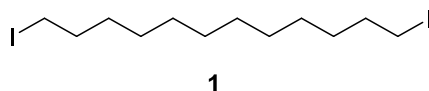
Dynamic whole body PET and CT images were acquired on the Sedecal SuperArgus 2R PET scanner (Sedecal, Spain). Rats were induced with 5% isoflurane/oxygen (v/v) anaesthesia before maintenance at 2%, using a flow rate of 1 L/min. Rats were cannulated in the tail vein using a bespoke catheter before being placed into an imaging cell where temperature and respiration were monitored (Minerve, France).

All PET /CT imaging studies were carried out under the project licence of Dr Anne Marie Seymour and supervised by Dr Chris Cawthorne. The imaging studies and data processing were carried out by Chris Cawthorne, Rob Atkinson, Faisal Nuhu and Shubhanchi Nigam.

## 7.4 Experimental procedures

### 7.4.1 Synthesis of 4-thiapalmitic acid/palmitate derivatives (TPD)

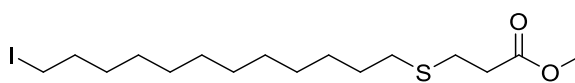
#### 7.4.1.1 1,12-Diodododecane (**1**)<sup>115</sup>



The synthetic procedure was completed following literature methods.<sup>115</sup> To a solution of 1,12-dibromododecane (3.00 g, 9 mmol) in acetone (40 mL) was added NaI (5.36 g, 36 mmol) and reaction mixture was heated at reflux under nitrogen blanket for 24 h. Then, solvent was evaporated under vacuum and crude product suspended in water (20 mL). The aqueous phase was extracted with dichloromethane (3 × 20 mL), dried over (MgSO<sub>4</sub>) and concentrated under vacuum. The crude product was crystallized from acetone yielding expected product as white crystals **1** (1.68 g, 57%).

<sup>1</sup>H NMR (400 MHz, CDCl<sub>3</sub>) δ 3.19 (t, *J*<sub>1,2</sub> = 7.0, 4H, 2(CH<sub>2</sub>- I), 1.93 – 1.68 (m, 4H, CH<sub>2</sub>-CH<sub>2</sub>-I), 1.43 – 1.12 (m, 16H, 8(CH<sub>2</sub>)).

### 7.4.1.2 Methyl 16-iodo-4-thiapalmitate (**2**)<sup>115</sup>



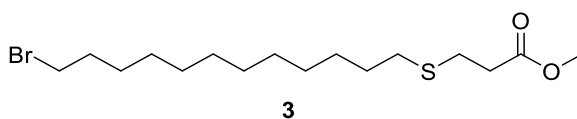
**2**

The synthetic procedure was completed following literature methods.<sup>115</sup> Bromo or iodo ester compound was dissolved in anhydrous acetonitrile. Methyl 3-mercaptopropionate and anhydrous  $K_2CO_3$  were added, and the reaction mixture was stirred at room temperature for 72 h. Then, the reaction mixture was acidified with ice-diluted 1N HCl and extracted with diethyl ether ( $3 \times 20$  mL). The combined ether fractions were washed successively with 5%  $NaHCO_3$ , water and brine, dried over  $MgSO_4$  and evaporated under reduced pressure.

Amounts: **1**, 12-diiodododecane **1** (1.33 g, 3.15 mmol), anhydrous acetonitrile (10 mL), methyl 3-mercaptopropionate (0.38 mL, 3.15 mmol), anhydrous  $K_2CO_3$  (0.55 g, 3.98 mmol), 1N HCl, diethyl ether ( $3 \times 20$  mL), 5%  $NaHCO_3$  ( $3 \times 20$  mL), water ( $3 \times 20$  mL), brine ( $1 \times 50$  mL) and amount of anhydrous  $MgSO_4$  (approximate). Following by chromatographic purification of the crude on silica gel eluted with n-hexane:ethyl acetate 97.5: 2.5 mixture and crystallisation from methanol, gave the expected iodinated thiapalmitate **2** with a (0.16 g, 24%) yield.

$^1H$  NMR (400 MHz,  $CDCl_3$ )  $\delta$  3.71 (s, 3H, O- $CH_3$ ), 3.20 (t,  $J_{1,2} = 7.1$ , 2H,  $CH_2-I$ ), 2.79 (t,  $J_{1,2} = 7.3$ , 2H,  $CH_2-S$ ), 2.62 (t,  $J_{1,2} = 7.4$ , 2H,  $CH_2-S$ ), 2.52 (m, 2H,  $CH_2-CH_2-S$ ), 1.82 (t,  $J_1 = 14.6$ ,  $J_2 = 7.2$ , 2H,  $CH_2$ ), 1.27 (s, 18H, 9( $CH_2$ )).

### 7.4.1.3 Methyl 16-bromo-4-thiapalmitate (**3**)<sup>4</sup>

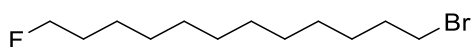


The synthetic procedure was completed following literature methods.<sup>4</sup> Sodium hydride was added to a stirred solution of methyl 3-mercaptopropanoate in dry THF. The reaction mixture was cooled to 0°C under nitrogen. The reaction mixture was stirred at 0°C for 15 min before THF solution of bromo or iodo protected compound was added drop wise. The reaction was stirred at 0°C for 30 min and at room temperature for 3 h. Then, it was quenched with water and extracted with the dichloromethane. The combined organic fractions were dried over Na<sub>2</sub>SO<sub>4</sub> and concentrated under vacuum.

Amounts: NaH (60% in oil, 0.30 g, 12.7 mmol), methyl 3-mercaptopropanoate (1.52 g, 12.7 mmol), dry THF (300 mL), THF (30 mL) of **1**, 12-dibromododecane (3.74 g, 11.3 mmol), water (50 mL), dichloromethane (3 × 100 mL) and amount of anhydrous Na<sub>2</sub>SO<sub>4</sub> (approximate). Following by chromatographic purification of the crude on silica gel eluted with n-hexane: ethyl acetate 95: 5 mixture, gave the expected brominated thiapalmitate **3** as a white solid with a (1.9 g, 41%) yield.

<sup>1</sup>H NMR (400 MHz, CDCl<sub>3</sub>) δ 3.70 (s, 3H, OCH<sub>3</sub>), 3.40 (t, *J*<sub>1,2</sub> = 6.9, 2H, CH<sub>2</sub>-Br), 2.77 (t, *J*<sub>1,2</sub> = 7.4, 2H, CH<sub>2</sub>-S), 2.60 (t, *J*<sub>1</sub> = 11.1, *J*<sub>2</sub> = 3.9, 2H, CH<sub>2</sub>-S), 2.54 – 2.44 (m, 2H CH<sub>2</sub>-CH<sub>2</sub>-S), 1.84 (m, 2H, CH<sub>2</sub>), 1.64 – 1.50 (m, 2H, CH<sub>2</sub>), 1.49 – 1.14 (m, 16H, 8(CH<sub>2</sub>)).<sup>13</sup>C NMR (150.81 MHz, CDCl<sub>3</sub>) δ ppm: 172.59 (COO-CH<sub>3</sub>), 51.88 (O-CH<sub>3</sub>), 34.82, 34.1, 32.9, 30.4, 29.6 – 29.4, 29.3, 29.2 6(CH<sub>2</sub>), 28.25, 28.1, 27.06; MS (ESI) *m/z*: 368 [M+H]<sup>+</sup>.

#### 7.4.1.4 1-Bromo-12-fluorododecane (4)



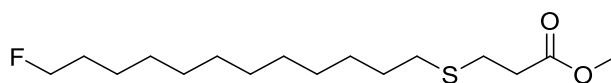
4

18-Crown-6 was dissolved in anhydrous acetonitrile was mixed with KF dissolved in water, and the KF/18-crown-6 complex was azeotropically dried. Then, tosylate or halogen compound dissolved in anhydrous acetonitrile was added to the flask and the reaction mixture was refluxed under nitrogen blanket overnight. The solvent was evaporated and the residue redissolved in dichloromethane; the organic phase was washed with water, dried over  $\text{Na}_2\text{SO}_4$  and evaporated under vacuum.

Amounts: 18-crown-6 (0.80 g, 3.04 mmol), anhydrous acetonitrile (10 mL), KF (0.17 g, 3.04 mmol), water, 1, 12-dibromododecane (1 g, 3.04 mmol), anhydrous acetonitrile, dichloromethane, water ( $3 \times 10$  mL), and amount of anhydrous  $\text{Na}_2\text{SO}_4$  (approximate).

Providing crude mixture containing 87% of expected product as quantified GC-MS and identified by  $^{19}\text{F}$  NMR, used directly in the next step.

#### 7.4.1.5 Methyl 16-fluoro-4-thiapalmitate (**5**)



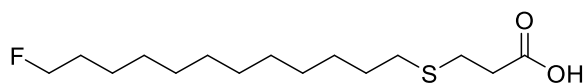
**5**

The product has been synthesised previously using a different synthetic route.<sup>4</sup> Sodium hydride was added to a stirred solution of methyl 3-mercaptopropanoate in dry THF. The reaction mixture was cooled to 0°C under a nitrogen blanket. The reaction mixture was stirred at 0°C for 15 min before THF solution of bromo or iodo protected compound was added dropwise. The reaction was stirred at 0°C for 30 min and at room temperature for 3 h. Then, it was quenched with water and extracted with the dichloromethane. The combined organic fractions were dried over Na<sub>2</sub>SO<sub>4</sub> and concentrated under vacuum.

Amounts: NaH (60% in oil, 0.12 g, 5.22 mmol), methyl 3-mercaptopropanoate (0.62 g, 5.22 mmol), dry THF (150 mL), THF (10 mL), 1-bromo-12-fluorododecane **4** (0.7 g, 2.61 mmol), water (50 mL), dichloromethane (3 × 100 mL) and amount of anhydrous Na<sub>2</sub>SO<sub>4</sub> (approximate). Following by chromatographic purification of the crude on silica gel eluted with n-hexane: ethyl acetate 95:5 mixture, gave the expected fluorinated thiapalmitate **5** as a colourless oil with a (0.12 g, 13 %) yield.

<sup>1</sup>H NMR (400 MHz, CDCl<sub>3</sub>) δ 4.53 – 4.37 (dt, 2H, *J*<sub>1</sub> = 47.3, *J*<sub>2</sub> = 6.2, CH<sub>2</sub>-F), 3.72 (s, 3H, O-CH<sub>3</sub>), 2.79 – 2.74 (m, 2H, CH<sub>2</sub>-S), 2.59 (t, *J*<sub>1</sub> = 11.1, *J*<sub>2</sub> = 4.1, 2H, CH<sub>2</sub>-S), 2.50 (m, CH<sub>2</sub>-CH<sub>2</sub>-S), 1.65 (t, *J*<sub>1</sub> = 17.0, *J*<sub>2</sub> = 7.8, 4H, 2(CH<sub>2</sub>)), 1.40 – 1.24 (m, 16H, 8(CH<sub>2</sub>)); <sup>19</sup>F NMR (376 MHz, CDCl<sub>3</sub>) δ 149.11; GC-MS: 306; MS (ESI) *m/z*: 307 [M+H]<sup>+</sup>. HPLC: Method 3 – retention time = 14:20 min.

#### 7.4.3.6 16-Fluoro-4-thiapalmitic acid (FTP) (**6**)



**6**

The product has been synthesised previously using a different synthetic route.<sup>135</sup> To ester compound was added LiOH × H<sub>2</sub>O dissolved in 60% EtOH and reaction mixture was stirred at room temperature for 1 h. Then, solvent was evaporated and the residue redissolved in dichloromethane and organic phase was washed with 1 N HCl, dried over Na<sub>2</sub>SO<sub>4</sub> and concentrated under vacuum.

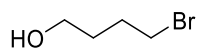
Amounts: methyl 16-fluoro-4-thiapalmitate **5** (0.03 g, 0.09 mmol), LiOH × H<sub>2</sub>O (0.012 g, 0.29 mmol), 60% EtOH (5 mL), dichloromethane (50 mL), 1 N HCl (50 mL) and amount of anhydrous Na<sub>2</sub>SO<sub>4</sub> (approximate). 16-fluoro-4-thiapalmitic acid **6** as colourless oil with a (20 mg, 71%) yield.

<sup>1</sup>H NMR (400 MHz, CDCl<sub>3</sub>) δ 4.43 (dt, *J*<sub>1</sub> = 47.4, *J*<sub>2</sub> = 6.2, 2H, CH<sub>2</sub>-F), 2.81 – 2.75 (m, 2H, CH<sub>2</sub>-S), 2.70 – 2.62 (m, 2H, CH<sub>2</sub>-S), 2.53 (t, *J*<sub>1</sub> = 9.8, *J*<sub>2</sub> = 5.1, 2H, CH<sub>2</sub>-CH<sub>2</sub>-S), 1.74 – 1.55 (m, 2H, 2(CH<sub>2</sub>)), 1.42 – 1.23 (m, 16H, 8(CH<sub>2</sub>)), 0.88 (s, 1H, OH); <sup>19</sup>F NMR (376 MHz, CDCl<sub>3</sub>) δ 149.11; MS (ESI) *m/z*: 331 [M+K]<sup>+</sup>. HPLC: Method 3 – retention time = 12:28 min.



## 7.4.2 Synthesis of 4-thiacaprylic acid/caprylate derivatives (TCD1)

### 7.4.2.1 4-Bromo-1-butanol (**7**)<sup>123</sup>

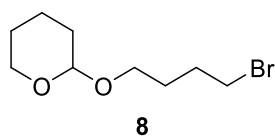


**7**

The synthetic procedure was completed following literature methods.<sup>123</sup> To tetrahydrofuran (THF) (67.5 mL, 832.2 mmol) cooled to 0°C was drop wise added HBr (48% w/v in water, 31 mL, 274 mmol) and the yellow reaction mixture was stirred at reflux for 2 h. After cooling to room temperature, the reaction was diluted with water (100 mL) and carefully neutralized with solid NaHCO<sub>3</sub>. The bromoalcohol product **7** was extracted with Et<sub>2</sub>O (3×100 mL), the organic fractions were combined, dried (Na<sub>2</sub>SO<sub>4</sub>) and the solvent was removed under a vacuum, providing expected product as a yellow oil (13.7 g, 33% yield).

<sup>1</sup>H NMR (400 MHz, CDCl<sub>3</sub>) δ 3.67 (t, *J*<sub>1,2</sub> = 6.4, 2H, CH<sub>2</sub>-O), 3.46 (t, *J*<sub>1,2</sub> = 6.7, 2H, CH<sub>2</sub>-Br), 2.44 (s, 1H, OH), 2.00 – 1.91 (m, 2H, CH<sub>2</sub>), 1.79 – 1.62 (m, 2H, CH<sub>2</sub>); MS (ESI) *m/z*: 152 [M+H]<sup>+</sup>.

#### 7.4.2.2 2-(4-Bromobutyloxy)tetrahydro-2H-pyran (**8**)<sup>126</sup>

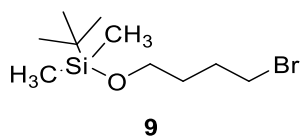


The synthetic procedure was completed following modified literature methods.<sup>126</sup> The alcohol precursor **7** was dissolved in anhydrous diethyl ether, and resulting solution was cooled to 0°C. A catalytic amount of *p*-toluenesulfonic acid and 3, 4-dihydro-2*H*-pyran were added, and the reaction was stirred at room temperature for 24 h. Then, the reaction mixture was washed with saturated sodium bicarbonate solution and brine. The organic layer was dried over anhydrous K<sub>2</sub>CO<sub>3</sub> and solvent removed under vacuum.

Amounts: 4-bromo-1-butanol **7** (13 g, 84.9 mmol), anhydrous diethyl ether (85 mL), *p*-toluenesulfonic acid (29.3 mg, 154 mmol), 3, 4-dihydro-2*H*-pyran (9.4 mL, 111.7 mmol), saturated sodium bicarbonate solution (2 × 60 mL), brine (1 × 40 mL) and amount of anhydrous K<sub>2</sub>CO<sub>3</sub> (approximate). THP protected bromoalcohol **8** was purified on a silica gel column eluted with a n-hexane : ethyl acetate 95: 5 mixture and was isolated a colourless oil (14 g, 70%).

<sup>1</sup>H NMR (400 MHz, CDCl<sub>3</sub>) δ 4.60 (t, *J*<sub>1,2</sub> = 3.5, 1H, O-CH-O), 3.94 – 3.75 (m, 2H, CH<sub>2</sub>-Br), 3.57 – 3.39 (m, 4H, 2(CH<sub>2</sub>-O)), 2.04 – 1.92 (m, 2H, CH<sub>2</sub>), 1.89 – 1.68 (m, 4H, 2(CH<sub>2</sub>)), 1.57 (m, 4H, 2(CH<sub>2</sub>)); GC-MS: 8:45 min, 237 (M<sup>+</sup>).

### 7.4.2.3 4-Bromo-1-(*tert*-butyldimethylsilyloxy)butane (**9**)<sup>127</sup>

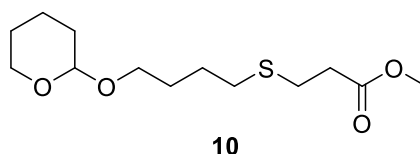


The synthetic procedure was completed following literature methods.<sup>127</sup> To an anhydrous solution of dichloromethane containing alcohol compound **7**, imidazole and 4-(dimethylamino)pyridine maintained at 0°C was added *tert*-butyldimethylsilyl chloride (TBDMSCl) and the reaction mixture was stirred at room temperature overnight. Then, the reaction was quenched with a saturated aqueous NH<sub>4</sub>Cl solution, and the aqueous phase was extracted with diethyl ether. The combined organic extracts were washed with brine, dried over MgSO<sub>4</sub> and concentrated under vacuum.

Amounts: anhydrous dichloromethane (300 mL), 4-bromo-1-butanol **7** (6.0 g, 39.21 mmol), imidazole (5.34 g, 78.4 mmol), 4-(dimethylamino)pyridine (2.4 g, 19.64 mmol), NH<sub>4</sub>Cl solution (50 mL) diethyl ether (3 × 100 mL), brine (3 × 40 mL) and amount of anhydrous MgSO<sub>4</sub> (approximate). Providing the silyl ether **9** as a colorless oil (10 g, 96%).

<sup>1</sup>H NMR (400 MHz, CDCl<sub>3</sub>) δ 3.63 (t, *J*<sub>1,2</sub> = 6.1, 2H, CH<sub>2</sub>-O), 3.43 (t, *J*<sub>1,2</sub> = 6.8, 2H, CH<sub>2</sub>-Br), 1.92 (t, *J*<sub>1,2</sub> = 12.4, 2H, CH<sub>2</sub>), 1.68 – 1.60 (m, 2H, CH<sub>2</sub>), 0.90 – 0.85 (m, 9H, 3(CH<sub>3</sub>)), 0.03 (d, *J* = 1.8, 6H, 2(CH<sub>3</sub>)); GC-MS: 12:22 min, 267 (M<sup>+</sup>).

#### 7.4.2.4 Methyl 8-(tetrahydro-2H-pyran-2-yl)-4-thiacaprylate (**10**)



##### Method 1

Bromo or iodo protected compound was dissolved in anhydrous acetonitrile. Methyl 3-mercaptopropionate and anhydrous  $K_2CO_3$  were added, and the reaction mixture was stirred at room temperature for 72 h. Then, the reaction mixture was acidified with ice-diluted 1N HCl and extracted with diethyl ether ( $3 \times 20$  mL). The combined ether fractions were washed successively with 5%  $NaHCO_3$ , water and brine, dried over  $MgSO_4$  and evaporated under reduced pressure.

Amounts: 4-Bromobutyl tetrahydropyranyl ether **2** (1.49 g, 6.3 mmol), anhydrous acetonitrile (20 mL), methyl 3-mercaptopropionate (0.69 mL, 6.3 mmol), anhydrous  $K_2CO_3$  (1.10 g, 8 mmol), 1N HCl, diethyl ether ( $3 \times 20$  mL), 5%  $NaHCO_3$  ( $3 \times 50$  mL), water ( $3 \times 50$  mL), brine ( $1 \times 50$  mL) and amount of anhydrous  $MgSO_4$  (approximate). Product **10** was purified by column chromatography on silica gel eluted with n-hexane: ethyl acetate 9: 1 mixture, and was isolated as colourless oil (0.75 g, 50%).

$^1H$  NMR (400 MHz,  $CDCl_3$ )  $\delta$  4.58 (t,  $J_{1,2} = 4.4$ , 1H, O-CH-O), 3.86 (t,  $J_{1,2} = 11.2$ , 2H,  $CH_2$ -O), 3.80 – 3.72 (m, 2H,  $CH_2$ -O), 3.71 (s, 3H, O- $CH_3$ ), 3.56 – 3.48 (m, 2H,  $CH_2$ -S), 3.45 – 3.38 (m, 2H,  $CH_2$ -S), 2.79 (t,  $J_{1,2} = 7.5$ , 2H,  $CH_2$ - $CH_2$ -S), 2.65 – 2.53 (m, 2H,  $CH_2$ ), 1.91 – 1.67 (m, 2H, 2( $CH_2$ )), 1.67 – 1.45 (m, 2H, 2( $CH_2$ )); MS (ESI) m/z: 277 [ $M+H$ ] $^+$ .

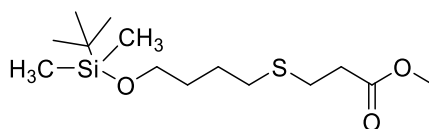
## Method 2

Sodium hydride was added to a stirred solution of methyl 3-mercaptopropanoate in dry THF. The reaction mixture was cooled to 0°C under a nitrogen blanket. The reaction mixture was stirred at 0°C for 15 min before THF solution of bromo or iodo protected compound was added drop wise. The reaction was stirred at 0°C for 30 min and at room temperature for 3 h. Then, it was quenched with water and extracted with the dichloromethane. The combined organic fractions were dried over Na<sub>2</sub>SO<sub>4</sub> and concentrated under vacuum.

Amounts: NaH (60% in oil, 1.29 g, 53.9 mmol), methyl 3-mercaptopropanoate (6.47 g, 53.9 mmol), dry THF (1000 mL), THF (100 mL), 4-bromobutyl tetrahydropyranyl ether **2** (11.37 g, 47.94 mmol), water (50 mL), dichloromethane (3 × 100 mL) and amount of anhydrous Na<sub>2</sub>SO<sub>4</sub> (approximate). Product **10** was purified by column chromatography on silica gel eluted with n-hexane: ethyl acetate 9:1 mixture and was isolated as colourless oil (7.42 g, 57%).

<sup>1</sup>H NMR (400 MHz, CDCl<sub>3</sub>) δ 4.58 (t, *J*<sub>1,2</sub> = 4.4, 1H, O-CH-O), 3.86 (t, *J*<sub>1,2</sub> = 11.2, 2H, CH<sub>2</sub>-O), 3.80 – 3.72 (m, 2H, CH<sub>2</sub>-O), 3.71 (s, 3H, O-CH<sub>3</sub>), 3.56 – 3.48 (m, 2H, CH<sub>2</sub>-S), 3.45 – 3.38 (m, 2H, CH<sub>2</sub>-S), 2.79 (t, *J*<sub>1,2</sub> = 7.5, 2H, CH<sub>2</sub>-CH<sub>2</sub>-S), 2.65 – 2.53 (m, 2H, CH<sub>2</sub>), 1.91 – 1.67 (m, 2H, 2(CH<sub>2</sub>)), 1.67 – 1.45 (m, 2H, 2(CH<sub>2</sub>)); MS (ESI) *m/z*: 277 [M+H]<sup>+</sup>.

#### 7.4.2.5 Methyl 8-(*tert*-butyldimethylsilyl)-4-thiacaprylate (**11**)



**11**

##### Method 1

Bromo or iodo protected compound was dissolved in anhydrous acetonitrile. Methyl 3-mercaptopropionate and anhydrous  $K_2CO_3$  were added, and the reaction mixture was stirred at room temperature for 72 h. Then, the reaction mixture was acidified with ice-diluted 1 N HCl and extracted with diethyl ether ( $3 \times 20$  mL). The combined ether fractions were washed successively with 5%  $NaHCO_3$ , water and brine, dried over  $MgSO_4$  and evaporated under reduced pressure.

Amounts: 4-Bromo-1-(*tert*-butyldimethylsilyloxy)butane **9** (1.21 g, 4.48 mmol), anhydrous acetonitrile (20 mL), methyl 3-mercaptopropionate (0.53 mL, 4.48 mmol) and anhydrous  $K_2CO_3$  (0.78 g, 5.68 mmol), 1N HCl, diethyl ether ( $3 \times 20$  mL), 5%  $NaHCO_3$  ( $3 \times 50$  mL), water ( $3 \times 50$  mL), brine ( $1 \times 50$  mL) and amount of anhydrous  $MgSO_4$  (approximate). Product **11** was purified by column chromatography on silica gel eluted with n-hexane: ethyl acetate 9:1 mixture, and was isolated as colourless oil (0.91 g, 66%).

$^1H$  NMR (400 MHz,  $CDCl_3$ )  $\delta$  3.69 (s, 3H, O- $CH_3$ ), 3.61 (t,  $J_{1,2} = 6.0$ , 2H,  $CH_2O$ ), 2.81 – 2.74 (m, 2H,  $CH_2-S$ ), 2.63 – 2.50 (m, 4H,  $CH_2-CH_2-S$ ), 1.69 – 1.57 (m, 4H, 2( $CH_2$ )), 0.90 – 0.85 (m, 9H, 3( $CH_3$ )), 0.04 (s, 6H, 2( $CH_3$ )); MS (ESI) m/z: 329  $[M+Na]^+$ .

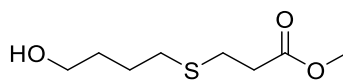
## Method 2

Sodium hydride was added to a stirred solution of methyl 3-mercaptopropanoate in dry THF. The reaction mixture was cooled to 0°C under a nitrogen blanket. The reaction mixture was stirred at 0°C for 15 min before THF solution of bromo or iodo protected compound was added drop wise. The reaction was stirred at 0°C for 30 min and at room temperature for 3 h. Then, it was quenched with water and extracted with the dichloromethane. The combined organic fractions were dried over Na<sub>2</sub>SO<sub>4</sub> and concentrated under vacuum.

Amounts: NaH (60% in oil, 0.10 g, 4.20 mmol), methyl 3-mercaptopropanoate (0.50 g, 4.20 mmol), dry THF (100 mL), THF (10 mL), 4-bromo-1-(*tert*-butyldimethylsilyloxy)butane **9** (1 g, 3.74 mmol), water (50 mL), dichloromethane (3 × 100 mL) and amount of anhydrous Na<sub>2</sub>SO<sub>4</sub> (approximate). To yield Product **11** as colourless oil (0.85 g, 75%).

<sup>1</sup>H NMR (400 MHz, CDCl<sub>3</sub>) δ 3.69 (s, 3H, O-CH<sub>3</sub>), 3.61 (t, *J*<sub>1,2</sub> = 6.0, 2H, CH<sub>2</sub>-O), 2.81 – 2.74 (m, 2H, CH<sub>2</sub>-S), 2.63 – 2.50 (m, 4H, CH<sub>2</sub>-CH<sub>2</sub>-S), 1.69 – 1.57 (m, 4H, 2(CH<sub>2</sub>)), 0.90 – 0.85 (m, 9H, 3(CH<sub>3</sub>)), 0.04 (s, 6H, 2(CH<sub>3</sub>)); MS (ESI) *m/z*: 329 [M+Na]<sup>+</sup>.

#### 7.4.2.6 Methyl 8-hydroxy-4-thiacaprylate (**12**)



**12**

##### Method 1-preferred route

To a solution of THP protected compound dissolved in MeOH was added *p*-toluene sulfonic acid monohydrate (TsOH × H<sub>2</sub>O) and the reaction was stirred at room temperature for 5 h. The methanol was evaporated and the residue redissolved in DCM, and the organic phase was washed successively with 10% NaHCO<sub>3</sub> solution, water and brine, dried over MgSO<sub>4</sub> and evaporated under reduced pressure.

Amounts: methyl 8-(tetrahydro-2*H*-pyran-2-yl)-4-thiacaprylate **9** (0.32 g, 1.15 mmol), MeOH (25 mL), TsOH × H<sub>2</sub>O (222 mg, 1.15 mmol), DCM (50 mL), 10% NaHCO<sub>3</sub> solution (3 × 50 mL), water (3 × 50 mL), brine (1 × 50 mL) and amount of anhydrous Na<sub>2</sub>SO<sub>4</sub> (approximate). Product **12** was purified by column chromatography on silica gel eluted with n-hexane: ethyl acetate 7:3 mixture and was isolated as a colourless oil (0.11 g, 51%).

<sup>1</sup>H NMR (400 MHz, CDCl<sub>3</sub>) δ 4.10 (s, 1H, OH), 3.69 (s, 3H, O-CH<sub>3</sub>), 3.67 – 3.64 (m, 2H, CH<sub>2</sub>-O), 2.81 – 2.74 (m, 2H, CH<sub>2</sub>-S), 2.64 – 2.51 (m, 4H, CH<sub>2</sub>-CH<sub>2</sub>-S), 1.67 (m, 4H, 2(CH<sub>2</sub>)); MS (ESI) m/z: 193 [M+H]<sup>+</sup>.

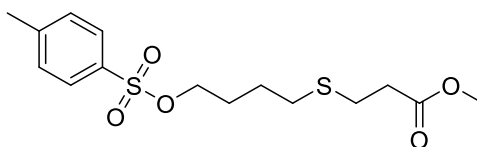


### Method 2- Attempted synthesis

To a solution of TBDMS protected compound dissolved in THF was added TBAF (1 M in THF, 9 mL, 9.0 mmol) and the reaction mixture was stirred at room temperature for 8h. Then, THF was evaporated and replaced by ethyl acetate, and the organic phase was washed with water, dried over MgSO<sub>4</sub> and evaporated under vacuum.

Amounts: tert-butyldimethyl derivative **11** (0.9 g, 3.0 mmol), THF (5 mL) and tetra-*n*-butylammonium fluoride in tetrahydrofuran (TBAF) (1 M in THF, 9 mL, 9.0 mmol), ethyl acetate (25 mL), water (3 × 50 mL) and amount of anhydrous Na<sub>2</sub>SO<sub>4</sub> (approximate). According to <sup>1</sup>H NMR, the obtained crude contained mainly still protected starting material.

#### 7.4.2.7 Methyl 8-tosyl-4-thiacaprylate (**13**)



**13**

##### Method 1- Attempted synthesis

To a solution of alcohol **12** (0.38 g, 1.97 mmol) in anhydrous dichloromethane (70 mL) maintained at 0°C was added diisopropylethylene amine (0.46 mL, 2.93 mmol) followed by tosyl chloride (0.43 g, 2.34 mmol) and the reaction mixture was stirred at room temperature for 24 h. Then, the reaction was diluted with dichloromethane (70 mL), the organic phase was washed successively with 10% citric acid, 10% NaHCO<sub>3</sub>, water, dried over Na<sub>2</sub>SO<sub>4</sub> and evaporated under vacuum. TLC analysis showed a complex mixture of products. <sup>1</sup>H NMR analysis indicated that only traces of starting alcohol remained, however, no expected product was isolated after liquid chromatography purification on silica gel.

##### Method 2- Attempted synthesis

To a stirred solution of an alcohol **12** (0.5 g, 2.60 mmol), K<sub>2</sub>CO<sub>3</sub> (0.5 g, 2.62 mmol) and Me<sub>3</sub>N×HCl (4.06 g, 42.58 mmol) in anhydrous dichloromethane (108 mL) maintained at 0°C was added tosyl chloride (0.49 g, 2.60 mmol) and the reaction mixture was stirred at room temperature for 72 h. Then, the solvent was evaporated and the residue redissolved in ethanol, the resulting solution filtered through celite and concentrated under vacuum. According to <sup>1</sup>H NMR, only traces of product **11** were formed.

### Method 3- Attempted synthesis

To a solution of alcohol **12** (0.1 g, 0.5 mmol), Et<sub>3</sub>N (16.3 mg, 0.16 mmol) and Me<sub>3</sub>N.HCl (0.9 mg, 0.01 mmol) in anhydrous acetonitrile (60 mL) maintained at -6°C was added tosyl chloride (19 mg, 0.1 mmol) in one portion. The reaction mixture was stirred at -10°C for 40 min warmed to room temperature, quenched with water (60 mL), extracted with ethyl acetate (3×100 mL). The combined organic fractions were washed with half-saturated aqueous NH<sub>4</sub>Cl and brine, dried over Na<sub>2</sub>SO<sub>4</sub> and concentrated under vacuum. According to <sup>1</sup>H NMR, only traces of product **11** were formed.

### Method 4- Attempted synthesis

To a solution of alcohol **12** (0.1 g, 0.5 mmol) in anhydrous dichloromethane (7.7 mL) maintained at 0°C was added 4-(dimethyl amino)pyridine (2 mg, 0.5 mmol) followed by tosyl chloride (0.095 g, 0.5 mmol). The reaction mixture was stirred at room temperature for 18 h. Then, it was quenched with 1N aqueous HCl (10mL), and the aqueous phase was extracted with dichloromethane (3×5 mL). The combined organic fractions were dried over Na<sub>2</sub>SO<sub>4</sub> and evaporated under vacuum. TLC analysis showed a complex mixture of products. <sup>1</sup>H NMR analysis indicated that only traces of starting alcohol remained, however, no expected product was isolated after liquid chromatography purification on silica gel.

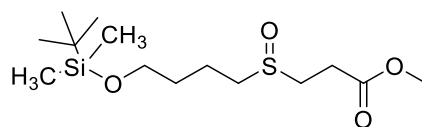
### Method 5-preferred route

To a solution of alcohol compound in anhydrous acetonitrile containing triethylamine (Et<sub>3</sub>N) and trimethylamine hydrochloride (Me<sub>3</sub>N × HCl) maintained at -5°C was added tosyl chloride dissolved in anhydrous acetonitrile. The reaction mixture was stirred at room temperature for 2 h. Acetonitrile was evaporated and the residue redissolved in ethyl acetate, washed with water and brine, dried over Na<sub>2</sub>SO<sub>4</sub> and evaporated under vacuum.

Amounts: compound **12** (0.1 g, 0.52 mmol), anhydrous acetonitrile (3 mL), Et<sub>3</sub>N (0.13 mL, 1.04 mmol), Me<sub>3</sub>N×HCl (49 mg, 0.052 mmol), tosyl chloride (0.14 g, 0.78 mmol), anhydrous acetonitrile (3 mL), ethyl acetate (10 mL), water (3 × 10 mL), brine (1 × 10 mL) and amount of anhydrous Na<sub>2</sub>SO<sub>4</sub> (approximate). Providing pure expected product as white crystals (0.13 g, 72%).

<sup>1</sup>H NMR (400 MHz, CDCl<sub>3</sub>) δ 7.93 (d, *J* = 8.4, 2H, Ar-H), 7.41 (dd, *J*<sub>1</sub> = 8.6, *J*<sub>2</sub> = 0.6, 2H, Ar-H), 3.73 – 3.68 (m, 3H, O-CH<sub>3</sub>), 3.72 – 3.65 (m, 2H, CH<sub>2</sub>-O), 2.84 – 2.74 (m, 2H, CH<sub>2</sub>-S), 2.65 – 2.56 (m, 4H, CH<sub>2</sub>-CH<sub>2</sub>-S), 2.47 (d, *J* = 15.7, 3H, Ar-CH<sub>3</sub>), 1.68 (d, *J* = 6.6, 4H, 2(CH<sub>2</sub>)); MS (ESI) *m/z*: 175 [M-tosylate]<sup>+</sup>.

#### 7.4.2.8 Methyl 8-(*tert*-butyldimethylsilyl)-4-sulfinylcaprylate (**14**)



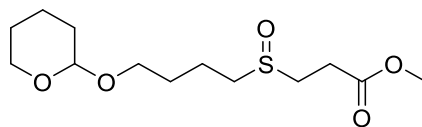
**14**

Protected compound dissolved in ethyl acetate was added  $\text{NaBO}_3 \times 4\text{H}_2\text{O}$  dissolved in water followed by glacial acetic acid. The reaction mixture was stirred at room temperature overnight. Then, the organic phase was separated, and the aqueous phase was extracted with ethyl acetate. The combined organic fractions were washed with water and brine, dried over  $\text{Na}_2\text{SO}_4$  and evaporated under reduced pressure.

Amounts: TBDMS protected thia-ester **11** (0.85 g, 2.77 mmol), ethyl acetate (20 mL),  $\text{NaBO}_3 \times 4\text{H}_2\text{O}$  (0.42g, 2.77 mmol), water (5 mL) and glacial acetic acid (3 mL, 49.9 mmol), ethyl acetate (3  $\times$  30 mL), water (3  $\times$  30 mL), brine (1  $\times$  30 mL) and amount of anhydrous  $\text{Na}_2\text{SO}_4$  (approximate). Providing expected product as a colorless oil (0.88 g, 99%).

$^1\text{H}$  NMR (400 MHz,  $\text{CDCl}_3$ )  $\delta$  3.69 (s, 3H, O- $\text{CH}_3$ ), 3.61 (t,  $J_{1,2} = 6.0$ , 2H,  $\text{CH}_2\text{-O}$ ), 2.81 – 2.74 (m, 4H,  $\text{CH}_2\text{-CH}_2\text{-S}$ ), 2.63 – 2.50 (m, 2H,  $\text{CH}_2\text{-S}$ ), 1.69 – 1.57 (m, 4H, 4( $\text{CH}_2$ )), 0.90 – 0.85 (m, 9H, 3( $\text{CH}_3$ )), 0.04 (s, 6H, 2( $\text{CH}_3$ )); MS (ESI)  $m/z$ : 323 [ $\text{M}+\text{H}$ ] $^+$ .

#### 7.4.2.9 Methyl 8-(tetrahydro-2H-pyran-2-yl)-4-sulfinylcaprylate (16)



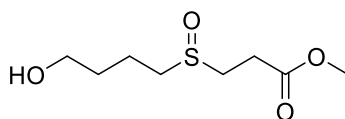
16

Protected compound dissolved in ethyl acetate was added  $\text{NaBO}_3 \times 4\text{H}_2\text{O}$  dissolved in water followed by glacial acetic acid. The reaction mixture was stirred at room temperature overnight. Then, the organic phase was separated, and the aqueous phase was extracted with ethyl acetate. The combined organic fractions were washed with water and brine, dried over  $\text{Na}_2\text{SO}_4$  and evaporated under reduced pressure.

Amounts: THP protected thiaester **9** (0.5 g, 1.8 mmol), ethyl acetate (40 mL),  $\text{NaBO}_3 \times 4\text{H}_2\text{O}$  (0.27 g, 1.8 mmol), water (5 mL), glacial acetic acid (3 mL, 49.9 mmol), ethyl acetate (3  $\times$  30 mL), water (3  $\times$  30 mL), brine (1  $\times$  30 mL) and amount of anhydrous  $\text{Na}_2\text{SO}_4$  (approximate). Product **16** was purified by liquid chromatography on silica gel eluted with hexane: ethyl acetate 97.5:2.5 mixture to give expected product as a colourless oil (0.3 g, 60%).

$^1\text{H}$  NMR (400 MHz,  $\text{CDCl}_3$ )  $\delta$  4.57 (t,  $J_{1,2} = 4.1$ , 1H, O-CH-O), 3.93 – 3.78 (m, 2H,  $\text{CH}_2\text{-O}$ ), 3.75 (s, 3H, O- $\text{CH}_3$ ), 3.56 – 3.34 (m, 2H,  $\text{CH}_2\text{-O}$ ), 2.97 – 2.68 (m, 4H,  $\text{CH}_2\text{-CH}_2\text{-S}$ ), 2.66 – 2.48 (m, 2H,  $\text{CH}_2\text{-S}$ ), 1.85 – 1.63 (m, 6H, 3( $\text{CH}_2$ )), 1.60 – 1.43 (m, 4H, 2( $\text{CH}_2$ )); MS (ESI)  $m/z$ : 315  $[\text{M}+\text{Na}]^+$ .

#### 7.4.2.10 Methyl 8-hydroxy-4-sulfinylcaprylate (**15**)



**15**

#### SYNTHESISED FROM **14**

To a solution of TBDMS protected compound dissolved in THF was added TBAF (1 M in THF, 9 mL, 9.0 mmol) and the reaction mixture was stirred at room temperature for 8 h. Then, THF was evaporated and replaced by ethyl acetate, and the organic phase was washed with water, dried over MgSO<sub>4</sub> and evaporated under vacuum.

#### Method 1- Attempted synthesis

Amounts: TBDMS derivative **14** (0.1g, 0.3 mmol), anhydrous THF (3 mL), TBAF (1 M in THF, 0.3 mL, 0.3 mmol), ethyl acetate (20 mL), water (3 × 20 mL) and amount of anhydrous Na<sub>2</sub>SO<sub>4</sub> (approximate). According to <sup>1</sup>H NMR, the obtained crude mainly contained protected starting material **14** with GC-MS showing 9% of expected de-protected alcohol **7**.

#### Method 2- Attempted synthesis

To TBDMS derivative **14** (0.16 mg, 0.5 mmol) dissolved in acetonitrile (15 mL) was added CeCl<sub>3</sub> × 6H<sub>2</sub>O (0.35 g, 1 mmol) followed by a few drops of glacial acetic acid. The reaction mixture was heated at reflux for 8 h. Then, acetonitrile was evaporated and the residue redissolved in ethyl acetate, and the organic layer was washed with brine, dried over Na<sub>2</sub>SO<sub>4</sub> and evaporated under vacuum to give a complex mixture of products containing de-protected sulfinyl alcohol as identified by MS (ESI) m/z: 209 [M+H]<sup>+</sup>.

## SYNTHESISED FROM **16**

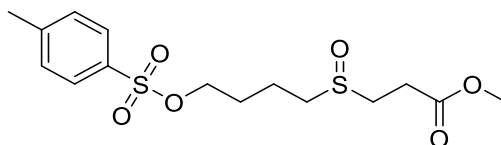
To a solution of THP protected compound dissolved in MeOH was added *p*-toluene sulfonic acid monohydrate (TsOH × H<sub>2</sub>O) and the reaction was stirred at room temperature for 5 h. The methanol was evaporated and the residue redissolved in DCM, and the organic phase was washed successively with 10% NaHCO<sub>3</sub> solution, water and brine, dried over MgSO<sub>4</sub> and evaporated under reduced pressure.

Amounts: THP derivative **16** (3.3 g, 11.35 mmol), MeOH (130 mL) and TsOH × H<sub>2</sub>O (2.15g, 11.33 mmol), DCM (100 mL), 10% NaHCO<sub>3</sub> solution (3 × 100 mL), water (3 × 100 mL), brine (1 × 100 mL) and amount of anhydrous Na<sub>2</sub>SO<sub>4</sub> (approximate). The expected product was isolated by column chromatography on silica gel eluted with hexane: ethyl acetate 65:35 mixture (0.83 g, 35%).

<sup>1</sup>H NMR (400 MHz, CDCl<sub>3</sub>) δ 3.69 (s, 3H, O-CH<sub>3</sub>), 3.72 – 3.59 (m, 2H, CH<sub>2</sub>-O), 2.87 – 2.70 (m, 2H, CH<sub>2</sub>-S), 2.58 (t, *J*<sub>1,2</sub> = 16.3, 2H, CH<sub>2</sub>-S) 2.59 (t, *J*<sub>1,2</sub> = 7.1, 2H, CH<sub>2</sub>-CH<sub>2</sub>-S), 1.83 – 1.55 (m, 4H, 2(CH<sub>2</sub>)), 1.42 (s, 1H, OH). <sup>13</sup>C NMR (100 MHz, CDCl<sub>3</sub>) 172.58, 62.47, 51.92, 34.77, 32.82, 31.00, 26.98, 25.85, MS (ESI) *m/z*: 209 [M+H]<sup>+</sup>.



#### 7.4.2.11 Methyl 8-tosyl-4- sulfinylcaprylate (**17**)



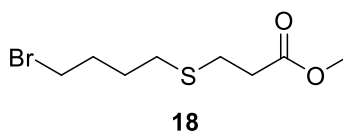
**17**

To a solution of alcohol compound in anhydrous acetonitrile containing triethylamine (Et<sub>3</sub>N) and trimethylamine hydrochloride (Me<sub>3</sub>N × HCl) maintained at -5°C was added tosyl chloride dissolved in anhydrous acetonitrile. The reaction mixture was stirred at room temperature for 2 h. Acetonitrile was evaporated and the residue redissolved in ethyl acetate, washed with water and brine, dried over Na<sub>2</sub>SO<sub>4</sub> and evaporated under vacuum.

Amounts: compound **15** (0.1 g, 0.48 mmol), anhydrous acetonitrile (5 mL), Et<sub>3</sub>N (0.097 mL, 0.96 mmol), Me<sub>3</sub>N × HCl (45 mg, 0.048 mmol), tosyl chloride (0.13 g, 0.72 mmol), anhydrous acetonitrile (5 mL), water (3 × 10 mL), brine (1 × 10 mL) and amount of anhydrous Na<sub>2</sub>SO<sub>4</sub> (approximate). Providing a crude mixture containing mainly expected compound **17** (<sup>1</sup>H NMR, TLC). However, chromatographic purification on silica gel yielded only de-protected alcohol intermediate **7**. Crude compound **17** was identified by <sup>1</sup>H NMR.

<sup>1</sup>H NMR (400 MHz, CDCl<sub>3</sub>) δ 7.79 (d, *J* = 8.3, 2H, Ar-H), 7.35 (d, *J* = 7.9, 2H, Ar-H), 3.71 (s, 3H, O-CH<sub>3</sub>), 2.59 (t, *J*<sub>1,2</sub> = 7.3, 2H, CH<sub>2</sub>-S), 2.51 – 2.30 (m, 4H, CH<sub>2</sub>-CH<sub>2</sub>-S), 2.17 (s, 3H, Ar-CH<sub>3</sub>), 1.94 – 1.54 (m, 4H, 2(CH<sub>2</sub>)).

#### 7.4.2.12 Methyl 8-bromo-4-thiacaprylate (**18**)



##### Method 1-preferred route

To a solution of tosylated precursor **13** (0.66 g, 1.90 mmol) in 10 mL of anhydrous dimethylformamide was added lithium bromide (1.32 g, 5.2 mmol) and reaction mixture was stirred at room temperature overnight. Then, solvent was evaporated and the residue redissolved in ethyl acetate (50 mL) and organic phase was washed with 5% NaHCO<sub>3</sub> (2 × 50 mL), water (2 × 50 mL) and brine (2 × 50 mL) respectively, dried over MgSO<sub>4</sub> and concentrated under vacuum. Following by chromatographic purification of the crude on silica gel eluted with n-hexane: ethyl acetate 90: 10 mixture, gave the expected product **18** as colorless oil with a (20 mg, 4%) yield.

<sup>1</sup>H NMR (400 MHz, CDCl<sub>3</sub>) δ 3.70 (s, 3H, O-CH<sub>3</sub>), 3.55 (t, *J*<sub>1,2</sub> = 6.5, 2H, CH<sub>2</sub>-Br), 2.79 (t, *J*<sub>1,2</sub> = 11.0, 3.8, 2H, CH<sub>2</sub>-S), 2.65 – 2.53 (m, 4H, CH<sub>2</sub>-CH<sub>2</sub>-S), 1.87 (d, *J* = 8.6, 2H, CH<sub>2</sub>), 1.76 (d, *J* = 7.2, 2H, CH<sub>2</sub>).

##### Method 2- Attempted synthesis

To a solution of tosylated precursor **7** (0.72 g, 2.08 mmol) in (10 mL) of anhydrous DCM was added CBr<sub>4</sub> (0.85 g, 2.59 mmol) and reaction mixture was cooled to 0°C. Then, PPh<sub>3</sub> (0.97 g, 3.72 mmol) was added to the reaction mixture. The reaction mixture was stirred at room temperature for 18 h.

### Method 3- Attempted synthesis

Bromo or iodo protected compound was dissolved in anhydrous acetonitrile. Methyl 3-mercaptopropionate and anhydrous  $K_2CO_3$  were added, and the reaction mixture was stirred at room temperature for 72 h. Then, the reaction mixture was acidified with ice-diluted 1 N HCl and extracted with diethyl ether ( $3 \times 20$  mL). The combined ether fractions were washed successively with 5%  $NaHCO_3$ , water and brine, dried over  $MgSO_4$  and evaporated under reduced pressure.

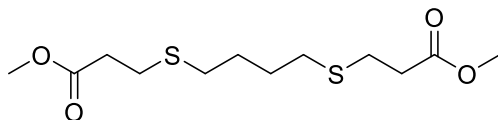
Amounts: 1, 4-dibromobutane (1 g, 4.63 mmol), anhydrous acetonitrile (10 mL), methyl 3-mercaptopropionate (0.27 mL, 2 mmol) and anhydrous  $K_2CO_3$  (1.10 g, 8 mmol), 1N HCl, diethyl ether ( $3 \times 20$  mL), 5%  $NaHCO_3$  ( $3 \times 50$  mL), water ( $3 \times 50$  mL), brine ( $1 \times 50$  mL) and amount of anhydrous  $MgSO_4$  (approximate). The method failed to deliver expected compound **18**. Instead, bis-substituted product **13** was isolated as confirmed by  $^1H$  NMR (400 MHz,  $CDCl_3$ )  $\delta$  3.61 (s, 6H, 2(O-CH<sub>3</sub>)), 2.70 – 2.66 (m, 4H, 2(CH<sub>2</sub>-S)), 2.52 (m, 4H, 2(CH<sub>2</sub>-S)), 2.48 – 2.39 (m, 2H, CH<sub>2</sub>), 1.64 – 1.57 (m, 2H, CH<sub>2</sub>), 1.18 (t,  $J_{1,2}$ = 5.1, 2H, CH<sub>2</sub>), 0.79 (t,  $J_{1,2}$ = 8.5, 2H, CH<sub>2</sub>).

### Method 4- Attempted synthesis

Sodium hydride was added to a stirred solution of methyl 3-mercaptopropanoate in dry THF. The reaction mixture was cooled to 0°C under a nitrogen blanket. The reaction mixture was stirred at 0°C for 15 min before THF solution of bromo or iodo protected compound was added drop wise. The reaction was stirred at 0°C for 30 min and at room temperature for 3 h. Then, it was quenched with water and extracted with the dichloromethane. The combined organic fractions were dried over  $Na_2SO_4$  and concentrated under vacuum.

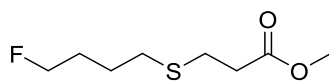
Amounts: NaH (60% in oil, 0.62 g, 25.9 mmol), methyl 3-mercaptopropanoate (3.1 g, 25.9 mmol), dry THF (500 mL), THF (50 mL), 1, 4-dibromobutane (5 g, 23.15 mmol) water (50 mL), dichloromethane ( $3 \times 100$  mL) and amount of anhydrous  $Na_2SO_4$  (approximate). The method failed to deliver expected compound **18**. Instead, bis-substituted product **19** was isolated as confirmed by  $^1H$  NMR spectroscopy.

$^1\text{H}$  NMR (400 MHz,  $\text{CDCl}_3$ )  $\delta$  3.61 (s, 6H, 2(O-CH<sub>3</sub>)), 2.70 – 2.66 (m, 4H, 2(CH<sub>2</sub>-S)), 2.52 (m, 4H, 2(CH<sub>2</sub>-S)), 2.48 – 2.39 (m, 2H, CH<sub>2</sub>), 1.64 – 1.57 (m, 2H, CH<sub>2</sub>), 1.18 (t,  $J_{1,2} = 5.1$ , 2H, CH<sub>2</sub>), 0.79 (t,  $J_{1,2} = 8.5$ , 2H, CH<sub>2</sub>).



19

### 7.4.2.13 Methyl 8-fluoro-4-thiacaprylate (**20**)



**20**

#### Method 1-preferred route

Sodium hydride was added to a stirred solution of methyl 3-mercaptopropanoate in dry THF. The reaction mixture was cooled to 0°C under a nitrogen blanket. The reaction mixture was stirred at 0°C for 15 min before THF solution of bromo or iodo protected compound was added drop wise. The reaction was stirred at 0°C for 30 min and at room temperature for 3 h. Then, it was quenched with water and extracted with the dichloromethane. The combined organic fractions were dried over Na<sub>2</sub>SO<sub>4</sub> and concentrated under vacuum.

Amounts: NaH (60% in oil, 0.174 g, 7.25 mmol), methyl 3-mercaptopropanoate (0.78 g, 7.25 mmol), dry THF (175 mL), THF (10 mL), 1-bromo-4-fluorobutane (1 g, 6.45 mmol), water (50 mL), dichloromethane (3 × 100 mL) and amount of anhydrous Na<sub>2</sub>SO<sub>4</sub> (approximate). Product **20** was purified by column chromatography on silica gel eluted with n-hexane: ethyl acetate 95:5 mixture and was isolated as a colourless oil (0.69 g, 54%).

<sup>1</sup>H NMR (400 MHz, CDCl<sub>3</sub>) δ 4.46 (dt, *J*<sub>1</sub> = 47.1, *J*<sub>2</sub> = 5.7, 2H, CH<sub>2</sub>-F), 3.70 (s, 3H, O-CH<sub>3</sub>), 2.82 – 2.74 (m, 2H, CH<sub>2</sub>-S), 2.65 – 2.56 (m, 4H, CH<sub>2</sub>-CH<sub>2</sub>-S), 1.89 – 1.68 (m, 4H, 2(CH<sub>2</sub>)). <sup>19</sup>F NMR (376 MHz, CDCl<sub>3</sub>) δ 149.11. GC-MS: 194; MS (ESI) *m/z*: 195 [M+H]<sup>+</sup>. HPLC: Method 1 – retention time = 18 min.

### Method 2- Attempted synthesis

18-crown-6 dissolved in anhydrous acetonitrile was mixed with KF dissolved in water, and the KF/18-crown-6 complex was azeotropically dried. Then, tosylate or halogen compound dissolved in anhydrous acetonitrile was added to the flask and the reaction mixture was refluxed under nitrogen blanket overnight. The solvent was evaporated and the residue redissolved in dichloromethane; the organic phase was washed with water, dried over Na<sub>2</sub>SO<sub>4</sub> and evaporated under vacuum.

Amounts: 18-crown-6 (0.05 g, 0.19 mmol), anhydrous acetonitrile (5 mL), KF (0.011 g, 0.19 mmol), water, tosylate precursor **13**, anhydrous acetonitrile, dichloromethane, water (3 × 10 mL), and amount of anhydrous Na<sub>2</sub>SO<sub>4</sub> (approximate). According to the <sup>1</sup>H & <sup>19</sup>F NMR the reaction didn't successful.

### Method 3- Attempted synthesis

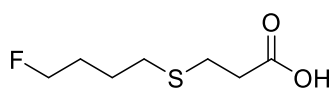
To tosylated or halogen compound dissolved in anhydrous acetonitrile was added tetra-*n*-butylammonium fluoride TBAF (1 M THF solution) and reaction was stirred under nitrogen blanket at room temperature for 72 h. at 24 and 48 h, additional doses of TBAF were added. At the end of 72 h period, reaction mixture was concentrated under vacuum and resulting crude retaken in dichloromethane. Organic phase was washed with water, dried over Na<sub>2</sub>SO<sub>4</sub> and evaporated under vacuum.

Tosylated precursor **13** (80 mg, 0.20 mmol), anhydrous acetonitrile (3 mL), TBAF (1 M THF solution, 3 mL, 3.0 mmol), TBAF (0.5 mL, 0.5 mmol), TBAF (0.5 mL, 0.5 mmol), dichloromethane (100 mL), and amount of anhydrous Na<sub>2</sub>SO<sub>4</sub> (approximate). The <sup>1</sup>H and <sup>19</sup>F NMR spectra indicated that the desired product had not been formed.

#### Method 4- Attempted synthesis

Alcohol compound **12** (0.1 g, 0.5 mmol) was dissolved in anhydrous dichloromethane (14 mL). Reaction mixture was cooled to -40°C, diethylaminosulfur trifluoride (DAST) (0.17 g, 1.06 mmol) was carefully added and reaction stirred under nitrogen blanket at -40°C for 2 h. Then dichloromethane was evaporated and the residue redissolved in ethyl acetate, organic phase was washed with water, dried over MgSO<sub>4</sub> and concentrated under vacuum. <sup>1</sup>H NMR, <sup>19</sup>F NMR and GC-MS analytical data showed that the expected fluorinated product **17** was not formed.

#### 7.4.2.14 8-Fluoro-4-thiacaprylic acid (**21**)



**21**

To ester compound was added LiOH  $\times$  H<sub>2</sub>O dissolved in 60% EtOH and reaction mixture was stirred at room temperature for 1 h. Then, solvent was evaporated and the residue redissolved in dichloromethane and organic phase was washed with 1 N HCl, dried over Na<sub>2</sub>SO<sub>4</sub> and concentrated under vacuum.

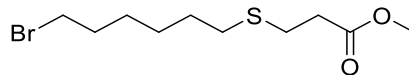
Amounts: Methyl 3-(4-fluorobutylthio)propanoate **17** (0.03 g, 0.15 mmol), LiOH  $\times$  H<sub>2</sub>O (0.01g, 0.45 mmol), 60% EtOH (5 mL), dichloromethane (50 mL), 1 N HCl (50 mL) and amount of anhydrous Na<sub>2</sub>SO<sub>4</sub> (approximate).

<sup>1</sup>H NMR (400 MHz, CDCl<sub>3</sub>)  $\delta$  4.46 (dt,  $J_1 = 47.1$ ,  $J_2 = 5.7$  Hz, 2H, CH<sub>2</sub>-F), 2.79 (t,  $J_{1,2} = 11.1$ , 2H, CH<sub>2</sub>-S), 2.68 – 2.57 (m, 4H, CH<sub>2</sub>-CH<sub>2</sub>-S), 1.87 – 1.68 (m, 4H, 2(CH<sub>2</sub>)), 1.25 (s, 1H, OH); <sup>19</sup>F NMR (376 MHz, CDCl<sub>3</sub>)  $\delta$  149.11; MS (ESI)  $m/z$ : 203 [M-H]<sup>-</sup>. HPLC: Method 1 – retention time = 15:00 min.



## 7.4.2 Synthesis of 4-thiacapric acid/caprate derivatives

### 7.4.3.1 Methyl 10-bromo-4-thiacaprate (**22**)



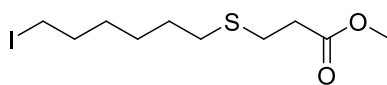
**22**

The synthetic procedure was completed following modified literature methods.<sup>136</sup> Bromo or iodo protected compound was dissolved in anhydrous acetonitrile. Methyl 3-mercaptopropionate and anhydrous  $K_2CO_3$  were added, and the reaction mixture was stirred at room temperature for 72 h. Then, the reaction mixture was acidified with ice-diluted 1N HCl and extracted with diethyl ether ( $3 \times 20$  mL). The combined ether fractions were washed successively with 5%  $NaHCO_3$ , water and brine, dried over  $MgSO_4$  and evaporated under reduced pressure.

Amounts: 1, 6-dibromohexane (1 g, 4.09 mmol), anhydrous acetonitrile (20 mL), methyl 3-mercaptopropionate (0.24 mL, 2 mmol), anhydrous  $K_2CO_3$  (0.27 g, 2 mmol), 1N HCl, diethyl ether ( $3 \times 20$  mL), 5%  $NaHCO_3$  ( $3 \times 50$  mL), water ( $3 \times 50$  mL), brine ( $1 \times 50$  mL) and amount of anhydrous  $MgSO_4$  (approximate). Following by chromatographic purification of the crude on silica gel eluted with n-hexane: ethyl acetate 97: 3 mixture, gave the expected brominated thia-caprate **22** as colourless oil with a (0.32 g, 28%) yield.

$^1H$  NMR (400 MHz,  $CDCl_3$ )  $\delta$  3.70 (s, 3H, O- $CH_3$ ), 3.40 (t,  $J_{1,2} = 6.8$  Hz, 2H,  $CH_2$ -Br), 2.80 – 2.73 (m, 2H,  $CH_2$ -S), 2.63 – 2.50 (m, 4H,  $CH_2$ - $CH_2$ -S), 1.90 – 1.81 (m, 2H,  $CH_2$ ), 1.64 – 1.57 (m, 2H,  $CH_2$ ), 1.48 – 1.37 (m, 4H, 2( $CH_2$ )).  $^{13}C$  NMR (100 MHz,  $CDCl_3$ ) (172.55, C=O), (51.91,  $CH_3$ ), (34.78, 33.39,  $CH_2$ - $CH_2$ -S), (32.69,  $CH_2$ -S), (30.11,  $CH_2$ ), (29.37,  $CH_2$ ), (28.01,  $CH_2$ ), (27.95,  $CH_2$ ), (27.06,  $CH_2$ -Br). MS (ESI) m/z: 322 [ $M+K$ ] $^+$ .

### 7.4.3.2 Methyl 10-iodo-4-thiacaprate (**23**)



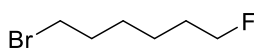
**23**

Bromo or iodo protected compound was dissolved in anhydrous acetonitrile. Methyl 3-mercaptopropionate and anhydrous  $K_2CO_3$  were added, and the reaction mixture was stirred at room temperature for 72 h. Then, the reaction mixture was acidified with ice-diluted 1N HCl and extracted with diethyl ether ( $3 \times 20$  mL). The combined ether fractions were washed successively with 5%  $NaHCO_3$ , water and brine, dried over  $MgSO_4$  and evaporated under reduced pressure.

Amounts: 1, 6-diiodohexane (1 g, 2.95 mmol), anhydrous acetonitrile (20 mL), methyl 3-mercaptopropionate (0.12 mL, 1 mmol), anhydrous  $K_2CO_3$  (0.13 g, 1 mmol), 1N HCl, diethyl ether ( $3 \times 20$  mL), 5%  $NaHCO_3$  ( $3 \times 50$  mL), water ( $3 \times 50$  mL), brine ( $1 \times 50$  mL) and amount of anhydrous  $MgSO_4$  (approximate). Following by chromatographic purification of the crude on silica gel eluted with n-hexane: ethyl acetate 97:3 mixture, gave the expected iodo thia-ester **23** as colourless oil with a (0.24 g, 31%) yield.

$^1H$  NMR (400 MHz,  $CDCl_3$ )  $\delta$  3.70 (s, 3H, O- $CH_3$ ), 3.19 (t,  $J_{1,2} = 7.0$ , 2H,  $CH_2-I$ ), 2.78 (t,  $J_{1,2} = 7.3$ , 2H,  $CH_2-S$ ), 2.65 – 2.46 (m, 4H,  $CH_2-CH_2-S$ ), 1.89 – 1.74 (m, 2H,  $CH_2$ ), 1.67 – 1.50 (m, 2H,  $CH_2$ ), 1.47 – 1.33 (m, 4H, 2( $CH_2$ )).  $^{13}C$  NMR (100 MHz,  $CDCl_3$ ) (172.52, C=O), (62.47,  $CH_3$ ), (51.89, 34.79,  $CH_2-CH_2-S$ ), (33.39,  $CH_2-S$ ), (32.12,  $CH_2$ ), (30.13,  $CH_2$ ), (29.10,  $CH_2$ ), (27.99,  $CH_2$ ), (27.08,  $CH_2-I$ ). MS (ESI) m/z: 331  $[M+H]^+$ .

### 7.4.3.3 1-Bromo-6-fluorohexane (**24**)



**24**

#### Method 1-preferred route

To tosylated or halogen compound dissolved in anhydrous acetonitrile was added tetra-*n*-butylammonium fluoride TBAF (1 M THF solution) and reaction was stirred under nitrogen blanket at room temperature for 72 h, with additional amounts of TBAF added at 24 h and 48 h. At the end of 72 h period, reaction mixture was concentrated under vacuum and resulting crude retaken in dichloromethane. Organic phase was washed with water, dried over Na<sub>2</sub>SO<sub>4</sub> and evaporated under vacuum.

Amounts: 1, 6-dibromohexane (9.67 g, 40 mmol), anhydrous acetonitrile (80 mL), TBAF (1 M THF solution, 20 mL, 20 mmol), TBAF (3 mL, 3 mmol), TBAF (3 mL, 3 mmol), dichloromethane (100 mL), and amount of anhydrous Na<sub>2</sub>SO<sub>4</sub>. Following by simple distillation of the crude, gave the expected 1-bromo-6-fluorohexane **24** as colourless oil with a (0.76 g, 10%) yield.

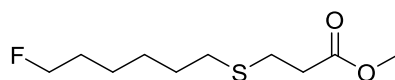
<sup>1</sup>H NMR (400 MHz, CDCl<sub>3</sub>) δ 4.45 (dt, *J*<sub>1</sub> = 47.3, *J*<sub>2</sub> = 6.1, 2H, CH<sub>2</sub>-F), 3.41 (t, *J*<sub>1,2</sub> = 6.8, 2H, CH<sub>2</sub>-Br), 1.87 (m, 2H, CH<sub>2</sub>), 1.46 (m, 4H, 2(CH<sub>2</sub>)); <sup>19</sup>F NMR (376 MHz, CDCl<sub>3</sub>) δ 149.11.

## Method 2- Attempted synthesis

18-Crown-6 dissolved in anhydrous acetonitrile was mixed with KF dissolved in water, and the KF/18-crown-6 complex was azeotropically dried. Then, tosylate or halogen compound dissolved in anhydrous acetonitrile was added to the flask and the reaction mixture was refluxed under nitrogen blanket overnight. The solvent was evaporated and the residue redissolved in dichloromethane; the organic phase was washed with water, dried over Na<sub>2</sub>SO<sub>4</sub> and evaporated under vacuum.

Amounts: 18-crown-6 (0.93 g, 3.55 mmol), anhydrous acetonitrile (10 mL), KF (0.17 g, 2.96 mmol), water, 1, 6-diiodohexane, anhydrous acetonitrile, dichloromethane, water (3 × 20 mL), and amount of anhydrous Na<sub>2</sub>SO<sub>4</sub> (approximate). Analysis of the <sup>1</sup>H and <sup>19</sup>F NMR spectra indicated that the desired product was not formed.

#### 7.4.3.4 Methyl 10-fluoro-4-thiacapratoate (**25**)



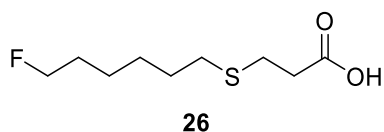
**25**

The product has been synthesised previously using a different synthetic route.<sup>4</sup> Sodium hydride was added to a stirred solution of methyl 3-mercaptopropanoate in dry THF. The reaction mixture was cooled to 0°C under a nitrogen blanket. The reaction mixture was stirred at 0°C for 15 min before THF solution of Bromo or iodo protected compound was added drop wise. The reaction was stirred at 0°C for 30 min and at room temperature for 3 h. Then, it was quenched with water and extracted with the dichloromethane. The combined organic fractions were dried over Na<sub>2</sub>SO<sub>4</sub> and concentrated under vacuum.<sup>115</sup>

Amounts: NaH (60% in oil, 0.19 g, 8.30 mmol), methyl 3-mercaptopropanoate (0.99 g, 8.30 mmol), dry THF (150 mL), THF (10 mL), 1-bromo-6-fluorohexane **18** (0.76 g, 4.15 mmol), water (50 mL), dichloromethane (3 × 100 mL) and amount of anhydrous Na<sub>2</sub>SO<sub>4</sub> (approximate). Following by chromatographic purification of the crude on silica gel eluted with n-hexane: ethyl acetate 95:5 mixture. Providing the expected product **19** as colourless oil with a (0.53 g, 58%) yield.

<sup>1</sup>H NMR (400 MHz, CDCl<sub>3</sub>) δ 4.53 (dt, *J*<sub>1</sub> = 47.3, *J*<sub>2</sub> = 6.1, 2H, CH<sub>2</sub>-F), 3.70 (s, 3H, O-CH<sub>3</sub>), 2.78 (t, *J*<sub>1,2</sub> = 7.4, 2H, CH<sub>2</sub>-S), 2.60 (t, *J*<sub>1,2</sub> = 7.4, 2H, CH<sub>2</sub>-S), 2.56 – 2.51 (m, 2H, CH<sub>2</sub>-CH<sub>2</sub>-S), 1.77-1.60 (t, *J*<sub>1,2</sub> = 7.4, 4H, 2(CH<sub>2</sub>)), 1.43 (t, *J*<sub>1,2</sub> = 3.7, 4H, 2(CH<sub>2</sub>); <sup>13</sup>C NMR (100 MHz, CDCl<sub>3</sub>) δ 84.86, 83.23, 62.96, 33.82, 32.70, 30.41, 30.21, 27.86, 24.57, 24.52.<sup>19</sup>F NMR (376 MHz, CDCl<sub>3</sub>) δ 149.11. HPLC: Method 2 – retention time = 19:08 min.

#### 7.4.3.5 10-Fluoro-4-thiacapric acid (**26**)



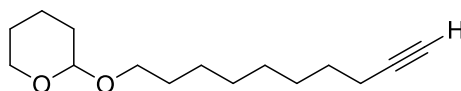
The product has been synthesised previously using a different synthetic route.<sup>135</sup> To ester compound **25** was added LiOH.xH<sub>2</sub>O dissolved in 60% EtOH and reaction mixture was stirred at room temperature for 1 h. Then, solvent was evaporated and the residue redissolved in dichloromethane and organic phase was washed with 1 N HCl, dried over Na<sub>2</sub>SO<sub>4</sub> and concentrated under vacuum.

Amounts: methyl 3-((6-fluorohexyl)thio)propanoate **25** (0.3 g, 1.34 mmol), LiOH × H<sub>2</sub>O (0.09 g, 2.23 mmol), 60% EtOH (50 mL), dichloromethane (50 mL), 1 N HCl (50 mL) and amount of anhydrous Na<sub>2</sub>SO<sub>4</sub> (approximate). 10-fluoro-4-thiacapric acid **26** as colourless oil with a 96% yield.

<sup>1</sup>H NMR (400 MHz, CDCl<sub>3</sub>) δ 4.44 (dt, *J*<sub>1</sub> = 47.3, *J*<sub>2</sub> = 6.1, 2H, CH<sub>2</sub>-F), 2.77 (t, *J*<sub>1,2</sub> = 7.2, 2H, CH<sub>2</sub>-S), 2.65 (t, *J*<sub>1,2</sub> = 1.2, 2H, CH<sub>2</sub>-S), 2.54 (t, *J*<sub>1,2</sub> = 6.7, 2H, CH<sub>2</sub>-CH<sub>2</sub>-S), 1.66 (t, *J*<sub>1,2</sub> = 21.6, 4H, 2(CH<sub>2</sub>)), 1.42 (t, *J*<sub>1,2</sub> = 7.1, 4H, 2(CH<sub>2</sub>)). <sup>19</sup>F NMR (376 MHz, CDCl<sub>3</sub>) δ 149.11.  
HPLC: Method 2 – retention time = 14:14 min.

## 7.4.4 Synthesis of 4-thiaoleic acid/oleate derivatives (TOD)

### 7.4.4.1 2-(Dec-9-yn-1-yloxy)tetrahydro-2H-pyran (**27**)<sup>137</sup>

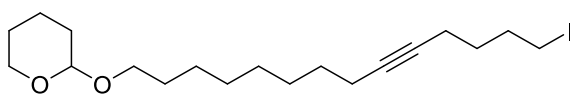


**27**

The synthetic procedure was completed following literature methods.<sup>137</sup> To dec-9-yn-1-ol (2.20 g, 14.2 mmol) dissolved in anhydrous dichloromethane (5 mL) was added pyridinium *p*-toluenesulfonate (PPTS) (0.35g, 1.42 mmol) followed by 3,4-dihydro-2H-pyran (1.43 g, 17.1 mmol) and reaction mixture was stirred at room temperature for 4 h. Then, reaction mixture was washed with 5% NaHCO<sub>3</sub> (2 x 10 mL) and brine (10 mL), dried over anhydrous K<sub>2</sub>O<sub>3</sub> and concentrated under vacuum. Short path silica gel plug purification (*n*-hexane : ethyl acetate 9 : 1) gave **27** as a colourless oil in quantitative yield (3.52 g, 100%).

<sup>1</sup>H NMR (400 MHz, CDCl<sub>3</sub>) δ 4.57 (t, *J*<sub>1,2</sub> = 4.4, 1H, O-CH-O), 3.87 (t, *J*<sub>1,2</sub> = 11.2, 2H, CH<sub>2</sub>-O), 3.73 (t, *J*<sub>1,2</sub> = 9.6, 2H, CH<sub>2</sub>-O), 2.29 – 2.05 (m, 2H, H<sub>2</sub>C≡CH), 1.93 (t, *J*<sub>1,2</sub> = 2.6, 1H, H<sub>2</sub>C≡CH), 1.82 (t, *J*<sub>1,2</sub> = 11.6, 2H, CH<sub>2</sub>), 1.72 (t, *J*<sub>1,2</sub> = 11.8, 2H, CH<sub>2</sub>), 1.64 – 1.44 (m, 8H, 4(CH<sub>2</sub>)), 1.44 – 1.24 (m, 6H, 3(CH<sub>2</sub>)). <sup>13</sup>C NMR (100 MHz, CDCl<sub>3</sub>): 98.94 (O-CH-O), 84.85 (H<sub>2</sub>C≡CH), 68.14 (H<sub>2</sub>C≡CH), 67.74, 62.45 (CH<sub>2</sub>-O), 30.87, 29.81, 29.41, 29.12, 28.77, 28.54, 26.26, 25.58, 19.79, 18.47 9(CH<sub>2</sub>); GC-MS: 10:00 min, 239 [M+H]<sup>+</sup>.

#### 7.4.4.2 2-(14-Iodotetradec-9-yn-1-yl)oxytetrahydro-2H-pyran (**28**)



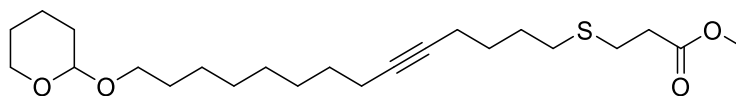
**28**

To THF (50 mL) solution of **27** (2.84 g, 11.91 mmol) cooled to  $-78^{\circ}\text{C}$  was added n-BuLi (1.6 M in hexane, 9.3 mL, 15 mmol) and reaction was allowed to warm to room temperature before 1, 4-diiodobutane (11.07 g, 35.84 mmol) was added. The reaction mixture was stirred at room temperature for 2 hours and then heated at reflux for further 24 h. Then, it was quenched with water (50 mL), evaporated to dryness under vacuum and redissolved in diethyl ether. Organic phase was washed with 10% citric acid solution, water, dried over  $\text{MgSO}_4$  and concentrated under vacuum. Chromatographic purification on silica gel eluted with hexane: ethyl acetate 97:3 mixture gave the expected product **28** as a colourless oil (3.03 g, 61%).

$^1\text{H}$  NMR (400 MHz,  $\text{CDCl}_3$ )  $\delta$  4.57 (t,  $J_{1,2} = 4.4$ , 1H, O-CH-O), 3.86 (t,  $J_{1,2} = 7.3$ , 2H, CH<sub>2</sub>-O), 3.73 (t,  $J_{1,2} = 9.6$ , 2H, CH<sub>2</sub>-O), 3.21 (t,  $J_{1,2} = 7.0$ , 2H, CH<sub>2</sub>-I), 2.21-2.13 (m, 4H, H<sub>2</sub>C $\equiv$ CH<sub>2</sub>), 1.96-1.91 (m, 2H, CH<sub>2</sub>), 1.88 – 1.78 (m, 2H, CH<sub>2</sub>), 1.72 (t,  $J_{1,2} = 11.7$ , 2H, CH<sub>2</sub>), 1.65 – 1.48 (m, 10H, 5(CH<sub>2</sub>)), 1.44 – 1.27 (m, 6H, 3(CH<sub>2</sub>)).  $^{13}\text{C}$  NMR (100 MHz,  $\text{CDCl}_3$ ): 100.71 (O-CH-O), 98.95, 81.12 (H<sub>2</sub>C $\equiv$ CH<sub>2</sub>), 79.22 (CH), 67.77, 67.47 (CH-O), 32.57, 30.88, 29.82, 29.47, 29.14, 28.90, 26.29, 25.58, 19.80, 18.79, 17.82, 8.56, 6.52 13(CH<sub>2</sub>). GC-MS: 12:47 min, 421 [M+H]<sup>+</sup>.



#### 7.4.4.3 Methyl 18-(tetrahydro-2H-pyran-2-yl)-4-thiaoleate (**29**)



29

##### Method 1

Bromo or iodo protected compound was dissolved in anhydrous acetonitrile. Methyl 3-mercaptopropionate and anhydrous  $K_2CO_3$  were added, and the reaction mixture was stirred at room temperature for 72 h. Then, the reaction mixture was acidified with ice-diluted 1N HCl and extracted with diethyl ether ( $3 \times 20$  mL). The combined ether fractions were washed successively with 5%  $NaHCO_3$ , water and brine, dried over  $MgSO_4$  and evaporated under reduced pressure.

Amounts: 2-(14-Iodotetradec-9-yn-1-yl)oxytetrahydro-2H-pyran **28** (3.44 g, 8.21 mmol), anhydrous acetonitrile (30 mL), methyl 3-mercaptopropionate (0.98 mL, 8.21 mmol), anhydrous  $K_2CO_3$  (1.34 g, 10.42 mmol), 1N HCl, diethyl ether ( $3 \times 20$  mL), 5%  $NaHCO_3$  ( $3 \times 50$  mL), water ( $3 \times 50$  mL), brine ( $1 \times 50$  mL) and amount of anhydrous  $MgSO_4$  (approximate). Chromatographic purification on silica gel eluted with hexane: ethyl acetate 9: 1 mixture gave the expected product **29** as a colourless oil (1.05 g, 31%).

$^1H$  NMR (400 MHz,  $CDCl_3$ ):  $\delta$  4.57 (t,  $J_{1,2} = 3.5$ , 1H, O-CH-O), 3.95 – 3.80 (m, 2H,  $CH_2$ -O), 3.78 – 3.71 (m, 2H,  $CH_2$ -O), 3.72 – 3.63 (s, 3H, O- $CH_3$ ), 2.78 (t,  $J_{1,2} = 7.5$ , 2H,  $CH_2$ -S), 2.68 – 2.48 (m, 4H,  $CH_2$ - $CH_2$ -S), 2.14 (m, 4H,  $H_2C \equiv CH_2$ ), 1.83 (m, 2H,  $CH_2$ ), 1.76 – 1.64 (m, 2H,  $CH_2$ ), 1.76 – 1.63 (m, 2H,  $CH_2$ ), 1.64 – 1.40 (m, 6H, 3( $CH_2$ )), 1.31 (m, 10H, 5( $CH_2$ )).  $^{13}C$  NMR (100 MHz,  $CDCl_3$ ): 172.53 ( $\underline{C}OOCH_3$ ), 98.95 (O- $\underline{C}H$ -O), 81.86 ( $H_2C \equiv CH_2$ ), 79.53, 67.76, 62.46 ( $CH_2$ -O), 51.88 (O- $CH_3$ ), 49.02, 34.77 ( $CH_2$ -S), 31.00, 30.88, 29.83, 29.47, 29.19, 28.93, 28.61, 28.18, 27.00, 26.11, 25.59, 19.80, 18.81, 18.60 14( $CH_2$ ). GC-MS: 15:45 min, 412 ( $M^+$ ).

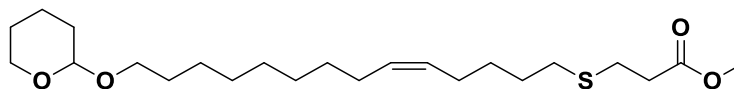
## Method 2

Sodium hydride was added to a stirred solution of methyl 3-mercaptopropanoate in dry THF. The reaction mixture was cooled to 0°C under a nitrogen blanket. The reaction mixture was stirred at 0°C for 15 min before THF solution of bromo or iodo protected compound was added drop wise. The reaction was stirred at 0°C for 30 min and at room temperature for 3 h. Then, it was quenched with water and extracted with the dichloromethane. The combined organic fractions were dried over Na<sub>2</sub>SO<sub>4</sub> and concentrated under vacuum.

Amounts: NaH (60% in oil, 0.51 g, 21.46 mmol), methyl 3-mercaptopropanoate (2.58 g, 21.46 mmol), dry THF (1000 mL), THF (100 mL), 2-(14-Iodotetradec-9-yn-1-yl)oxytetrahydro-2*H*-pyran **25** (4.53 g, 10.77 mmol), water (50 mL), dichloromethane (3 × 100 mL) and amount of anhydrous Na<sub>2</sub>SO<sub>4</sub> (approximate). Product **30** was purified by column chromatography on silica gel eluted with n-hexane: ethyl acetate 9:1 mixture and was isolated as colourless oil (3.24 g, 73%).

<sup>1</sup>H NMR (400 MHz, CDCl<sub>3</sub>): δ 4.57 (t, *J*<sub>1,2</sub> = 3.5, 1H, O-CH-O), 3.95 – 3.80 (m, 2H, CH<sub>2</sub>-O), 3.78 – 3.71 (m, 2H, CH<sub>2</sub>-O), 3.72 – 3.63 (s, 3H, O-CH<sub>3</sub>), 2.78 (t, *J*<sub>1,2</sub> = 7.5, 2H, CH<sub>2</sub>-S), 2.68 – 2.48 (m, 4H, CH<sub>2</sub>-CH<sub>2</sub>-S), 2.14 (m, 4H, H<sub>2</sub>C≡CH<sub>2</sub>), 1.83 (m, 2H, CH<sub>2</sub>), 1.76 – 1.64 (m, 2H, CH<sub>2</sub>), 1.76 – 1.63 (m, 2H, CH<sub>2</sub>), 1.64 – 1.40 (m, 6H, 3(CH<sub>2</sub>)), 1.31 (m, 10H, 5(CH<sub>2</sub>)). <sup>13</sup>C NMR (100 MHz, CDCl<sub>3</sub>): 172.53 (C=O), 98.95 (O-CH-O), 81.86 (H<sub>2</sub>C≡CH<sub>2</sub>), 79.53, 67.76, 62.46 (CH<sub>2</sub>-O), 51.88 (O-CH<sub>3</sub>), 49.02, 34.77 (CH<sub>2</sub>-S), 31.00, 30.88, 29.83, 29.47, 29.19, 28.93, 28.61, 28.18, 27.00, 26.11, 25.59, 19.80, 18.81, 18.60 14(CH<sub>2</sub>). GC-MS: 15:45 min, 412 (M<sup>+</sup>).

#### 7.4.4.4 Methyl (Z)-18-(2-tetrahydropyranyloxy)-4-thia-octadec-9-enoate (**30**)

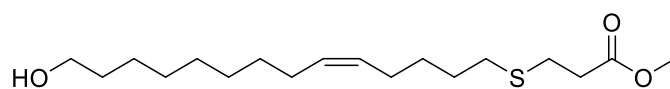


**30**

The reaction flask of a low-pressure hydrogenation apparatus is charged with (2.38 g, 5.77 mmol) of compound **29** (2.38 g) of the palladium catalyst, (6.8 mL, 57.76 mmol) of quinoline, and 50 mL of hexane. The apparatus is evacuated, and hydrogen is admitted to a pressure slightly above 1 bar stirring or shaking is started, causing rapid absorption of hydrogen. The hydrogen pressure is kept close to 1 bar overnight. The reaction was then filtered through celite, the hexane evaporated and the residue redissolved in ethyl acetate (200 mL), washed with (3 × 100 mL) 10% citric acid, water (3 × 100 mL), brine (100 mL) and dried over Na<sub>2</sub>SO<sub>4</sub> and then concentrated under vacuum. Product **30** was purified by column chromatography on silica gel eluted with n-hexane: ethyl acetate 95:5 mixture and was isolated as a colourless oil (1.89 g, 79%) yield.

<sup>1</sup>H NMR (400 MHz, CDCl<sub>3</sub>) δ 5.41 – 5.29 (m, 2H, HC=CH), 4.57 (t, *J*<sub>1,2</sub> = 4.4, 1H, O-CH-O), 3.91 – 3.82 (m, 2H, CH<sub>2</sub>-O), 3.74 (t, *J*<sub>1,2</sub> = 8.2, 2H, CH<sub>2</sub>-O), 3.70 (s, 3H, O-CH<sub>3</sub>), 2.78 (t, *J*<sub>1,2</sub> = 11.0, 2H, CH<sub>2</sub>-S), 2.66 – 2.46 (m, 4H, CH<sub>2</sub>-CH<sub>2</sub>-S), 2.02 (dd, *J*<sub>1</sub> = 13.9, *J*<sub>2</sub> = 6.7, 4H, H<sub>2</sub>CHC=CHCHH<sub>2</sub>), 1.71 (m, 2H, CH<sub>2</sub>), 1.62 – 1.51 (m, 12H, 6(CH<sub>2</sub>)), 1.41 (m, 6H, 3(CH<sub>2</sub>)). <sup>13</sup>C NMR (100 MHz, CDCl<sub>3</sub>): 172.56 (C=O), 130.52 (C=C), 98.94 (O-C-O), 67.78 (CH<sub>2</sub>-O), 62.45 (O-C), 51.87 (O-CH<sub>3</sub>), 34.80 (C-C=O), 32.15 (CH<sub>2</sub>-S), 30.88, 29.87, 29.56, 29.40, 29.25, 28.97, 27.40, 27.05, 26.88, 26.32, 25.59, 19.80 12(CH<sub>2</sub>).

#### 7.4.4.5 Methyl (Z)-18-hydroxy-4-thiaoctadec-9-enoate (**31**)<sup>125</sup>



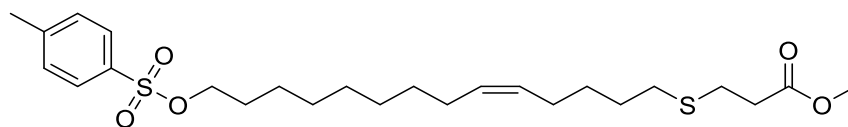
**31**

The synthetic procedure was completed following literature methods.<sup>125</sup> To a solution of THP protected compound dissolved in MeOH was added *p*-toluene sulfonic acid monohydrate (TsOH × H<sub>2</sub>O) and the reaction was stirred at room temperature for 5 h. The methanol was evaporated and the residue taken up into DCM, and the organic phase was washed successively with 10% NaHCO<sub>3</sub> solution, water and brine, dried over MgSO<sub>4</sub> and evaporated under reduced pressure.

Amounts: THP derivative **30** (1.71 g, 4.12 mmol), MeOH (80 mL) and TsOH × H<sub>2</sub>O (0.78 g, 4.12 mmol), DCM (100 mL), 10% NaHCO<sub>3</sub> solution (3 × 100 mL), water (3 × 100 mL), brine (1 × 100 mL) and amount of anhydrous Na<sub>2</sub>SO<sub>4</sub> (approximate). The expected product was isolated by column chromatography on silica gel eluted with hexane: ethyl acetate 9: 1 mixture (1.21 g, 89%).

<sup>1</sup>H NMR (400 MHz, CDCl<sub>3</sub>) δ 5.44 – 5.27 (m, 2H, HC=CH), 3.70 (s, 3H, O-CH<sub>3</sub>), 2.63 – 2.51 (m, 2H, CH<sub>2</sub>-S), 2.06 – 1.97 (m, 4H, CH<sub>2</sub>-CH<sub>2</sub>-S), 1.62 – 1.52 (m, 4H, H<sub>2</sub>CHC≡CHCH<sub>2</sub>), 1.58 (m, 14H, 7(CH<sub>2</sub>)), 1.46 – 1.28 (m, 6H, 3(CH<sub>2</sub>)). <sup>13</sup>C NMR (100 MHz, CDCl<sub>3</sub>): 172.56 (C=O), 130.05, 129.25 (C=C), 63.16 (CH<sub>2</sub>-OH), 51.89 (O-CH<sub>3</sub>), 34.81 (C-C=O), 32.88 (CH<sub>2</sub>-S), 32.15, 29.88, 29.47, 28.88, 28.56, 27.41, 27.05, 26.97, 25.81- 9(CH<sub>2</sub>).

#### 7.4.4.6 Methyl (Z)-18-(tosyloxy)-4-thia-octadec-9-enoate (**32**)



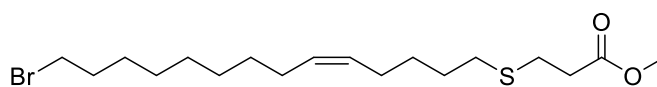
**32**

The product has been synthesised previously using a different synthetic route.<sup>117</sup> To a solution of alcohol compound in anhydrous acetonitrile containing triethylamine (Et<sub>3</sub>N) and trimethylamine hydrochloride (Me<sub>3</sub>N.HCl) maintained at -5°C was added tosyl chloride dissolved in anhydrous acetonitrile. The reaction mixture was stirred at room temperature for 2 h. Acetonitrile was evaporated and the residue redissolved in ethyl acetate, washed with water and brine, dried over Na<sub>2</sub>SO<sub>4</sub> and evaporated under vacuum.

Amounts: compound **31** (0.3 g, 0.90 mmol), anhydrous acetonitrile (5 mL), Et<sub>3</sub>N (0.097 mL, 0.96 mmol), Me<sub>3</sub>N × HCl (86 mg, 0.09 mmol), tosyl chloride (0.25 g, 1.35 mmol), anhydrous acetonitrile (5 mL), water (3 × 10 mL), brine (1 × 10 mL) and amount of anhydrous Na<sub>2</sub>SO<sub>4</sub> (approximate). Purifying by column chromatography on silica gel eluted with n-hexane: ethyl acetate 95:5 mixture and was isolated as a colourless oil (0.3 g, 70%) yield.

<sup>1</sup>H NMR (400 MHz, CDCl<sub>3</sub>) δ 7.80 – 7.77 (m, 2H, Ar-H), 7.34 (d, *J*<sub>1</sub> = 8.5, 2H, Ar-H), 5.33 (m, 2H, HC=CH), 4.01 (t, *J*<sub>1,2</sub> = 6.5, 2H, CH<sub>2</sub>-O), 3.69 (s, 3H, O-CH<sub>3</sub>), 2.74 (t, *J*<sub>1,2</sub> = 7.5, 2H, CH<sub>2</sub>-S), 2.55 – 2.50 (m, 4H, CH<sub>2</sub>-CH<sub>2</sub>-S), 2.44 (m, 4H, H<sub>2</sub>CHC=CHCH<sub>2</sub>), 2.06 – 1.95 (m, 3H, CH<sub>3</sub>-Ar), 1.61 (t, *J*<sub>1,2</sub> = 14.7, 2H, CH<sub>2</sub>), 1.39 (m, 2H, CH<sub>2</sub>), 1.36 – 1.22 (m, 10H, 5(CH<sub>2</sub>)). <sup>13</sup>C NMR (100 MHz, CDCl<sub>3</sub>): 172.56 (C=O), 144.70 (Ar-C-S), 133.31 (Ar-C-CH<sub>3</sub>), 130.41-129.88 (2 Ar-C, C=C), 129.60-127.97 (2 Ar-C), 70.78 (CH<sub>2</sub>-O), 51.88 (O-CH<sub>3</sub>), 34.80 (C-C=O), 32.15 (CH<sub>2</sub>-S), 29.97, 29.47, 29.21, 29.00, 27.10, 27.05, 26.97, 25.81, 25.41 (CH<sub>2</sub>), 21.73 (Ar-CH<sub>3</sub>).

#### 7.4.4.7 Methyl (Z)-18-bromo-4-thia-octadec-9-enoate (**33**)<sup>117</sup>

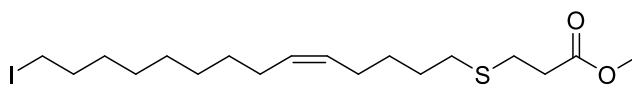


**33**

The product has been synthesised previously using a different synthetic route.<sup>117</sup> Compound **32** (0.2 g, 0.41 mmol) and lithium bromide (0.17 g, 2.05 mmol) were dissolved in dry acetone (10 mL) and stirred at RT for 5 h under nitrogen. After that the solvent was evaporated under vacuum to give product **33** which was purified by column chromatography on silica gel eluted with n-hexane: ethyl acetate 98:2 mixture and was isolated as a colourless oil (0.12 g, 75%).

<sup>1</sup>H NMR (400 MHz, CDCl<sub>3</sub>) δ 5.34 (m, 2H, HC=CH), 3.70 (s, 3H, O-CH<sub>3</sub>), 3.42 (t, *J*<sub>1,2</sub> = 6.9, 2H, CH<sub>2</sub>-Br), 2.78 (t, *J*<sub>1,2</sub> = 7.5, 2H, CH<sub>2</sub>-S), 2.63 – 2.50 (m, 4H, CH<sub>2</sub>-CH<sub>2</sub>-S), 2.03 (m, 4H, H<sub>2</sub>CHC=CHCH<sub>2</sub>), 1.85 (t, *J*<sub>1,2</sub> = 7.2, 2H, CH<sub>2</sub>), 1.57 – 1.24 (m, 14H, 7(CH<sub>2</sub>)). HPLC: Method 4 – retention time = 24.38 min.

#### 7.4.4.8 Methyl (Z)-18-iodo-4-thia-octadec-9-enoate (**34**)

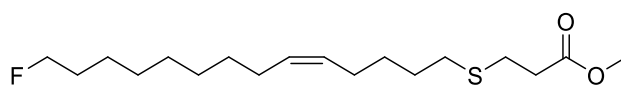


**34**

Compound **32** (0.45 g, 0.92 mmol) and sodium iodide (0.68 g, 4.6 mmol) were dissolved in dry acetone (10 mL) and stirred at RT for 5 h under nitrogen. After that the solvent was evaporated under vacuum to give product **34** which was purified by column chromatography on silica gel eluted with n-hexane: ethyl acetate 90:10 mixture and was isolated as a colourless oil (0.3 g, 75%).

$^1\text{H NMR}$  (400 MHz,  $\text{CDCl}_3$ )  $\delta$  5.35 (m, 2H, HC=CH), 3.70 (s, 3H, O- $\text{CH}_3$ ), 3.19 (t,  $J_{1,2} = 7.0$ , 2H,  $\text{CH}_2\text{-I}$ ), 2.78 (t,  $J_{1,2} = 7.4$ , 2H,  $\text{CH}_2\text{-S}$ ), 2.61 (t,  $J_{1,2} = 7.4$ , 2H,  $\text{CH}_2\text{-S}$ ), 2.57 – 2.50 (m, 2H,  $\text{CH}_2\text{-CH}_2\text{-S}$ ), 2.11 – 1.97 (m, 4H,  $\text{H}_2\text{CHC}=\text{CHCH}_2$ ), 1.86 – 1.78 (m, 2H,  $\text{CH}_2$ ), 1.65 – 1.57 (m, 2H,  $\text{CH}_2$ ), 1.48 – 1.22 (m, 12H, 6( $\text{CH}_2$ )). HPLC: Method 4 – retention time = 26.08 min.

#### 7.4.4.8 Methyl 18-fluoro-4-thiaoleate (**35**)<sup>235</sup>



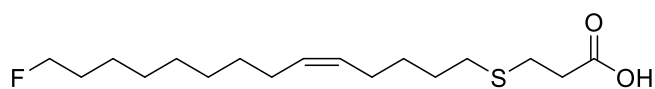
**35**

The product has been synthesised previously using a different synthetic route.<sup>235</sup> To a solution of alcohol **31** (0.1 g, 0.30 mmol) in anhydrous acetonitrile (3 mL) was slowly added diethylaminosulfur trifluoride (0.14 g, 0.9 mmol) dissolved in anhydrous acetonitrile (10 mL) cooled to  $-78^{\circ}\text{C}$  and the reaction mixture was stirred at room temperature for 5 h. Acetonitrile was evaporated and the residue redissolved in ethyl acetate, washed with 10%  $\text{NaHCO}_3$  solution, water and brine, dried over  $\text{Na}_2\text{SO}_4$  and evaporated under vacuum. Product **35** was purified by column chromatography on silica gel eluted with n-hexane: ethyl acetate 95: 5 mixture and was isolated as a colourless oil (0.04 g, 45%) yield.

$^1\text{H}$  NMR (400 MHz,  $\text{CDCl}_3$ )  $\delta$  5.35 (m, 2H,  $\text{HC}=\text{CH}$ ), 4.43 (dt,  $J_1 = 47.4$ ,  $J_2 = 6.2$ , 2H,  $\text{CH}_2\text{-F}$ ), 3.70 (s, 3H,  $\text{O-CH}_3$ ), 2.78 (t,  $J_{1,2} = 7.5$ , 2H,  $\text{CH}_2\text{-S}$ ), 2.62 – 2.50 (m, 4H,  $\text{CH}_2\text{-CH}_2\text{-S}$ ), 2.06 – 1.96 (m, 4H,  $\text{H}_2\text{CHC}\equiv\text{CHCH}_2$ ), 1.66 (m, 4H,  $2(\text{CH}_2)$ ), 1.44 – 1.27 (m, 12H,  $6\text{CH}_2$ ).  
 $^{13}\text{C}$  NMR (100 MHz,  $\text{CDCl}_3$ ): 172.56 (C=O), 130.00-129.28 (C=C), 85.15-86.41 ( $\text{CH}_2\text{F}$ ), 51.87 (O- $\text{CH}_3$ ), 34.81 ( $\text{C-C=O}$ ), 32.15 ( $\text{CH}_2\text{-S}$ ), 30.30, 30.29, 29.76, 29.56, 29.21, 29.00, 27.30, 27.05, 26.83, 25.25  $10(\text{CH}_2)$ . HPLC: Method 4-retention time = 22:28 min.



#### 7.4.4.9 Methyl 18-fluoro-4-thiaoleic acid (**36**)<sup>135</sup>



**36**

The product has been synthesised previously using a different synthetic route.<sup>135</sup> To ester compound was added LiOH × H<sub>2</sub>O dissolved in 60% EtOH and reaction mixture was stirred at room temperature for 1 h. Then, solvent was evaporated and the residue redissolved in dichloromethane and organic phase was washed with 1 N HCl, dried over Na<sub>2</sub>SO<sub>4</sub> and concentrated under vacuum.

Amounts: methyl 18-fluoro-4-thiaoleate **32** (10 g, 0.03 mmol), LiOH × H<sub>2</sub>O (2 mg, 0.05 mmol), 60% EtOH (5 mL), dichloromethane (25 mL), 1 N HCl (5 mL) and amount of anhydrous Na<sub>2</sub>SO<sub>4</sub> (approximate). 10-fluoro-4-thiacapric acid **36** as colourless oil with a (5 mg, 60%) yield.

<sup>1</sup>H NMR (400 MHz, CDCl<sub>3</sub>) δ 5.46 – 5.27 (m, 2H, HC=CH), 4.44 (dt, *J*<sub>1</sub> = 47.4, *J*<sub>2</sub> = 6.2, 2H, CH<sub>2</sub>-F), 2.79 (t, *J*<sub>1,2</sub> = 11.2, 2H, CH<sub>2</sub>-S), 2.66 (t, *J*<sub>1,2</sub> = 7.0, 2H, CH<sub>2</sub>-CH<sub>2</sub>-S), 2.58 – 2.51 (m, 2H, CH<sub>2</sub>-CH<sub>2</sub>-S), 2.02 (m, 4H, H<sub>2</sub>CHC=CHCH<sub>2</sub>), 1.71 – 1.36 (m, 16H, 8(CH<sub>2</sub>)). HPLC: Method 4 – retention time = 18:48 min.

## 7.4.5 Radio-fluorination of thia-fatty acid tracers

### General procedure A

Cyclotron-produced [ $^{18}\text{F}$ ] fluoride was purified on weak anion exchange cartridge (QMA Light). Water solution containing activity was loaded onto the cartridge, which was then dried with air and activity eluted with  $\text{K}_2\text{CO}_3$ . Kryptofix 2.2.2 dissolved in acetonitrile was then added and the mixture was dried at  $90^\circ\text{C}$  under 0.5 bar current of argon. The residue was further dried by azeotropic distillation by addition of acetonitrile. A solution of the labeling precursor in acetonitrile was added onto the dried  $\text{K}^{18}\text{F}/\text{K}_{222}$  complex and reaction mixture was heated in a closed vial at  $90^\circ\text{C}$  for 10 min. Subsequent hydrolysis of the resulting [ $^{18}\text{F}$ ]fluoroester was performed in the same vessel by addition of KOH solution and heating at  $90^\circ\text{C}$  for 5 min. Reaction was quenched by addition  $\text{NaH}_2\text{PO}_4$ . After that, crude mixture was centrifuged to set down the insoluble and purified by semi-preparative HPLC on ACE 5 C-18, 5  $\mu\text{m}$ , 10 mm  $\times$  250 mm). The fraction containing [ $^{18}\text{F}$ ]fluoro fatty acid was diluted in water and loaded on an (Oasis C18 Sep-Pak cartridge). Cartridge was washed water, dried with current of Argon and flushed with tiny amount of ether. The product was eluted with more of ether, solvent was evaporated at room temperature by a current of argon and radiolabeled product was formulated in 3% BSA in isotonic NaCl solution, filtered through a 0.22  $\mu\text{m}$  filter and dispensed for animal administration.

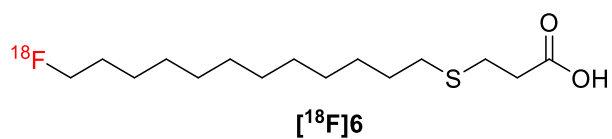
In general, radioactive decay is the process by which an unstable isotope emits energy to reach a more stable state. Radioactive material decays until the only stable substance is left and the decay of a substance is fixed and measurable. The decay corrected radiochemical yield was determined by dividing the activity in a formulated product ([<sup>18</sup>F]-thia-fatty acid) by decay corrected starting activity.

**Decay corrected radiochemical yield = Activity in a formulated product / decay corrected starting activity × 100%**

The radiochemical purity is the percentage of desired product in the formulated solution, which is measured by integration of HPLC or TLC.<sup>94, 236, 237</sup>

**Radiochemical purity = the proportion of the total activity of a specific radionuclide in a specific chemical or biologic form**

#### 7.4.5.1 Radiosynthesis of [<sup>18</sup>F]FTP/[<sup>18</sup>F]6

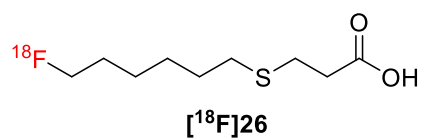


General procedure A was followed.

Amounts: methyl 16-iodo-4-thiopalmitate (4-5 mg), [<sup>18</sup>F] fluoride (900-1200 MBq), K<sub>2</sub>CO<sub>3</sub> (3.6 mg in 1 mL of water), Kryptofix 2.2.2 (10 mg in 1 mL ACN), KOH (250 μL, 0.2 M), NaH<sub>2</sub>PO<sub>4</sub> (250 μL, 0.5 M).

Decay corrected radiochemical yield (18 ± 1.2 %), purity > 95% and total synthesis time (120 min).

#### 7.4.5.2 Radiosynthesis of [<sup>18</sup>F]FTC2/[<sup>18</sup>F]26

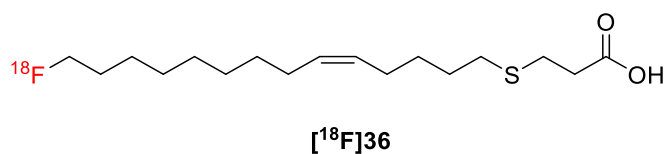


General procedure A was followed.

Amounts: methyl 10-iodo-4-thiacaprate (4-5 mg), [<sup>18</sup>F] fluoride (900-1200 MBq), K<sub>2</sub>CO<sub>3</sub> (3.6 mg in 1 mL of water), Kryptofix 2.2.2 (10 mg in 1 mL ACN), KOH (250 μL, 0.2 M), NaH<sub>2</sub>PO<sub>4</sub> (250 μL, 0.5 M).

Radiochemical decay corrected yield (16.15 ± 2.6 %), purity > 98% and total synthesis time (120 min).

### 7.4.5.3 Radiosynthesis of [<sup>18</sup>F]FTO/[<sup>18</sup>F]36



General procedure A was followed

Amounts: methyl 18-bromo-4-thiaoleate (4-5 mg), [<sup>18</sup>F] fluoride (900-1200 MBq), K<sub>2</sub>CO<sub>3</sub> (3.6 mg in 1 mL of water), Kryptofix 2.2.2 (10 mg in 1 mL ACN), KOH (250 μL, 0.2 M), NaH<sub>2</sub>PO<sub>4</sub> (250 μL, 0.5 M).

Radiochemical decay corrected yield (17.7 ± 1.7 %), purity > 96% and total synthesis time (120 min)

## 7.4.6 Stability in serum

General procedure B:

[<sup>18</sup>F]-Fluoro-4-thia fatty acids were incubated in human serum at 37°C for 3 h. This was followed by precipitation of the protein component using acetonitrile and centrifugation at 5000 rpm for 2 min. The supernatant layer was then sampled and analyzed by HPLC under the conditions described above.

#### 7.4.6.1 Study the stability of [<sup>18</sup>F]FTP/[<sup>18</sup>F]6 in serum

General procedure B was followed.

Amounts: [<sup>18</sup>F]-16-fluoro-4-thiapalmitic acid ([<sup>18</sup>F]FTP) (100 μL, 10 MBq), human serum (500 μL).

HPLC analysis of the serum sample revealed that the [<sup>18</sup>F]FTP remained stable (95%) during incubation at 37°C up to 3 hours.



#### 7.4.6.2 Study the stability of [<sup>18</sup>F]FTC2/[<sup>18</sup>F]**26** in serum

General procedure B was followed.

Amounts: [<sup>18</sup>F]-10-fluoro-4-thiacapric acid ([<sup>18</sup>F]FTC2) (100 μL, 10 MBq), human serum (500 μL).

HPLC analysis of the serum sample revealed that the [<sup>18</sup>F]FTC2 remained stable (98%) during incubation at 37°C up to 3 hours.

#### 7.4.6.2 Study the stability of [<sup>18</sup>F]FTO/[<sup>18</sup>F]**36** in serum

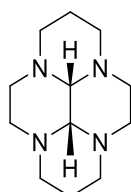
General procedure B was followed.

Amounts: [<sup>18</sup>F]-18-fluoro-4-thiaoleic acid ([<sup>18</sup>F]FTO) (100 μL, 10 MBq), human serum (500 μL).

HPLC analysis of the plasma sample revealed that the [<sup>18</sup>F]FTO remained stable (90%) during incubation at 37°C up to 3 hours.

## 7.4.7 Synthesis of copper-cross bridge cyclam complex which functionalise and not functionalise with a triphenylphosphonium

### 7.4.7.1 *Cis-3a, 5a, 8a, 10a*-tetraazaperhydropyrene (**37**)<sup>201</sup>

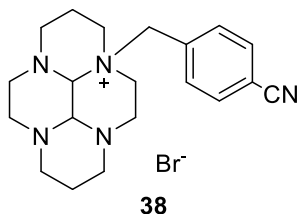


**37**

The synthetic procedure was completed following literature methods.<sup>201</sup> 1,4,8,11-tetraazacyclotetradodecane (4.06 g, 20.3 mmol) was dissolved in MeOH (400 mL) and cooled to  $-10^{\circ}\text{C}$ . A cold ( $0^{\circ}\text{C}$ ) aqueous solution of glyoxal (40% w/w, 2.94 g, 50.9 mmol) was added dropwise over 90 min. The clear solution was stirred at  $-10^{\circ}\text{C}$  for 30 min, then at RT for 3 hours. The solvent was removed *in vacuo* and the crude solid was re-dissolved in diethyl ether (100 mL). The filtrate was dried ( $\text{MgSO}_4$ ), filtered and solvent removed *in vacuo*.

To yield a white solid (5.22 g, 95%).  $^1\text{H}$  NMR (400 MHz,  $\text{CDCl}_3$ )  $\delta$  3.52 (t,  $J_{1,2} = 10.2$ , 2H, N- $\beta$ - $\text{CH}_2$ ), 3.07 (s, 2H,  $\text{H}_{\text{aminal}}$ ), 3.00 – 2.68 (m, 8H, 4(N- $\alpha$ - $\text{CH}_2$ )), 2.36 – 2.03 (m, 8H, 4(N- $\alpha$ - $\text{CH}_2$ )), 1.24 – 1.18 (m, 2H, N- $\beta$ - $\text{CH}_2$ ). MS (ESI) m/z: 223  $[\text{M}+\text{H}]^+$ .

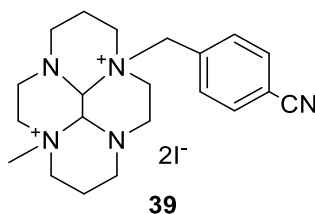
7.4.7.2 10a-[4-cyanobenzyl]-dodecahydro-6H-3a,5a,8a,10a-tetraaza-pyrenium bromide (**38**)<sup>196, 199</sup>



The synthetic procedure was completed following literature methods.<sup>196, 199</sup> *Cis*-3a,5a,8a,10a-tetraazaperhydropyrene **37** (3.50 g, 15.7 mmol) was dissolved in dry MeCN (150 mL), 4-(bromomethyl)benzonitrile (7.72 g, 39.4 mmol) was added and the solution was stirred under argon for 2 days. The resulting precipitate was filtered and washed with diethyl ether (2 x 25 mL).

To yield a white solid (5.95 g, 92%). <sup>1</sup>H NMR (400 MHz, CDCl<sub>3</sub>) δ 7.96 (d, *J* = 8.2, 2H, Ar H), 7.70 (d, *J* = 8.3, 2H, Ar H), 5.83 (d, *J* = 13.1, 1H, H<sub>aminal</sub>), 5.66 (d, *J* = 13.1, 1H, H<sub>aminal</sub>), 4.44 – 4.26 (m, 2H, Ar CH<sub>2</sub>), 4.13 – 3.94 (m, 2H, N-α-CH<sub>2</sub>), 3.84 (d, *J* = 12.2, 2H, CH<sub>2</sub>), 3.63 – 3.46 (m, 2H, N-α-CH<sub>2</sub>), 2.91 (m, 8H, 4(N-α-CH<sub>2</sub>)), 2.70 – 2.40 (m, 2H, N-α-CH<sub>2</sub>), 2.41 – 2.14 (m, 2H, N-α-CH<sub>2</sub>), 1.77 (d, *J* = 14.7, 2H, N-β-CH<sub>2</sub>), 1.37 (d, *J* = 13.7, 2H, N-β-CH<sub>2</sub>). <sup>13</sup>C NMR (100 MHz, CDCl<sub>3</sub>, δ): 18.18 (N-β-CH<sub>2</sub>), 19.34 (N-β-CH<sub>2</sub>), 43.10 (N-α-CH<sub>2</sub>), 46.55 (N-α-CH<sub>2</sub>), 48.62 (N-α-CH<sub>2</sub>), 51.34 (N-α-CH<sub>2</sub>), 52.27 (N-α-CH<sub>2</sub>), 55.56 (N-α-CH<sub>2</sub>), 58.94 (N-α-CH<sub>2</sub>), 60.03 (N-α-CH<sub>2</sub>), 61.54 (Ar-CH<sub>2</sub>), 70.19 (CH<sub>2</sub>), 82.56 (CH<sub>2</sub>), 113.79 (Ar-C), 117.19 (CN), 131.05 (Ar-C), 132.67 (Ar-C), 134.83 (Ar-C). MS (ESI) *m/z*: 338 [M-Br]<sup>+</sup>.

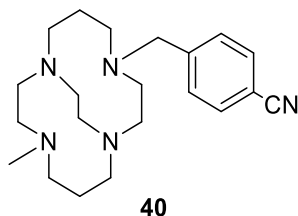
7.4.7.3 10a-[4-cyanobenzyl]-5a-[methyl]-decahydro-3a,5a,8a,10a-tetraaza-pyrenium diiodide (**39**)<sup>196, 199</sup>



The synthetic procedure was completed following literature methods.<sup>196, 199</sup> The 10a-[4-cyanobenzyl]-dodecahydro-6*H*-3a,5a,8a,10a-tetraaza-pyrenium bromide **38** (1.95 g, 5.76 mmol) was suspended in anhydrous MeCN (100 mL) under nitrogen. Iodomethane (25 mL, 415.0 mmol) was added dropwise. The white suspension was left to stir for 10 days. A second portion of iodomethane (13 mL, 208.0 mmol) was added after 5 days. Excess iodomethane was removed by flowing nitrogen through the suspension for 30 min. The solid was collected by filtration, washed with ether (2 x 50 mL) and dried.

To yield a white powder (3 g, 86%). <sup>1</sup>H NMR (400 MHz, D<sub>2</sub>O) δ 7.78 (d, *J* = 8.1, 2H, Ar-H), 7.58 (d, *J* = 8.2, 2H, Ar-H), 5.14 (d, *J* = 13.1, 1H, H<sub>aminal</sub>), 4.77 (m, 1H, H<sub>aminal</sub>), 4.34 (dd, *J* = 36.4, 4.2, 2H, Ar-CH<sub>2</sub>), 3.70 – 2.95 (m, 17H, 7(N-α-CH<sub>2</sub>), CH<sub>3</sub>), 2.70 (d, *J* = 3.0, 1H, CH), 2.55 (d, *J* = 2.7, 2H, N-α-CH<sub>2</sub>), 2.29 (d, *J* = 15.3, 2H, CH<sub>2</sub>), 2.15 – 1.98 (m, 2H, CH<sub>2</sub>), 1.75 (t, *J*<sub>1,2</sub> = 41.1, 2H, N-α-CH<sub>2</sub>). <sup>13</sup>C NMR (100 MHz, D<sub>2</sub>O, δ): 18.03 (N-β-CH<sub>2</sub>), 18.33 (N-β-CH<sub>2</sub>), 46.35 (CH<sub>3</sub>), 46.55 (N-α-CH<sub>2</sub>), 47.99 (N-α-CH<sub>2</sub>), 49.49 (N-α-CH<sub>2</sub>), 51.08 (N-α-CH<sub>2</sub>), 51.33 (N-α-CH<sub>2</sub>), 60.79 (N-α-CH<sub>2</sub>), 61.21 (N-α-CH<sub>2</sub>), 65.28 (N-α-CH<sub>2</sub>), 77.05 (Ar-CH<sub>2</sub>), 77.42 (CH<sub>2</sub>), 114.18 (Ar-C), 118.45 (CN), 130.06 (Ar-CH), 131.10 (Ar-CH), 132.18 (Ar-C). MS (ESI) *m/z*: 176 [M-2I]<sup>+</sup>, 480 [M+I]<sup>+</sup> and 607 [M+2I]<sup>+</sup>.

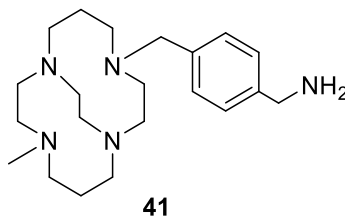
7.4.7.4 1-[4-Cyanobenzyl]-8-[methyl]-1,4,8,11-tetraazabicyclo[6.6.2] hexadecane (**40**)<sup>196, 199</sup>



The synthetic procedure was completed following literature methods.<sup>196, 199</sup> The 10a-[4-cyanobenzyl]-5a-[methyl]-decahydro-3a,5a,8a,10a-tetraaza-pyrenium diiodide **39** (3 g, 4.94 mmol) was dissolved in ethanol (300 mL) and sodium borohydride (6.5 g, 167.30 mmol) was added in small portions. The mixture was stirred for 14 days at RT. Water (100 mL) was added to decompose excess sodium borohydride and the solvent was removed *in vacuo*. The residue was taken up into water (100 mL) and made strongly basic (pH 14, KOH). The basic solution was extracted with DCM (4 x 100 mL), the combined organic extracts were dried (Na<sub>2</sub>SO<sub>4</sub>), filtered and solvent removed *in vacuo*.

To yield a yellow/cream oil (1.64 g, 94%). Anal. calcd for C<sub>21</sub>H<sub>33</sub>N<sub>5</sub>: C, 70.95; H, 9.36; N, 19.70. Found: C, 70.58; H, 9.58; N, 19.36. <sup>1</sup>H NMR (400 MHz, CDCl<sub>3</sub>) δ 7.62 – 7.56 (m, 2H, Ar-H), 7.45 (d, *J* = 8.1, 2H, Ar-H), 4.09 (m, 2H, N-α-CH<sub>2</sub>), 3.81 – 3.70 (m, 2H, Ar-CH<sub>2</sub>), 3.24 (d, *J* = 14.3, 2H, N-α-CH<sub>2</sub>), 3.11 – 3.00 (m, 2H, N-α-CH<sub>2</sub>), 2.85 – 2.62 (m, 3H, CH<sub>3</sub>), 2.48 – 2.21 (m, 16H, 8(N-α-CH<sub>2</sub>)), 1.53 – 1.37 (m, 4H, 2(N-β-CH<sub>2</sub>)). <sup>13</sup>C NMR (101 MHz, CDCl<sub>3</sub>, δ) 27.03 (N-β-CH<sub>2</sub>), 28.05 (N-β-CH<sub>2</sub>), 42.87 (CH<sub>3</sub>), 52.02 (N-α-CH<sub>2</sub>), 52.27 (N-α-CH<sub>2</sub>), 54.15 (N-α-CH<sub>2</sub>), 55.14 (N-α-CH<sub>2</sub>), 56.04 (N-α-CH<sub>2</sub>), 56.29 (N-α-CH<sub>2</sub>), 56.76 (N-α-CH<sub>2</sub>), 57.08 (N-α-CH<sub>2</sub>), 57.98 (N-α-CH<sub>2</sub>), 59.67 (N-α-CH<sub>2</sub>), 60.06 (N-α-CH<sub>2</sub>), 76.79 (Ar-C), 77.11 (N-α-CH<sub>2</sub>), 77.37 (N-α-CH<sub>2</sub>), 110.42 (N-α-CH<sub>2</sub>), 119.23 (CN), 126.39 (Ar-CH), 126.84 (Ar-CH), 129.19 (Ar-CH), 129.49 (Ar-CH), 132.0 (Ar-CH), 147.11 (Ar-C). MS (ESI) *m/z*: 355 [M]<sup>+</sup>.

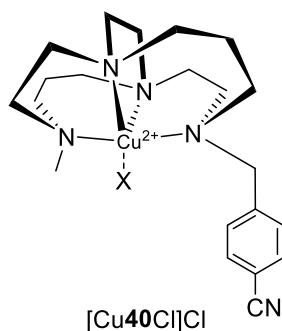
#### 7.4.7.5 1-[4-Aminomethylbenzyl]-8-[methyl]-1,4,8,11-tetraazabicyclo [6.6.2]hexadecane (**41**)<sup>196, 199</sup>



The synthetic procedure was completed following literature methods.<sup>196, 199</sup> LiAlH<sub>4</sub> (0.19 g, 5.0 mmol) was dissolved in anhydrous THF (20 mL). The 1-[4-cyanobenzyl]-8-[methyl]-1,4,8,11-tetraazabicyclo[6.6.2] hexadecane (**6**) (1.45 g, 4.1 mmol) in anhydrous THF (20 mL) was added dropwise under ice-cooling. After complete addition the mixture was stirred for 30 min and then heated to reflux for 3 hours. The reaction was cooled in an ice-bath, water (0.21 mL) was added dropwise followed by 15% sodium hydroxide (0.21 mL) solution followed by a second portion of water (0.62 mL). The resulting white precipitate was filtered and washed with THF (2 x 10 mL) then water (2 x 5 mL). The aqueous layer was made strongly basic (pH > 12, KOH) and extracted with THF (5 x 25 mL). The organic phases were dried (Na<sub>2</sub>SO<sub>4</sub>), filtered and solvents removed *in vacuo*.

To yield a yellow oil (1.13 g, 77%). <sup>1</sup>H NMR (400 MHz, CDCl<sub>3</sub>) δ 7.29 (s, 1H, Ar-H), 7.24 (s, 1H, Ar-H), 6.98 (s, 1H, Ar H), 3.87 – 3.72 (m, 4H, CH<sub>2</sub>NH<sub>2</sub> + Ar-CH<sub>2</sub>), 3.25 – 2.97 (m, 2H, N-α-CH<sub>2</sub>), 2.91 – 2.81 (m, 2H, N-α-CH<sub>2</sub>), 2.77 – 2.61 (m, 2H, N-α-CH<sub>2</sub>), 2.54 – 2.39 (m, 8H, 4(N-α-CH<sub>2</sub>)), 2.29 – 2.17 (m, 6H, 3(N-α-CH<sub>2</sub>)), 1.94 – 1.80 (m, 3H, CH<sub>3</sub>), 1.46 – 1.33 (m, 6H, 2(N-β-CH<sub>2</sub>)+ N-α-CH<sub>2</sub>), <sup>13</sup>C NMR (100 MHz, CDCl<sub>3</sub>, δ): 26.82 (N-β-CH<sub>2</sub>), 30.29 (N-β-CH<sub>2</sub>), 42.96 (CH<sub>3</sub>), 52.06 (N-α-CH<sub>2</sub>), 52.27 (N-α-CH<sub>2</sub>), 53.93 (N-α-CH<sub>2</sub>), 54.84 (N-α-CH<sub>2</sub>), 55.92 (N-α-CH<sub>2</sub>), 56.25 (N-α-CH<sub>2</sub>), 56.46 (N-α-CH<sub>2</sub>), 56.52 (N-α-CH<sub>2</sub>), 57.90 (N-α-CH<sub>2</sub>), 59.15 (N-α-CH<sub>2</sub>), 59.63 (Ar-CH<sub>2</sub>), 67.95 (CH<sub>2</sub>-NH<sub>2</sub>), 125.49 (Ar-C), 126.72 (Ar-CH), 127.65 (Ar-CH), 129.07 (Ar-C). HRMS (m/z): [M + H]<sup>+</sup> calcd for C<sub>21</sub>H<sub>38</sub>N<sub>5</sub>, 360.3124; found, 360.3122. MS (ESI) m/z: 359 [M]<sup>+</sup>.

7.4.7.6 1-[4-Cyanobenzyl]-8-[methyl]-1,4,8,11-tetraazabicyclo[6.6.2] hexadecane copper(II) chloride [Cu**40**Cl]Cl

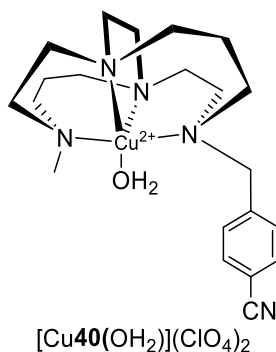


The macrocycle was dissolved in MeOH (10 mL), a methanolic (5 mL) solution of the metal salt was added dropwise. The mixture was left to stir at RT for 3 days under argon. Solvent was concentrated *in vacuo* to *ca.* 5 mL then purified either *via* size exclusion chromatography (Sephadex LH20) or filtration.

Amount: 1-[4-Cyanobenzyl]-8-[methyl]-1, 4, 8, 11-tetraazabicyclo[6.6.2] hexadecane **40** (0.1 g, 0.28 mmol), copper(II) chloride (0.045 g, 0.336 mmol), Sephadex LH20. To yield a blue solid (0.1 g, 71%). Anal. calcd for  $C_{21}H_{35}Cl_2CuN_5O \cdot 2CH_3OH$ : C, 48.67; H, 7.69; N, 12.67. Found: C, 48.29; H, 7.58; N, 12.24. ICP for  $C_{21}H_{35}Cl_2CuN_5O \cdot 2CH_3OH$ : 11.11. Found: 10.96. MS (ESI)  $m/z$ : 453  $[M^{2+}+Cl]^{+}$  and 463  $[M^{2+}+HCOO]^{+}$ . HRMS ( $m/z$ ):  $[M^{2+}+HCOO]^{+}$  calcd for  $C_{22}H_{34}CuN_5O_2^{+}$ , 463.1978; found, 463.1985.



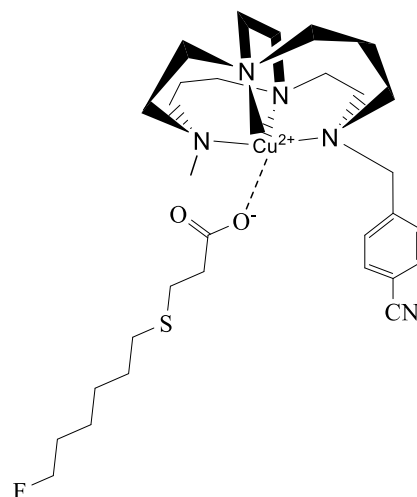
7.4.7.7 1-[4-Cyanobenzyl]-8-[methyl]-1,4,8,11-tetraazabicyclo[6.6.2] hexadecane copper(II) perchlorate [Cu**40**(OH<sub>2</sub>)](ClO<sub>4</sub>)<sub>2</sub>



The macrocycle was dissolved in MeOH (10 mL), a methanolic (5 mL) solution of the metal salt was added dropwise. The mixture was stirred and left at RT for 3 days under argon. Solvent was concentrated *in vacuo* to ca. 5 mL than purified either *via* size exclusion chromatography (Sephadex LH20) or filtration.

Amount: 1-[4-Cyanobenzyl]-8-[methyl]-1,4,8,11-tetraazabicyclo[6.6.2] hexadecane **40** (0.2 g, 0.56 mmol), copper(II) perchlorate hexahydrate (0.25 g, 0.676 mmol), filtration. To yield a blue solid (0.23 g, 66%). Anal. calcd for C<sub>21</sub>H<sub>35</sub>Cl<sub>2</sub>CuN<sub>5</sub>O<sub>9</sub>·0.5CH<sub>3</sub>OH·1.5H<sub>2</sub>O: C, 37.83; H, 5.68; N, 10.11. Found: C, 38.03; H, 05.94; N, 10.31. ICP for C<sub>21</sub>H<sub>35</sub>Cl<sub>2</sub>CuN<sub>5</sub>O<sub>9</sub>·0.5CH<sub>3</sub>OH·1.5H<sub>2</sub>O: 9.36. Found: 8.96. MS (ESI) *m/z*: 467 [M<sup>2+</sup>+HCOO<sup>-</sup>]<sup>+</sup> and 521 [M<sup>2+</sup>+ClO<sub>4</sub><sup>-</sup>]<sup>+</sup>. HRMS (*m/z*): [M<sup>2+</sup>+HCOO<sup>-</sup>]<sup>+</sup> calcd for C<sub>22</sub>H<sub>34</sub>CuN<sub>5</sub>O<sub>2</sub><sup>+</sup>, 463.1983; found, 463.1995.

7.4.7.8 Forming of F-thiacapric acid with copper complex of 1-[4-cyanobenzyl]-8-[methyl]-1,4,8,11-tetraazabicyclo[6.6.2] hexadecane [Cu40(26)]<sup>+</sup>



[Cu40(26)]<sup>+</sup>

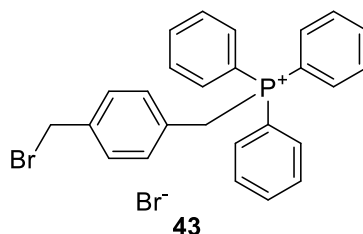
The metal macrocycle complex was dissolved in a solvent mixture (1 mL) was added to (750  $\mu$ L) solution (same solvent mixture) of the 10-fluoro-4-thiacapric acid **26**. The mixture was shaken for 1 hour at the selected temperature. Solvent was removed *in vacuo*.

Amount: 1-[4-Cyanobenzyl]-8-[methyl]-1,4,8,11-tetraazabicyclo[6.6.2] hexadecane copper(II) chloride [Cu40Cl]Cl (0.002 g, 0.0037 mmol), 1-[4-cyanobenzyl]-8-[methyl]-1,4,8,11-tetraazabicyclo[6.6.2] hexadecane copper(II) perchlorate [Cu40(OH<sub>2</sub>)](ClO<sub>4</sub>)<sub>2</sub> (0.002 g, 0.0028 mmol), 10-fluoro-4-thiacapric acid **26** (0.00058 g, 0.0028 mmol), solvent (see Table 18) MS/MS: 625 [M]<sup>+</sup>, 463 [copper complex]<sup>2+</sup> and 300 [FTC2]<sup>+</sup>. HRMS (*m/z*): [M]<sup>+</sup> calcd for C<sub>30</sub>H<sub>49</sub>CuFN<sub>5</sub>O<sub>2</sub>S, 625.2882; found, 625.2877.

Complex No.	Tem.	Solvent mixture		MS (ESI) m/z
		MeCN	H <sub>2</sub> O	
[Cu40(OH <sub>2</sub> )](ClO <sub>4</sub> ) <sub>2</sub>	RT	7	3	625 [M] <sup>+</sup> and 463 [M <sup>2+</sup> + HCOO] <sup>-</sup>
[Cu40(OH <sub>2</sub> )](ClO <sub>4</sub> ) <sub>2</sub>	RT	6	4	625 [M] <sup>+</sup> and 463 [M <sup>2+</sup> + HCOO] <sup>-</sup>
[Cu40(OH <sub>2</sub> )](ClO <sub>4</sub> ) <sub>2</sub>	RT	5	5	625 [M] <sup>+</sup> and 463 [M <sup>2+</sup> + HCOO] <sup>-</sup>
[Cu40(OH <sub>2</sub> )](ClO <sub>4</sub> ) <sub>2</sub>	RT	4	6	625 [M] <sup>+</sup> and 463 [M <sup>2+</sup> + HCOO] <sup>-</sup>
[Cu40(OH <sub>2</sub> )](ClO <sub>4</sub> ) <sub>2</sub>	RT	3	7	625 [M] <sup>+</sup> and 463 [M <sup>2+</sup> + HCOO] <sup>-</sup>
[Cu40(OH <sub>2</sub> )](ClO <sub>4</sub> ) <sub>2</sub>	RT	2	8	625 [M] <sup>+</sup> and 463 [M <sup>2+</sup> + HCOO] <sup>-</sup>
[Cu40(OH <sub>2</sub> )](ClO <sub>4</sub> ) <sub>2</sub>	RT	1	9	625 [M] <sup>+</sup> and 463 [M <sup>2+</sup> + HCOO] <sup>-</sup>
[Cu40(OH <sub>2</sub> )](ClO <sub>4</sub> ) <sub>2</sub>	50°C	7	3	625 [M] <sup>+</sup> and 463 [M <sup>2+</sup> + HCOO] <sup>-</sup>
[Cu40(OH <sub>2</sub> )](ClO <sub>4</sub> ) <sub>2</sub>	50°C	6	4	625 [M] <sup>+</sup> and 463 [M <sup>2+</sup> + HCOO] <sup>-</sup>
[Cu40(OH <sub>2</sub> )](ClO <sub>4</sub> ) <sub>2</sub>	50°C	5	5	625 [M] <sup>+</sup> and 463 [M <sup>2+</sup> + HCOO] <sup>-</sup>
[Cu40(OH <sub>2</sub> )](ClO <sub>4</sub> ) <sub>2</sub>	50°C	4	6	625 [M] <sup>+</sup> and 463 [M <sup>2+</sup> + HCOO] <sup>-</sup>
[Cu40(OH <sub>2</sub> )](ClO <sub>4</sub> ) <sub>2</sub>	50°C	3	7	625 [M] <sup>+</sup> and 463 [M <sup>2+</sup> + HCOO] <sup>-</sup>
[Cu40(OH <sub>2</sub> )](ClO <sub>4</sub> ) <sub>2</sub>	50°C	2	8	625 [M] <sup>+</sup> and 463 [M <sup>2+</sup> + HCOO] <sup>-</sup>
[Cu40Cl]Cl & [Cu40(OH <sub>2</sub> )](ClO <sub>4</sub> ) <sub>2</sub>	50°C	1	9	625 [M] <sup>+</sup> and 463 [M <sup>2+</sup> + HCOO] <sup>-</sup>
Complex No.	Temp eratur e	Solvent mixture		MS (ESI) m/z
		MeCN	PBS	
[Cu40(OH <sub>2</sub> )](ClO <sub>4</sub> ) <sub>2</sub>	RT	1	9	625 [M] <sup>+</sup> and 463 [M <sup>2+</sup> + HCOO] <sup>-</sup>
[Cu40(OH <sub>2</sub> )](ClO <sub>4</sub> ) <sub>2</sub>	50°C	1	9	625 [M] <sup>+</sup> and 463 [M <sup>2+</sup> + HCOO] <sup>-</sup>
Complex No.	Temp eratur e	Solvent mixture		MS (ESI) m/z
		3% BSA	H <sub>2</sub> O	
[Cu40(OH <sub>2</sub> )](ClO <sub>4</sub> ) <sub>2</sub>	RT	1	9	625 [M] <sup>+</sup> and 463 [M <sup>2+</sup> + HCOO] <sup>-</sup>
[Cu40(OH <sub>2</sub> )](ClO <sub>4</sub> ) <sub>2</sub>	50°C	1	9	625 [M] <sup>+</sup> and 463 [M <sup>2+</sup> + HCOO] <sup>-</sup>
Complex No.	Temp eratur e	Solvent		MS (ESI) m/z
		H <sub>2</sub> O		
[Cu40(OH <sub>2</sub> )](ClO <sub>4</sub> ) <sub>2</sub>	RT	1.5 mL		625 [M] <sup>+</sup> and 463 [M <sup>2+</sup> + HCOO] <sup>-</sup>
[Cu40(OH <sub>2</sub> )](ClO <sub>4</sub> ) <sub>2</sub>	50°C	1.5 mL		625 [M] <sup>+</sup> and 463 [M <sup>2+</sup> + HCOO] <sup>-</sup>
Complex No.	Temp eratur e	Solvent		MS (ESI) m/z
		MeCN		
[Cu40(OH <sub>2</sub> )](ClO <sub>4</sub> ) <sub>2</sub>	RT	1.5 mL		625 [M] <sup>+</sup> and 463 [M <sup>2+</sup> + HCOO] <sup>-</sup>
[Cu40(OH <sub>2</sub> )](ClO <sub>4</sub> ) <sub>2</sub>	50°C	1.5 mL		625 [M] <sup>+</sup> and 463 [M <sup>2+</sup> + HCOO] <sup>-</sup>
Complex No.	Temp eratur e	Solvent		MS (ESI) m/z
		DMF		
[Cu40(OH <sub>2</sub> )](ClO <sub>4</sub> ) <sub>2</sub>	RT	1.5 mL		625 [M] <sup>+</sup> and 463 [M <sup>2+</sup> + HCOO] <sup>-</sup>
[Cu40(OH <sub>2</sub> )](ClO <sub>4</sub> ) <sub>2</sub>	50°C	1.5 mL		625 [M] <sup>+</sup> and 463 [M <sup>2+</sup> + HCOO] <sup>-</sup>

Table 18: Conditions, which use to synthesis compound [Cu40(26)]<sup>+</sup>

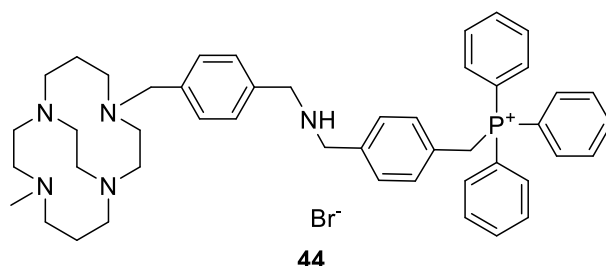
#### 7.4.7.9 (4-(Bromomethyl)benzyl)triphenylphosphonium bromide (**43**)<sup>205</sup>



The synthetic procedure was completed following literature methods.<sup>205</sup> Triphenylphosphine (2 g, 7.63 mmol) was dissolved in anhydrous toluene (25 mL) and added dropwise to the solution of  $\alpha, \alpha'$ -dibromomethyl-p-xylene (2.01 g, 7.63 mmol) in anhydrous toluene (25 mL). The mixture was heated under reflux for 18 hours. Then, the reaction cooled to RT, filtered and washed with (30 mL) toluene and (30 mL) diethylether. Following by chromatographic purification of the crude on silica gel eluted with dichloromethane: acetone 80: 20 mixture.

To yield a white powder (3.6 g, 90%). <sup>1</sup>H NMR (400 MHz, CDCl<sub>3</sub>)  $\delta$  7.82 – 7.71 (m, 9H, Ar-H), 7.67 – 7.58 (m, 6H, Ar-H), 7.15 – 7.07 (m, 4H, Ar-H), 4.38 (s, 2H, CH<sub>2</sub>-Br), 1.68 (s, 2H, CH<sub>2</sub>-P). <sup>31</sup>P NMR (162 MHz, CDCl<sub>3</sub>)  $\delta$  24.08. Anal. calcd for C<sub>26</sub>H<sub>23</sub>Br<sub>2</sub>P: C, 59.34; H, 4.41. Found: C, 58.97; H, 4.54. MS (ESI) m/z: 445 [M<sup>+</sup>-Br]<sup>+</sup>.

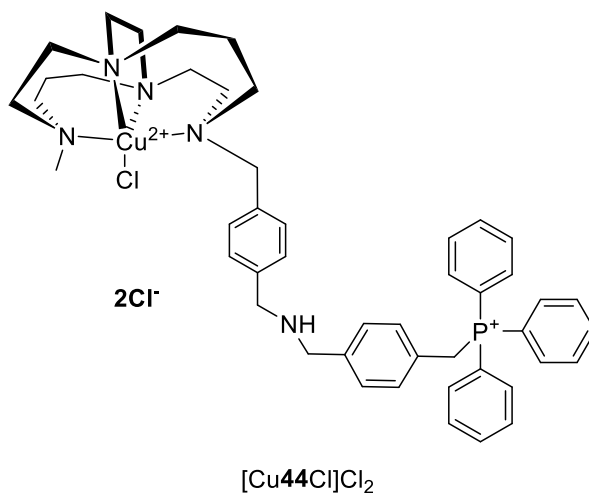
7.4.7.10 (4-(((4-((11-methyl-1,4,8,11-tetraazabicyclo[6.6.2]hexadecane-4-yl)methyl)benzyl)amino)methyl)benzyl)triphenylphosphonium bromide (**44**)



To a solution of 1-[4-aminomethylbenzyl]-8-[methyl]-1,4,8,11-tetraazabicyclo[6.6.2]hexadecane **41** (0.5 g, 1.39 mmol) in dry MeCN (20 mL) added (4-(bromomethyl)benzyl)triphenylphosphonium bromide **43** (0.43 g, 0.83 mmol) in dry MeCN (20 mL) and the solution was stirred under argon at RT for 24 hours. The solvents were removed *in vacuo*. The residue was taken up into water (50 mL) and made strongly basic (pH 14, KOH). The basic solution was extracted with benzene (3 x 50 mL), the combined organic extracts were dried (Na<sub>2</sub>SO<sub>4</sub>), filtered and solvent removed *in vacuo*. It is likely that the excess of aminobenzyl cross bridged cyclam starting material **41** is still present in the isolated compound.

To yield a yellow/cream oil (0.4 g, 60%). Anal. calcd for C<sub>47</sub>H<sub>59</sub>BrN<sub>5</sub>P<sup>+</sup>: C, 70.13; H, 7.39; N, 8.70. Found: C, 71.41; H, 7.65; N, 6.41 (due to presence of unreacted starting material). <sup>1</sup>H NMR (400 MHz, CDCl<sub>3</sub>) δ 7.85 – 7.52 (m, 19H, Ar- H), 7.09 (m, 4H, Ar-H), 5.43 – 5.18 (m, 2H, CH<sub>2</sub>-P), 3.40 (s, 2H, CH<sub>2</sub>-NH), 3.49 (s, 2H, CH<sub>2</sub>-NH), 2.84 (t, *J*<sub>1,2</sub> = 64.4, 8H, 4(N-α-CH<sub>2</sub>)), 2.47 – 2.21 (m, 2H, N-α-CH<sub>2</sub>), 2.14 – 1.98 (m, 9H, CH<sub>3</sub>, 3(N-α-CH<sub>2</sub>)), 1.84 (t, *J*<sub>1,2</sub> = 11.1, 6H, 3(N-α-CH<sub>2</sub>)), 1.41 (d, *J* = 2.8, 4H, N-β-CH<sub>2</sub> + N-α-CH<sub>2</sub>), 1.22 (d, *J* = 12.9, 2H, N-β-CH<sub>2</sub> + N-α-CH<sub>2</sub>). <sup>31</sup>P NMR (162 MHz, CDCl<sub>3</sub>) δ 23.71. MS (ESI) *m/z*: 363 [M<sup>+</sup>+H<sup>+</sup>]<sup>2+</sup>. HRMS (*m/z*): [M<sup>+</sup>+H<sub>2</sub>O] calcd for C<sub>47</sub>H<sub>61</sub>N<sub>5</sub>OP<sup>+</sup>, 742.4608; found, 742.4592.

7.4.7.11 (4-(((4-((11-methyl-1,4,8,11-tetraazabicyclo[6.6.2] hexadecane-4-yl)methyl)benzyl)amino)methyl)benzyl) triphenylphosphonium bromide copper(II) chloride [Cu**44**Cl]Cl<sub>2</sub>

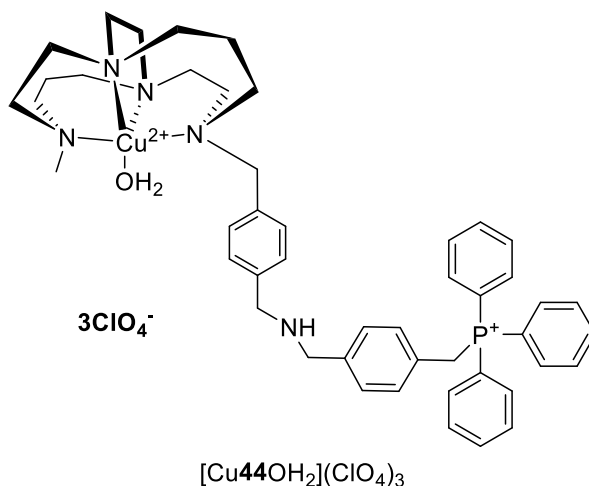


The crude macrocycle was dissolved in dry DMF (10 mL), a DMF (10 mL) solution of the metal salt was added dropwise. The reaction mixture refluxed overnight under argon. Solvent was removed *in vacuo* and added MeOH ca. 3 mL then purified *via* size exclusion chromatography (Sephadex LH20). The impurity of **41** in the starting material is likely to carry through to formation of a copper(II) complex impurity in the product.

Amounts: (4-(((4-((11-Methyl-1,4,8,11-tetraazabicyclo[6.6.2] hexadecane-4-yl)methyl)benzyl)amino)methyl)benzyl) triphenylphosphonium bromide **44** (0.04 g, 0.049 mmol), copper(II) chloride (0.008 g, 0.059 mmol).

To yield a blue solid (0.031 g, 67%). Anal. calcd for C<sub>47</sub>H<sub>59</sub>Cl<sub>3</sub>CuN<sub>5</sub>P: C, 63.06; H, 6.65; N, 7.83. Found: C, 56.31; H, 6.36; N, 6.23. ICP for C<sub>47</sub>H<sub>59</sub>Cl<sub>3</sub>CuN<sub>5</sub>P: 7.10. Found: 9.42. (due to presence of **41** allowing formation of another complex). MS (ESI) m/z: 452 [M<sup>3+</sup>+Cl<sup>-</sup>+H<sup>+</sup>+H<sub>2</sub>O]<sup>3+</sup>. HRMS (m/z): [M<sup>3+</sup>+ 2Cl<sup>-</sup>]<sup>+</sup> calcd for C<sub>47</sub>H<sub>59</sub>Cl<sub>2</sub>CuN<sub>5</sub>P<sup>+</sup>, 857.3143; found, 857.3176.

7.4.7.11 (4-(((4-((11-methyl-1,4,8,11-tetraazabicyclo[6.6.2] hexadecane-4-yl)methyl)benzyl)amino)methyl)benzyl) triphenylphosphonium bromide copper(II) perchlorate [Cu**44**(OH<sub>2</sub>)](ClO<sub>4</sub>)<sub>2</sub>

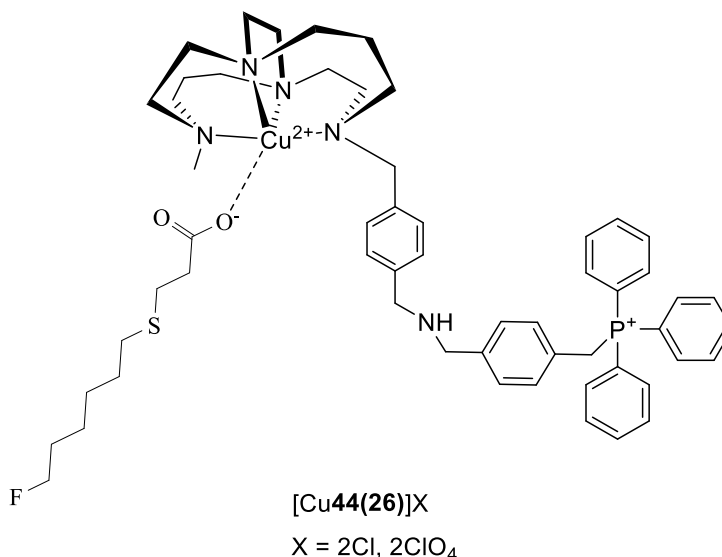


The macrocycle was dissolved in dry DMF (10 mL), a DMF (10 mL) solution of the metal salt was added dropwise. The reaction mixture refluxed overnight under argon. Solvent was removed *in vacuo* and added MeOH ~3 mL than purified *via* size exclusion chromatography (Sephadex LH20). The impurity of **41** in the starting material is likely to carry through to formation of a copper(II) complex impurity in the product.

Amounts: (4- (((4-((11-Methyl-1,4,8,11-tetraazabicyclo[6.6.2] hexadecane-4-yl)methyl)benzyl)amino)methyl)benzyl) triphenylphosphonium bromide **44** (0.1 g, 0.12 mmol), copper(II) perchlorate hexahydrate (0.05 g, 0.14 mmol).

To yield a blue solid (0.09 g, 69%). Anal. calcd for C<sub>47</sub>H<sub>61</sub>Cl<sub>3</sub>CuN<sub>5</sub>O<sub>13</sub>P: C, 51.09; H, 5.57; N, 6.34. Found: C, 49.43; H, 6.45; N, 8.48. ICP for C<sub>47</sub>H<sub>61</sub>Cl<sub>3</sub>CuN<sub>5</sub>O<sub>13</sub>P: 5.75. Found: 3.49. (due to presence of **41** allowing formation of this complex as impurity). MS (ESI) m/z: 452 [M<sup>3+</sup>+ClO<sub>4</sub><sup>-</sup>]<sup>2+</sup>. HRMS (m/z): [M<sup>3+</sup>+ 3ClO<sub>4</sub><sup>-</sup> + 3H<sub>2</sub>O + 2H<sup>+</sup>]<sup>2+</sup> calcd for C<sub>47</sub>H<sub>69</sub>Cl<sub>3</sub>CuN<sub>5</sub>O<sub>16</sub>P<sup>2+</sup>, 579.1415; found, 579.1414.

7.4.7.12 (4-(((4-((11-methyl-1,4,8,11-tetraazabicyclo[6.6.2] hexadecane-4-yl)methyl)benzyl)amino)methyl)benzyl) triphenylphosphonium bromide copper(II) chloride and perchlorate [Cu**44(26)**]**X**



The metal macrocycle complex (known to contain an impurity) was dissolved in mixture solvent (1 mL) was added to (750  $\mu$ L) solution (same mixture solvent) of the 10-fluoro-4-thiacapric acid **26**. The mixture was shaken and the reaction was performed multiple times at a series of different temperature for 1 hour. Solvent was removed *in vacuo*.

Compound [Cu**44(26)**]**Cl**<sub>2</sub>

Amounts: (4-(((4-((11-Methyl-1,4,8,11-tetraazabicyclo[6.6.2] hexadecane-4-yl)methyl)benzyl)amino)methyl)benzyl) triphenylphosphonium bromide copper(II) chloride [Cu**44Cl**]**Cl**<sub>2</sub> (0.001 g, 0.001 mmol) 10-fluoro-4-thiacapric acid **26** (0.0002 g, 0.001 mmol), solvent (see Table 19).



Complex	Temperature	Solvent mixture		MS (ESI) <i>m/z</i>	Yield
		3% BSA	H <sub>2</sub> O		
[Cu <b>44</b> Cl]Cl <sub>2</sub>	RT	1	9	533 [M <sup>2+</sup> +2Cl <sup>-</sup> +3H <sup>+</sup> ] <sup>3+</sup>	Blue solid (0.53 mg, 53%)

Table 19: Conditions, which use to synthesis compound [Cu**44**(**26**)]Cl<sub>2</sub>

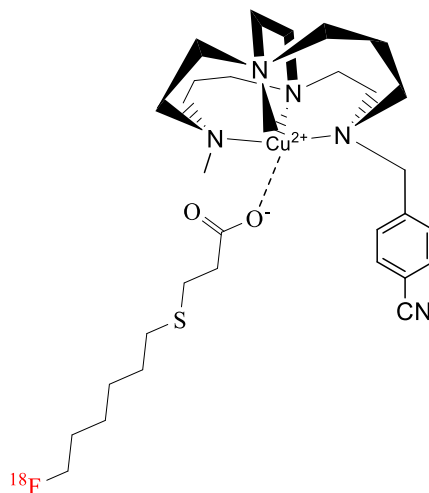
Compound [Cu**44**(**26**)](ClO<sub>4</sub>)<sub>2</sub>

Amounts: 4-(((4-((11-methyl-1,4,8,11-tetraazabicyclo[6.6.2] hexadecane-4-yl)methyl)benzyl)amino)methyl)benzyl) triphenylphosphonium bromide copper(II) perchlorate [Cu**44**(OH<sub>2</sub>)](ClO<sub>4</sub>)<sub>3</sub> (0.001 g, 0.0007 mmol), 10-fluoro-4-thiacapric acid **26** (0.0001 g, 0.0007 mmol), solvent (see Table 20). HRMS (*m/z*): [M<sup>3+</sup> + ClO<sub>4</sub><sup>-</sup> + HCOO<sup>-</sup> + 2H<sup>+</sup> + H<sub>2</sub>O]<sup>+</sup> calcd for C<sub>57</sub>H<sub>80</sub>ClCuFN<sub>5</sub>O<sub>9</sub>PS<sup>2+</sup>, 579.1606; found, 579.1607.

Complex	Temperature	Solvent mixture		MS (ESI) <i>m/z</i>	Yield
		3% BSA	H <sub>2</sub> O		
[Cu <b>44</b> (OH <sub>2</sub> )](ClO <sub>4</sub> ) <sub>3</sub>	RT	1	9	616 [M <sup>2+</sup> +2ClO <sub>4</sub> <sup>-</sup> +2H <sup>+</sup> +H <sub>2</sub> O] <sup>2+</sup>	Blue solid (0.6 mg, 75%)

Table 20: Conditions, which use to synthesis compound [Cu**44**(**26**)](ClO<sub>4</sub>)<sub>2</sub>

7.4.7.8 Copper complexes of (4-(((4-((11-methyl-1,4,8,11-tetraazabicyclo[6.6.2] hexadecane-4-yl)methyl)benzyl)amino)methyl)benzyl) triphenylphosphonium bromide  $[^{18}\text{F}][\text{Cu40(26)}]^+$



$[^{18}\text{F}][\text{Cu40(26)}]^+$

The metal macrocycle complex was dissolved in mixture solvent was added to the  $[^{18}\text{F}]$ -10-4-thiacapric acid  $[^{18}\text{F}]\mathbf{26}$ . The mixture was shaken and the reaction performed multiple times at different temperatures and for different reaction times (see Table 21). HPLC gradient-method-2— retention time = 9:26 min.

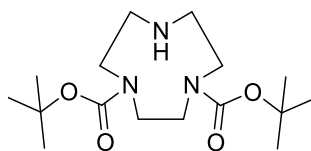
Reaction number	Complex number	Mass of complex used	Solvent used to dissolve complex	Solvent used for <sup>18</sup> F-FTC2	Total vol.	Time	Temp.	HPLC mobile phase	Yield (HPLC or TLC)
1	[Cu <sup>40</sup> (OH <sub>2</sub> )](ClO <sub>4</sub> ) <sub>2</sub>	1 mg	1000 μL (ACN: water 8:2)	1000 μL (ACN: water 8:2)	2000 μL	3 h	RT	TFA	HPLC: 1h: 04.8, 2h: 17.9%, 3h: 49.54%
2	[Cu <sup>40</sup> (OH <sub>2</sub> )](ClO <sub>4</sub> ) <sub>2</sub>	1 mg	1000 μL (ACN: water 8:2)	1000 μL (ACN: water 8:2)	2000 μL	3 h	RT	TFA	HPLC: 1h: 15.85%, 2h: 14.21%, 3h: 13.58%
3	[Cu <sup>40</sup> (OH <sub>2</sub> )](ClO <sub>4</sub> ) <sub>2</sub>	1 mg	100 μL (ACN: water 8:2)	1000 μL (ACN: water 8:2)	1100 μL	3 h	RT	TFA	HPLC: 1h: 09.1%, 2h: 13.4%, 3h: 04.3%
4	[Cu <sup>40</sup> (OH <sub>2</sub> )](ClO <sub>4</sub> ) <sub>2</sub>	1 mg	500 μL (ACN: water 8:2)	500 μL (ACN: water 8:2)	1000 μL	3 h	RT	TFA	TLC: 1h: 11.11%, 2h: 13%, 3h: 3%
5	[Cu <sup>40</sup> (OH <sub>2</sub> )](ClO <sub>4</sub> ) <sub>2</sub>	1 mg	100 μL (ACN: water 8:2)	100 μL (ACN: water 8:2)	200 μL	3 h	RT	TFA	HPLC: 1h: 12.1%, 2h: 3%, 3h: 10.59%
6	[Cu <sup>40</sup> (OH <sub>2</sub> )](ClO <sub>4</sub> ) <sub>2</sub>	1 mg	100 μL (ACN: water 8:2)	100 μL (ACN: water 8:2)	200 μL	3 h	50°C	TFA	HPLC: 1h: 5.30%, 3h: 05.50%
7	[Cu <sup>40</sup> (OH <sub>2</sub> )](ClO <sub>4</sub> ) <sub>2</sub>	1 mg	500 μL (ACN: water 8:2)	500 μL (ACN: water 8:2)	1000 μL	3 h	50°C	TFA	TLC: 1h: 6.59%, 2h: 13%, 3h: 3%
8	[Cu <sup>40</sup> (OH <sub>2</sub> )](ClO <sub>4</sub> ) <sub>2</sub>	1 mg	100 μL (ACN: water 3:7)	500 μL (ACN: water 3:7)	600 μL	3 h	RT	TFA	HPLC: 1h: 0%, 2h: 6.2%, 3h: 05.1%
9	[Cu <sup>40</sup> (OH <sub>2</sub> )](ClO <sub>4</sub> ) <sub>2</sub>	1 mg	100 μL (ACN: water 3:7)	500 μL (ACN: water 3:7)	600 μL	3 h	50°C	TFA	HPLC: 1 h: 0%, 2 h: 2.6%, 3 h: 05.04%
10	[Cu <sup>40</sup> (OH <sub>2</sub> )](ClO <sub>4</sub> ) <sub>2</sub>	1 mg	100 μL (ACN: water 7:3)	100 μL (ACN: water 7:3)	200 μL	3 h	RT	TFA	HPLC: 1 h: 11%, 2 h: 0%, 3 h: 0%
11	[Cu <sup>40</sup> (OH <sub>2</sub> )](ClO <sub>4</sub> ) <sub>2</sub>	1 mg	100 μL (ACN: water 9:1)	100 μL (ACN: water 9:1)	200 μL	3 h	RT	TFA	HPLC: 1 h: 8.8%, 2 h: 0%, 3 h: 0%
12	[Cu <sup>40</sup> (OH <sub>2</sub> )](ClO <sub>4</sub> ) <sub>2</sub>	1 mg	100 μL (EtOH: water 9:1)	100 μL (EtOH: water 9:1)	200 μL	3 h	RT	TFA	HPLC: 30 min: 31%, 1 h: 31.44%, 3 h: 34.34%
13	[Cu <sup>40</sup> Cl]Cl	1 mg	1000 μL (EtOH: water 8:2)	dry	1000 μL	3 h	50°C	TFA & HClO <sub>4</sub>	TFA: 3 h: 3.61% , HClO <sub>4</sub> : 3 h: 4.05%
14	[Cu <sup>40</sup> Cl]Cl	1 mg	1000 μL (EtOH: water 8:2)	dry	1000 μL	3 h	50°C	TFA & HClO <sub>4</sub>	TFA: 3 h: 5% , HClO <sub>4</sub> : 3 h: 8.77%
15	[Cu <sup>40</sup> Cl]Cl	1 mg	1000 μL EtOH	dry	1000 μL	3 h	RT	TFA	TLC: 30 min: 31%, 1 h: 31.44%, 3 h: 34.34%
16	[Cu <sup>40</sup> (OH <sub>2</sub> )](ClO <sub>4</sub> ) <sub>2</sub>	1 mg	1000 μL (PBS:water 100:900)	dry	1000 μL	1 h	50°C	TFA	HPLC: 30 min: 60.19%, 1 h: 62.81%

17	[Cu <sub>40</sub> (OH <sub>2</sub> )](ClO <sub>4</sub> ) <sub>2</sub>	1 mg	1000 μL (PBS:water 100:900)	dry	1000 μL	1 h	50°C	TFA	HPLC: 93%
18	[Cu <sub>40</sub> (OH <sub>2</sub> )](ClO <sub>4</sub> ) <sub>2</sub>	1 mg	1000 μL (PBS:water 100:900)	dry	1000 μL	1 h	50°C	TFA	HPLC: 24%
19	[Cu <sub>40</sub> (OH <sub>2</sub> )](ClO <sub>4</sub> ) <sub>2</sub>	1 mg	1000 μL (PBS:water 100:900)	dry	1000 μL	1 h	50°C	TFA	HPLC: 7%
20	[Cu <sub>40</sub> (OH <sub>2</sub> )](ClO <sub>4</sub> ) <sub>2</sub>	1 mg	1000 μL (PBS:water 100:900)	dry	1000 μL	1 h	50°C	TFA & HClO <sub>4</sub>	TFA: 2% HClO <sub>4</sub> : 3.48%
21	[Cu <sub>40</sub> Cl]Cl	1 mg	1000 μL (PBS: water 100:900)	dry	1000 μL	1 h	50°C	TFA & HClO <sub>4</sub>	TFA: 2% HClO <sub>4</sub> : 3.48%
22	[Cu <sub>40</sub> Cl]Cl	1 mg+ 1 equiv. Cs <sub>2</sub> CO <sub>3</sub>	1000 μL EtOH	dry	1000 μL	1 h	RT	TFA & HClO <sub>4</sub>	TFA: 0% HClO <sub>4</sub> : 0%
23	[Cu <sub>40</sub> Cl]Cl	1 mg+ 1 equiv. Cs <sub>2</sub> CO <sub>3</sub>	1000 μL (EtOH: water 8:2)	dry	1000 μL	1h	RT	TFA & HClO <sub>4</sub>	TFA: 3.61% HClO <sub>4</sub> : 4.05%
24	[Cu <sub>40</sub> (OH <sub>2</sub> )](ClO <sub>4</sub> ) <sub>2</sub>	1 mg	950 μL (PBS: water 100:900)	Dry + (FTC2OH 2mg, 10 μmol, 1000 μL (PBS: water 100:900)) 50 μL	1000 μL	1h	50°C	TFA & HClO <sub>4</sub>	TFA: 5.71% HClO <sub>4</sub> : 5.45%
25	[Cu <sub>40</sub> (OH <sub>2</sub> )](ClO <sub>4</sub> ) <sub>2</sub>	1 mg	900 μL (PBS: water 100:900)	Dry + (FTC2OH 2mg, 10 μmol, 1000 μL (PBS: water 100:900)) 100 μL	1000 μL	1h	50°C	TFA & HClO <sub>4</sub>	TFA: 2.73% HClO <sub>4</sub> : 2.74%
26	[Cu <sub>40</sub> (OH <sub>2</sub> )](ClO <sub>4</sub> ) <sub>2</sub>	1 mg	800 μL (PBS: water 100:900)	Dry + (FTC2OH 2mg, 10 μmol, 1000 μL (PBS: water 100:900)) 200 μL	1000 μL	1 h	50°C	TFA & HClO <sub>4</sub>	TFA: 3.50% HClO <sub>4</sub> : 2.91%
27	[Cu <sub>40</sub> (OH <sub>2</sub> )](ClO <sub>4</sub> ) <sub>2</sub>	1 mg	700 μL (PBS: water 100:900)	Dry + (FTC2OH 2mg, 10 μmol, 1000 μL (PBS: water 100:900)) 300 μL	1000 μL	1 h	50°C	TFA & HClO <sub>4</sub>	TFA: 2.18% HClO <sub>4</sub> : 1.94%

Table 21: Reaction conditions used in the synthesis of [<sup>18</sup>F][Cu<sub>40</sub>(26)]<sup>+</sup>

## 7.4.8 Synthesis of a novel TACN-thia fatty acids (palmitic and oleic acids) and $^{99m}\text{Tc}$ radiolabeled

### 7.4.8.1 Di-*tert*-butyl 1,4,7-triazonane-1,4-dicarboxylate (**47**)<sup>225</sup>

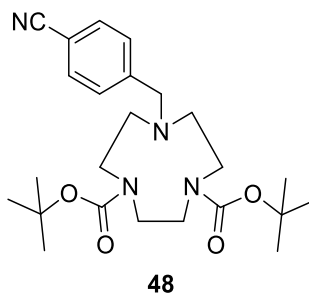


**47**

The synthetic procedure was completed following literature methods.<sup>225</sup> To a solution of TACN (1 g, 7.7 mmol) in  $\text{CHCl}_3$  (25 mL) was added in portions BOC-ON (3.77 g, 15.3 mmol). The resulting mixture was stirred for 72 h and the solvent evaporated under vacuum. The residue was partitioned between 10% NaOH solution (10 mL) and diethyl ether (30 mL). The ether layer was separated and washed with 10% NaOH solution (10 mL) and water (10 mL) several times. The ether layer was dried ( $\text{MgSO}_4$ ), filtered, and concentrated under vacuum.

To yield a colourless oil (2.4 g, 92%).  $^1\text{H}$  NMR (400 MHz,  $\text{CDCl}_3$ )  $\delta$  3.51 – 2.91 (m, 12H, 6( $\text{N}-\alpha\text{-CH}_2$ )), 1.48 (s, 18H, 6( $\text{CH}_3$ )), 1.20 (t,  $J_{1,2} = 7.0$ , 1H, NH).  $^{13}\text{C}$  NMR (100 MHz,  $\text{CDCl}_3$ )  $\delta$  155.90 2(CO), 79.98 2( $\text{C}(\text{CH}_3)_3$ ), 51.29 (2 $\text{N}-\alpha\text{-CH}_2$ ), 50.51 (2 $\text{N}-\alpha\text{-CH}_2$ ), 49.83 ( $\text{N}-\alpha\text{-CH}_2$ ), 49.62 ( $\text{N}-\alpha\text{-CH}_2$ ), 28.62 6( $\text{CH}_3$ ). MS (ESI)  $m/z$ : 330 [ $\text{M}+\text{H}^+$ ]<sup>+</sup>.

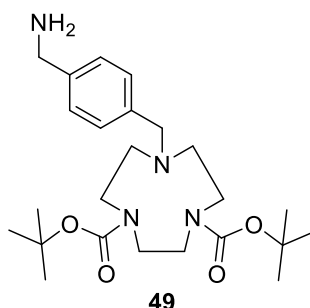
#### 7.4.8.2 Di-*tert*-butyl 7-(4-(cyanomethyl)benzyl)-1,4,7, triazonane-1,4-dicarboxylate (**48**)



Compound **47** (2.35g, 7.13mmol) was added to a flask containing 4-(bromomethyl) benzonitrile (1.4g, 7.13mmol) and acetonitrile (160 mL) and potassium carbonate (1.97 g, 14.26 mmol) and is stirred and heated at 60 °C for 48 hours. The resulting solution is filtered and dried under vacuum before being purified *via* column chromatography on silica gel eluted with mixture of n-hexane: ethyl acetate 93: 17.

To yield a white crystal (2.42 g, 76%). <sup>1</sup>H NMR (400 MHz, CDCl<sub>3</sub>) δ 7.64 – 7.46 (m, 4H, Ar-H), 3.70 (t, *J*<sub>1,2</sub> = 11.8, 2H, Ar-CH<sub>2</sub>), 3.53 – 3.23 (m, 8H, 4(N-α-CH<sub>2</sub>)), 2.63 (m, 4H, 2(N-α-CH<sub>2</sub>)), 1.56 – 1.42 (s, 18H, 6(CH<sub>3</sub>)). MS (ESI) *m/z*: 445 [M+H]<sup>+</sup>.

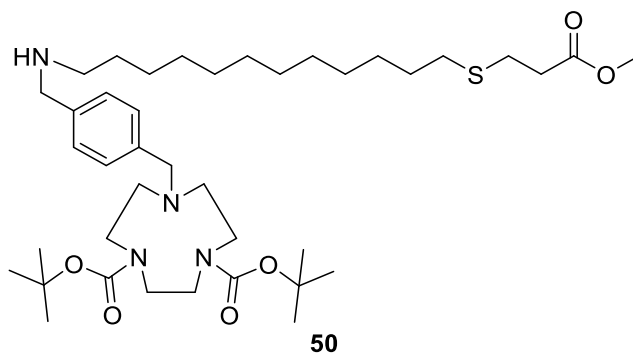
7.4.8.3 Di-*tert*-butyl 7-(4-(aminomethyl)benzyl)-1,4,7, triazonane-1, 4-dicarboxylate (**49**)



Compound **48** (2.42 g, 5.44 mmol) was dissolved in a mixture of dioxane (175 mL) and water (45 mL). Raney-nickel (0.93 g, 0.3 mL, 10.88 mmol) as a 50% suspension in water and 10% palladium on charcoal (0.33 g, 0.30 mmol) were added together with lithium hydroxide monohydrate (0.59 g, 14.14 mmol) and the reaction mixture was stirred under hydrogen atmosphere at 50°C for 24 hours. The catalyst was then filtered off, the solvents were removed in vacuum, and a mixture of water (100 mL) and CH<sub>2</sub>Cl<sub>2</sub> (30 mL) was added. After phase separation, the aqueous phase was extracted three times using CH<sub>2</sub>Cl<sub>2</sub> (3x10 mL). The combined organic layers were dried over sodium sulfate and the solvent was removed under vacuo before being purified using column chromatography on silica gel eluted with mixture of DCM: MeOH 75: 25.

To yield a white crystal (1.98 g, 81%). <sup>1</sup>H NMR (400 MHz, CDCl<sub>3</sub>) δ 7.32 (d, *J* = 8.0, 2H, Ar-H), 7.24 – 7.18 (m, 2H, Ar-H), 3.85 (t, *J*<sub>1,2</sub> = 3.9, 2H, Ar-CH<sub>2</sub>), 3.64 (t, *J*<sub>1,2</sub> = 8.3, 2H, CH<sub>2</sub>-NH<sub>2</sub>), 3.47 (t, *J*<sub>1,2</sub> = 19.8, 4H, 2(N-α-CH<sub>2</sub>)), 3.33 – 3.14 (m, 4H, 2(N-α-CH<sub>2</sub>)), 2.73 – 2.57 (m, 4H, 2(N-α-CH<sub>2</sub>)), 1.47 (s, 18H, 6(CH<sub>3</sub>)). MS (ESI) *m/z*: 449 [M+H]<sup>+</sup>.

7.4.8.4 Di-*tert*-butyl 7-(4-(((12-((3-methoxy-3-oxopropyl)thio)dodecyl)amino)methyl)benzyl)-1, 4, 7-triazonane-1, 4-dicarboxylate (bisprotection TACN-thiapalmitate) (**50**)

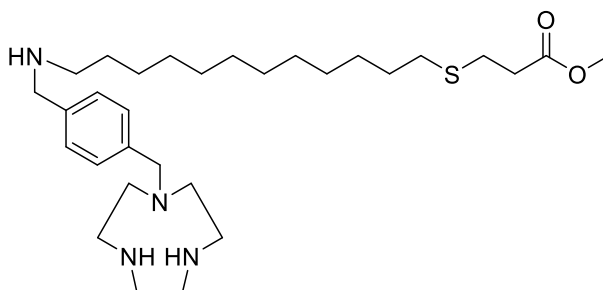


To a solution of compound **50** (0.1g, 0.22mmol) in 10mL dry DMF, add methyl 16-iodo-4-thiapalmitate **22** (0.091g, 0.22mmol) which is dissolved in 5mL dry DMF, dropwise under argon. Then, add 1 equivalents of base (triethylamine, 30 $\mu$ L), the mixture leave at 50°C for five days. Solvent was removed *in vacuo*, replaced by 10mL of dichloromethane and washed with with water (3x10mL). The organic layer was dried over sodium sulfate and solvent removed under *in vacuo*.

To yield a yellow oil (0.12 g, 75%).  $^1\text{H}$  NMR (400 MHz,  $\text{CDCl}_3$ )  $\delta$  8.01 (s, 1H, NH), 7.36 (m, 4H, Ar-H), 3.70 (s, 3H, COO- $\text{CH}_3$ ), 3.65 (d,  $J = 6.7$ , 4H,  $\text{CH}_2\text{-NH}_2$ , Ar- $\text{CH}_2$ ), 3.48 (m, 8H,  $\text{CH}_2\text{-S}$ ,  $\text{CH}_2\text{-CH}_2\text{-S}$ ), 3.33 – 3.10 (m, 8H, 4(N- $\alpha\text{-CH}_2$ )), 2.78 (t,  $J_{1,2} = 7.5$ , 2H, N- $\alpha\text{-CH}_2$ ), 2.71 – 2.59 (m, 10H, N- $\alpha\text{-CH}_2$ , 4( $\text{CH}_2$ )), 2.55 – 2.47 (m, 2H,  $\text{CH}_2$ ), 1.77 – 1.53 (m, 10H, 5( $\text{CH}_2$ )), 1.44 (s, 18H, 6( $\text{CH}_3$ )). MS (ESI)  $m/z$ : 736 [ $\text{M}+\text{H}^+$ ] $^+$ .



7.4.8.5 Methyl 3-((12-((4-((1, 4, 7-triazonan-1-yl)methyl)amino)dodecyl)thio)propanoate (TACN-thiapalmitate) (**51**)



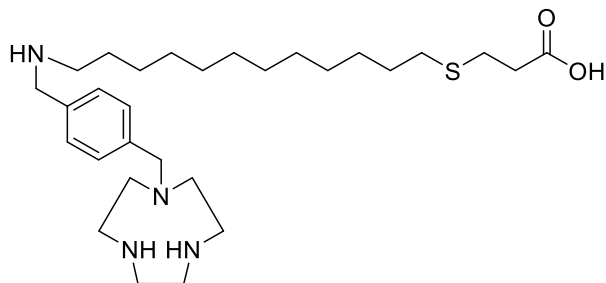
**51**

Bis-protection TACN-thia-fatty acid dissolved in methanol and added to 3 N HCl. Then, left at RT for 24 hours. Solvent was removed *in vacuo*.

Amounts: compound **50** (0.166 g, 0.22 mmol), MeOH (5 mL), 3 N HCl (10 mL).

To yield a yellow crystal (0.075 g, 88%).  $^1\text{H}$  NMR (400 MHz,  $\text{CD}_3\text{OH}$ )  $\delta$  7.53 (m, 4H, Ar-H), 4.26 – 3.87 (m, 4H,  $\text{CH}_2\text{-NH}_2$ , Ar- $\text{H}_2$ ), 3.67 (m, 5H,  $\text{COO-CH}_3$ ,  $\text{CH}_2\text{-S}$ ), 3.25 – 3.15 (m, 4H,  $\text{CH}_2\text{-CH}_2\text{-S}$ ), 3.09 – 2.49 (m, 12H, 6(N- $\alpha\text{-CH}_2$ )), 1.82 – 1.22 (m, 24H, 11( $\text{CH}_2$ ), 2(NH)). MS (ESI) m/z: 535  $[\text{M}+\text{H}^+]^+$ .

7.4.8.6 3-((12-((4-((1,4,7-Triazonan-1-yl)methyl)benzyl)amino)-dodecyl)thio)propanoic acid (TACN-thiapalmitic acid) (**52**)



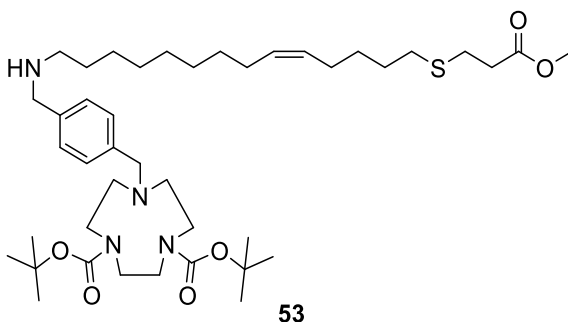
**52**

To ester compound was added LiOH  $\times$  H<sub>2</sub>O dissolved in 60% EtOH and reaction mixture was stirred at room temperature for 5 h. Adjust pH to 7-8 then remove ethanol *in vacuo* making sure water is retained. Purify using C18 cartridge and remove solvent *in vacuo*.

Amounts: compound **51** (0.075 g, 0.14 mmol), LiOH  $\times$  H<sub>2</sub>O (0.02 g, 0.50 mmol), 60% EtOH (30 mL), 1 N HCl (50 mL).

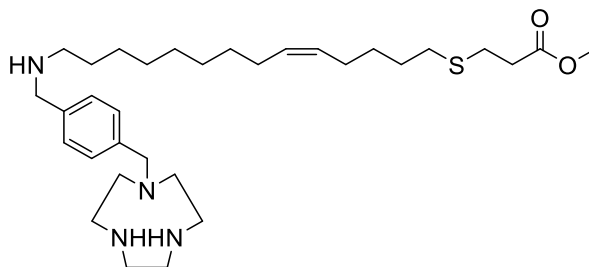
To yield a yellow oil (0.07 g, 95%). Anal. calcd for C<sub>29</sub>H<sub>52</sub>N<sub>4</sub>O<sub>2</sub>S.1.75HCl.2.75EtOH: C, 58.66; H, 9.54; N, 7.24; S, 5.19. Found: C, 58.26; H, 09.96; N, 07.88; S, 04.51. <sup>1</sup>H NMR (400 MHz, CD<sub>3</sub>OD)  $\delta$  7.46 (m, 4H, Ar-H), 4.15 (s, 2H, CH<sub>2</sub>-NH<sub>2</sub>), 3.83 (s, 2H, Ar-CH<sub>2</sub>), 3.65 (m, 2H, CH<sub>2</sub>-S), 3.16 (m, CH<sub>2</sub>-CH<sub>2</sub>-S), 2.98 (d, *J* = 7.5, 6H, 3(N- $\alpha$ -CH<sub>2</sub>)), 2.88 – 2.82 (m, 4H, 2(N- $\alpha$ -CH<sub>2</sub>)), 2.73 (t, *J*<sub>1,2</sub> = 6.5, 8H, 2(N- $\alpha$ -CH<sub>2</sub>)), 1.55 (d, *J* = 4.6, 2H, 2NH), 1.30 (m, 24H, 2(NH), 11(CH<sub>2</sub>)). MS (ESI) *m/z*: 521 [M+H]<sup>+</sup>. HRMS (*m/z*): [M-H]<sup>-</sup> calcd for C<sub>29</sub>H<sub>51</sub>N<sub>4</sub>O<sub>2</sub>S, 519.3733; found, 519.3738.

7.4.8.7 Di-*tert*-butyl (Z)-7-(4-(((14-((3-methoxy-3-oxopropyl)thio)-tetradec-9-en-1-yl)amino)methyl)benzyl)-1, 4, 7-triazonane-1, 4-dicarboxylate (bisprotection TACN-thia-oleate) (**53**)



To a solution of compound **49** (0.1 g, 0.22 mmol) in 10 mL dry DMF, add methyl 18-iodo-4-thiaoleate **34** (0.098 g, 0.22 mmol) which is dissolved in 10 mL dry DMF, dropwise under argon. Then, add 1 equivalents of base (triethylamine, 30  $\mu$ L), the mixture leave at 50°C for six days. Solvent was removed *in vacuo*, replaced by 10 mL of dichloromethane and washed with with water (3 x 10 mL). The organic layer was dried over sodium sulfate and solvent removed under *in vacuo*. To yield a yellow oil (0.16 g, 97%). MS (ESI) m/z: 761 [M+H]<sup>+</sup>.

7.4.8.8 Methyl (Z) 3-((14-((4-((1,4,7-triazonan-1-yl)benzyl)amino)-tetradec-5-en-1-yl)thio)propanoate (TACN-thiaoleate) (**54**)

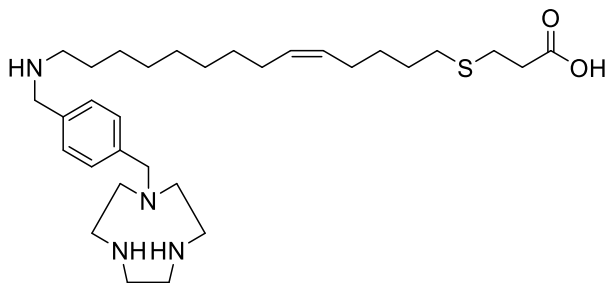


**54**

Bis-protection TACN-thia-fatty acid dissolved in methanol and added to 3N HCl. Then, left at RT for 24 hours. Solvent was removed *in vacuo*.

Amounts: compound **53** (0.166 g, 0.22 mmol), MeOH (5 mL), 3 N HCl (10 mL). To yield a yellow oil (0.31 g). MS (ESI) m/z: 561 [M+H]<sup>+</sup>.

7.4.8.9 (Z)-3-((14-((4-((1,4,7-triazonan-1-yl)methyl)benzyl)amino)-tetradec-5-en-1-yl)thio)propanoic acid (TACN-thiaoleic acid) (**55**)



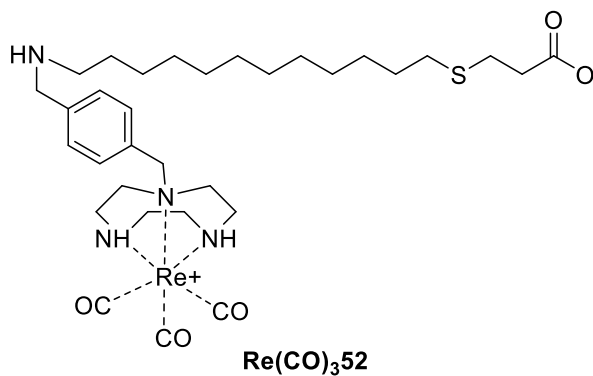
**55**

To ester compound was added LiOH  $\times$  H<sub>2</sub>O dissolved in 60% EtOH and reaction mixture was stirred at room temperature for 5 h. Adjust pH to 7-8 then remove ethanol *in vacuo* making sure water is retained. Purify using C18 cartridge and remove solvent *in vacuo*.

Amounts: compound **54** (0.31g, 0.55 mmol), LiOH  $\times$  H<sub>2</sub>O (0.093g, 0.0022 mmol), 60% EtOH (10 mL), 1 N HCl (50 mL).

To yield a yellow oil (0.07 g, 23%). Anal. calcd for C<sub>31</sub>H<sub>54</sub>N<sub>4</sub>O<sub>2</sub>S + 1.9HCl+1.75EtOH: C, 59.47; H, 9.61; N, 8.04; S, 4.60. Found: C, 59.70; H, 8.82; N, 7.61; S, 03.40. <sup>1</sup>H NMR (400 MHz, CD<sub>3</sub>OD)  $\delta$  7.65 – 7.36 (m, 4H, Ar H), 5.41 – 5.32 (m, 2H, HC=CH), 4.14 (s, 2H, CH<sub>2</sub>-NH<sub>2</sub>), 3.59 – 3.43 (m, 2H, Ar-CH<sub>2</sub>), 3.19 – 3.11 (m, 2H, CH<sub>2</sub>-S), 3.03 – 2.86 (m, 6H, CH<sub>2</sub>-S, CH<sub>2</sub>-CH<sub>2</sub>-S), 2.74 – 2.66 (m, 4H, 2(N- $\alpha$ -CH<sub>2</sub>)), 2.48 (m, 8H, 4(N- $\alpha$ -CH<sub>2</sub>)), 2.06 – 1.99 (m, 4H, H<sub>2</sub>CHC=CHCH<sub>2</sub>), 1.33 – 1.22 (m, 20H, 9(CH<sub>2</sub>), 2(NH)). MS (ESI) m/z: 547 [M+H]<sup>+</sup>.

7.4.8.10 Rhenium(I) complex of 3-((12-((4-((1, 4, 7-triazonan-1-yl)methyl)benzyl)amino)dodecyl)thio)propanoic acid (TACN-thiapalmitic acid)  $\text{Re}(\text{CO})_3$ **52**

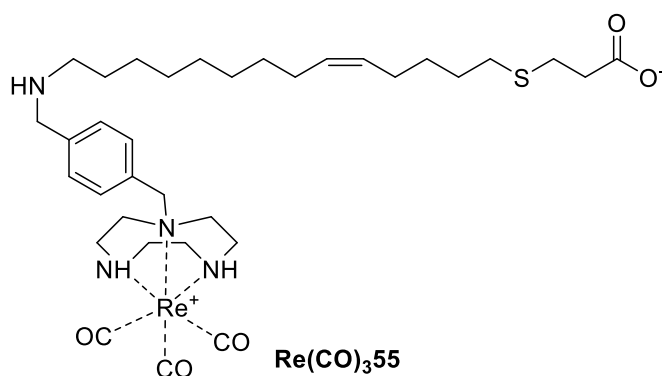


TACN-thiapalmitic acid **52** or TACN-thia-oleic acid **55** was dissolved in DMF and added to  $[\text{Re}(\text{CO})_3\text{Br}_3][\text{Et}_4\text{N}]_2$  (synthesised by Rebecca L Hargreaves) in dry DMF. The mixture solution is heated to 50°C for 18 hours. Solvent removed *in vacuo* and washed with water.

Amounts: TACN-thiapalmitic acid **52** (0.002 g, 0.0038 mmol), (1 mL) DMF,  $[\text{Re}(\text{CO})_3\text{Br}_3][\text{Et}_4\text{N}]_2$  (0.0019 g, 0.0038 mmol), (0.5 mL) DMF, (15 mL) water.

To yield a yellow oil (2 mg, 25%). MS (ESI)  $m/z$ : 353  $[\text{M}^+ + \text{H}^+ - 3\text{CO}]^{2+}$ . HPLC: Method 6 – retention time = 17:17 min.

7.4.8.11 Rhenium(I) complex of (Z)3-((14-((4-((1,4,7-triazonan-1-yl)methyl)benzyl)amino)tetradec-5-en-1-yl)thio)propanoic acid (TACN-thiaoleic acid)  $\text{Re}(\text{CO})_3$ **55**

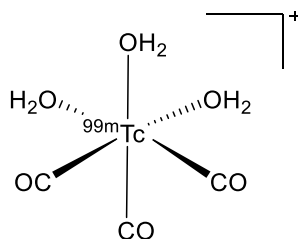


TACN-thiapalmitic acid **52** or TACN-thia-oleic acid **55** was dissolved in DMF and added to  $[\text{Re}(\text{CO})_3\text{Br}_3][\text{Et}_4\text{N}]_2$  (synthesised by Rebecca L Hargreaves) in dry DMF. The mixture solution is heated to  $50^\circ\text{C}$  for 18 hours. Solvent removed *in vacuo* and washed with water.

Amounts: TACN-thia-oleic acid **55** (0.010 g, 0.010 mmol), DMF (3 mL),  $[\text{Re}(\text{CO})_3\text{Br}_3][\text{Et}_4\text{N}]_2$  (0.009 g, 0.010 mmol), DMF (2 mL), water (30 mL).

To yield a yellow oil (4.7 mg, 31%). MS (ESI)  $m/z$ : 431  $[\text{M}+2\text{Na}^+]^{2+}$ . HPLC: Method 6 – retention time = 19:27 min.

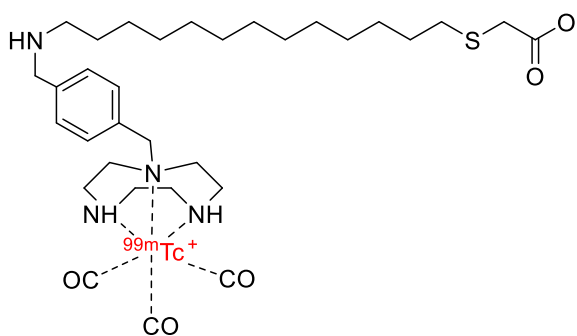
#### 7.4.8.12 Synthesis of organometallic precursor [<sup>99m</sup>Tc(OH<sub>2</sub>)<sub>3</sub>(CO)<sub>3</sub>]<sup>+</sup> (**56**)<sup>58</sup>



[<sup>99m</sup>Tc(OH<sub>2</sub>)<sub>3</sub>(CO)<sub>3</sub>]<sup>+</sup> **56** was synthesised following literature.<sup>58</sup> (2.9 mg, 7.6 μmol) Sodium tetraborate decahydrate, (7.8 mg, 73.6 μmol) sodium carbonate, (9.0 mg, 31.9 μmol) potassium sodium tetrataurate tetrahydrate and (4.5 mg, 43.3 μmol) disodium boranocarbonate were added to HPLC vial and purged with argon for 5 min. TcO<sub>4</sub><sup>-</sup> (740- 3000 MBq recommended but less dose work) was added directly from the generator to the vial under argon. The degassed mixture was heated at 90°C for 20 minutes. The vial containing the product is placed into a lead pot and transferred to the HPLC. A 20 μL portion containing typically ~20 MBq of the reaction mixture is injected into the HPLC for analysis. HPLC: Method 6 – retention time = 5:5 min.



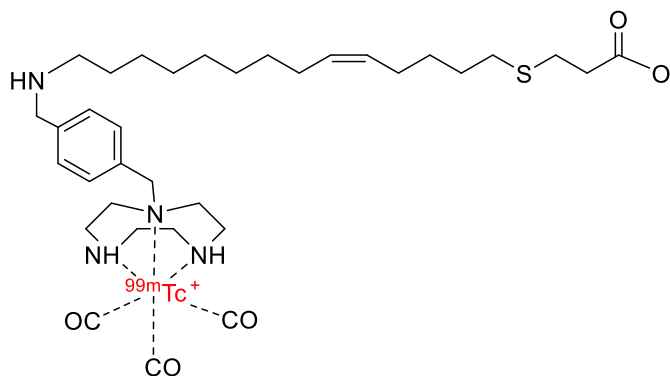
7.4.8.13  $^{99m}\text{Tc}$  radiolabeling of 3-((12-((4-((1, 4, 7-triazonan-1-yl)methyl)benzyl)amino)dodecyl)thio)propanoic acid (TACN-thiopalmitic acid)  $^{99m}\text{Tc}(\text{CO})_3\mathbf{52}$



$^{99m}\text{Tc}(\text{CO})_3\mathbf{52}$

The corresponding ligand TACN-thiopalmitic acid **52** (3.22 mmol) was dissolved in a 1 mL glass vial with 150  $\mu\text{L}$  of sodium acetate pH 11. The reaction vial was then tightly closed, and flushed with argon for 10 min. Freshly prepared  $[\text{}^{99m}\text{Tc}(\text{CO})_3(\text{H}_2\text{O})_3]^+$  (50  $\mu\text{L}$ ) was added to the reaction and the mixture heated at 90°C while being shaken at 500 RPM for 30 min. The reaction solution was cooled before being checked by radio-HPLC. HPLC: Method 6 – retention time  $R_t = 17:36$  min.

7.4.8.14  $^{99m}\text{Tc}$  radiolabeling of (Z)-3-((14-((4-((1,4,7-triazonan-1-yl)methyl)benzyl)amino)tetradec-5-en-1-yl)thio)propanoic acid (TACN-thia-oleic acid)  $^{99m}\text{Tc}(\text{CO})_3\mathbf{55}$



$^{99m}\text{Tc}(\text{CO})_3\mathbf{55}$

The corresponding ligand TACN-thiaoleic acid **55** (4.58 mmol) was dissolved in a 1 mL glass vial with 150  $\mu\text{L}$  of sodium acetate pH 11. The reaction vial was then tightly closed, and flushed with argon for 10 min. Freshly prepared  $[\text{}^{99m}\text{Tc}(\text{CO})_3(\text{H}_2\text{O})_3]^+$  (50  $\mu\text{L}$ ) was added to the reaction and the mixture heated at  $90^\circ\text{C}$  while being shaken at 500 RPM for 30 min. The reaction solution was cooled before being checked by radio-HPLC. HPLC: Method 6 – retention time  $R_t = 19:27$  min.

## References

1. <http://www.who.int/mediacentre/factsheets/fs317/en/>, (Accessed on 29-08-2017).
2. S. Vallabhajosula, *Molecular Imaging: Radiopharmaceuticals for PET and SPECT*, Springer Science & Business Media, Berlin, 2009.
3. R. C. Hendel, M. R. Patel, C. M. Kramer, M. Poon, J. C. Carr, N. A. Gerstad, L. D. Gillam, J. M. Hodgson, R. J. Kim and J. R. Lesser, *J. Am. Coll. Cardiol.*, 2006, **48**, 1475-1497.
4. M. K. Pandey, A. P. Belanger, S. Wang and T. R. DeGrado, *J. Med. Chem.*, 2012, **55**, 10674-10684.
5. D. B. Mark, J. L. Anderson, J. A. Brinker, J. A. Brophy, D. E. Casey Jr, R. R. Cross, D. Edmundowicz, R. Hachamovitch, M. A. Hlatky, J. E. Jacobs, S. Jaskie, K. G. Kett, V. Malhotra, F. A. Masoudi, M. V. McConnell, G. D. Rubin, L. J. Shaw, M. E. Sherman, S. Stanko and R. P. Ward, *J. Am. Coll. Cardiol.*, 2014, **63**, 698-721.
6. <http://www.nhlbi.nih.gov/>, (Accessed on 15-09-2017).
7. T. Geva and A. C. Marshall, *Circulation*, 2006, **113**, 1051-1052.
8. R. Y. Kwong and E. K. Yucel, *Circulation*, 2003, **108**, e104-e106.
9. L. R. Peterson and R. J. Gropler, *Circ. Cardiovasc. Imag.*, 2010, **3**, 211-222.
10. Z. Li and P. S. Conti, *Adv. Drug. Deliver. Rev.*, 2010, **62**, 1031-1051.
11. <https://pancreaticcanceraction.org/pancreatic-cancer/diagnosis/mri-scan/>, (Accessed on 15-09-2017).

12. <http://pixshark.com/spect-scan-machine.htm>, (Accessed on 15-05-2017).
13. <http://www.iambiomed.com/equipments/ct>, (Accessed on 15-09-2017).
14. <http://nutaq.com/en/blog/pet-scanners-rapid-data-acquisition-daq-hardware>, , (Accessed on 15-09-2017).
15. <http://www.drclaireboccia.com/services-offered.shtml>, (Accessed on 15-09-2017).
16. G. D. Lopaschuk, J. R. Ussher, C. D. Folmes, J. S. Jaswal and W. C. Stanley, *Physiol. Rev.*, 2010, **90**, 207-258.
17. G. D. Lopaschuk, R. L. Collins-Nakai and T. Itoi, *Cardiovasc. Res.*, 1992, **26**, 1172-1180.
18. A. P. Belanger, M. K. Pandey and T. R. DeGrado, *Nucl. Med. Biol.*, 2011, **38**, 435-441.
19. N. Fillmore, J. Mori and G. D. Lopaschuk, *Br. J. Pharmacol.*, 2014, **171**, 2080-2090.
20. J. R. Dyck, J.-F. Cheng, W. C. Stanley, R. Barr, M. P. Chandler, S. Brown, D. Wallace, T. Arrhenius, C. Harmon and G. Yang, *Circ. Res.*, 2004, **94**, e78-e84.
21. J. D. McGarry, G. Mannaerts and D. W. Foster, *J. Clin. Invest.*, 1977, **60**, 265.
22. S. M. Houten and R. J. Wanders, *J. Inherit. Metab. Dis.*, 2010, **33**, 469-477.
23. E. Gertz, J. Wisneski, W. Stanley and R. Neese, *J. Clin. Invest.*, 1988, **82**, 2017.

24. P. Randle, P. Garland, C. Hales and E. Newsholme, *Lancet*, 1963, **281**, 785-789.
25. A. Kadkhodayan, A. R. Coggan and L. R. Peterson, *Heart Fail. Rev.*, 2013, **18**, 567-574.
26. K. N. Giedd and S. R. Bergmann, *Curr. Cardiol. Rep.*, 2011, **13**, 121-131.
27. K. Yoshinaga, M. Naya, T. Shiga, E. Suzuki and N. Tamaki, *Eur. J. Nucl. Med. Mol. Imaging*, 2014, **41**, 384-393.
28. S. L. Pimlott and A. Sutherland, *Chem. Soc. Rev.*, 2011, **40**, 149-162.
29. W. E. Connor, *Am. J. Clin. Nutr.*, 2000, **71**, 171S-175S.
30. N. Willumsen, H. Vaagenes, A. C. Rustan, H. Grav, M. Lundquist, L. Skattebøl, J. Songstad and R. K. Berge, *J. Lipid Mediat. Cell Signal.*, 1997, **17**, 115-134.
31. M. Taylor, T. R. Wallhaus, T. R. DeGrado, D. C. Russell, P. Stanko, R. J. Nickles and C. K. Stone, *J. Nucl. Med.*, 2001, **42**, 55-62.
32. R. K. Berge, A. Aarsland, H. Kryvi, J. Bremer and N. Aarsaether, *Biochem. Pharmacol.*, 1989, **38**, 3969-3979.
33. R. K. Berge, J. Skorve, K. J. Tronstad, K. Berge, O. A. Gudbrandsen and H. Grav, *Curr. Opin. Lipidol.*, 2002, **13**, 295-304.
34. S. Skrede, H. Sørensen, L. Larsen, H. Steineger, K. Høvik, O. Spydevold, R. Horn and J. Bremer, *Biochim. Biophys. Acta*, 1997, **1344**, 115.

35. P. Wu, H. J. Grav, R. Horn and J. Bremer, *Biochem. Pharmacol.*, 1996, **51**, 751-758.
36. S. M. Lau, R. K. Brantley and C. Thorpe, *Biochemistry*, 1989, **28**, 8255-8262.
37. D. Wallach, *Biochem. Pharmacol.*, 1961, **5**, 323-331.
38. G. W. Goodwin, P. M. Rougraff, E. J. Davis and R. A. Harris, *J. Biol. Chem.*, 1989, **264**, 14965-14971.
39. K. Kurdziel, G. Ravizzini, B. Croft, J. Tatum, P. Choyke and H. Kobayashi, *Expert Opin. Med. Diagn.*, 2008, **2**, 829-842.
40. M. L. James and S. S. Gambhir, *Physiol. Rev.*, 2012, **92**, 897-965.
41. K. Chen and X. Chen, *Curr. Top. Med. Chem.*, 2010, **10**, 1227-1236.
42. K. Glunde, A. P. Pathak and Z. M. Bhujwala, *Trends Mol. Med.*, 2007, **13**, 287-297.
43. D. Papathanassiou, C. Bruna-Muraille, C. Jouannaud, L. Gagneux-Lemoussu, J.-P. Eschard and J.-C. Liehn, *Joint Bone Spine*, 2009, **76**, 474-480.
44. S. Liu, *Adv. Drug. Deliver. Rev.*, 2008, **60**, 1347-1370.
45. S. Banerjee, M. R. Pillai and N. Ramamoorthy, *Semin. Nucl. Med.*, 2001, **31**, 260-277.
46. P. Blower, *Dalton T.*, 2006, 1705-1711.
47. R. J. Kowalsky and S. W. Falen, *Radiopharmaceuticals in Nuclear Pharmacy and Nuclear Medicine*, American Pharmacists Association, Washington, 2004.

48. K. Iniewski, *Medical Imaging: Principles, Detectors, and Electronics*, Wiley-Blackwell, New Jersey, 2009.
49. A. F. Chatziioannou, *Proc. Am. Thorac. Soc.*, 2005, **2**, 533-536.
50. G. T. Gullberg, B. W. Reutter, A. Sitek, J. S. Maltz and T. F. Budinger, *Phys. Med. Biol.*, 2010, **55**, R111.
51. M. M. Khalil, J. L. Tremoleda, T. B. Bayomy and W. Gsell, *Int. J. Mol. Imaging.*, 2011, **2011**.
52. M. D. Bartholomä, A. S. Louie, J. F. Valliant and J. Zubieta, *Chem. Rev.*, 2010, **110**, 2903-2920.
53. I. Zolle, *Technetium-99m Pharmaceuticals*, Springer, Spain, 2007.
54. M. J. Welch, *Handbook of Radiopharmaceuticals: Radiochemistry and Applications*, John Wiley & Sons, Price, 2003.
55. S. Liu, *Chem. Soc. Rev.*, 2004, **33**, 445-461.
56. T. Storr, Y. Sugai, C. A. Barta, Y. Mikata, M. J. Adam, S. Yano and C. Orvig, *Inorg. Chem.*, 2005, **44**, 2698-2705.
57. R. Alberto, R. Schibli, A. Egli, A. P. Schubiger, U. Abram and T. A. Kaden, *J. Am. Chem. Soc.*, 1998, **120**, 7987-7988.
58. R. Alberto, K. Ortner, N. Wheatley, R. Schibli and A. P. Schubiger, *J. Am. Chem. Soc.*, 2001, **123**, 3135-3136.

59. N. Lazarova, S. James, J. Babich and J. Zubieta, *Inorg. Chem. Commun.*, 2004, **7**, 1023-1026.
60. R. Waibel, R. Alberto, J. Willuda, R. Finnern, R. Schibli, A. Stichelberger, A. Egli, U. Abram, J.-P. Mach and A. Plückthun, *Nat. Biotechnol.*, 1999, **17**.
61. R. Schibli and A. P. Schubiger, *Eur. J. Nucl. Med. Mol. Imaging*, 2002, **29**, 1529-1542.
62. R. M. Reilly, *Monoclonal antibody and peptide-targeted radiotherapy of cancer*, John Wiley & Sons, 2010.
63. A. Vértes, S. Nagy, Z. Klencsár, R. G. Lovas and F. Rösch, *Handbook of Nuclear Chemistry: Vol. 4: Radiochemistry and Radiopharmaceutical Chemistry in Life Sciences*, Springer Science & Business Media, 2010.
64. J. Fichna and A. Janecka, *Bioconjugate Chem.*, 2003, **14**, 3-17.
65. T. A. Holly, B. G. Abbott, M. Al-Mallah, D. A. Calnon, M. C. Cohen, F. P. DiFilippo, E. P. Ficaro, M. R. Freeman, R. C. Hendel and D. Jain, *J. Nucl. Cardiol.*, 2010, **17**, 941-973.
66. O. O. Sogbein, M. Pelletier-Galarneau, T. H. Schindler, L. Wei, R. G. Wells and T. D. Ruddy, *BioMed Res. Int.*, 2014, **2014**.
67. N. Tamaki, K. Morita, Y. Kuge and E. Tsukamoto, *J. Nucl. Med.*, 2000, **41**, 1525.
68. S. T. Treves, *Pediatric Nuclear Medicine and Molecular Imaging*, Springer, 2014.



69. E. Cazzola, E. Benini, M. Pasquali, P. Mirtschink, M. Walther, H.-J. Pietzsch, L. Uccelli, A. Boschi, C. Bolzati and A. Duatti, *Bioconjugate Chem.*, 2008, **19**, 450-460.
70. A. Mathur, S. Subramanian, M. B. Mallia, S. Banerjee, G. Samuel, H. D. Sarma and M. Venkatesh, *Bioorg. Med. Chem.*, 2008, **16**, 7927-7931.
71. E. D. Michelakis, *Circulation*, 2008, **117**, 2431-2434.
72. M. Walther, C. M. Jung, R. Bergmann, J. Pietzsch, K. Rode, K. Fahmy, P. Mirtschink, S. Stehr, A. Heintz, G. Wunderlich, W. Kraus, H. J. Pietzsch, J. Kropp, A. Deussen and H. Spies, *Bioconjugate Chem.*, 2007, **18**, 216-230.
73. T. Uehara, T. Uemura, S. Hirabayashi, S. Adachi, K. Odaka, H. Akizawa, Y. Magata, T. Irie and Y. Arano, *J. Med. Chem.*, 2007, **50**, 543-549.
74. A. C. Heintz, C. M. Jung, S. N. Stehr, P. Mirtschink, M. Walther, J. Pietzsch, R. Bergmann, H.-J. Pietzsch, H. Spies, G. Wunderlich, J. Kropp and A. Deussen, *Nucl. Med. Commun.*, 2007, **28**, 637-645.
75. Y. Magata, T. Kawaguchi, M. Ukon, N. Yamamura, T. Uehara, K. Ogawa, Y. Arano, T. Temma, T. Mukai and E. Tadamura, *Bioconjugate Chem.*, 2004, **15**, 389-393.
76. T. Chu, Y. Zhang, X. Liu, Y. Wang, S. Hu and X. Wang, *Appl. Radiat. Isot.*, 2004, **60**, 845-850.
77. G. S. Jones, D. R. Elmaleh, H. W. Strauss and A. J. Fischman, *Bioorg. Med. Chem. Lett.*, 1996, **6**, 2399-2404.

78. G. S. Jones, D. R. Elmaleh, H. W. Strauss and A. J. Fischman, *Nucl. Med. Biol.*, 1994, **21**, 117-123.
79. R. H. Mach, H. F. Kung, P. Jungwiwattanaporn and Y. Z. Guo, *Int. J. Rad. Appl. Instrum. B*, 1991, **18**, 215-226.
80. H. Coenen, *Fluorine-18 Labeling Methods: Features and Possibilities of Basic Reactions*, Springer, Berlin, Heidelberg, 2007.
81. R. P. Beaney, *Clin. Oncol.*, 2004, **16**, 161.
82. C. M. West, T. Jones and P. Price, *Nat. Rev. Cancer*, 2004, **4**, 457-469.
83. A. Takano, *Curr. Pharm. Des.*, 2010, **16**, 371-377.
84. S. V. Ankala and G. Fenteany, *Tetrahedron Lett.*, 2002, **43**, 4729-4732.
85. R. P. Woods, J. C. Mazziotta and S. R. Cherry, *J. Comput. Assist. Tomogr.*, 1993, **17**, 536-546.
86. D. W. Townsend, T. Beyer, P. E. Kinahan, T. Brun, R. Roddy, R. Nutt and L. G. Byars, 1998.
87. A. Sanchez-Crespo, *Appl. Radiat. Isot.*, 2013, **76**, 55-62.
88. N. A. Meanwell, *J. Med. Chem.*, 2018, DOI: 10.1021/acs.jmedchem.7b01788.
89. Q. A. Huchet, B. Kuhn, B. Wagner, N. A. Kratochwil, H. Fischer, M. Kansy, D. Zimmerli, E. M. Carreira and K. Müller, *J. Med. Chem.*, 2015, **58**, 9041-9060.

90. E. P. Gillis, K. J. Eastman, M. D. Hill, D. J. Donnelly and N. A. Meanwell, *J. Med. Chem.*, 2015, **58**, 8315-8359.
91. S. Preshlock, M. Tredwell and V. Gouverneur, *Chem. Rev.*, 2016, **116**, 719-766.
92. O. Jacobson, D. O. Kiesewetter and X. Chen, *Bioconjugate Chem.*, 2015, **26**, 1-18.
93. D. van der Born, A. Pees, A. J. Poot, R. V. A. Orru, A. D. Windhorst and D. J. Vugts, *Chem. Soc. Rev.*, 2017, **46**, 4709-4773.
94. P. W. Miller, N. J. Long, R. Vilar and A. D. Gee, *Angew. Chem.*, 2008, **120**, 9136-9172.
95. D. W. Kim, H.-J. Jeong, S. T. Lim and M.-H. Sohn, *Recent Trends in the Nucleophilic [18F]-Radiolabeling Method with No-Carrier-Added [18F]Fluoride*, Springer, 2010.
96. J. De Goeij and M. Bonardi, *J. Radioanal. Nucl. Chem.*, 2005, **263**, 13-18.
97. H. Gewirtz, *Jacc. Cardiovasc. Imag.*, 2011, **4**, 292-302.
98. A. Abraham, G. Nichol, K. A. Williams, A. Guo, L. Garrard, R. A. Davies, L. Duchesne, H. Haddad, B. Chow and J. DaSilva, *J. Nucl. Med.*, 2010, **51**, 567-574.
99. A. Kadkhodayan, A. R. Coggan and L. R. Peterson, *Heart Failure Rev.*, 2013, **18**, 567-574.
100. S. S. Gambhir, M. Schwaiger, S.-C. Huang, J. Krivokapich, H. R. Schelbert, C. A. Nienaber and M. E. Phelps, *J. Nucl. Med.*, 1989, **30**, 359-366.

101. P. Herrero, C. S. Dence, A. R. Coggan, Z. Kisrieva-Ware, P. Eisenbeis and R. J. Gropler, *J. Nucl. Med.*, 2007, **48**, 2046-2055.
102. R. S. Driessen, P. G. Raijmakers, W. J. Stuijzand and P. Knaapen, *Int. J. Cardiovasc. Imaging*, 2017, **33**, 1021-1031.
103. P. Arumugam, D. Tout and C. Tonge, *Br. Med. Bull.*, 2013, **107**, 87-100.
104. H. R. Schelbert, M. E. Phelps, S. Huang, N. MacDonald, H. Hansen, C. Selin and D. Kuhl, *Circulation*, 1981, **63**.
105. B. Rauch, F. Helus, M. Grunze, E. Braunwell, G. Mall, W. Hasselbach and W. Kuebler, *Circulation*, 1985, **71**.
106. S. Senthamizhchelvan, P. E. Bravo, C. Esaias, M. A. Lodge, J. Merrill, R. F. Hobbs, G. Sgouros and F. M. Bengel, *J. Nucl. Med.*, 2010, **51**, 1592-1599.
107. O. Gaemperli and P. A. Kaufmann, *Ann. N. Y. Acad. Sci.*, 2011, **1228**, 109-136.
108. L. I. Araujo, A. A. Lammertsma, C. G. Rhodes, E. McFalls, H. Iida, E. Rechavia, A. Galassi, R. De Silva, T. Jones and A. Maseri, *Circulation*, 1991, **83**, 875-885.
109. K. J. Mather and T. R. DeGrado, *BBA-Mol. Cell Biol. L.*, 2016, **1861**, 1535-1543.
110. M. K. Pandey, A. Bansal and T. R. DeGrado, *Heart Metab.*, 2011, **51**, 15-19.
111. A. A. Papamandjaris, D. E. MacDougall and P. J. Jones, *Life Sci.*, 1998, **62**, 1203-1215.
112. L. A. Pon, *Mitochondria, Elsevier Inc.*, 2 edn., 2007.

113. T. R. DeGrado and D. C. Moka, *Int. J. Rad. Appl. Instrum. B*, 1992, **19**, 389-397.
114. T. Takala, P. Nuutila, K. Pulkki, V. Oikonen, T. Grönroos, T. Savunen, T. Vähäsilta, M. Luotolahti, M. Kallajoki, J. Bergman, S. Forsback and J. Knuuti, *Eur. J. Nucl. Med. Mol. Imaging*, 2002, **29**, 1617-1622.
115. T. R. DeGrado, S. Wang, J. E. Holden, R. J. Nickles, M. Taylor and C. K. Stone, *Nucl. Med. Biol.*, 2000, **27**, 221-231.
116. A. P. Belanger, M. K. Pandey and T. R. DeGrado, *Nucl. Med. Biol.*, 2011, **38**, 435-441.
117. T. R. DeGrado, F. Bhattacharyya, M. K. Pandey, A. P. Belanger and S. Wang, *J. Nucl. Med.*, 2010, **51**, 1310-1317.
118. Z. Cai, N. S. Mason, C. J. Anderson and W. B. Edwards, *Nucl. Med. Biol.*, 2016, **43**, 108-115.
119. E. Sheibani and K. Wärnmark, *Org. Biomol. Chem.*, 2012, **10**, 2059-2067.
120. K. Nagao and T. Yanagita, *Pharmacol. Res.*, 2010, **61**, 208-212.
121. K. Hamacher, H. H. Coenen and G. Stocklin, *J Nucl Med*, 1986, **27**, 235-238.
122. E. Briard and V. W. Pike, *J. Labelled Compd. Radiopharm.*, 2004, **47**, 217-232.
123. J. I. Ambrus, PhD thesis, University of Wollongong, 2008.

124. M. J. Dagani, H. J. Barda, T. J. Benya and D. C. Sanders, in *Ullmann's Encyclopedia of Industrial Chemistry*, Wiley-VCH Verlag GmbH & Co. KGaA, 2000, DOI: 10.1002/14356007.a04\_405.
125. P. G. Wuts and T. W. Greene, *Greene's protective groups in organic synthesis*, John Wiley & Sons, 2006.
126. P. A. Grieco and S. D. Larsen, *J. Org. Chem.*, 1986, **51**, 3553-3555.
127. P. Tauh and A. G. Fallis, *J. Org. Chem.*, 1999, **64**, 6960-6968.
128. E. Corey and A. Venkateswarlu, *J. Am. Chem. Soc.*, 1972, **94**, 6190-6191.
129. M. Billinger, M. Fleisch, F. R. Eberli, A. Garachemani, B. Meier and C. Seiler, *J. Am. Coll. Cardiol.*, 1999, **33**, 1027-1035.
130. Y. Yoshida, Y. Sakakura, N. Aso, S. Okada and Y. Tanabe, *Tetrahedron*, 1999, **55**, 2183-2192.
131. D. Urabe, H. Todoroki, K. Masuda and M. Inoue, *Tetrahedron*, 2012, **68**, 3210-3219.
132. S. Funakoshi, N. Fujii, K. Akaji, H. Irie and H. Yajima, *Chem. Pharm. Bull.*, 1979, **27**, 2151-2156.
133. S. Lu, S. D. Lepore, S. Y. Li, D. Mondal, P. C. Cohn, A. K. Bhunia and V. W. Pike, *J. Org. Chem.*, 2009, **74**, 5290-5296.
134. W. J. Middleton, *J. Org. Chem.*, 1975, **40**, 574-578.

135. B. Dayal, G. Salen, B. Toome, G. S. Tint, S. Shefer and J. Padia, *Steroids*, 1990, **55**, 233-237.
136. *United States Pat.*, US6362352B1, 2002.
137. M. M. Goerger and B. S. Hudson, *J. Org. Chem.*, 1988, **53**, 3148-3153.
138. T. V. Ovaska, V. Snieckus and B. Nolte, *e-EROS Encyclopedia of Reagents for Organic Synthesis*, Pblished online, 2009.
139. B. Tripathi, L. Paniwnyk, N. Cherkasov, A. Ibhaddon, T. Lana-Villarreal and R. Gómez, *Ultrason. Sonochem.*, 2015, **26**, 445-451.
140. T. R. DeGrado, H. H. Coenen and G. Stocklin, *J. Nucl. Med.*, 1991, **32**, 1888-1896.
141. B. Renstrom, S. Rommelfanger, C. K. Stone and T. R. DeGrado, *J. Nucl. Med.*, 1998, **39**, 1684.
142. T. R. DeGrado, M. T. Kitapci, S. Wang, J. Ying and G. D. Lopaschuk, *J. Nucl. Med.*, 2006, **47**, 173-181.
143. G.-J. Meyer, H. H. Coenen, S. L. Waters, B. Långström, R. Cantineau, K. Strijckmans, W. Vaalburg, C. Halldin, C. Crouzel and B. Mazière, in *Radiopharmaceuticals for Positron Emission Tomography*, Springer, 1993, pp. 91-150.
144. H. Vera-Ruiz, C. Marcus, V. Pike, H. Coenen, J. Fowler, G. Meyer, P. Cox, W. Vaalburg, R. Cantineau and F. Helus, *Int. J. Rad. Appl. Instrum. B*, 1990, **17**, 445-456.

145. D. J. Schlyer, *Handbook of Radiopharmaceuticals: Radiochemistry and Applications*, 2003, 1-70.
146. P. J. Riss and F. Roesch, *Bioorg. Med. Chem.*, 2009, **17**, 7630-7634.
147. J. H. Clark, *Chem. Rev.*, 1980, **80**, 429-452.
148. V. Vlasov, *J. Fluorine Chem.*, 1993, **61**, 193-216.
149. I. AlJammaz, B. Al-Otaibi, H. AlHindas and S. M. Okarvi, *Nucl. Med. Biol.*, 2015, **42**, 804-808.
150. A. Tressaud and G. Haufe, *Fluorine and health: molecular imaging, biomedical materials and pharmaceuticals*, Elsevier, 2008.
151. F. Cicone, D. Viertl, A. M. Quintela Pousa, T. Denoël, S. Gnesin, F. Scopinaro, M.-C. Vozenin and J. O. Prior, *Front. Med. (Lausanne)*, 2017, **4**, 35.
152. K. N. Giedd and S. R. Bergmann, *Curr. Cardiol. Rep.*, 2011, **13**, 121-131.
153. J. A. Wisneski, E. W. Gertz, R. A. Neese and M. Mayr, *J. Clin. Invest.*, 1987, **79**, 359.
154. W. C. Stanley, G. D. Lopaschuk, J. L. Hall and J. G. McCormack, *Cardiovasc. Res.*, 1997, **33**, 243-257.
155. S. R. Bergmann, C. J. Weinheimer, J. Markham and P. Herrero, *J. Nucl. Med. Allied Sci.*, 1996, **37**, 1723-1730.
156. D. W. Myears, B. E. Sobel and S. R. Bergmann, *Am. J. Physiol. Heart Circ. Physiol.*, 1987, **253**, H107-H114.



157. J. Li, J. Lu and Y. Zhou, *BioMed Res. Int.*, 2017, **2017**, 11.
158. T. Storr, K. H. Thompson and C. Orvig, *Chem. Soc. Rev.*, 2006, **35**, 534-544.
159. L. Ronconi and P. J. Sadler, *Coord. Chem. Rev.*, 2007, **251**, 1633-1648.
160. T. J. Hubin, *Coord. Chem. Rev.*, 2003, **241**, 27-46.
161. S. P. Fricker, V. Anastassov, J. Cox, M. C. Darkes, O. Grujic, S. R. Idzan, J. Labrecque, G. Lau, R. M. Mosi, K. L. Nelson, L. Qin, Z. Santucci and R. S. Wong, *Biochem. Pharmacol.*, 2006, **72**, 588-596.
162. D. P. Singh, K. Kumar, S. S. Dhiman and J. Sharma, *J. Enzyme Inhib. Med. Chem.*, 2010, **25**, 21-28.
163. S. P. Fricker, V. Anastassov, J. Cox, M. C. Darkes, O. Grujic, S. R. Idzan, J. Labrecque, G. Lau, R. M. Mosi, K. L. Nelson, L. Qin, Z. Santucci and R. S. Y. Wong, *Biochem. Pharmacol.*, 2006, **72**, 588-596.
164. R. Delgado, V. Felix, L. M. P. Lima and D. W. Price, *Dalton T.*, 2007, DOI: 10.1039/B704360K, 2734-2745.
165. D. K. Cabbiness and D. W. Margerum, *J. Am. Chem. Soc.*, 1969, **91**, 6540-6541.
166. N. F. Curtis, *Supramol. Chem.*, 2012, **24**, 439-447.
167. R. J. A. Wanders, J. P. N. Ruiten, L. IJlst, H. R. Waterham and S. M. Houten, *J. Inherit. Metab. Dis.*, 2010, **33**, 479-494.
168. D. G. Nicholls, *Int. J. Biochem. Cell Biol.*, 2002, **34**, 1372-1381.

169. M.-C. Frantz and P. Wipf, *Environ. Mol. Mutagen.*, 2010, **51**, 462-475.
170. M. R. Duchon, *Mol. Aspects Med.*, 2004, **25**, 365-451.
171. J. S. Modica-Napolitano and K. Singh, *Expert Reviews in Molecular Medicine*, 2002, **4**, 1-19.
172. H. W. Strauss and H. Schoder, *JACC. Cardiovasc. Imaging*, 2012, **5**, 293-296.
173. B. Agarwal, D. F. Stowe, R. K. Dash, Z. J. Bosnjak and A. K. Camara, *Front. Psychol.*, 2014, **5**.
174. M. P. Murphy and R. A. J. Smith, *Annu. Rev. Pharmacol. Toxicol.*, 2007, **47**, 629-656.
175. A. T. Hoye, J. E. Davoren, P. Wipf, M. P. Fink and V. E. Kagan, *Acc. Chem. Res.*, 2008, **41**, 87-97.
176. L. F. Yousif, K. M. Stewart and S. O. Kelley, *ChemBioChem*, 2009, **10**, 1939-1950.
177. K. L. Horton, K. M. Stewart, S. B. Fonseca, Q. Guo and S. O. Kelley, *Chem. Biol.*, 2008, **15**, 375-382.
178. A. Capello, E. P. Krenning, B. F. Bernard, W. A. Breeman, J. L. Erion and M. de Jong, *J. Nucl. Med.*, 2006, **47**, 122-129.
179. K. L. Horton and S. O. Kelley, *J. Med. Chem.*, 2009, **52**, 3293-3299.
180. M. P. Murphy, *Trends Biotechnol.*, 1997, **15**, 326-330.
181. M. Ross, G. Kelso, F. Blaikie, A. James, H. Cocheme, A. Filipovska, T. Da Ros, T. Hurd, R. Smith and M. Murphy, *Biochemistry (Moscow)*, 2005, **70**, 222-230.

182. B. J. Krause, Z. Szabo, L. C. Becker, R. F. Dannals, U. Scheffel, C. Seki, H. T. Ravert, A. F. Dipaola, Jr. and H. N. Wagner, Jr., *J. Nucl. Biol. Med.*, 1994, **38**, 521-526.
183. I. Madar, J. H. Anderson, Z. Szabo, U. Scheffel, P. F. Kao, H. T. Ravert and R. F. Dannals, *J. Nucl. Med.*, 1999, **40**, 1180-1185.
184. I. Madar, L. Weiss and G. Izbicki, *J. Nucl. Med.*, 2002, **43**, 234-238.
185. H. T. Ravert, I. Madar and R. F. Dannals, *J. Labelled Compd. Radiopharm.*, 2004, **47**, 469-476.
186. I. Madar, H. T. Ravert, Y. Du, J. Hilton, L. Volokh, R. F. Dannals, J. J. Frost and J. M. Hare, *J. Nucl. Med.*, 2006, **47**, 1359-1366.
187. Z. Cheng, M. Subbarayan, X. Chen and S. S. Gambhir, *J. Labelled Compd. Radiopharm.*, 2005, **48**, 131-137.
188. Z. Cheng, R. C. Winant and S. S. Gambhir, *J. Nucl. Med.*, 2005, **46**, 878-886.
189. J.-J. Min, S. Biswal, C. Deroose and S. S. Gambhir, *J. Nucl. Med.*, 2004, **45**, 636-643.
190. S. S. Denisov, E. A. Kotova, E. Y. Plotnikov, A. A. Tikhonov, D. B. Zorov, G. A. Korshunova and Y. N. Antonenko, *Chem. Commun.*, 2014, **50**, 15366-15369.
191. Y. T. Ko, C. Falcao and V. P. Torchilin, *Mol. Pharm.*, 2009, **6**, 971-977.
192. A. Khan, G. Nicholson, J. Greenman, L. Madden, G. McRobbie, C. Pannecouque, E. De Clercq, R. Ullom, D. L. Maples, R. L. Maples, J. D.

- Silversides, T. J. Hubin and S. J. Archibald, *J. Am. Chem. Soc.*, 2009, **131**, 3416-3417.
193. R. Kolinski, *J. Cheminformatics*, 1995, **26**.
194. E. H. Wong, G. R. Weisman, D. C. Hill, D. P. Reed, M. E. Rogers, J. S. Condon, M. A. Fagan, J. C. Calabrese, K. C. Lam, I. A. Guzei and A. L. Rheingold, *J. Am. Chem. Soc.*, 2000, **122**, 10561-10572.
195. C. A. Boswell, X. Sun, W. Niu, G. R. Weisman, E. H. Wong, A. L. Rheingold and C. J. Anderson, *J. Med. Chem.*, 2004, **47**, 1465-1474.
196. T. J. Hubin, J. M. McCormick, S. R. Collinson, D. H. Busch and N. W. Alcock, *Chem. Commun.*, 1998, DOI: 10.1039/A802060D, 1675-1676.
197. J. D. Silversides, C. C. Allan and S. J. Archibald, *Dalton T.*, 2007, DOI: 10.1039/b615329a, 971-978.
198. S. Hatse, K. Princen, E. D. Clercq, M. M. Rosenkilde, T. W. Schwartz, P. E. Hernandez-Abad, R. T. Skerlj, G. J. Bridger and D. Schols, *Biochem. Pharmacol.*, 2005, **70**, 752-761.
199. G. Weisman, M. Rogers, E. Wong, J. Jasinski and E. Paight, *J. Am. Chem. Soc.*, 1990, **112**, 8604-8605.
200. R. Smith, D. Huskens, D. Daelemans, R. E. Mewis, C. D. Garcia, A. N. Cain, T. N. C. Freeman, C. Pannecouque, E. D. Clercq, D. Schols, T. J. Hubin and S. J. Archibald, *Dalton T.*, 2012, **41**, 11369-11377.
201. M. Le Baccon, F. Chuburu, L. Toupet, H. Handel, M. Soibinet, I. Déchamps-Olivier, J.-P. Barbier and M. Aplincourt, *New J. Chem.*, 2001, **25**, 1168-1174.

202. J. Costamagna, G. Ferraudi, B. Matsuhira, M. Campos-Vallette, J. Canales, M. Villagrán, J. Vargas and M. Aguirre, *Coord. Chem. Rev.*, 2000, **196**, 125-164.
203. A. Hackling, R. Ghosh, S. Perachon, A. Mann, H.-D. Höltje, C. G. Wermuth, J.-C. Schwartz, W. Sippl, P. Sokoloff and H. Stark, *J. Med. Chem.*, 2003, **46**, 3883-3899.
204. T. J. Wadas, E. H. Wong, G. R. Weisman and C. J. Anderson, *Curr. Pharm. Des.*, 2007, **13**, 3-16.
205. J. Wang, C.-T. Yang, Y.-S. Kim, S. G. Sreerama, Q. Cao, Z.-B. Li, Z. He, X. Chen and S. Liu, *J. Med. Chem.*, 2007, **50**, 5057-5069.
206. G. Van der Vusse, J. Glatz, H. Stam and R. S. Reneman, *Physiol. Rev.*, 1992, **72**, 881-940.
207. J. Neely, M. a. Rovetto and J. Oram, *Prog. Cardiovasc. Dis.*, 1972, **15**, 289-329.
208. S. Nishimura and Y. Ohta, *Int. J. Card. Imaging*, 1999, **15**, 35-39.
209. S. K. Biswas, M. Sarai, A. Yamada, S. Motoyama, H. Harigaya, T. Hara, K. Sugimoto, H. Toyama, H. Hishida and Y. Ozaki, *Int. J. Cardiol.*, 2010, **138**, 290-299.
210. M. Pillai and A. Duatti, *J. Labelled Compd. Radiopharm.*, 2008, **51**, 329-335.
211. R. Alberto and U. Abram, *<sup>99m</sup>Tc: labeling chemistry and labeled compounds*, Springer, Boston, 2011.
212. S. M. Karesh, W. C. Eckelman and R. C. Reba, *J. Pharm. Sci.*, 1977, **66**, 225-228.

213. H. Zeng and H. Zhang, *Eur. J. Med. Chem.*, 2014, **72**, 10-17.
214. B. C. Lee, D. H. Kim, J. H. Lee, H. J. Sung, Y. S. Choe, D. Y. Chi, K.-H. Lee, Y. Choi and B.-T. Kim, *Bioconjugate Chem.*, 2007, **18**, 1332-1337.
215. B. C. Lee, D. H. Kim, I. Lee, Y. S. Choe, D. Y. Chi, K.-H. Lee, Y. Choi and B.-T. Kim, *J. Med. Chem.*, 2008, **51**, 3630-3634.
216. A. Mathur, M. B. Mallia, H. D. Sarma, S. Banerjee and M. Venkatesh, *J. Labelled Compd. Radiopharm.*, 2010, **53**, 580-585.
217. L. I. Wiebe, *J. Nucl. Med.*, 2008, **49**, 1901-1901.
218. L. I. Wiebe, *J. Nucl. Med.*, 2008, **49**, 1900-1900.
219. T. Uehara, H. Akizawa and Y. Arano, *Technetium-99m Radiopharmaceuticals for Lymphoscintigraphy. Chapter 13*, International Atomic Energy Agency, Vienna (Austria), 2009.
220. S. J. Archibald, *J. Cheminformatics*, 2010, **41**.
221. K. Suzuki, N. Shimmura, K. Thipyapong, T. Uehara, H. Akizawa and Y. Arano, *Inorg. Chem.*, 2008, **47**, 2593-2600.
222. T. Liu, Q. Gan and J. Zhang, *J. Radioanal. Nucl. Chem.*, 2016, **310**, 1215-1221.
223. A. Isidro-Llobet, M. Alvarez and F. Albericio, *Chemical reviews*, 2009, **109**, 2455-2504.
224. U. Ragnarsson and L. Grehn, *RSC Advances*, 2013, **3**, 18691-18697.

225. H.-S. Chong, X. Ma, T. Le, B. Kwamena, D. E. Milenic, E. D. Brady, H. A. Song and M. W. Brechbiel, *J. Med. Chem.*, 2007, **51**, 118-125.
226. G. Ortiz, S. Brandès, Y. Rousselin and R. Guillard, *Chem. Eur. J.*, 2011, **17**, 6689-6695.
227. B. Klenke and I. H. Gilbert, *J. Org. Chem.*, 2001, **66**, 2480-2483.
228. J. Dilworth and S. Parrott, *Chem. Soc. Rev.*, 1998, **27**, 43-55.
229. E. Wong, T. Fauconnier, S. Bennett, J. Valliant, T. Nguyen, F. Lau, L. F. Lu, A. Pollak, R. A. Bell and J. R. Thornback, *Inorg. Chem.*, 1997, **36**, 5799-5808.
230. E. Deutsch, K. Libson, J.-L. Vanderheyden, A. R. Ketring and H. R. Maxon, *Int. J. Rad. Appl. Instrum. B*, 1986, **13**, 465-477.
231. M. K. Dewanjee, *Semin. Nucl. Med.*, 1990, **20**, 5-27.
232. U. Abram and R. Alberto, *J. Braz. Chem. Soc.*, 2006, **17**, 1486-1500.
233. D. B. G. Williams and M. Lawton, *J. Org. Chem.*, 2010, **75**, 8351-8354.
234. A. Zakrzewska, A. Parczewski, D. Kazmierczak, W. Ciesielski and J. Kochana, *Acta Chim. Slov.*, 2007, **54**, 106.
235. J. F. Carvalho and G. D. Prestwich, *J. Org. Chem.*, 1984, **49**, 1251-1258.
236. M. Tredwell and V. Gouverneur, *Angew. Chem. Int. Edit.*, 2012, **51**, 11426-11437.

237. G. E. Smith, H. L. Sladen, S. C. Biagini and P. J. Blower, *Dalton T.*, 2011, **40**, 6196-6205.